

EUROPEAN JOURNAL OF BIOLOGY

Owner

Yesim Oktem
Istanbul University, Turkey

Editor in Chief

Sehnaz Bolkent
Istanbul University, Turkey

Deputy Editor in Chief

Fusun Oztay
Istanbul University, Turkey

Editorial Board

Hafiz Ahmed
University of Maryland, USA

Ahmed Asan
Trakya University, Turkey

Ricardo Antunes de Azevedo
Universidade de Sao Paulo, Brazil

Levent Bat
Sinop University, Turkey

Mahmut Caliskan
Istanbul University, Turkey

Carmela Caroppo
Institute for Coastal Marine Environment, Italy

Cihan Demirci
Istanbul University, Turkey

Mustafa Djamgoz
Imperial College, United Kingdom

Editors

Amal Amer
The Ohio State University, USA

Gulriz Baycu Kahyaoglu
Istanbul University, Turkey

Aysegul Mulayim
Istanbul University, Turkey

Jan Zima
Charles University, Czech Republic

Aglıka Edrewa
Bulgarian Academy of Science, Bulgaria

Refet Gojak
University of Sarajevo, Bosnia

Ufuk Gunduz
Middle East Technical University, Turkey

Dietmar Keyser
University of Hamburg, Germany

Ayten Kimiran
Istanbul University, Turkey

Domenico Morabito
Université d'Orléans, France

Michael Moustakas
Aristotle University, Greece

Nurdan Ozkucur
Tufts University, USA

Statistical Editor

Ahmet Dirican
Istanbul University, Turkey

Language Editors

Elizabeth Mary Earl
Istanbul University, Turkey

Alan James Newson
Istanbul University, Turkey

Nesrin Ozoren
Bogazici University, Turkey

Majeti Narasimha Vara Prasad
University of Hyderabad, India

Thomas Sawidis
Aristotle University, Greece

Alex Sivan
The Hebrew University of Jerusalem, Israel

Nico M. Van Straalen
Vrije Universiteit, The Netherlands

Ismail Turkan
Ege University, Turkey

Argyro Zenetos
Hellenic Centre for Marine Research, Greece

Coert J. Zuurbier
*Academisch Medisch Centrum Universiteit,
The Netherlands*

Owner on behalf of the Istanbul University Faculty of Science: Yesim Oktem – Publication Type: Biannually – Printed at: İlbey Matbaa Kağıt Reklam Org. M.Üc. San. Tic. Ltd. Şti. 2.Matbaacılar Sitesi 3NB 3 Topkapı/Zeytinburnu, İstanbul, Turkey www.ilbeymatbaa.com.tr, Sertifika No: 17845 – Printing Date: December 2019

Publishing Company

Istanbul University Press
İstanbul Üniversitesi Merkez Kampüsü,
34452 Beyazıt, Fatih / İstanbul - Turkey
Phone: +90 (212) 440 00 00



İSTANBUL
UNIVERSITY
P R E S S

Aims and Scope

European Journal of Biology (Eur J Biol) is an international, scientific, open access periodical published in accordance with independent, unbiased, and double-blinded peer-review principles. The journal is the official publication of Istanbul University Faculty of Science and it is published biannually on June and December. The publication language of the journal is English. European Journal of Biology has been previously published as IUFS Journal of Biology. It has been published in continuous publication since 1940.

European Journal of Biology aims to contribute to the literature by publishing manuscripts at the highest scientific level on all fields of biology. The journal publishes original research and review articles, and short communications that are prepared in accordance with the ethical guidelines in all fields of biology and life sciences.

The scope of the journal includes but not limited to; botany, zoology, hydrobiology, animal and plant systematics, ecology, environmental biology, microbiology, radiobiology, molecular biology, biochemistry, genetics, biotechnology, physiology, toxicology, cell biology, cancer biology, neurobiology, developmental biology, stem cell biology, regenerative and reparative biology, nanobiotechnology, system biology, tissue engineering, biomaterials, and omic sciences.

The target audience of the journal includes specialists and professionals working and interested in all disciplines of biology.

The editorial and publication processes of the journal are shaped in accordance with the guidelines of the International Committee of Medical Journal Editors (ICMJE), World Association of Medical Editors (WAME), Council of Science Editors (CSE), Committee on Publication Ethics (COPE), European Association of Science Editors (EASE), and National Information Standards Organization (NISO). The journal is in conformity with the Principles of Transparency and Best Practice in Scholarly Publishing (doaj.org/bestpractice).

European Journal of Biology is currently indexed by Web of Science Zoological Record, CAB Abstracts (CABI), Chemical Abstracts Service (CAS) and TUBITAK-ULAKBIM TR Index.

Processing and publication are free of charge with the journal. No fees are requested from the authors at any point throughout the evaluation and publication process. All manuscripts must be submitted via the online submission system, which is available at dergipark.gov.tr/iufsjb. The journal guidelines, technical information, and the required forms are available on the journal's web page.

All expenses of the journal are covered by the Istanbul University.

Statements or opinions expressed in the manuscripts published in the journal reflect the views of the author(s) and not the opinions of the Istanbul University Faculty of Science, editors, editorial board, and/or publisher; the editors, editorial board, and publisher disclaim any responsibility or liability for such materials.

All published content is available online, free of charge at dergipark.gov.tr/iufsjb. Printed copies of the journal are distributed free of charge.



Editor in Chief: Prof. Sehnaz BOLKENT

Address: Istanbul University, Faculty of Science, Department of Biology, 34134 Vezneciler, Fatih, Istanbul, TURKEY

Phone: +90 212 4555700 (Ext. 15079)

Fax: +90 212 5280527

E-mail: sbolkent@istanbul.edu.tr

Instructions to Authors

European Journal of Biology (Eur J Biol) is an international, scientific, open access periodical published in accordance with independent, unbiased, and double-blinded peer-review principles. The journal is the official publication of Istanbul University Faculty of Science and it is published biannually on June and December. The publication language of the journal is English. European Journal of Biology has been previously published as IUFS Journal of Biology. It has been published in continuous publication since 1940.

European Journal of Biology aims to contribute to the literature by publishing manuscripts at the highest scientific level on all fields of biology. The journal publishes original research and review articles, and short communications that are prepared in accordance with the ethical guidelines in all fields of biology and life sciences.

The scope of the journal includes but not limited to; botany, zoology, hydrobiology, animal and plant systematics, ecology, environmental biology, microbiology, radiobiology, molecular biology, biochemistry, genetics, biotechnology, physiology, toxicology, cell biology, cancer biology, neurobiology, developmental biology, stem cell biology, regenerative and reparative biology, nanobiotechnology, system biology, tissue engineering, biomaterials, and omic sciences.

The editorial and publication processes of the journal are shaped in accordance with the guidelines of the International Council of Medical Journal Editors (ICMJE), the World Association of Medical Editors (WAME), the Council of Science Editors (CSE), the Committee on Publication Ethics (COPE), the European Association of Science Editors (EASE), and National Information Standards Organization (NISO). The journal conforms to the Principles of Transparency and Best Practice in Scholarly Publishing (doaj.org/bestpractice).

Originality, high scientific quality, and citation potential are the most important criteria for a manuscript to be accepted for publication. Manuscripts submitted for evaluation should not have been previously presented or already published in an electronic or printed medium. Manuscripts that have been presented in a meeting should be submitted with detailed information on the organization, including the name, date, and location of the organization.

Manuscripts submitted to European Journal of Biology will go through a double-blind peer-review process. Each submission will be reviewed by at least three external, independent peer reviewers who are experts in their fields in order to ensure an unbiased evaluation process. The editorial board will invite an external and independent editor to manage the evaluation processes of manuscripts submitted by editors or by the editorial board members of the journal. The Editor in Chief is the final authority in the decision-making process for all submissions.

An approval of research protocols by the Ethics Committee in accordance with international agreements (World Medical Association Declaration of Helsinki "Ethical Principles for Medi-

cal Research Involving Human Subjects," amended in October 2013, www.wma.net) is required for experimental, clinical, and drug studies. If required, ethics committee reports or an equivalent official document will be requested from the authors.

For manuscripts concerning experimental research on humans, a statement should be included that shows the written informed consent of patients and volunteers was obtained following a detailed explanation of the procedures that they may undergo. Information on patient consent, the name of the ethics committee, and the ethics committee approval number should also be stated in the Materials and Methods section of the manuscript. It is the authors' responsibility to carefully protect the patients' anonymity. For photographs that may reveal the identity of the patients, signed releases of the patient or of their legal representative should be enclosed.

European Journal of Biology requires experimental research studies on vertebrates or any regulated invertebrates to comply with relevant institutional, national and/or international guidelines. The journal supports the principles of Basel Declaration (basel-declaration.org) and the guidelines published by International Council for Laboratory Animal Science (ICLAS) (iclas.org). Authors are advised to clearly state their compliance with relevant guidelines.

European Journal of Biology advises authors to comply with IUCN Policy Statement on Research Involving Species at Risk of Extinction and the Convention on the Trade in Endangered Species of Wild IUCN Policy Statement on Research Involving Species at Risk of Extinction and the Convention on the Trade in Endangered Species of Wild Fauna and Flora.

All submissions are screened by a similarity detection software (iThenticate by CrossCheck).

In the event of alleged or suspected research misconduct, e.g., plagiarism, citation manipulation, and data falsification/fabrication, the Editorial Board will follow and act in accordance with COPE guidelines.

Each individual listed as an author should fulfil the authorship criteria recommended by the International Committee of Medical Journal Editors (ICMJE - www.icmje.org). The ICMJE recommends that authorship be based on the following 4 criteria:

- 1 Substantial contributions to the conception or design of the work; or the acquisition, analysis, or interpretation of data for the work; AND
- 2 Drafting the work or revising it critically for important intellectual content; AND
- 3 Final approval of the version to be published; AND
- 4 Agreement to be accountable for all aspects of the work in ensuring that questions related to the accuracy or integrity of any part of the work are appropriately investigated and resolved.

In addition to being accountable for the parts of the work he/she has done, an author should be able to identify which co-authors are responsible for specific other parts of the work. In addition, authors should have confidence in the integrity of the contributions of their co-authors.

All those designated as authors should meet all four criteria for authorship, and all who meet the four criteria should be identified as authors. Those who do not meet all four criteria should be acknowledged in the title page of the manuscript.

European Journal of Biology requires corresponding authors to submit a signed and scanned version of the authorship contribution form (available for download through the journal's web page) during the initial submission process in order to act appropriately on authorship rights and to prevent ghost or honorary authorship. If the editorial board suspects a case of "gift authorship," the submission will be rejected without further review. As part of the submission of the manuscript, the corresponding author should also send a short statement declaring that he/she accepts to undertake all the responsibility for authorship during the submission and review stages of the manuscript.

European Journal of Biology requires and encourages the authors and the individuals involved in the evaluation process of submitted manuscripts to disclose any existing or potential conflicts of interests, including financial, consultant, and institutional, that might lead to potential bias or a conflict of interest. Any financial grants or other supports received for a submitted study from individuals or institutions should be disclosed to the Editorial Board. To disclose a potential conflict of interest, the ICMJE Potential Conflict of Interest Disclosure Form should be filled and submitted by all contributing authors. Cases of a potential conflict of interest of the editors, authors, or reviewers are resolved by the journal's Editorial Board within the scope of COPE and ICMJE guidelines.

The Editorial Board of the journal handles all appeal and complaint cases within the scope of COPE guidelines. In such cases, authors should get in direct contact with the editorial office regarding their appeals and complaints. When needed, an ombudsperson may be assigned to resolve cases that cannot be resolved internally. The Editor in Chief is the final authority in the decision-making process for all appeals and complaints.

When submitting a manuscript to European Journal of Biology, authors accept to assign the copyright of their manuscript to Istanbul University Faculty of Science. If rejected for publication, the copyright of the manuscript will be assigned back to the authors. European Journal of Biology requires each submission to be accompanied by a Copyright Transfer Form (available for download at the journal's web page). When using previously published content, including figures, tables, or any other material in both print and electronic formats, authors must obtain permission from the copyright holder. Legal, financial and criminal liabilities in this regard belong to the author(s).

Statements or opinions expressed in the manuscripts published in European Journal of Biology reflect the views of the author(s) and not the opinions of the editors, the editorial board, or the publisher; the editors, the editorial board, and the publisher disclaim any responsibility or liability for such materials. The final responsibility in regard to the published content rests with the authors.

MANUSCRIPT SUBMISSION

European Journal of Biology endorses ICMJE-Recommendations for the Conduct, Reporting, Editing, and Publication of Scholarly Work in Medical Journals (updated in December 2015 - <http://www.icmje.org/icmje-recommendations.pdf>). Authors are required to prepare manuscripts in accordance with the CONSORT guidelines for randomized research studies, STROBE guidelines for observational original research studies, STARD guidelines for studies on diagnostic accuracy, PRISMA guidelines for systematic reviews and meta-analysis, ARRIVE guidelines for experimental animal studies, TREND guidelines for non-randomized public behaviour, and COREQ guidelines for qualitative research.

Manuscripts can only be submitted through the journal's online manuscript submission and evaluation system, available at the journal's web page. Manuscripts submitted via any other medium will not be evaluated.

Manuscripts submitted to the journal will first go through a technical evaluation process where the editorial office staff will ensure that the manuscript has been prepared and submitted in accordance with the journal's guidelines. Submissions that do not conform to the journal's guidelines will be returned to the submitting author with technical correction requests.

During the initial submission, authors are required to submit the following:

- Copyright Transfer Form,
- Author Contributions Form, and

ICMJE Potential Conflict of Interest Disclosure Form (should be filled in by all contributing authors). These forms are available for download at the journal's web page.

Preparation of the Manuscript

Title page: A separate title page should be submitted with all submissions and this page should include:

- The full title of the manuscript as well as a short title (running head) of no more than 50 characters,
- Name(s), affiliations, and highest academic degree(s) of the author(s),
- Grant information and detailed information on the other sources of support,
- Name, address, telephone (including the mobile phone number) and fax numbers, and email address of the corresponding author,
- Acknowledgment of the individuals who contributed to the preparation of the manuscript but who do not fulfil the authorship criteria.

Abstract: Abstract with subheadings should be written as structured abstract in submitted papers except for Review Articles and Letters to the Editor. Please check Table 1 below for word count specifications (250 words).

Keywords: Each submission must be accompanied by a minimum of three to a maximum of six keywords for subject indexing at the end of the abstract. The keywords should be listed in full without abbreviations.

Manuscript Types

Original Articles: This is the most important type of article since it provides new information based on original research. A structured abstract is required with original articles and it should include the following subheadings: Objective, Materials and Methods, Results and Conclusion. The main text of original articles should be structured with Introduction, Materials and Methods, Results, Discussion, and Conclusion subheadings. Please check Table 1 for the limitations of Original Articles.

Statistical analysis to support conclusions is usually necessary. Statistical analyses must be conducted in accordance with international statistical reporting standards. Information on statistical analyses should be provided with a separate subheading under the Materials and Methods section and the statistical software that was used during the process must be specified.

Units should be prepared in accordance with the International System of Units (SI).

Short Communications: Short communication is for a concise, but independent report representing a significant contribution to Biology. Short communication is not intended to publish preliminary results. But if these results are of exceptional interest and are particularly topical and relevant will be considered for publication.

Short Communications should include an abstract and should be structured with the following subheadings: "Introduction", "Materials and Methods", "Results and Discussion".

Editorial Comments: Editorial comments aim to provide a brief critical commentary by reviewers with expertise or with high reputation in the topic of the research article published in the journal. Authors are selected and invited by the journal to provide such comments. Abstract, Keywords, and Tables, Figures, Images, and other media are not included.

Review Articles: Reviews prepared by authors who have extensive knowledge on a particular field and whose scientific background has been translated into a high volume of publications with a high citation potential are welcomed. These authors may even be invited by the journal. Reviews should describe, discuss, and evaluate the current level of knowledge of a topic in clinical practice and should guide future studies. The main text should contain Introduction, Experimental and Clinical Research Consequences, and Conclusion sections. Please check Table 1 for the limitations for Review Articles.

Letters to the Editor: This type of manuscript discusses important parts, overlooked aspects, or lacking parts of a previously published article. Articles on subjects within the scope of the journal that might attract the readers' attention, particularly educative cases, may also be submitted in the form of a "Letter to the Editor." Readers can also present their comments on the published manuscripts in the form of a "Letter to the Editor." Abstract, Keywords, and Tables, Figures, Images, and other media should not be included. The text should be unstructured. The manuscript that is being commented on must be properly cited within this manuscript.

Tables

Tables should be included in the main document, presented after the reference list, and they should be numbered consecutively in the order they are referred to within the main text. A descriptive title must be placed above the tables. Abbreviations used in the tables should be defined below the tables by footnotes (even if they are defined within the main text). Tables should be created using the "insert table" command of the word processing software and they should be arranged clearly to provide easy reading. Data presented in the tables should not be a repetition of the data presented within the main text but should be supporting the main text.

Figures and Figure Legends

Figures, graphics, and photographs should be submitted as separate files (in TIFF or JPEG format) through the submission system. The files should not be embedded in a Word document or the main document. When there are figure subunits, the subunits should not be merged to form a single image. Each subunit should be submitted separately through the submission system. Images should not be labeled (a, b, c, etc.) to indicate figure sub-

Table 1. Limitations for each manuscript type

Type of manuscript	Word limit	Abstract word limit	Reference limit	Table limit	Figure limit
Original Article	4500	250 (Structured)	No limit	6	Maximum 10
Short Communication	2500	200	30	3	4
Review Article	5500	250	No limit	5	6
Letter to the Editor	500	No abstract	5	No tables	No media

nits. Thick and thin arrows, arrowheads, stars, asterisks, and similar marks can be used on the images to support figure legends. Like the rest of the submission, the figures too should be blind. Any information within the images that may indicate an individual or institution should be blinded. The minimum resolution of each submitted figure should be 300 DPI. To prevent delays in the evaluation process, all submitted figures should be clear in resolution and large in size (minimum dimensions: 100 × 100 mm). Figure legends should be listed at the end of the main document.

All acronyms and abbreviations used in the manuscript should be defined at first use, both in the abstract and in the main text. The abbreviation should be provided in parentheses following the definition.

When a drug, chemical, product, hardware, or software program is mentioned within the main text, product information, including the name of the product, the producer of the product, and city and the country of the company (including the state if in USA), should be provided in parentheses in the following format: "Discovery St PET/CT scanner (General Electric, Milwaukee, WI, USA)"

All references, tables, and figures should be referred to within the main text, and they should be numbered consecutively in the order they are referred to within the main text.

Limitations, drawbacks, and the shortcomings of original articles should be mentioned in the Discussion section before the conclusion paragraph.

References

While citing publications, preference should be given to the latest, most up-to-date publications. If an ahead-of-print publication is cited, the DOI number should be provided. Authors are responsible for the accuracy of references. Journal titles should be abbreviated in accordance with the journal abbreviations in Index Medicus/ MEDLINE/PubMed. When there are six or fewer authors, all authors should be listed. If there are seven or more authors, the first six authors should be listed followed by "et al." In the main text of the manuscript, references should be cited using Arabic numbers in parentheses. The reference styles for different types of publications are presented in the following examples.

Journal Article: Rankovic A, Rancic N, Jovanovic M, Ivanović M, Gajo-ović O, Lazić Z, et al. Impact of imaging diagnostics on the budget – Are we spending too much? *Vojnosanit Pregl* 2013; 70: 709-11.

Book Section: Suh KN, Keystone JS. Malaria and babesiosis. Gorbach SL, Barlett JG, Blacklow NR, editors. *Infectious Diseases*. Philadelphia: Lippincott Williams; 2004.p.2290-308.

Books with a Single Author: Sweetman SC. *Martindale the Complete Drug Reference*. 34th ed. London: Pharmaceutical Press; 2005.

Editor(s) as Author: Huizing EH, de Groot JAM, editors. *Functional reconstructive nasal surgery*. Stuttgart-New York: Thieme; 2003.

Conference Proceedings: Bengissson S, Sothemin BG. Enforcement of data protection, privacy and security in medical informatics. In: Lun KC, Degoulet P, Piemme TE, Rienhoff O, editors.

MEDINFO 92. Proceedings of the 7th World Congress on Medical Informatics; 1992 Sept 6-10; Geneva, Switzerland. Amsterdam: North-Holland; 1992. pp.1561-5.

Scientific or Technical Report: Cusick M, Chew EY, Hoogwerf B, Agrón E, Wu L, Lindley A, et al. Early Treatment Diabetic Retinopathy Study Research Group. Risk factors for renal replacement therapy in the Early Treatment Diabetic Retinopathy Study (ETDRS), *Kidney Int*: 2004. Report No: 26.

Thesis: Yılmaz B. Ankara Üniversitesindeki Öğrencilerin Beslenme Durumları, Fiziksel Aktiviteleri ve Beden Kitle İndeksleri Kan Lipidleri Arasındaki İlişkiler. H.Ü. Sağlık Bilimleri Enstitüsü, Doktora Tezi. 2007.

Epub Ahead of Print Articles: Cai L, Yeh BM, Westphalen AC, Roberts JP, Wang ZJ. Adult living donor liver imaging. *Diagn Interv Radiol*. 2016 Feb 24. doi: 10.5152/dir.2016.15323. [Epub ahead of print].

Manuscripts Published in Electronic Format: Morse SS. Factors in the emergence of infectious diseases. *Emerg Infect Dis* (serial online) 1995 Jan-Mar (cited 1996 June 5): 1(1): (24 screens). Available from: URL: [http:// www.cdc.gov/ncidod/EID/cid.htm](http://www.cdc.gov/ncidod/EID/cid.htm).

REVISIONS

When submitting a revised version of a paper, the author must submit a detailed "Response to the reviewers" that states point by point how each issue raised by the reviewers has been covered and where it can be found (each reviewer's comment, followed by the author's reply and line numbers where the changes have been made) as well as an annotated copy of the main document. Revised manuscripts must be submitted within 30 days from the date of the decision letter. If the revised version of the manuscript is not submitted within the allocated time, the revision option may be cancelled. If the submitting author(s) believe that additional time is required, they should request this extension before the initial 30-day period is over.

Accepted manuscripts are copy-edited for grammar, punctuation, and format. Once the publication process of a manuscript is completed, it is published online on the journal's webpage as an ahead-of-print publication before it is included in its scheduled issue. A PDF proof of the accepted manuscript is sent to the corresponding author and their publication approval is requested within 2 days of their receipt of the proof.

Editor in Chief: Prof. Sehnaz BOLKENT

Address: Istanbul University, Faculty of Science, Department of Biology, 34134 Vezneciler, Fatih, Istanbul, TURKEY

Phone: +90 212 4555700 (Ext. 15079)

Fax: +90 212 5280527

E-mail: sbolkent@istanbul.edu.tr

Contents

Research Articles

- 63** **Determination of Oxidative Stress Parameters and Tissue Factor Activity in the Saliva of Patients with Periodontitis**
Sehkar Oktay, Ozge Ozoner, Ebru Emekli Alturfan, Ulku Noyan
- 69** **Karrikinolide Promotes Seed Germination but has no Effect on Leaf Segment Senescence in *Triticum aestivum* L.**
Nihal Goren-Saglam, Kevser Duygun, Gulay Kaya, Filiz Vardar
- 75** **N-Acetylcysteine Improves Acrylamide-Induced Changes in Ovarian Tissue and Serum Levels of Pituitary-Ovarian Axis Hormones in Adult Rats**
Marziyeh Naimi, Mehrdad Shariati, Syrus Naimi, Mohammad Amin Edalatmanesh
- 82** **Acibenzolar-S-Methyl Inhibits MEK1/2 Signaling in SH-SY5Y Neuroblastoma Cells**
Aysegul Yildiz
- 88** **Genetic Diversity of Gazelles (*Gazella marica* and *Gazella gazella*) in Southeast Turkey: A Special Emphasis on Ongoing Conservation Studies of *Gazella marica* in Turkey***
Fikriye Dilan Saatoglu, Melis Denizci Oncu, Hasan Emir, Taner Hatipoglu, Sinan Can Acan, Tolga Kankilic, Inci Togan, Evren Koban Bastanlar
- 103** **First Report on the Occurrence of Invasive Macrophyte *Elodea canadensis* Michx. in Sapanca Lake**
Sezgi Ersoy, Yelda Aktan Turan
- 108** **Karyotypes of Southeastern Turkish Scorpions *Hottentotta saulcyi* and *Buthacus macrocentrus* (Scorpiones: Buthidae)**
Halil Koc, Ersen Aydin Yagmur, Frantisek Šťáhlavský
- 114** **Investigation of Antimicrobial, Antibiofilm, and Cytotoxic Effects of Straight-Chain Sulfanyl Members of Arylamino-1,4-naphthoquinones as Potential Antimicrobial Agents**
Emel Mataraci Kara, Ayse Tarbin Jannuzzi, Nilufer Bayrak, Hatice Yildirim, Mahmut Yildiz, Amac Fatih Tuyun, Buket Alpertunga, Berna Ozbek Celik
- 121** **Antioxidant Effects of Epigallocatechin Gallate in Cerulein-Induced Pancreatitis**
Elif Karacaoglu, Gozde Girgin, Guldeniz Selmanoglu, Terken Baydar
- 129** **Larvicidal Activities of Essential Oils Extracted from Five Algerian Medicinal Plants against *Culiseta longiareolata* Macquart. Larvae (Diptera: Culicidae).**
Ismahane Nabti, Mustapha Bounechada
- 136** **Isolation, Identification and Pathogenicity of *Flavobacterium columnare* SGM4 in Catfish *Clarias batrachus* (Linnaeus 1758)**
Sudeshna Sarker, Thangapalam Jawahar Abraham
- 144** **Effects of Tempol in Lipopolysaccharide-Induced Liver Injury**
Perihan Sinem Serin, Asli Kandil, Huri Bulut, Tugba Kaskavalci, Erman Caner Bulut, Cihan Demirci-Tansel

Review Article

- 153** **CRISPR-Cas: Removing Boundaries of the Nature**
Nicat Cebrailoglu, Ali Burak Yildiz, Ozlem Akkaya, Yelda Ozden Ciftci

Short Communication

- 161** **The Effect of Body Shape Type on Differentiability of Traditional and Geometric Morphometric Methods: A Case Study of *Channa gachua* (Hamilton, 1822)**
Atta Mouludi-Saleh, Soheil Eagderi, Hadi Poorbagher, Shirin Kazemzadeh

Determination of Oxidative Stress Parameters and Tissue Factor Activity in the Saliva of Patients with Periodontitis

Sehkar Oktay¹ , Ozge Ozoner² , Ebru Emekli Alturfan¹ , Ulku Noyan³ 

¹Marmara University, Faculty of Dentistry, Department of Biochemistry, Istanbul, Turkey

²Ataşehir Hospital, Oral and Dental Health Clinics, Istanbul, Turkey

³Acibadem Hospital, Oral and Dental Health Clinics, Istanbul, Turkey

ORCID IDs of the authors: S.O. 0000-0002-2878-288X; O.O. 0000-0001-8103-0700; E.E.A. 0000-0003-2419-8587; U.N. 0000-0002-5489-9758

Please cite this article as: Oktay S, Ozoner O, Emekli Alturfan E, Noyan U. Determination of Oxidative Stress Parameters and Tissue Factor Activity in the Saliva of Patients with Periodontitis. Eur J Biol 2019; 78(2): 63-68.
DOI: 10.26650/EurJBiol.2019.0002

ABSTRACT

Objective: Periodontitis, an inflammatory disease, leads to the destruction of the periodontium and results in tooth loss. Reactive oxygen species are involved in the destruction of periodontal tissues and systemic inflammation. The aim of the study was to evaluate and compare the oxidative status in different kinds of periodontal disease and whether the treatment amends these effects.

Materials and Methods: Whole saliva was collected from 30 patients with chronic marginal gingivitis, chronic periodontitis and generalized aggressive periodontitis at baseline and after non-surgical periodontal therapy and 10 healthy control subjects. Lipid peroxidation (LPO) and glutathione (GSH) levels and glutathione-s-transferase, superoxide dismutase catalase and tissue factor (TF) activities were determined in the whole saliva.

Results: Antioxidant enzyme activities were significantly higher in periodontitis groups before non-surgical periodontal therapy and also increased LPO levels and decreased TF activities were found in these groups. Significant decreases in antioxidant enzymes and LPO levels, and increases in TF activities were detected after treatment. GSH levels increased after treatment.

Conclusion: Increased antioxidant enzyme activities and LPO levels indicate destruction of periodontal tissues due to excessive radical production. Treatment of periodontitis and restoring the balance of oxidant-antioxidants ameliorates tissue damage caused by oxygen species and inflammation.

Keywords: Oxidative stress, periodontitis, saliva

INTRODUCTION

Gingivitis and periodontitis, which are called periodontal diseases are among the most common chronic conditions affecting world's populations (1,2). Periodontal disease is a polymicrobial subgingival inflammatory disease of the periodontal tissues (3). Chronic marginal gingivitis (CMG) is a non-destructive periodontal disease and characterized by inflammation of the gums due to the accumulation of plaque at or near the gingival sulcus (1). Chronic periodontitis (CP)

is a widespread periodontal disease of the oral cavity involving of chronic inflammation of the surrounding and supporting structures of the teeth which is caused by aggregation of plenty of dental plaque (4). Generalized aggressive periodontitis (GAgP) which is characterized by rapid loss of attachment and bone destruction and familial aggregation, is mostly affects younger patients (5).

Periodontitis is a multifactor phenomenon and it has a strong relationship with generation of reactive



Corresponding Author: Sehkar Oktay E-mail: nihal.oktay@marmara.edu.tr

Submitted: 03.04.2019 • **Revision Requested:** 04.04.2019 • **Last Revision Received:** 18.05.2019 • **Accepted:** 24.05.2019

© Copyright 2019 by The Istanbul University Faculty of Science • Available online at <http://ejb.istanbul.edu.tr> • DOI: 10.26650/EurJBiol.2019.0002

oxygen species (ROS) and the destruction of the connective tissues during periodontal disease (6). In all organisms, there is a balance between antioxidants and oxidants. Antioxidants, consisting of enzymatic and non-enzymatic, prevent, limit or intercept oxidative tissue injury caused by ROS. If the balance is disrupted by physical-chemical, environmental or pathological agents, the level of oxidants outweigh the level of antioxidants and the cell will be under oxidative stress (7). During periodontitis, oxidative stress is enhanced as a result of excessive production of ROS and if immune system cannot defend enough, connective tissue and bone damage occurs. This damage leads to the formation of other systemic diseases and spreads to other organs from the mouth (8,9). Thus, early detection and control of periodontal disease is critical for the prevention of diseases that may occur in other organs.

Whole saliva is a mixture of gingival fluids and secretions of the salivary glands. Determination of the saliva components levels reflect the microbial condition and severity of periodontitis (10). Because of saliva's ready availability it is suitable for study. Thus, saliva may be used as a cost effective and noninvasive sample in determination of oxidative stress and analysis for periodontal diagnosis. We therefore evaluated and compared some oxidative stress and coagulation parameters in whole saliva of patients with CMG, CP and GAgP baseline and after non-surgical periodontal therapy.

MATERIALS AND METHODS

Study Groups

The study was approved by the Ethical Committee of Marmara University (No. MAR-YC-2009-0282). Written informed assent was obtained from patients who participated in this study.

A total of 30 adult patients, who referred to Marmara University Faculty of Dentistry, Department of Periodontology and systemically and periodontally healthy 10 person were included in the study. The study groups consisted of: CMG; non-surgical periodontal therapy applied with CMG diagnose, CP; non-surgical periodontal therapy applied with CP diagnose, GAgP; non-surgical periodontal therapy applied with AgP diagnose, Control; periodontally healthy individuals. Then, patient groups were divided into 2 subgroups: Baseline (B), 90th days after the end of the treatment (AT).

The patients in the study groups were otherwise healthy, with no history of systemic disease and consumption of anti-inflammatory or other drugs and antioxidants for at least six months. Subjects having past illness and undergoing any periodontal treatment, pregnant, lactating mothers, alcoholics and smokers were not included the study. Control subjects also had the same criteria and also did not have any history of periodontal disease.

According to research methods, periodontal treatment which includes scaling and root planing (SRP) was applied to the CMG, CP and GAgP patients. Whole saliva samples were taken at baseline and 90th days after the end of the treatment. All

patients were checked once in a month in a 3 months follow up period and if necessary, oral hygiene instructions were repeated and professional dental cleaning was done to the patients.

Clinical Measurements and Periodontal Therapy

The periodontal status of all participants was evaluated by measurement of plaque index (PI) as developed by Löe H and Silness P (11), gingival index (GI) as developed by Silness P and Löe H (12) and pocket depth (PD) and clinical attachment loss (CAL). The periodontal examination of the study was carried out at 4 sites per tooth. PD and CAL were measured on sites of each tooth such as mesial, distal, median points at vestibular and lingual surfaces. All clinical measurements were saved at baseline and 90 days after the end of the initial periodontal therapy in CMG, CP, GAgP groups and one time point in periodontally healthy group after the collection of saliva samples.

Patients with periodontal diseases received the initial periodontal therapy, including scaling and root planing within 14 days and oral hygiene was taught to each one. All patients were checked once in a month in a 3 months follow up period and if necessary, oral hygiene instructions were repeated and professional dental cleaning was done to the patients.

Collection of Samples

Unstimulated whole saliva samples of the groups were collected in the morning following an overnight fast and the collection of the saliva was performed at the same time of the day, as much as possible. The participants were told not to drink or eat that morning before collection of the saliva. The saliva samples of the individuals were gotten in the morning while the patients were seated with the instructions to allow saliva to pool in the bottom of the mouth and drain into a tube for collection. The saliva was aliquoted into storage vials and kept in -20°C until analysis.

Determination of Glutathione

Glutathione (GSH) concentrations of samples were determined by the method of Beutler (13) and the results are expressed in % mg GSH.

Determination of Lipid Peroxidation

Yagi's method was used for determination as thiobarbituric acid reactive substances (14). Results are expressed as nmol malondialdehyde (MDA)/ml.

Determination of Glutathione-S-transferase

Glutathione-S-Transferase (GST) activities of samples are monitored at 340 nm by a spectrophotometer and results were expressed as U GST/ml.min (15).

Determination of Catalase Activity

Catalase (CAT) activities of samples were measured with the Aebi's method (16) and results were expressed as U CAT/ml.min.

Determination of Superoxide Dismutase Activity

Superoxide dismutase (SOD) activities of samples were assayed by the previously described method and results were expressed in U SOD/ml.min (17).

Determination of Tissue Factor Activity

Tissue factor (TF) activities of samples were evaluated according to Quick's method (18). The clotting time is inversely proportional to the TF activity and the lengthed clotting time is a manifestation of decreased TF activity.

Statistical Analysis

All data were presented as mean ±SD. Differences in biochemical parameters between groups were analyzed using the Mann-Whitney U-test and an unpaired two-tailed Student t test was used for comparing two independent groups. Statistical analyses were performed using GraphPad Prism 5.0 (GraphPad Software, San Diego, California, USA).

RESULTS

Enzymatic Biochemical Parameters

The results of salivary GST, SOD and CAT activities are shown in Figure 1.

In salivary GST activity, a significant decrease was observed in the CP-AT group compared with the control group (p<0.05) and

also in the CMG-AT group compared with the CMG-B and CP-AT group compared with the CP-B group (p<0.05).

A significant decrease in salivary SOD activity was detected in the CMG-AT and GAgP-AT groups compared with the control group (p<0.05), additionally in the CMG-AT group compared with the CMG-B and CP-AT group compared with the CP-B (p<0.01, p<0.05, respectively).

In salivary CAT activity, a significant decrease was detected in the CMG-AT, CP-AT and GAgP-AT groups compared with the control group (p<0.05), also in the CMG-AT group compared with the CMG-B, CP-AT group compared with the CP-B and GAgP-AT group compared with the GAgP-B group (p<0.01, p<0.001, p<0.05, respectively).

Nonenzymatic Biochemical Parameters

The results of saliva GSH, lipid peroxidation (LPO) levels and TF activities are shown in Figure 2.

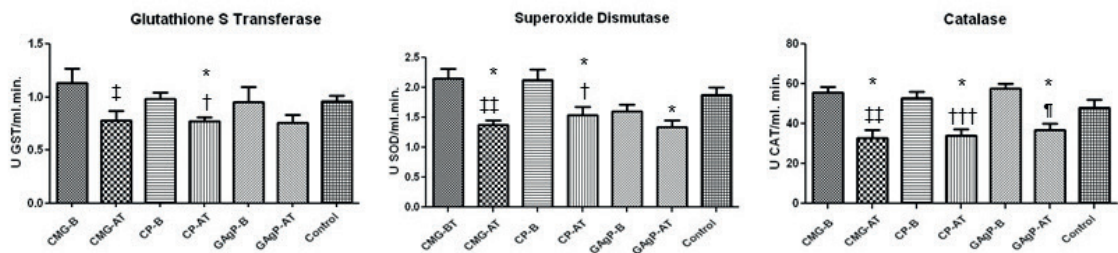


Figure 1. Enzymatic biochemical parameters in saliva. GST: Glutathione-S-Transferase, SOD: Superoxide Dismutase, CAT: Catalase, CMG-AT: Chronic Marginal Gingivitis-After Treatment, CMG-B: Chronic Marginal Gingivitis-Baseline, CP-AT: Chronic Periodontitis-After Treatment, CP-B: Chronic Periodontitis-Baseline, GAgP-AT: Generalized Aggressive Periodontitis-After Treatment, GAgP-B: Generalized Aggressive Periodontitis-Baseline. The bars represent mean ± SD for each group. *p<0.05 vr Control; †p<0.05, ‡p<0.01 vr CMG-B; ††p<0.001, †††p<0.001 vr CP-B; ¶p<0.05 vr GAgP-B.

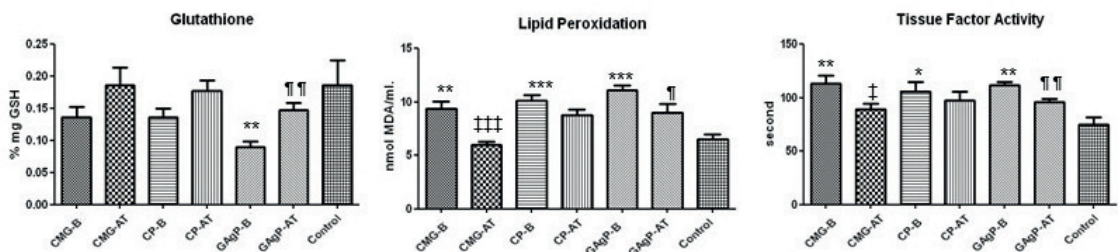


Figure 2. Nonenzymatic biochemical parameters in saliva. GSH: Glutathione, LPO: Lipid Peroxidation, TF: Tissue Factor, CMG-AT: Chronic Marginal Gingivitis-After Treatment, CMG-B: Chronic Marginal Gingivitis-Baseline, CP-AT: Chronic Periodontitis-After Treatment, CP-B: Chronic Periodontitis-Baseline, GAgP-AT: Generalized Aggressive Periodontitis-After Treatment, GAgP-B: Generalized Aggressive Periodontitis-Baseline. Since the clotting time is inversely proportional to the TF activity, the lengthening of the clotting time is a manifestation of decreased TF activity. The bars represent mean ± SD for each group. **p<0.01, ***p<0.001 vr Control; †p<0.05, ‡p<0.01 vr CMG-B; ¶p<0.05, ¶¶p<0.01 vr GAgP-B. In salivary GSH levels, a significant decrease was detected in GAgP-B group compared with the control group (p<0.01), on the other hand a significant increase was detected in GAgP-AT group compared with GAgP-B group (p<0.01).

Significant increases in salivary LPO levels were detected in the CMG-B, CP-B and GAgP-B groups compared with the control group ($p < 0.01$, $p < 0.001$, $p < 0.001$, respectively) while significant decreases were observed in the CMG-AT group compared with the CMG-B and GAgP-AT group compared with the GAgP-B ($p < 0.001$, $p < 0.05$, respectively).

Significant decreases in salivary TF activity were detected in the CMG-B, CP-B and GAgP-B groups compared with the control group ($p < 0.01$, $p < 0.05$, $p < 0.01$ respectively). On the other hand significant increases were observed in the CMG-AT group compared with the CMG-B group and in the GAgP-AT group compared with the GAgP-B group. ($p < 0.05$, $p < 0.01$, respectively).

DISCUSSION

In the present study the results show that the presence of inflammation and excessive production of ROS accelerate tissue damage and actuate coagulation cascade in periodontium. Supporting periodontitis treatment by antioxidants may facilitate these damage and provides to tissue renewing itself faster.

Periodontitis is a common, chronic inflammation disease caused by infection of periodontium with especially gram negative bacteria. The response of the host is generally chronic inflammation and this response has both local and systemic inflammatory symptoms (19).

In many studies it was shown that ROS is the cause of LPO and oxidative stress in the pathogenesis of periodontal disease. As it was demonstrated by various studies that ROS trigger and/or progress of periodontal disease (6,20-22). Free radicals are capable of inducing and increasing destruction of periodontal tissue and are associated with bone resorption, also free radical induced tissue injury increased in individuals with periodontitis (23). Additionally, an increase in free radicals causes overproduction of MDA, is one of the final products of LPO in the cell. Enhanced levels of LPO was reported by previous studies with periodontitis patients (24-28). In accordance to this results, we found increased LPO levels in the CMG-B, CP-B, CP-AT, GAgP-B and GAgP-AT groups compared with the controls and significantly decreased levels of LPO in the CMG and GAgP groups after treatment compared with baseline which means treatment provides protection to cell against cellular damage via the inhibition of LPO.

Glutathione transferases are a family of detoxifying enzymes that have been shown to be over-expressed in tumor tissues and suggested as biomarkers for some specific tissues. However there are a few reports about the level and the presence of these enzymes in human saliva (29). Accordingly there are few studies focused on the activity of GST in periodontitis patients and the results are contradictory. Borges et al. found increased GST activities in periodontitis patients compared with control group while Amarnath et al. found decreased activity of this enzyme (23,30). In the present study, increased GST activities

were determined in periodontitis groups, additionally a decrease was observed in treatment groups. As these enzymes are devoted to cell protection in organism, catalyzing the conjugation reaction to the center of the toxic compounds increased activities in periodontitis groups may be related with the defence mechanism of the organism.

SOD is the antioxidant enzyme which catalyzes dismutation of superoxide radicals to hydrogen peroxide. It has an important function to remove ROS from the cellular environment and avoid the cell from damaging effect of ROS. Previous studies have found increased SOD activities in periodontitis patients before treatment that support our results (21,28,30-33). CAT is also an antioxidant enzyme of the defence system in organisms and helps to detoxify hydrogen peroxide. Increased levels of CAT activities were found in previous studies in periodontitis patients in accordance with our results (21,25,28,30).

The antioxidant enzymes are protective molecules of organism which prevent ROS and they play an important role in periodontal disease by providing protection against oxidative stress. Excessive production of free radicals trigger immune system and activate antioxidant enzymes. For that reason, increased activities of GST, SOD, CAT may be a defense system of saliva against destructivity of radicals in periodontal tissues. Increased levels of GST may indicate the oxidative damage in cell and increased superoxide radicals via bacterial inflammation may induce an increase in SOD production in cell. Also, increased CAT activity in periodontitis patients may be attributed to elevated oxidative damage via ROS.

Reduced form of GSH, is a nonenzymatic antioxidant, has many functions including the removing hydroperoxides and detoxification of membranes. Similar to GST, there are limited studies about GSH in periodontitis and the results are conflicting. Panjamurthy et al. found decreased levels of GSH levels in plasma but increased levels in gingival tissue in periodontitis patients (21). Also Tsai et al. found decreased levels of GSH levels in their study which supports our result (26). This findings may suggest that immune system needs large amount of GSH for protection the periodontal tissues and GSH is consumed during inflammatory defense.

Due to the inflammation caused by periodontal pathogens, inflammatory and endothelial cells get activated and by the beginning of the inflammatory response, onset and progression of atherosclerosis is induced (34). TF is the key initiator of the coagulation cascade and has a crucial role in thrombosis. TF initiates coagulation and thrombus formation following to injury of vessel wall by a reason. Previous studies have demonstrated that periodontitis patients have tendency to atherosclerotic complications (35-37). In the present study, we found decreased activity of TF in periodontitis patients which means there is a tendency to bleeding and after treatment, an increase was observed in TF activity. Periodontal pathogens may cause defects in coagulation mechanism by progression of inflammation and damage to the veins.

CONCLUSION

In this study, we support the fact that patients with periodontitis have a tendency towards the destruction of periodontal tissues due to excessive free radical production. The severity of periodontitis may effect the immune response and the consumption of antioxidants. Thus, selection of a periodontal treatment which supports antioxidant system may be effective in preventing of other inflammatory diseases. Increased levels of radicals during periodontitis makes the organism unprotective, and therefore, an additional antioxidant treatment may be useful during periodontal treatment. Also based on the results from our study, saliva analysis to determine oxidant-antioxidant parameters in inflammatory oral diseases may be suggested as an alternative to other invasive methods.

Periodontal diseases have been recently re-classified and some descriptions to define the diseases have been changed according to the new classification report (38). But due to the present study started before the publications of these report, the descriptions were not changed.

The limited number of patients in this study may impair the validity of results. Further studies need to be conducted with large study population.

Peer-review: Externally peer-reviewed.

Author Contributions: Conception/Design of study: S.O., O.O.; Data Acquisition: S.O., O.O.; Data Analysis/Interpretation: S.O., E.E.A., U.N.; Final Approval and Accountability: S.O., O.O., E.E.A., U.N.; Drafting Manuscript: S.O., E.E.A., O.O.; Critical Revision of Manuscript: U.N., E.E.A.; Technical or Material Support: S.O., E.E.A., O.O., U.N.; Supervision: S.O., E.E.A.

Conflict of Interest: The authors declare that they have no conflicts of interest.

Financial Disclosure: There are no funders to report for this submission

Acknowledgements: No conflicts of interest related to this study.

REFERENCES

1. Ridgeway EE. Periodontal disease: diagnosis and management. *J Am Acad Nurse Pract* 2000; 12: 79-83.
2. Silva N, Abusleme L, Bravo D, Dutzan N, Garcia-Sesnich J, Vernal R, et al. Host response mechanisms in periodontal diseases. *J Appl Oral Sci* 2015; 23(3):329-55.
3. Armitage GC. Development of a classification system for periodontal diseases and conditions. *Ann Periodontol* 1999; 4(1): 1-6.
4. Lamont RJ, Hajishengallis G. Polymicrobial synergy and dysbiosis in inflammatory disease. *Trends Mol Med* 2015; 21(3): 172-83.
5. Liu G, Luan Q, Chen F, Chen Z, Zhang Q, Yu X. Shift in the subgingival microbiome following scaling and root planing in generalized aggressive periodontitis. *J Clin Periodontol* 2018; 45(4): 440-52.
6. Waddington RJ, Moseley R, Embery G. Reactive oxygen species: A potential role in the pathogenesis of periodontal diseases. *Oral Dis* 2000; 6: 138-51.
7. Piedrafita G, Keller M A, Ralser M. The impact of non-enzymatic reactions and enzyme promiscuity on cellular metabolism during (oxidative) stress conditions. *Biomolecules* 2015; 5(3): 2101-122.
8. Sculley DV, Langley-Evans SC. Periodontal disease is associated with lower antioxidant capacity in whole saliva and evidence of increased protein oxidation. *Clin Sci (Lond)* 2003; 105: 167-72.
9. Spiekerman CF, Hujoel PP, DeRouen TA. Bias induced by self-reported smoking on periodontitis-systemic disease associations. *J Dent Res* 2003;82(5) : 345-49.
10. Kuboniwa M, Sakanaka A, Hashino E, Bamba T, Fukusaki E, Amano A. Prediction of periodontal inflammation via metabolic profiling of saliva. *J Dent Res* 2016; 95(12): 1381-86.
11. Løe H. and Silness J. Periodontal disease in pregnancy. Prevalance and severity. *Acta Odontol Scand* 1963; 21(6): 533-55.
12. Silnes J and Løe H. Periodontal disease in pregnancy II. Correlation between oral hygiene and periodontal condition. *Acta Odontol Scand* 1964; 22(1): 121-35.
13. Beutler E. Glutathione: red cell metabolism. A manual biochemical methods 1975; pp. 72-136, Grune and Stratton, New York.
14. Yagi K. Assay for blood plasma or serum. *Methods Enzymol* 1984; 105: 328-37.
15. Habig WH, Jacopy WB. Assays for differentiation of glutathione-S-transferases. *Method Enzymol* 1981; 77: 398-405.
16. Aebi H. Catalase in vitro. In (Ed. Bergmeyer HU) *Methods of enzymatic analysis* 1974; pp. 673-7, New York.
17. Mylroie AA, Collins H, Umbles C, Kyle J. Erythrocyte superoxide dismutase activity and other parameters of copper status in rats ingesting lead acetate. *Toxicol Appl Pharmacol* 1986; 82: 512-20.
18. Ingram GIC, Hills M. Reference method for the one stage prothrombin time test on human blood. *Thromb Haemostas* 1976; 36: 237-38.
19. Dave S, Balista EL Jr, Thomas E, Van D. Cardiovascular disease and periodontal disease: commonality and causation. *Compendium* 2004; 25(7): 26-37.
20. D' Aiuto F, Nibali L, Parkar M, Patel K, Suvan J, Donos N. Oxidative stress, systemic inflammation, and severe periodontitis. *J Dent Res* 2010; 89: 1241-46.
21. Panjamurthy K, Manoharan S, Ramachandran CR. Lipid peroxidation and antioxidant status in patients with periodontitis. *Cell Mol Biol Lett* 2005; 10: 255-64.
22. Patel SP, Pradeep AR, Chowdhry S. Crevicular fluid levels of plasma glutathione peroxidase (eGPx) in periodontal health and disease. *Arch Oral Biol* 2009; 54: 543-48.
23. Amarnath K, Nellore J. Antioxidant potential of phytonanoparticles in an emerging biofluid (saliva) of periodontitis patients. In *Nanoscience, Engineering and Technology (ICONSET), 2011 International Conference, 2011*; pp. 401-407. IEEE.
24. Akalin FA, Baltacioglu E, Alver A, Karabulut E. Lipid peroxidation levels and total oxidant status in serum, saliva and gingival crevicular fluid in patients with chronic periodontitis. *J Clin Periodontol* 2007; 34: 558-65.
25. Yagan A, Kesim S, Liman N. Effect of low-dose doxycycline on serum oxidative status, gingival antioxidant levels and alveolar bone loss in experimental periodontitis in rats. *J Periodontol* 2014; 85(3): 478-89.
26. Tsai CC, Chen HS, Chen SL, Ho YP, Ho KY, Wu YM, et al. Lipid peroxidation: a possible role in the induction and progression of chronic periodontitis. *J Periodontal Res* 2005; 40(5): 378-84.
27. Tonguc MO, Ozturk O, Sutcu R, Ceyhan BM, Kilinc G, Sonmez Y, et al. The impact of smoking status on antioxidant enzyme activity and malondialdehyde levels in chronic periodontitis. *J Periodontol* 2011; 82(9): 1320-28.

28. Oktay S, Chukkapalli SS, Rivera-Kweh MF, Velsko IM, Holliday LS, Kesavalu L. Periodontitis in rats induces systemic oxidative stress that is controlled by bone-targeted antirosorptives. *J Periodontol* 2015; 86(1): 137-45.
29. Fabrini R, Bocedi A, Camerini S, Fusetti M, Ottaviani F, Passali FM et al. Inactivation of human salivary glutathione transferase p1-1 by hypothiocyanite: A post-translational control system in search of a role. Ed. Fernando Rodrigues-Lima. *PLoS ONE* 2014; 9(11): e112797.
30. Borges I, Moreira EAM, Filho DW, Tiago Oliveira TB, Silva MBS, Frode TS. Proinflammatory and oxidative stress markers in patients with periodontal disease. *Mediators Inflamm* 2007; 2007: 1-5.
31. Akalin FA, Toklu E, Renda N. Analysis of superoxide dismutase activity levels in gingiva and gingival crevicular fluid in patients with chronic periodontitis and periodontally healthy controls. *J Clin Periodontol* 2005; 32:238-43.
32. Wei D, Zhang X-L, Wang Y-Z, Yang C-X, Chen G. Lipid peroxidation levels, total oxidant status and superoxide dismutase in serum, saliva and gingival crevicular fluid in chronic periodontitis patients before and after periodontal therapy. *Australian Dent J* 2010; 55: 70-8.
33. Aziz AS, Kalekar MG, Benjamin T, Suryakar AN, Prakashan MM. Effect of nonsurgical periodontal therapy on some oxidative stress markers in patients with chronic periodontitis: A biochemical study. *World J Dent* 2013; 4: 17-23.
34. Roth GA, Moser B, Roth-Walter E, GiacoDa MD, Harja E, Papapanou PN, et al. Infection with a periodontal pathogen increases mononuclear cell adhesion to human aortic endothelial cells. *Atherosclerosis* 2007; 190: 271-81.
35. Buhlin K, Gustafsson A, Hakansson J, Klinge B. Oral health and cardiovascular disease in Sweden. *J Clin Periodontol* 2002; 29: 254-59.
36. Arbes SJ, Slade GD, Beck JD. Association between extent of periodontal attachment loss and self-reported history of heart attack: an analysis of NHANES III data. *J Dent Res* 1999; 78: 1777-82.
37. Emekli Alturfan E, Basar I, Malali E, Elemek E, Oktay S, Ayan F, et al. Plasma tissue factor levels and salivary tissue factor activities of periodontitis patients with and without cardiovascular disease. *Pathophysiol Haemost Thromb* 2010; 37(2-4): 77-81.
38. Caton JG, Armitage G, Berglundh T, Chapple IL, Jepsen S, Kornman KS, Sanz M, Tonetti MS, Mealey BL, Papapanou PN, Sa Tonetti MS. A new classification scheme for periodontal and peri-implant diseases and conditions—Introduction and key changes from the 1999 classification. *J Periodontol* 2018; 89: 1-8.

Karrikinolide Promotes Seed Germination but has no Effect on Leaf Segment Senescence in *Triticum aestivum* L.

Nihal Goren-Saglam¹ , Kevser Duygun¹ , Gulay Kaya² , Filiz Vardar³ 

¹Istanbul University, Faculty of Science, Department of Biology, Istanbul, Turkey

²Recep Tayyip Erdogan University, Faculty of Arts and Sciences, Department of Biology, Rize, Turkey

³Marmara University, Faculty of Arts and Science, Department of Biology, Istanbul, Turkey

ORCID IDs of the authors: N.G.S. 0000-0003-1255-5188; K.D. 0000-0002-4582-3911; G.K. 0000-0002-4899-1494; F.V. 0000-0002-1051-5628

Please cite this article as: Goren Saglam N, Duygun K, Kaya G, Vardar F. Karrikinolide Promotes Seed Germination but has no Effect on Leaf Segment Senescence in *Triticum aestivum* L. Eur J Biol 2019; 78(2): 69-74. DOI: 10.26650/EurJBiol.2019.0005

ABSTRACT

Objective: Germination and senescence are the two most important developmental processes in the plant life cycle. While seed germination is an important physiological event for the continuity of species, leaf senescence is also an important developmental process that impacts crop yields. Karrikins are a group of plant growth regulators found in the smoke generated by burning plant material. It has been suggested that karrikinolide (KAR₁) is generally the most active karrikin in terms of stimulating germination.

Materials and Methods: In this study, the effect of karrikinolide on germination and leaf segment senescence in wheat was investigated. For this purpose, control, 1 nM, 0.01, 0.1, 1, and 10 μ M KAR₁ solutions were used. Firstly, the wheat seeds were germinated in the dark in these solutions and germination percentages and root lengths were measured. Secondly, 4 of first leaf segments (3cm. each) from 10-day-old wheat seedlings were placed in petri dishes containing 1, 10, 100 μ M KAR₁ and distilled water as a control. Following incubation, fresh weight, chlorophyll content, cell death amounts and total protein amounts were determined.

Results: The obtained data shows that 1 μ M KAR₁ promotes germination and root length to the greatest extent. This suggests that karrikins have a promoting effect on the germination of wheat seeds. Our results demonstrate that KAR₁ has no effect on leaf segment senescence.

Conclusion: Our study suggests that KAR₁ has the potential to be used in agriculture to improve germination and seedling growth of crop species.

Keywords: Seed germination, leaf senescence, KAR₁, *Triticum aestivum*

INTRODUCTION

Germination and senescence are the two most important developmental events in plant life. While the life cycle of plants begins with seed germination in higher plants, senescence is the last phase of the plant life cycle. Seed germination is an important physiological event for the continuity of species. Internal and external conditions must be suitable for seed germination. Germination is controlled by external environmental factors and internal factors such as plant growth regulators (1,2). Gibberellic acid (GA) and

abscisic acid (ABA) are well-known plant hormones that have an important role in the regulation of dormancy and germination (3-5). In addition, plant-derived smoke has been shown to promote the germination of numerous plant species with different life histories (6-8). These findings led to the discovery of compounds found in smoke (e.g. karrikins and glyceronitrile) that are responsible for the stimulation of germination (6,9). Researchers have found that karrikinolide (KAR₁) is the most abundant and active karrikin in smoke and that enhances germination and seedling growth in many plants even at very low concentrations (7,8,10-12).



Corresponding Author: Nihal Goren Saglam E-mail: goren@istanbul.edu.tr

Submitted: 11.04.2019 • **Revision Requested:** 28.04.2019 • **Last Revision Received:** 17.07.2019 • **Accepted:** 18.07.2019

© Copyright 2019 by The Istanbul University Faculty of Science • Available online at <http://ejb.istanbul.edu.tr> • DOI: 10.26650/EurJBiol.2019.0005

Leaf senescence is an important developmental stage affected by various internal and external factors, such as leaf age, hormone levels, exposure to darkness, and environmental stresses (13,14). Hormones are internal components that mediate the regulatory effects of environmental factors on leaf senescence. While some hormones such as ethylene, ABA, jasmonic acid (JA) and salicylic acid (SA) stimulate senescence, cytokinins and gibberellins play an important role in delaying senescence (15-19). In addition to these hormones, strigolactones (SLs) appear to be a class of plant hormones that regulate leaf senescence, because SL-deficient and SL-insensitive mutants show a phenotype with delayed leaf senescence (14). Karrikins and strigolactones have a butenolide ring in their structure. Even though both molecules have highly similar signaling mechanisms, it has been suggested that they have different effects on plant growth (20).

In literature, there has been no study showing the effect of karrikins on senescence so far. Our study is thus the first attempt to show the effect of KAR₁ on leaf segment senescence in wheat. For this reason, the aims of the current study were to investigate the effects of KAR₁ on seed germination and leaf segment senescence in wheat.

MATERIALS AND METHODS

Plant Material, Growth Conditions & Hormone Treatments

For the germination experiments, wheat (*Triticum aestivum* L.) seeds were sterilized with 10% commercial bleach and washed 5 times with sterile distilled water. Five replicates of 100 seeds each were placed in Petri dishes containing filter paper imbibed in a solution of KAR₁ (1 nM, 0.01, 0.1, 1, 10 μ M) and distilled water as a control and kept in darkness at 25 °C. The wheat seeds were germinated in the dark in these solutions and germination percentages and root lengths were measured.

For the leaf segment senescence experiments, wheat seeds were planted in moisturized perlite after surface sterilization with 10% commercial bleach and washed 5 times with sterile distilled water. They were grown in a growth chamber (16 h light, 8 h dark photoperiod and at 25 \pm 2 °C). Four of the first leaf segments (3 cm. each) from 10-day-old wheat seedlings were placed in 5 cm diameter petri dishes containing 4 mL of KAR₁ solutions (1, 10, 100 μ M). Distilled water was used as a control.

Fresh Weight Analysis for Senescence

After the harvest, the segments of wheat were weighed and placed in 1, 10 and 100 μ M KAR₁ solutions. After 10 days, the segments were weighed and the fresh weight change was calculated. It was analysed with 10 replicate tissue samples of 4 bulked leaf segments.

Analysis of Pigment Content for Senescence

The pigments were extracted by grinding the wheat segments in 90% ice-cold acetone with a pestle and mortar and added to a 15 mL tube. The samples were stored at 4 °C in the dark overnight. They were spun at 3000 g for 10 min

at 4 °C in a centrifuge and the supernatant was collected in a new tube. The total chlorophyll content was determined spectrophotometrically (Shimadzu 1601) (21). It was analysed with 10 replicate tissue samples of 4 bulked leaf segments.

Measurement of Cell Death for Senescence

Cell death was measured spectrophotometrically using Evans blue to stain the detached leaves (22). The detached leaves were submerged in a 0.1% (w/v) aqueous solution of Evans blue dye (Sigma-Aldrich). They were subjected to two 5-min cycles of vacuum followed by 30 min under vacuum. The leaves were then washed three times with distilled water (15 min each). The dye bound to dead cells was solubilized in 50% (v/v) methanol and 1% (w/v) SDS at 60 °C for 30 min and then quantified by absorbance at 600 nm. For 100% cell death, the detached leaves were heated at 100 °C for 5 min before staining. Four leaves were pooled for each sample. Ten samples were analysed and this experiment was repeated three times with equivalent results.

Analysis of Protein Content for Senescence

The segment samples were homogenized with an ice-cold 0.1 mmol/L sodium phosphate buffer (pH 7.0). The homogenates were centrifuged at 13000 rpm for 30 min at 4 °C and the supernatants were used to determine the total soluble protein content. The protein content of the extracts was determined according to Bradford (1976), using bovine serum albumin as a standard (23). It was analyzed with 10 replicate tissue samples of 4 bulked leaf segments.

Statistical Analysis

Each treatment was analysed with 10 replicate root and segment samples. The data presented here is the mean values \pm SE (n=10). All data was evaluated using one-way ANOVA followed by Dunnett's multiple comparison tests using Graph Pad PRISM software. * p < 0.05 was considered significant, p > 0.05 was considered not significant.

RESULTS

KAR₁ has a Stimulating Effect on the Germination and Root Growth of Wheat Seeds

To investigate the effect of different concentrations of KAR₁ on wheat seed germination we calculated the germination percentage. Our results showed that KAR₁ increased the germination percentage even at 1nM concentration (p < 0.05). However, 1 μ M KAR₁ was found to be the most effective concentration with 100% germination percentage. It increased the germination by 1.3 times compared to the control (Figure 1). When the root length data was examined, it was seen that the root length compared to the control increased in all concentrations and the most effective concentration was found to be 1 μ M KAR₁ (p < 0.05) (Figure 2). It was found 2.2 times higher compared to the control at 72th hours. Our data indicated that KAR₁ promotes seed germination and increases root length even at lower concentrations (1 nM KAR₁).

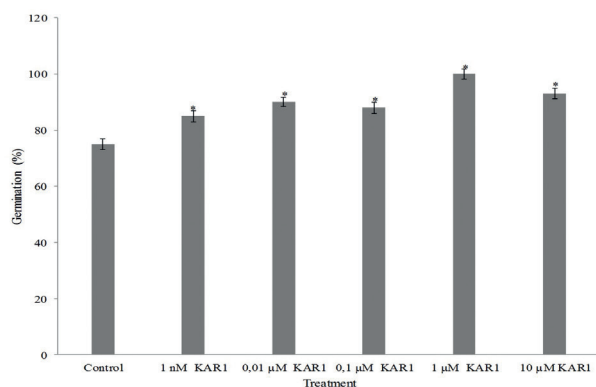


Figure 1. Comparisons of germination (%) after incubation in distilled water (control), 1 nM, 0.01, 0.1, 1 and 10 μM KAR₁ solutions. Values are means± S.E (n=10). (*p < 0.05; compared to control)

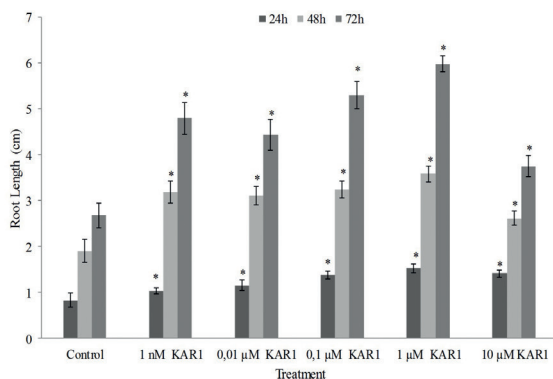


Figure 2. Comparisons of root length (cm) after 24h, 48h and 72h after incubation in distilled water (control), 1 nM, 0.01, 0.1, 1 and 10 μM KAR₁ solutions. Values are means± S.E (n=10). (*p < 0.05; compared to control)

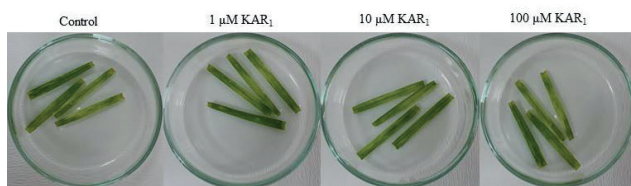


Figure 3. Wheat leaf segments after incubation in distilled water (control), 1, 10 and 100 μM KAR₁ solutions, respectively.

KAR₁ does not Show Any Promoting or Inhibitory Effect on Leaf Senescence

There are no studies showing the relationship between KAR₁ and leaf senescence. We designed this research to investigate the effect of KAR₁ on leaf segment senescence in wheat. The leaf segments were incubated in 1, 10 and 100 μM KAR₁ solutions and distilled water (as a control). We found that there was no significant change between the control and treatment groups (Figure 3). The amounts of fresh weight observed in wheat

segments soaked in 100, 10 and 1 μM KAR₁ solutions are given in Figure 4. Fresh weight was calculated by subtracting the final weights of the segments recorded after being soaked in KAR₁ solutions from their initial weights recorded before being soaked in KAR₁ solutions. It was determined that exposure to the control or KAR₁ treatments did not make a lot of difference ($p > 0.05$) (Figure 4).

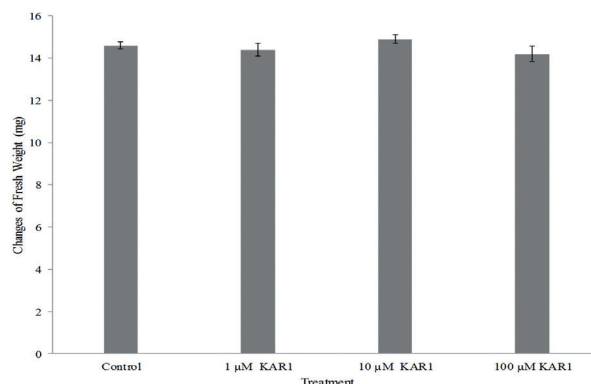


Figure 4. Comparisons of fresh weight after incubation in distilled water (control), 1, 10 and 100 μM KAR₁ solutions. Values are means± S.E (n=10). ($p > 0.05$; compared to control)

A loss of chlorophyll is the first visible symptom of leaf senescence. We measured the chlorophyll content and did not find a significant change ($p > 0.05$) (Figure 5). Cell death was indicated by a loss of plasma membrane integrity. An examination of cell viability showed that cell death was not significantly altered in the treatment group, as measured by Evans blue staining. Evans blue measures cell death for an entire leaf. Our results showed that different concentrations of KAR₁ had no effect on cell death amounts when compared to the control ($p > 0.05$) (Figure 6). Another senescence parameter is total protein amount. The amounts of total protein observed

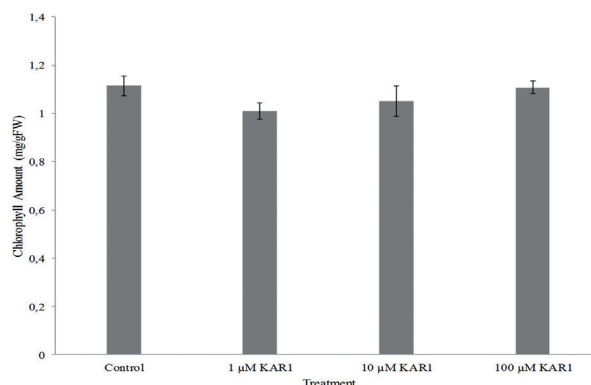


Figure 5. Effects of 1, 10 and 100 μM KAR₁ treatments on chlorophyll content in wheat leaf segments. Values are means± S.E (n=10). ($p > 0.05$; compared to control)

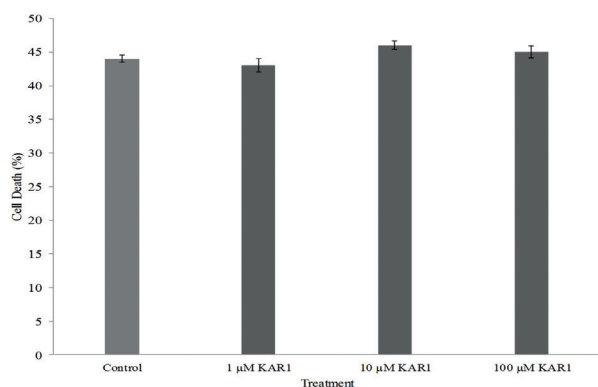


Figure 6. Effects of 1, 10 and 100 μM KAR1 treatments on cell death amount. Values are means± S.E (n=10). ($p > 0.05$; compared to control)

in wheat segments soaked in 100, 10 and 1 μM KAR₁ solutions are given in Figure 7. Our results showed that different concentrations of KAR₁ had no effect on total protein amount when compared to the control ($p > 0.05$) (Figure 7).

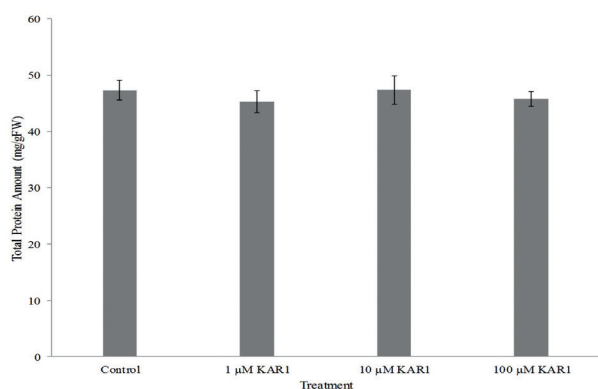


Figure 7. Effects of 1, 10 and 100 μM KAR1 treatments on total protein amount. Values are means± S.E (n=10). ($p > 0.05$; compared to control)

DISCUSSION

Seed germination and leaf senescence are important developmental processes that are affected by external and internal factors. Many plant hormones regulate seed germination and the initiation of leaf senescence. In recent years researchers have discovered new plant growth regulators such as karrikins. The discovery of karrikins is extremely important because of their potential usage in agriculture and horticulture. KAR₁ was discovered in 2004 (6) and following this discovery, studies on the karrikins have always been on the effect of seed germination and seedling growth (11,24-28). When the previous studies are examined, it is seen that there are no studies concerning the effect of KAR₁ on the germination of wheat seeds and on leaf senescence.

Global warming is causing a reduction in the productivity and survival of plants - including crops (29). It also adversely affects seed germination. Due to the role of wheat in nutrition, promoting the germination of wheat seeds is very important for yielding more crops from cultivated areas. For these reasons, it is important to identify new substances that will promote seed germination and to investigate their effectiveness. There is limited information on the effect of KAR₁ on germination in wheat seeds. To investigate the effect of KAR₁ on the germination of wheat seeds, we used different concentrations of KAR₁, ranging from 1 nm to 10 μM. Researchers found that 10 nm KAR₁ was an effective concentration for germination of lettuce seeds (26, 30). Our results showed that 1 μM KAR₁ was an effective concentration for wheat seeds. 1 μM KAR₁ accelerated both seed germination and root length. Our results indicate that KAR₁ is effective in stimulating root growth as previously suggested (31).

Senescence is a developmental process that results in the death of a cell, organ or organism. Considering the remobilisation and recycling of important nutrients such as nitrogen, sulphur, phosphorus and potassium, we can clearly see the vital importance of senescence in the plant life cycle. These nutrients are remobilised from the senescing leaves to the actively growing tissues, thus providing for the growth and reproduction of the plant (32,33). The photosynthetic capacity of the leaf suddenly drops due to the loss of chlorophyll during senescence. The production of carbohydrates, amino acids and other molecules is displaced by the degradation of macromolecules such as protein, lipids and nucleic acids (DNA and RNA), and the released nutrients are mobilised to plant parts such as new buds, young leaves, developing fruits and seeds or to storage organs for the future growing season (34,35).

Initiation of leaf senescence is affected by various factors including age, abiotic and biotic stress, and plant hormones (36,37). Effects of plant hormones on senescence such as auxin, cytokinin, gibberellin, ethylene ABA, SA and JA are well-known (29,35,36). Moreover, the effect of KAR₁ on leaf senescence is still lacking in the literature. To test the effect of KAR₁ on wheat leaf segment senescence, different concentrations of KAR₁ from 1 to 100 μM were used. We measured important leaf senescence parameters such as, chlorophyll amount, fresh weight changes, cell death amount and total protein amount.

Changes in fresh weight are one indication of leaf senescence because nutrients remobilise from senescing leaves to storage organs during senescence (38,39). The fresh weight tends to decrease when leaf senescence starts. Our data showed that there were no significant changes between the control and treatment groups (Figure 4). The dramatic metabolic transition from anabolism to catabolism, including the increased hydrolysis of macromolecules occurs during leaf senescence (38). Leaf cells are subject to structural and biochemical changes during senescence (40-44). Because of this, the changes of fresh weight are an important parameter for leaf senescence.

Another important leaf senescence indicator is a decreased chlorophyll amount. During leaf senescence, the death of the photosynthesizing tissues occurs and this results in chlorophyll catabolism (42-44). A yellowing of the leaves is the most obvious phenotypic change in leaf senescence (45). It is caused by the dismantling of the pigment-protein complexes of chloroplasts and a degradation of the constituent chlorophyll (46). We measured the chlorophyll amounts and did not see any significant changes compared to the control (Figure 5).

Membrane integrity is crucial to cell viability. High levels of membrane integrity loss are clear symptoms of cell death (47, 48). The percentage of death cells is an important parameter for leaf senescence. In parallel with our results, we did not detect any changes in cell death amounts compared to the control groups (Figure 6). Our results related to leaf senescence show that KAR₁ does not have any effect on leaf segment senescence in the 1-100 µM concentration range.

Biochemically, senescence is characterized by the degradation of macro-molecules, such as chlorophylls, proteins, membrane lipids and RNA, and metabolically these events replace carbon assimilation (49). In our study we found no changes in protein content following the KAR₁ application (Figure 7).

CONCLUSION

In the light of this data, this study suggests that KAR₁ promotes seed germination even at 1 nM in wheat. Our results indicate that 1 µM KAR₁ is more effective for promoting seed germination in wheat seeds. However, neither a stimulatory nor inhibitory effect of KAR₁ on the leaf segment senescence in wheat leaves was observed.

Peer-review: Externally peer-reviewed.

Author Contributions: Conception/Design of study: N.G.S., F.V.; Data Acquisition: N.G.S.; Data Analysis/Interpretation: N.G.S., K.D., G.K.; Final Approval and Accountability: N.G.S., K.G., G.K., F.V.; Drafting Manuscript: N.G.S.; Critical Revision of Manuscript: N.G.S.; Technical or Material Support: N.G.S., K.G., G.K., F.V.

Conflict of Interest: The authors declare that they have no conflicts of interest.

Financial Disclosure: There are no funders to report for this submission

Acknowledgements: The authors would like to thank to Dr. Gavin R. Flametti (University of Western Australia) for gifting the Karrikinolide.

REFERENCES

1. Yuan K, Wysocka-Diller J. Phytohormone signalling pathways interact with sugars during seed germination and seedling development. *J Exp Bot* 2006; 57(12):3359-67.
2. Merai, Z, Graeber K, Wilhelmsson P, Ullrich KK, Arshad W, Grosche C et al., A novel model plant to study the light control of seed germination. *J Exp Bot* 2019; erz146, doi:10.1093/jxb/erz146
3. Koornneef M, Bentsink L, Hilhorst H. Seed dormancy and germination. *Curr Opin Plant Biol* 2002; 5(1):33-6.
4. Penfield S. Seed dormancy and germination. *Curr Biol* 2017; 27(17):R874-78.
5. Kępczyński J. Induction of agricultural weed seed germination by smoke and smoke-derived karrikin (KAR 1), with a particular reference to *Avena fatua* L. *Acta Physiol Plant* 2018; 40(5):87-97.
6. Flematti GR, Ghisalberti EL, Dixon KW, Trengove RD. A compound from smoke that promotes seed germination. *Science* 2004; 305(5686):977-77.
7. Light ME, Daws MI, Van Staden J. Smoke-derived butenolide: towards understanding its biological effects. *S Afr J Bot* 2009; 75(1):1-7.
8. Flematti GR, Dixon KW, Smith SM. What are karrikins and how were they 'discovered' by plants? *BMC Biol* 2015; 13(1):108-12.
9. Flematti GR, Merritt DJ, Piggott MJ, Trengove RD, Smith SM, Dixon KW, Ghisalberti EL. Burning vegetation produces cyanohydrins that liberate cyanide and stimulate seed germination. *Nat Commun* 2011; 2:360. doi: 10.1038/ncomms1356
10. Nelson DC, Flematti GR, Ghisalberti EL, Dixon KW, Smith SM. Regulation of seed germination and seedling growth by chemical signals from burning vegetation. *Annu Rev Plant Biol* 2012; 63:107-30.
11. Reynolds CJ, Long RL, Flematti GR, Cherry H, Turner SR. Karrikins promote germination of physiologically dormant seeds of *C. hrysanthemoides monilifera* ssp. *monilifera* (boneseed). *Weed Res* 2014; 54(1):48-57.
12. Waters MT. From little things big things grow: karrikins and new directions in plant development. *Func Plant Biol* 2017; 44(4):373-85.
13. Sharabi-Schwager M, Samach A, Porat R. Overexpression of the CBF2 transcriptional activator in *Arabidopsis* counteracts hormone activation of leaf senescence. *Plant Signaling Behav* 2010; 5(3):296-99.
14. Yamada Y, Furusawa S, Nagasaka S, Shimomura K, Yamaguchi S, Umehara M. Strigolactone signaling regulates rice leaf senescence in response to a phosphate deficiency. *Planta* 2014; 240(2):399-408
15. Morris K, Mackerness SAH, Page T, John CF, Murphy AM, Carr JP, Buchanan-Wollaston V. Salicylic acid has a role in regulating gene expression during leaf senescence. *The Plant J* 2000; 23(5):677-85.
16. He Y, Fukushige H, Hildebrand DF, Gan S. Evidence supporting a role of jasmonic acid in *Arabidopsis* leaf senescence. *Plant Physiol* 2002; 128(3):876-84.
17. Lim PO, Nam HG. Aging and senescence of the leaf organ. *J Plant Biol* 2007; 50(3):291-300.
18. Jibrán R, Hunter DA, Dijkwel PP. Hormonal regulation of leaf senescence through integration of developmental and stress signals. *Plant Mol Biol* 2013; 82(6):547-61.
19. Yamada Y, Umehara M. Possible roles of strigolactones during leaf senescence. *Plants* 2015; 4(3):664-77.
20. Morffy N, Faure L, Nelson DC. Smoke and hormone mirrors: action and evolution of karrikin and strigolactone signaling. *Trends Genet* 2016; 32(3):176-88.
21. Parsons TR, Strickland JDH. Discussion of spectrophotometric determination of marine plant pigments, with revised equation for ascertaining chlorophylls and carotenoids. *J Mar Res* 1963; 21:155-63.
22. Guo FQ, Crawford NM. *Arabidopsis* nitric oxide synthase1 is targeted to mitochondria and protects against oxidative damage and dark-induced senescence. *The Plant Cell* 2005; 17(12):3436-50.
23. Bradford MM. A rapid and sensitive method for the quantitation of microgram quantities of protein utilizing the principle of protein-dye binding. *Anal Biochem* 1976; 72: 248-54.

24. Nelson DC, Flematti GR, Riseborough JA, Ghisalberti EL, Dixon KW, Smith SM. Karrikins enhance light responses during germination and seedling development in *Arabidopsis thaliana*. *Proc Natl Acad Sci USA* 2010; 107:7095-100.
25. Light ME, Burger BV, Staerk D, Kohout L, Van Staden J. Butenolides from plant-derived smoke: natural plant-growth regulators with antagonistic actions on seed germination. *J Nat Prod* 2010; 73(2):267-69.
26. Nair JJ, Pošta M, Papenfus HB, Munro OQ, Beier P, Van Staden J. Synthesis, X-ray structure determination and germination studies on some smoke-derived karrikins. *S Afr J Bot* 2014; 91:53-7.
27. Mousavinik M, Jowkar A, Rahimianboogar A. Positive effects of karrikin on seed germination of three medicinal herbs under drought stress. *Iran Agric Res* 2016; 35(2):57-64.
28. Laghmouchi Y, Belmehdi O, Bouyahya A, Senhaji NS, Abrini, J. Effect of temperature, salt stress and pH on seed germination of medicinal plant *Origanum compactum*. *Biocatal Agric Biotechnol* 2017; 10:156-60.
29. Zhao Y, Gao J, Kim J, Chen K, Bressan RA, Zhu JK. Control of plant water use by ABA induction of senescence and dormancy: an overlooked lesson from evolution. *Plant Cell Physiol* 2017; 58(8):1319-27.
30. Flematti GR, Goddard-Borger ED, Merritt DJ, Ghisalberti EL, Dixon KW, Trengove RD. Preparation of 2 H-furo [2, 3-c] pyran-2-one derivatives and evaluation of their germination-promoting activity. *J Agric Food Chem* 2007; 55(6):2189-94.
31. Çatav ŞS, Küçükakyüz K, Tavşanoğlu Ç, Pausas JG. Effect of fire-derived chemicals on germination and seedling growth in Mediterranean plant species. *Basic Appl Ecol* 2018; 30:65-75.
32. Balazadeh S, Parlitz S, Mueller-Roeber B, Meyer RC. Natural developmental variations in leaf and plant senescence in *Arabidopsis thaliana*. *Plant Biol* 2008; 10:136-47.
33. Kitonyo OM, Sadras VO, Zhou Y, Denton MD. Nitrogen supply and sink demand modulate the patterns of leaf senescence in maize. *Field Crop Res* 2018; 225:92-103.
34. Maillard A, Diquelou S, Billard V, Laine P, Garnica M, Prudent M, et al. Leaf mineral nutrient remobilization during leaf senescence and modulation by nutrient deficiency. *Front Plant Sci* 2015; 6: 317-22.
35. Tamary E, Nevo R, Naveh L, Levin-Zaidman S, Kiss V, Savidor A, et al. Chlorophyll catabolism precedes changes in chloroplast structure and proteome during leaf senescence. *Plant Direct* 2019; 3(3): e00127.
36. Kim J, Woo HR, Nam HG. Toward systems understanding of leaf senescence: an integrated multi-omics perspective on leaf senescence research. *Mol Plant* 2016; 9(6):813-25.
37. Ding F, Wang M, Zhang, S. Sedoheptulose-1, 7-bisphosphatase is involved in methyl jasmonate-and dark-induced leaf senescence in tomato plants. *Int J Mol Sci* 2018; 19(11):3673-80.
38. Woo HR, Kim HJ, Lim PO, Nam HG. Leaf senescence: Systems and dynamics aspects. *Annu Rev Plant Biol* 2019; 70:15.1-15.30.
39. Jan S, Abbas N, Ashraf M, Ahmad P. Roles of potential plant hormones and transcription factors in controlling leaf senescence and drought tolerance. *Protoplasma* 2019; 256(2):313-29.
40. Gregersen PL, Culetic A, Boschian L, Krupinska K. Plant senescence and crop productivity. *Plant Mol Biol* 2013; 82:603-22.
41. Li X, Ahmad S, Ali A, Guo C, Li H, Yu J, Guo Y. Characterization of somatic embryogenesis receptor-like kinase 4 as a negative regulator of leaf senescence in *Arabidopsis*. *Cells* 2019; 8(1):50-61.
42. Lim J, Park JH, Jung S, Hwang D, Nam HG, Hong S. Antagonistic roles of PhyA and PhyB in far-red light-dependent leaf senescence in *Arabidopsis thaliana*. *Plant Cell Physiol* 2018; 59(9):1753-64.
43. Krautler B. Breakdown of chlorophyll in higher plants- phyllobilins as abundant, yet hardly visible signs of ripening, senescence, and cell death. *Angewandte Chemie* 2016; 55:4882-907.
44. Lim PO, Kim HJ, Nam HG. Leaf Senescence. *Annu Rev Plant Biol* 2007; 58:115-36.
45. Kim HJ, Park JH, Kim J, Kim JJ, Hong S, Kim J et al. Time-evolving genetic networks reveal a NAC troika that negatively regulates leaf senescence in *Arabidopsis*. *PNAS* 2018; 115(21):E4930-39.
46. Mayta ML, Lodeyro AF, Guiamet JJ, Tognetti VB, Melzer M, Hajirezaei MR, Carrillo N. Expression of a plastid-targeted flavodoxin decreases chloroplast reactive oxygen species accumulation and delays senescence in aging tobacco leaves. *Front Plant Sci* 2018; 9:1039-57.
47. Blasi ÉA, Buffon G, Rativa AG, Lopes MC, Berger M, Santi L. et al. High infestation levels of *Schizotetranychus oryzae* severely affects rice metabolism. *J Plant Physiol* 2017; 219:100-111.
48. Cheng R, Gong L, Li Z, Liang, YK. Rice BIG gene is required for seedling viability. *J Plant Physiol* 2019; 232:39-50.
49. Balazadeh S, Riaño-Pachón DM, Mueller-Roeber B. Transcription factors regulating leaf senescence in *Arabidopsis thaliana*. *Plant Biol* 2008; 10: 63-75.

N-Acetylcysteine Improves Acrylamide-Induced Changes in Ovarian Tissue and Serum Levels of Pituitary-Ovarian Axis Hormones in Adult Rats

Marziyeh Naimi^{1,2} , Mehrdad Shariati³ , Syrus Naimi⁴ ,
Mohammad Amin Edalatmanesh² 

¹Islamic Azad University, Fars Science and Research Branch, Department of Biology, Fars, Iran

²Islamic Azad University, Shiraz Branch, Department of Biology, Shiraz, Iran

³Islamic Azad University, Kazerun Branch, Department of Biology, Kazerun, Iran

⁴Islamic Azad University, Kazerun Branch, Department of Genetics, Kazerun, Iran

ORCID IDs of the authors: M.N. 0000-0003-0014-9924; M.S. 0000-0001-7360-0208; S.N. 0000-0003-4557-1336; M.A.E. 0000-0002-7936-1145

Please cite this article as: Naimi M, Shariati M, Naimi S, Edalatmanesh MA. N-Acetylcysteine Improves Acrylamide-Induced Changes in Ovarian Tissue and Serum Levels of Pituitary-Ovarian Axis Hormones in Adult Rats. Eur J Biol 2019; 78(2): 75-81. DOI: 10.26650/EurJBiol.2019.0009

ABSTRACT

Objective: The purpose of this study was to evaluate the protective effect of N-acetylcysteine (NAC) on ovarian tissue and serum levels of follicle stimulating hormone (FSH), luteinizing hormone (LH), estradiol, and progesterone in Acrylamide (AA)-treated adult rats.

Materials and Methods: Forty-two adult female Wistar rats were randomly assigned into 7 groups of 6 including: a control group without treatment, a placebo group received distilled water intraperitoneally, an AA group received 50 mg/kg by oral gavage, a NAC group received 40 mg/kg intraperitoneally, an AA+NAC10, AA+NAC20 and an AA+NAC40 groups received 10, 20 and 40 mg/kg of NAC intraperitoneally, respectively and then also received 50 mg/kg AA by oral gavage for 28 days. Serum levels of FSH, LH, estradiol and progesterone were measured by radioimmunoassay method and ovarian tissue was evaluated histopathologically.

Results: Administering AA alone decreased the number of ovarian follicles, corpus luteum and the levels of FSH, estradiol and progesterone, while increased the number of atretic follicles and LH level compared to the control, placebo and NAC groups ($p < 0.05$). The administration of NAC alone had no effect on the number of ovarian follicles, corpus luteum and the level of hormones compared to the control and placebo groups ($p > 0.05$). Following AA+NAC20 and AA+NAC40 administration and not AA+NAC10, the number of ovarian follicles, corpus luteum and also the levels of FSH, estradiol and progesterone increased, while the number of atretic follicles and LH level decreased ($p < 0.05$), which was in a dose-dependent manner compared to the AA group.

Conclusion: NAC could recover the AA female rat reproductive toxicity in a dose-dependent manner, and improved folliculogenesis.

Keywords: Acrylamide, n-acetylcysteine, ovary, estradiol, rat



Corresponding Author: Mehrdad Shariati E-mail: mehrdadshariati@kau.ac.ir
Submitted: 17.05.2019 • **Revision Requested:** 11.06.2019 • **Last Revision Received:** 22.07.2019 • **Accepted:** 24.07.2019

© Copyright 2019 by The Istanbul University Faculty of Science • Available online at <http://ejb.istanbul.edu.tr> • DOI: 10.26650/EurJBiol.2019.0009

INTRODUCTION

Acrylamide (AA) also known as acrylic acid amide or propanamide is an unsaturated amide with the chemical formula $\text{CH}_2=\text{CH}-\text{CONH}_2$, which exists in two mono- and polymeric forms (1). The monomeric AA is mutagenic and tumorigenic in human and laboratory animals, but the toxic effects of its polymeric form have not yet been recognized (2). AA is produced in a large amount in starchy foods cooked at high-temperature (120°C) such as potato, corn, and wheat, which is due to the presence of asparagine amino acid (150-4000 µg/kg) and in foods containing protein in an average amount (5-50 µg/kg) and it has raised a general concern in societies that consume a large amount of AA-rich foods (3,4). AA is rapidly metabolized in the body, and its metabolites are normally excreted by urine (1). In humans and rodents, AA is oxidized by CYP450 2E1 and converts into glycidamide (GA) which is an epoxide derivative. Studies show that both *in vivo* and *in vitro*, GA has genotoxicity features (5). Glutathione S-transferase (GST) is a metabolic enzyme that plays an important role in reducing oxidative stress and eliminating free radicals. The conjugation of AA or its metabolite, i.e. GA with GST enzyme, disrupts cellular function and causes cell death. Studies have also indicated that the destructive effects of AA or GA are by influencing sulfhydryl groups of proteins (6,7). Due to AA poisoning, the level of glutathione decreases and the body's defense system against free radicals weakens (8). Free radicals combine with cell membrane and unsaturated fatty acids, producing radical lipids with oxygen molecule and as a result, phospholipids in the endoplasmic reticulum decompose and release enzymes, which ultimately lead to cell death (9). Some studies represent that AA has destructive effects on the reproductive system of both male and female (10-13). AA-treated rats have low-weight ovaries and low-quality or undeveloped oocytes due to increased oxidative stress and this can lead to a significant reduction in the fertilization rate or low-quality embryos and consequently subfertility or infertility (12).

N-acetylcystein (NAC) is a kind of acetylated L-amino acid, used as an antidote for acetaminophen poisoning, as well as for treating various disorders associated with oxidative stress (14). Studies have shown that during oxidative stress that decreases glutathione levels, NAC can act as an antioxidant by increasing glutathione and naturally neutralizes the effects of intracellular damage of free radicals by repairing oxidative damage or collecting oxygen reactive species (15). In previous studies, severe side effects associated with NAC consumption have not been reported so that its consumption at high doses for one year was uncomplicated (16). Therefore, in the current study, the protective effect of NAC on ovarian tissue and serum levels of follicle stimulating hormone (FSH), luteinizing hormone (LH), estradiol, and progesterone in AA-treated adult rats were studied.

MATERIALS AND METHODS

Animals

In the present experimental study, 42 adult female Wistar rats weighing 220 ± 20 g and 8 weeks old were provided from the animals' house at the Islamic Azad University of Kazerun. All animals were maintained on a 12 h/12 h light-dark cycle at $22\pm 2^\circ\text{C}$ and 70% relative humidity in polycarbonate cages and they had free access to sufficient water and food ad libitum. Before any experimental manipulation, the animals were kept together for two weeks to adapt to the laboratory conditions. The current study was approved by the Ethics Committee of the Islamic Azad University of Kazerun, Iran, regarding to work with laboratory animal care (Ethical No: IR.Kiau 16330525651006).

Experimental Design

Animals were randomly divided into 7 groups of 6 control, placebo, AA, NAC, AA+NAC10, AA+NAC20 and AA+NAC40 groups. The control group did not receive any treatment. Because the medications' solvent in this study was distilled water, animals in the placebo group received distilled water intraperitoneally. The animals in AA group received 50 mg/kg AA (Merck, Germany) by oral gavage. In NAC group, the animals received 40 mg/kg NAC (Merck, Germany) intraperitoneally. The rats in AA+NAC10, AA+NAC20 and AA+NAC40 groups received 10, 20 and 40 mg/kg NAC intraperitoneally, respectively at 9 o'clock in the morning and then received 50 mg/kg AA by oral gavage at 5 o'clock in the afternoon. All groups were treated over a period of 28 days. The basis for selecting the dose of AA and NAC was based on the previous studies (10,17). Regarding the above mentioned protocol, after receiving the last dose of AA, the animals were anesthetized using ether and blood sampling was carried out directly from the heart. Then, for histological evaluations, the left and right ovaries of all rats were removed from the abdominal cavity.

Before starting the treatment, vaginal smear was prepared to ensure that all rats were at one stage of the estrus cycle. For this purpose, 100 µg of estradiol valerate (Aboreyhan, Iran), dissolved in 0.2 ml of olive oil, was injected intramuscularly using an insulin syringe. After 42 hours, 50 µg of progesterone (Aboreyhan, Iran) was injected intramuscularly. Six hours after the injection of progesterone, the vaginal smear was prepared and examined by light microscope. The previous method was used to determine the stages of estrous cycle. In this method, each stage of the estrus cycle is detected based on the ratio between three types of cell population (epithelial cells, keratinized cells and leukocytes) observed in vaginal smear (18). Microscopic observations showed that all the rats were synchronized in the estrous phase.

Hormonal Analysis

Using a 5ml syringe, blood sampling was done directly from the heart. After agglutination process in the laboratory, the blood samples were centrifuged for 5 minutes at 3000 rpm to discrete the serum. The serums were stored at -20°C prior to FSH, LH, estradiol, and progesterone measurement. The serum

levels of FSH, LH, estradiol and progesterone were measured using radioimmunoassay (RIA) kits (FSH and LH: BT Lab, China; Estradiol and Progesterone: IBL, Germany) according to the manufacturer's instructions.

Based on the RIA kits, 125 µl of the standard solution was decanted into NSB tube and then 25 µl of the serum was added. 500 µl of the labeled solution was added and 100 µl of antiserum was added at the last step and incubated for 60 minutes at 37°C. Then, the amount of 1000 µl of the secondary antibody was added and incubated for 15 minutes at 20 to 35°C. At the final stage, the mixture was centrifuged at 2000 rpm for 20 minutes, and after separating the supernatant, the levels of hormones were counted using a gamma counter (Kentron, Switzerland).

Histopathologic Analysis of Ovarian Tissue

After blood sampling, the left and right ovaries of all animals were removed and once the surrounding adipose tissue was removed, they were fixed in a 10% buffered formalin solution. After standard histological processing, the samples were blocked in paraffin and then, using a microtome (Aisan, China), midsagittal and longitudinal serial sections of 5 µm thickness were prepared and stained with hematoxylin-eosin (Merck, Germany). Under the light microscope (Nikon, Tokyo, Japan), the number of primary follicles, secondary follicles, graafian follicles, atretic follicles and corpus luteum were counted in each section. Counting the follicles and corpus luteum were performed in a spiral way from a point at the cortex in clockwise direction toward the medulla.

Statistical Analysis

Data were analyzed using SPSS version 20 software (SPSS Inc., Chicago, IL, USA). The normal distribution of the resulting data was confirmed by non-parametric Kolmogorov-Smirnov test. Then, all data were analyzed applying one way ANOVA by bonferroni test at a significance level of $p < 0.05$. The data were described as mean \pm standard error (SE) in the graphs. GraphPad Prism version 6 (GraphPad Prism, Inc., San Diego, CA, USA) was used to represent the graphs.

RESULTS

Hormonal Findings

Based on the hormonal findings, there was no significant difference in the serum levels of FSH, LH, estradiol and progesterone among the control, placebo, NAC and AA+NAC40 groups ($p > 0.05$) (Figures 1A-1D). The serum Levels of FSH, estradiol and progesterone in the AA and AA+NAC10 groups were decreased significantly compared to the control, placebo, NAC and AA+NAC40 groups ($p < 0.05$) (Figures 1A, 1C and 1D), but the level of LH increased significantly in both groups compared to the control, placebo, NAC and AA+NAC40 groups ($p < 0.05$) (Figure 1B). The serum levels of FSH, estradiol and progesterone in AA+NAC10, AA+NAC20 and AA+NAC40 groups were increased in a dose-dependent manner compared to the AA group, and were significantly different in AA+NAC20 and AA+NAC40 groups. Conversely, the level of LH was decreased compared to AA group in a dose-dependent manner, and was significantly different in AA+NAC40 group ($p < 0.05$) (Figure 1B).

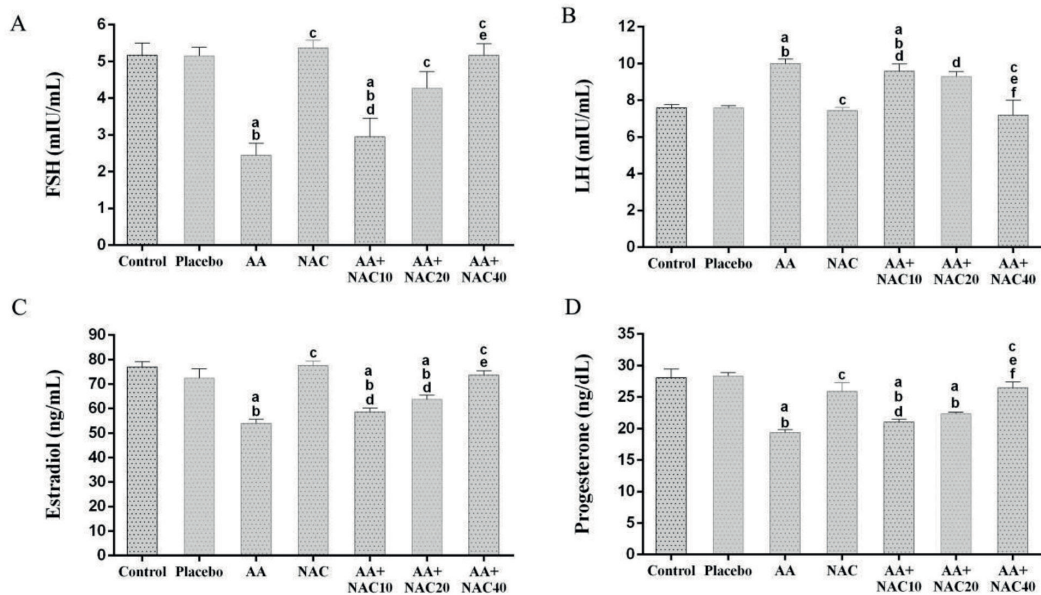


Figure 1. A-D. Comparison of mean and standard error of the serum levels of FSH, LH, estradiol and progesterone in control, placebo, AA-treated rats in AA group, NAC-treated rats in NAC group and AA+NAC-treated rats in AA+NAC10, AA+NAC20 and AA+NAC40 groups. a: compared to control group; b: compared to placebo group; c: compared to AA group; d: compared to NAC group; e: compared to AA+NAC10 group; f: compared to AA+NAC20 group (a, b, c, d, e and f= $p < 0.05$).

Histopathologic Findings

Figure 2 compares the mean and the standard error of the number of primary follicles, secondary follicles, graafian follicles and corpus luteum. There was no significant difference in the number of primary follicles, secondary follicles, graafian follicles and corpus luteum among the control, placebo, NAC, AA+NAC20 and AA+NAC40 groups ($p>0.05$) (Figures 2A-2D). Also, there was no significant difference in the number of primary follicles, secondary follicles, graafian follicles and corpus luteum among the control, placebo, NAC, AA+NAC20 and AA+NAC40 groups ($p>0.05$) (Figures 2A-2D). Also, there was no significant difference in the number of graafian follicles among the control, placebo, NAC and AA+NAC10 groups ($p>0.05$) (Figure 2C). The number of primary follicles, secondary follicles and corpus luteum in the AA group was significantly decreased compared to the control, placebo, NAC, AA+NAC20 and AA+NAC40 groups ($p<0.05$) (Figures 2A, 2B and 2D). Furthermore, the number of graafian follicles in the AA group was significantly decreased compared to the control, placebo, NAC, AA+NAC10, AA+NAC20 and AA+NAC40 groups ($p<0.05$) (Figure 2C). The number of primary follicles, secondary follicles and corpus luteum increased in a dose-dependent manner in the AA+NAC10, AA+NAC20 and AA+NAC40 groups in comparison to the AA group, and this increase was significant in the AA+NAC20 and AA+NAC40 groups ($p<0.05$) (Figures 2A, 2B and 2D). Also, the number of graafian follicles in the AA+NAC10, AA+NAC20 and AA+NAC40 groups was significantly increased in comparison with the AA group ($p<0.05$) (Figure 2C).

Figure 3 compares the mean and standard error of the number of atretic follicles. There was no significant difference in the number of atretic follicles among the control, placebo, NAC, AA+NAC20 and AA+NAC40 groups ($p>0.05$), but the number of atretic follicles increased significantly in AA and AA+NAC10 groups compared to the control, placebo, NAC, AA+NAC20 and AA+NAC40 groups ($p<0.05$).

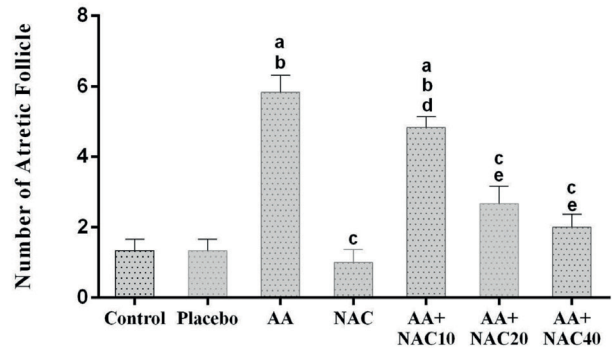


Figure 3. Comparison of mean and standard error of atretic follicles in control, placebo, AA-treated rats in AA group, NAC-treated rats in NAC group and AA+NAC-treated rats in AA+NAC10, AA+NAC20 and AA+NAC40 groups. a: compared to control group; b: compared to placebo group; c: compared to AA group; d: compared to NAC group; e: compared to AA+NAC10 group (a, b, c, d and e= $p<0.05$).

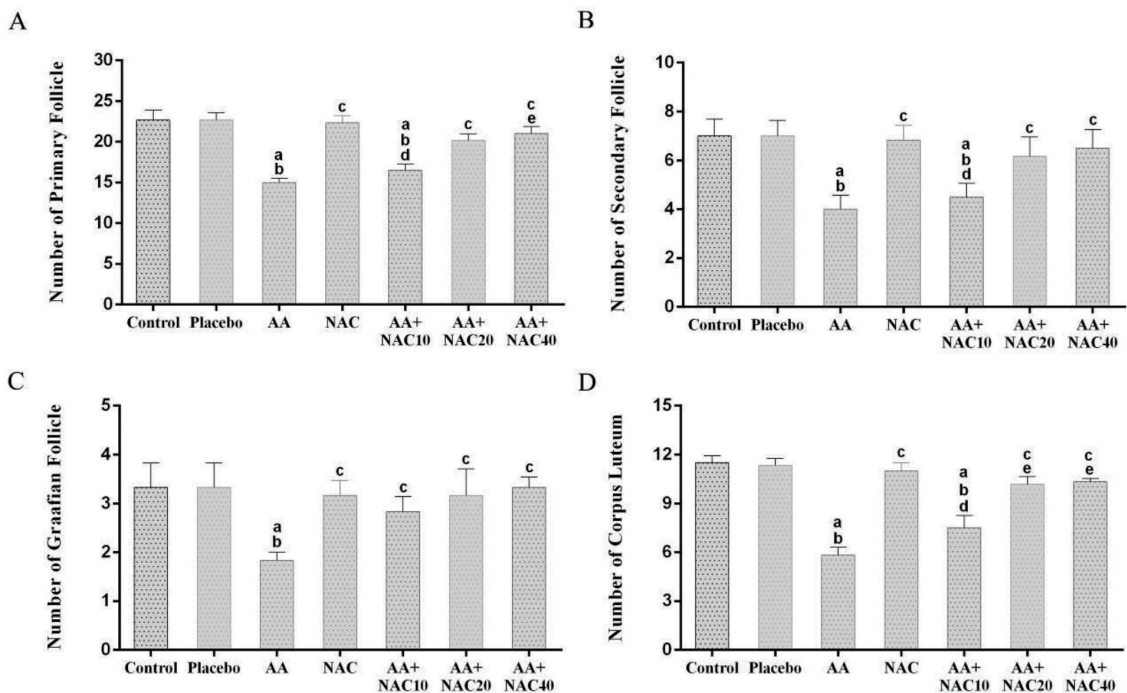


Figure 2. A-D. Comparison of mean and standard error of the number of primary follicles, secondary follicles, graafian follicles and corpus luteum in control, placebo, AA-treated rats in AA group, NAC-treated rats in NAC group and AA+NAC-treated rats in AA+NAC10, AA+NAC20 and AA+NAC40 groups. a: compared to control group; b: compared to placebo group; c: compared to AA group; d: compared to NAC group; e: compared to AA+NAC10 group (a, b, c, d and e= $p<0.05$).

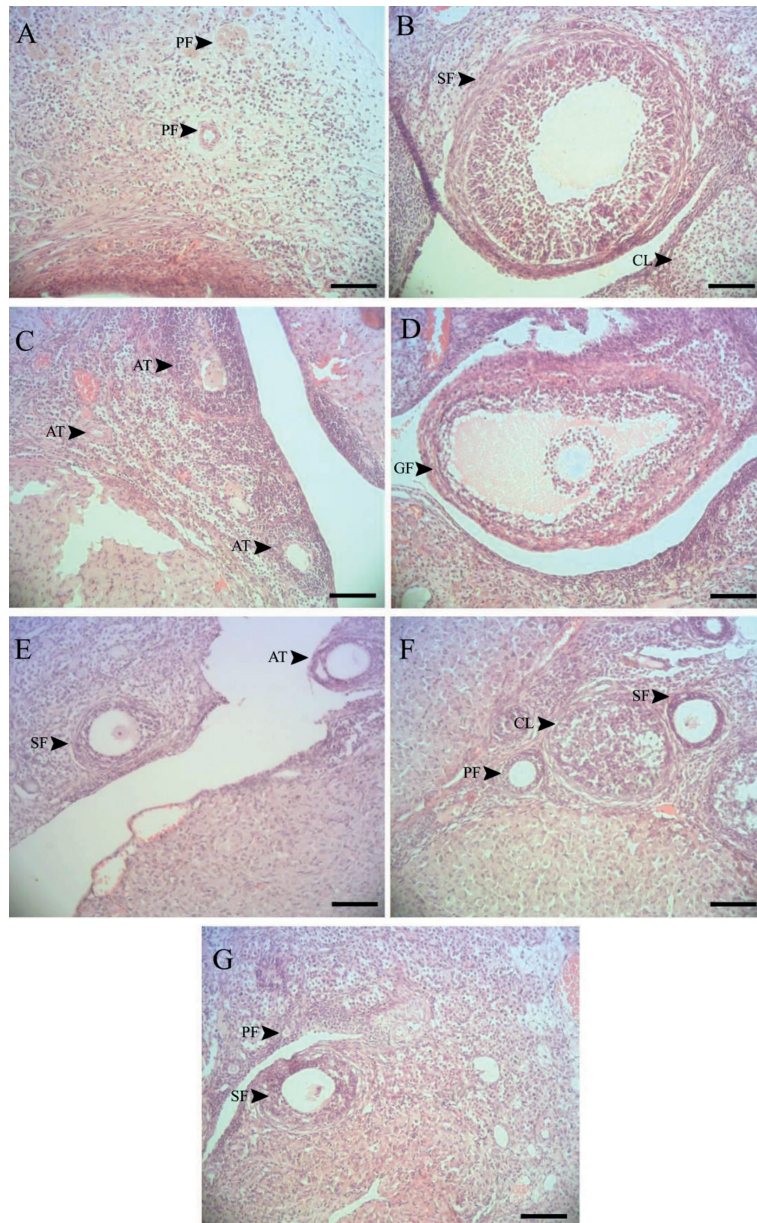


Figure 4. A-G. Photomicrograph of ovarian tissue in rats treated with AA, NAC and AA+NAC in different groups. In control (A) and placebo (B) groups, types of ovarian follicles and normal folliculogenesis are observed. In the AA group (C) the reduction of ovarian follicles and elevation of atretic follicles can be observed. In the NAC group (D) graafian follicles along with a thick layer of granulosa are observed. In AA+NAC10 group (E) a large number of atretic follicles are observed. In the AA+NAC20 (F) and AA+NAC40 (G) groups different ovarian follicles are seen. Folliculogenesis has been improved. PF: Primary follicle; SF: Secondary follicle; GF: Graafian follicle; CL: Corpus luteum; AT: Atretic follicle. H & E staining. The photos are with 10X magnification. Black bars: 50 μ m.

Figure 4 represents the morphology of ovarian tissue in different groups. The histological sections of the ovaries in the control, placebo, NAC, AA+NAC20 and AA+NAC40 groups show normal folliculogenesis with all types of follicles, including graafian follicles with a thick layer of granulosa cells and corpus luteum (Figures 4A, 4B, 4D, 4F and 4G). In AA and AA+NAC10 groups, atretic follicles with a very thin granulosa layer, which is characterized by cystic follicles and few corpus luteum indicating ovulation decrease, were observed (Figures 4C and 4E).

DISCUSSION

In the present study, the effect of NAC administration on the changes of ovarian tissue and the serum levels of FSH, LH, estradiol and progesterone was evaluated in AA-treated rats. Our results showed that the number of primary follicles, secondary follicles, graafian follicles and corpus luteum decreased significantly while the number of atretic follicles increased significantly by administering 50 mg/kg AA in AA group

compared to the control, placebo and NAC groups. Although toxic effects of AA on male reproductive system have been investigated in several studies, few quantitative studies have been done on the female reproductive system. It was suggested that administering different amounts of AA (20 and 40 mg/kg) in rats decreases the number of primordial follicles and corpus luteum, while the increase in the number of primary and antral follicles was observed in a dose-dependent manner (10).

The results of this study as well as our study suggest that AA can affect follicular growth, development and atresia in different stages and prevent the formation of corpus luteum as a normal ovarian function index. It was indicated that the low dose-administration of AA in rats, infertility can occur due to the reduction of mature follicles and cystic changes in the ovary (11). In this study, the administration of AA decreased FSH, estradiol and progesterone levels and increased LH level. It has been indicated that AA can decrease the FSH level in a dose-dependent manner, and also affect the proliferation and survival of granulosa cells, therefore, it seems that the reduction in estradiol level may be due to decreased level of FSH and the degradation of granulosa cells function (10,19). The main function of the corpus luteum is secreting progesterone, so reduced level of progesterone can be due to the reduction of the corpus luteum following AA administration (19). An elevated level of LH with a reduced level of estradiol and progesterone suggest that the pituitary-gonad axis can provide a suitable negative feedback after reducing estradiol and progesterone levels as a result of AA administration.

NAC is a low molecular weight thiol derived from cysteine amino acid and due to antioxidant, anti-aging and anti-inflammatory activities, it has an important role in reducing oxidative stress, eliminating ROS and improving nitric oxide activity (20,21). Some studies confirm the protective and positive effects of NAC on various tissues of the body, including the liver, kidney, intestine and ovary (22-25). In patients with polycystic ovarian syndrome, NAC can decrease and increase insulin level and peripheral insulin sensitivity, respectively, nevertheless, co-administering of NAC and assisted reproductive technology medications does not significantly increase the number of ovarian follicles in these patients (26). It was demonstrated that the NAC administration in AA-treated rats can decrease the level of Malondialdehyde and increase glutathione level and GST activity in the liver and intestine (27). The results of this study showed that administering NAC at a dose of 40 mg/kg in the NAC group does not influence the level of FSH, LH, estradiol and progesterone and also the number of ovarian follicles and corpus luteum compared to control and placebo groups. In confirmation of our results, it has been shown that in NAC-treated pregnant rats, the progesterone level and the number of corpus luteum did not change in comparison with the control group (28). What's more, it was revealed that the administration of 100 mg/kg of NAC in male rats did not affect the serum levels of FSH, LH and testosterone compared to the control group (13). It seems that administering NAC alone in this study does not affect the level of the pituitary-gonadal

axis hormones as well as the number of ovarian follicles and the corpus luteum. However, it has been shown that proper treatment with NAC delayed the rate of apoptosis and death of healthy follicles during the aging process of the ovary and since oocytes and follicles can be exposed to oxidative stress in the body, so the ovary can be a proper place for NAC activity (29).

Based on our observations in the current study, administering NAC at 20 and 40 mg/kg in AA-treated rats was significantly increased the number of primary follicles, secondary follicles, graafian follicles and corpus luteum, but the number of atretic follicles was significantly increased compared to AA groups; while there was no significant difference between control, placebo and NAC groups. Also, our study represented that the levels of FSH, LH, estradiol and progesterone after NAC administration at 40 mg/kg in AA-treated rats did not differ significantly with control, placebo and NAC groups. Follicular atresia is a natural process dependent on the developmental stage and apoptosis plays an important role in this process. AA has been shown to increase follicular atresia in primordial and primary follicles. It has been suggested that AA can induce caspase enzymes in oocytes and causes proteolysis of vimentin intermediate filament, which results in apoptosis promotion (30). Nitric oxide plays an important role in modulating oxidative stress, and its excessive increase can be cytotoxic by reacting with reactive oxygen and nitrogen species that impairs mitochondrial function (28). It has also been indicated that nitric oxide (NO) plays an important role in folliculogenesis, follicular atresia, oocyte development, ovulation, luteolysis, and steroidogenesis. NO is synthesized by nitric oxide synthase (NOS) and AA can exert its toxic effects through NOS pathway on the female reproductive system (10). Nevertheless, it appears that NAC can modulate the toxic effects of AA on the ovary by affecting the NOS activity (21,28).

CONCLUSION

Our study shows that AA has toxic effects on ovaries and could impair the folliculogenesis as well as the level of pituitary-gonadal axis hormones in the rats. The administration of NAC in healthy female rats did not influence the folliculogenesis and pituitary-gonadal hormones levels. Administering NAC at different doses in AA-treated rats doesn't have a similar effect on follicular development and atresia as well as pituitary-ovarian axis hormones. The lowest effect of NAC was observed at 10 mg/kg, while 20 and 40 mg/kg NAC had the highest effect on the folliculogenesis and levels of pituitary-ovarian axis hormones in AA-treated rats, respectively. Therefore, administering NAC in AA-treated rats could improve folliculogenesis and serum levels of pituitary-ovarian axis hormones in a dose-dependent manner. Therefore, NAC supplementation may be beneficial when there is a risk of AA female reprotoxicity.

Ethics Committee Approval: The current study was approved by the Ethics Committee of the Islamic Azad University of Kazerun, Iran, regarding to work with laboratory animal care (No: IR.Kiau 16330525651006).

Author Contributions: Conception/Design of study: M.N., M.S.; Data Acquisition: M.N., M.A.E.; Data Analysis/Interpretation: S.N., M.N.; Drafting Manuscript: M.N., M.S.; Critical Revision of Manuscript: M.N., M.S.; Final Approval and Accountability: M.S.; Technical or Material Support: M.S.; Supervision - S.N., M.S.

Acknowledgment: This study is the result of a Ph.D. thesis in developmental biology. The authors would like to thank the Islamic Azad University of Kazerun and the Islamic Azad University of Shiraz for their cooperation during this study.

Conflict of Interest: The authors have no conflict of interest to declare.

Financial Disclosure: This study was supported by the Research Fund of the Islamic Azad University of Shiraz (Grant No: IR.Shiraziau 1633052565).

References

- Rahangadale S, Jangir BL, Patil M, Verma T, Bhandarkar A, Sonkusale P, et al. Evaluation of protective effect of vitamin E on acrylamide induced testicular toxicity in wister rats. *Toxicol Int* 2012; 19(2): 158-61.
- Olesen PT, Olsen A, Frandsen H, Frederiksen K, Overvad K, Tjønneland A. Acrylamide exposure and incidence of breast cancer among postmenopausal women in the Danish Diet, Cancer and Health Study. *Int J Cancer* 2008; 122(9): 2094-100.
- Yener Y and Kalipci E. The carcinogenic effects of acrylamide formed during cooking of some foods. *Academic J Cancer Res* 2009; 2(1): 25-32.
- Lingnert H, Grivas S, Jagerstad M, Skog K, Tornqvist M, Aman P, et al. Acrylamide in food: mechanisms of formation and in influencing factors during heating of foods. *Scand J Nutr* 2002; 46(4): 159-72.
- Klaunig JE. Acrylamide carcinogenicity. *J Agric Food Chem* 2008; 56(15): 5984-8.
- Barber DS, Hunt JR, Ehrich MF, Lehning EJ, Lopachin RM. Metabolism, toxicokinetics and hemoglobin adduct formation in rats following subacute and subchronic acrylamide dosing. *Neurotoxicology* 2001; 22(3): 341-53.
- Tyl RW and Friedman MA. Effects of acrylamide on rodent reproductive performance. *Reprod Toxicol* 2003; 17(1): 1-13.
- Collí-Dulá RC, Friedman MA, Hansen B, Denslow ND. Transcriptomics analysis and hormonal changes of male and female neonatal rats treated chronically with a low dose of acrylamide in their drinking water. *Toxicol Rep* 2016; 19(3): 414-26.
- Zarei M and Shivanandappa T. Amelioration of cyclophosphamide-induced hepatotoxicity by the root extract of *Decalepis hamiltonii* in mice. *Food Chem Toxicol* 2013; 57: 179-84.
- Wei Q, Li J, Li X, Zhang L, Shi F. Reproductive toxicity in acrylamide-treated female mice. *Reprod Toxicol* 2014; 46: 121-8.
- ALKarim S, ElAssouli S, Ali S, Ayuob N, ElAssouli Z. Effects of low dose acrylamide on the rat reproductive organs structure, fertility and gene integrity. *Asian Pac J Reprod* 2015; 4(3): 179-87.
- Duan X, Qiao Wang C, Chen KL, Zhu CC, Liu J, Suna SC. Acrylamide toxic effects on mouse oocyte quality and fertility *in vivo*. *Sci Rep* 2015; 5: 11562.
- Kunle-Alabi OT, Akindele OO, Odoh MI, Oghenetega BO, Raji Y. Comparative effects of coconut water and N-Acetyl cysteine on the hypothalamo-pituitary-gonadal axis of male rats. *Songklanakarini J Sci Technol* 2017; 39(6): 759-64.
- Ercal N, Treeratphan P, Lutz P, Hammond TC, Matthews RH. N-acetylcysteine protects chinese hamster ovary (CHO) cells from lead-induced oxidative stress. *Toxicology* 1996; 108(1-2): 57-64.
- Xue C, Liu W, Wu J, Yang X, Xu H. Chemoprotective effect of N-acetylcysteine (NAC) on cellular oxidative damages and apoptosis induced by nano titanium dioxide under UVA irradiation. *Toxicol in Vitro* 2011(1); 25: 110-6.
- Demedts M, Behr J, Buhl R, Costabel U, Dekhuijzen R, Jansen HM, et al. High-dose acetylcysteine in idiopathic pulmonary fibrosis. *N Engl J Med*. 2005; 353(21): 2229-42.
- Chiew AL, Isbister GK, Duffull SB, Buckley NA. Evidence for the changing regimens of acetylcysteine. *Br J Clin Pharmacol* 2016; 81(3): 471-81.
- Marcondes FK, Bianchi FJ, Tanno AP. Determination of estrous cycle phases of rats: some helpful considerations. *Braz J Biol* 2002; 62(4A): 609-14.
- Camacho L, Latendresse JR, Muskhelishvili L, Patton R, Bowyer JF, Thomas M, et al. Effects of acrylamide exposure on serum hormones, gene expression, cell proliferation, and histopathology in male reproductive tissues of Fischer 344 rats. *Toxicol Lett* 2012; 211(2): 135-43.
- Pan X, Wu X, Yan D, Peng C, Rao C, Yan H. Acrylamide-induced oxidative stress and inflammatory response are alleviated by N-acetylcysteine in PC12 cells: Involvement of the crosstalk between Nrf2 and NF- κ B pathways regulated by MAPKs. *Toxicol Lett* 2018; 288: 55-64.
- Kojsová S, Jendeková L, Zicha J, Kunes J, Andriantsitohaina R, Pechánová O. The effect of different antioxidants on nitric oxide production in hypertensive rats. *Physiol Res* 2006; 55(Suppl): S3-16.
- Galhardo MA, Júnior CQ, Riboli Navarro PG, Morello RJ, De Jesus Simões M, De Souza Montero EF. Liver and lung late alterations following hepatic reperfusion associated to ischemic preconditioning or N-acetylcysteine. *Microsurgery* 2007; 27(4): 295-9.
- Usta U, Inan M, Erbas H, Aydogdu N, Puyan OF, Altaner S. Tissue damage in rat ovaries subjected to torsion and detorsion: effects of L-carnitine and N-acetyl cysteine. *Pediatr Surg Int* 2008; 24: 567-73.
- Danilovic A, Lucon AM, Srougi M, Shimizu MHM, Lanhez LE, Nahas WC, et al. Protective effect of N-acetylcysteine on early outcomes of deceased renal transplantation. *Transplant Proc* 2011; 43: 1443-9.
- Millea PJ. N-Acetylcysteine: Multiple clinical applications. *Am Fam Physician* 2009; 80: 265-9.
- Mokhtari V, Afsharian P, Shahhoseini M, Kalantar SM, Moini A. A review on various uses of n-acetyl cysteine. *Cell J* 2017; 19(1): 11-17.
- Altinoz E, Turkoz Y, Vardi N. The protective effect of N-acetylcysteine against acrylamide toxicity in liver and small and large intestine tissues. *Bratisl Lek Listy* 2015; 116(4): 252-8.
- Helal MA. The effects of N-acetyl-L-cysteine on the female reproductive performance and nephrotoxicity in rats. *Ren Fail* 2016; 38(2): 311-20.
- Liu J, Liu M, Ye X, Liu K, Huang J, Wang L, et al. Delay in oocyte aging in mice by the antioxidant N-acetyl-L-cysteine (NAC). *Hum Reprod* 2012; 27(5): 1411-20.
- Hulas-Stasiak M, Dobrowolski P, Tomaszewska E, Kostro K. Maternal acrylamide treatment reduces ovarian follicle number in newborn guinea pig offspring. *Reprod Toxicol*. 2013; 42: 125-31.

Acibenzolar-S-Methyl Inhibits MEK1/2 Signaling in SH-SY5Y Neuroblastoma Cells

Aysegul Yildiz¹ 

¹Mugla Sitki Kocman University, Faculty of Science, Department of Molecular Biology and Genetics, Mugla, Turkey

ORCID IDs of the author: A.Y. 0000-0001-6356-7459

Please cite this article as: Yildiz A. Acibenzolar-S-Methyl Inhibits MEK1/2 Signaling in SH-SY5Y Neuroblastoma Cells. Eur J Biol 2019; 78(2): 82-87. DOI: 10.26650/EurJBiol.2019.0020

ABSTRACT

Objective: Targeted cancer therapy using targeted cell proliferation inhibitors has become increasingly more critical. Studies conducted over the last decade have shown that non-steroidal drugs containing salicylic acid (SA) such as aspirin reduce mortality in many cancers. From this perspective, there are data suggesting SA as a potential inhibitor of the mitogenic MEK1/2 (mitogen-activated-protein-kinase, MAPK), extracellular-signal regulated-protein-kinase (ERK) signaling, which could be highly effective in the prevention of proliferation in cancer. To date, no study has been conducted on the effect of SA on MEK1/2 signaling in neuroblastoma cells. Thus, the aim of this study is to reveal whether SA has an effect on MEK1/2 signaling in neuroblastoma cancer which is a frequent pediatric cancer with poor prognosis.

Materials and Methods: The purpose of this study was to investigate whether a SA analog acibenzolar-S-methyl had an effect on the MEK1/2 signaling pathway and on cell viability in SH-SY5Y neuroblastoma cells by MTS (3-(4,5-dimethylthiazol-2-yl)-5-(3-carboxymethoxyphenyl)-2-(4-sulfophenyl)-2H-tetrazolium) cell viability analysis and MEK1/2 and active caspase-3 detection by western blotting technique.

Results: MTS cell viability test indicated that 10 mM acibenzolar-S-methyl reduces cell viability by 50%. Western blotting results of 10 mM acibenzolar-S-methyl-treated cells showed that MEK1/2 signaling was significantly inhibited in SH-SY5Y cells. Besides, an increase in active-caspase-3 levels provided insight into acibenzolar-S-methyl's apoptotic effect which needs further morphological apoptotic data.

Conclusion: Our research is the first to show that SA analog acibenzolar-S-methyl negatively affects MEK1/2 signaling causing the death of SH-SY5Y neuroblastoma cells. Our results can give insight not only into understanding the mechanisms of carcinogenesis but also into developing effective treatment methods.

Keywords: Salicylic acid, Acibenzolar-S-Methyl, MEK1/2, SH-SY5Y, neuroblastoma cancer

INTRODUCTION

Signal transduction is an important part of a complex system which organizes many cellular activities in the cell and regulates their behavior. Errors in signal transduction are, therefore the main cause of diseases such as cancer, autoimmunity, and diabetes. Thus, metabolic functions related to signal transduction have become the most important focus of cancer biology (1).

In this regard, targeting mitogenic and/or survival signals in order to suppress cell proliferation or cell growth through targeted inhibitors is getting more

attention. By means of targeted inhibitors, successful results can be achieved by suppressing cell proliferation or cell growth during tumorigenesis. To this end, several important studies have been performed and results showed that low dose aspirin which contains salicylic acid (SA) reduces the incidence and mortality of colorectal, breast, gastric, lung or other cancers (2-6).

Furthermore, researchers examining the effect of SA on a hepatoma cell line have shown that SA can inhibit proliferation and induce apoptosis of the hepatoma cell line in a time and dose-dependent manner (7). In addition, in a study of human colorectal tumor cell lines,



Corresponding Author: Aysegul Yildiz E-mail: aysegulunal@mu.edu.tr

Submitted: 18.07.2019 • **Revision Requested:** 04.09.2019 • **Last Revision Received:** 03.10.2019 • **Accepted:** 16.10.2019

© Copyright 2019 by The Istanbul University Faculty of Science • Available online at <http://ejb.ibul.edu.tr> • DOI: 10.26650/EurJBiol.2019.0020

the effect of salicylate, aspirin metabolite, on these cell lines was determined. Salicylate showed dose-dependent inhibitory effects in all cell lines (8). All these studies indicate that SA may be protective and preventive against cancer.

At this point, one could pose a question regarding what the mechanism of the apoptotic action of salicylate in cancer is. In this context, the high number of protein kinases modulated by salicylate may provide a strong explanation for the apoptotic effect of salicylate on cancer cells. From this perspective, a considerable amount of data suggests that SA may have an effect on the mitogenic MAPK/ERK (mitogen-activated protein kinase/extracellular signal-regulated kinases) signaling pathway, one of the cell's most vital signaling pathways (9,10).

MAPK enzymes found in all eukaryotic cells are the intersections and/or junctions of mitogenic stimuli received by different receptors. In response to the stimuli it receives, the intracellular signal is transferred to the small oncogenic G-protein Ras and then to the Raf (MEK kinase) protein, which then activates MEK1/2 (MAPK/ERK kinase or MAP kinase kinase) signal proteins. Activated MEK1/2 phosphorylates and activates ERK1/2 which ultimately regulates essential cellular events such as gene expression, mitosis, cell viability, apoptosis, cellular metabolism, differentiation and motility (11). As is evident from its function, MEK1/2 is one of the key regulators of MAPK/ERK signaling cascade.

There is a study conducted with A549 human lung cancer cells demonstrating that SA may have a suppressing effect on this vital signaling pathway (9). In the afore-mentioned study the said effect was demonstrated by disrupting the MAPK signaling pathway by inhibiting the binding of c-Raf to the Ras protein (9). This data is very important given the role of the MAPK signaling pathway in processes such as cell proliferation, differentiation, and survival.

Although it is true that in many cancers inhibiting MEK1/2 signaling results in apoptotic death, in certain types of cancer such as melanoma, inhibiting MEK1/2 signaling could contrarily contribute to resistance to apoptosis (10) pointing out the heterogeneous nature of the molecular and genetic basis of cancer.

However, little is known about the role and effect of MEK1/2 signaling in neuroblastoma cancer, and no studies have as yet been conducted on the effect of SA on this signaling pathway. There are only a few studies indicating that the MAPK signaling pathway plays a role in the transformation of neuroblastoma cells into transformed phenotype and in gaining resistance to chemotherapy (12). In addition, we have demonstrated through our recently completed study that inhibiting MEK1/2 signaling by specific MEK1/2 inhibitor U0126 in SH-SY5Y neuroblastoma cells results in a significant decrease in cell viability (unpublished data).

Taking into account that neuroblastoma is the most common type of pediatric extracranial solid tumor in which 98% of the

patients are under 10 years of age, and considering that the disease has a very poor prognosis with a 30% long-term survival rate (13,14), it would be of great value to investigate whether SA has an effect on the MEK1/2 signaling and correlatively on cell viability in neuroblastoma cells. With this aim in mind, we treated SH-SY5H neuroblastoma cell line with an SA analog, acibenzolar-S-methyl and we analyzed the effect of acibenzolar-S-methyl on MEK1/2 signaling and on cell viability. Western blotting results of acibenzolar-S-methyl-treated cells showed that MEK1/2 signaling was significantly inhibited. In addition, we determined that active caspase-3 levels increased upon acibenzolar-S-methyl treatment. Although this result is promising for the apoptotic effect of acibenzolar-S-methyl in SH-SY5Y cells, it needs further morphological analysis to be able to exactly point out apoptosis in acibenzolar-S-methyl-treated SH-SY5Y cells.

In this study, we showed for the first time that salicylic acid analog acibenzolar-S-methyl negatively affects MEK1/2 signaling causing death of SH-SY5Y neuroblastoma cells. Our study may become a guide not only for choosing the right targets but also for choosing the right weapons in the fight against cancer.

MATERIALS AND METHODS

Cell Culture

SH-SY5Y neuroblastoma cells were cultured at 37°C with 5% CO₂ at 1 atmospheric pressure in high-glucose Dulbecco's modified Eagle medium (DMEM) containing 10% fetal bovine serum (FBS), 2 mM L-Glutamine and antibiotics (100 U/mL penicillin and 100 µg/mL streptomycin). When the cells reached sufficient confluence, they were washed with sterile phosphate buffered saline (PBS). Then, the cells were removed from the petri dish with a 10X stock solution of 2.5% sterile trypsin-ethylene diamine tetraacetic acid (Trypsin-EDTA).

Acibenzolar-S-methyl Treatment of SH-SY5Y cells

Firstly, SH-SY5Y cells were grown on 96 well-plates as 10⁴ cells/well and they were incubated at 37°C with 5% CO₂ for ~18-20 hours in order to obtain 60-80% confluency. Then, Acibenzolar-S-methyl (Syngenta) was applied at 1, 10, 15 and 20 mM concentrations on cultured cells in order to investigate the effect of different concentrations of acibenzolar-S-methyl on SH-SY5Y cells to be able to determine the half-maximal inhibitory concentration (IC₅₀). For this aim, treated cells were incubated at 37°C with 5% CO₂ for 24 and 48 hours.

MTS Cell Viability Assay

In order to investigate IC₅₀ value for acibenzolar-S-methyl on SH-SY5Y cells, MTS Cell Viability Assay (ab197010, Abcam) was used according to the manufacturers' instructions. Briefly, 20 µl MTS solution was added onto both cultured control SH-SY5Y cells and SH-SY5Y cells which were treated with different concentrations of acibenzolar-S-methyl and incubated for 24 and 48 hours. Then the cells were incubated for 3.5 hours at 37°C with 5% CO₂. After that, spectrophotometric analysis was performed at 490 nm wavelength for absorbance measurement

using SpectraMax® i3 Platform (Molecular Devices, LLC, San Jose, CA, USA). Cell viability data were obtained from three independent experiments and performed in triplicate wells.

Western Blotting

Total protein from acibenzolar-S-methyl-treated and control SH-SY5Y cells was extracted using Whole Cell Extraction Kit (2910, Millipore). The protein concentration was measured using the Qubit™ Protein Assay Kit (Thermo Fisher Scientific) and Qubit™ 3.0 Fluorometer. Equal amounts of samples (100 µg protein/ lane) were separated by SDS-PAGE (12.5% sodium dodecyl sulfate-polyacrylamide electrophoresis according to the molecular weight of the proteins) and transferred to nitrocellulose membrane (sc-3724, Santa Cruz Biotechnology) using Trans-Blot Turbo Transfer System (BioRad). The membranes were blocked in 5% BSA/tris buffered saline-tween (TBS-T) for 1 h at room temperature, stained with the primary antibodies overnight at 4 °C and with the secondary antibody for 1 h at room temperature. The following primary antibodies were used at 1:1000 dilutions; mouse monoclonal anti- MEK1/2 (sc-81504, Santa Cruz Biotechnology), mouse monoclonal anti-calnexin (sc-80645, Santa Cruz Biotechnology) and mouse monoclonal anti-caspase-3 (sc-271759, Santa Cruz Biotechnology) at 1:500 dilution in 5%BSA/TBS-T. After primary antibody incubation, membranes were washed 6 times with 1XTBS-T buffer at room temperature each for 5 min and incubated with 1:1000 diluted anti-mouse IgGκ light chain binding protein (m-IgGκ BP) conjugated to HRP (sc-516102, Santa Cruz Biotechnology) for 1 h at room temperature. Blots were visualized using Clarity Western ECL Substrate Kit (170-5061, BioRad). Blots were scanned and the densities of the specific bands were quantified and normalized with calnexin as internal loading control using ChemiDoc™ Imaging Systems (BioRad) and Lab 4.0 Software.

Integrative Pixel Analysis

For western blot images, Photoshop CS6 Software was used to analyze the relative intensity of the protein bands. The relative expressional value was normalized to '1' in untreated control cells for each protein that was analyzed, and relative protein expression fold changes of experimental groups were then calculated.

Statistical Analysis

Statistical Package for the Social Sciences (SPSS) Statistical Analysis Program was used and results were statistically analyzed according to "paired-2 tailed student's t-test". p-value under 0.05 was considered significant and p-value under 0.001 was considered very significant for all statistical analysis. Error bars in the graphs were generated using \pm s.d. values for MTS cell viability and western blotting analysis.

RESULTS

Acibenzolar-S-methyl Inhibited SH-SY5Y Neuroblastoma Cell Line Proliferation

The MTS assay showed that the cell proliferation of SH-SY5Y neuroblastoma cells was inhibited by acibenzolar-S-methyl

treatment in a time and dose-dependent manner (Figures 1A-C). Inverted microscopy images were taken by Leica DMI1 Inverted Microscope for cell culture (Leica, Wetzlar, Germany). Compared with the control group, acibenzolar-S-methyl at lower concentrations (1 mM) showed little inhibition effect on cell viability, while the proliferation levels of 10, 15, and 20 mM acibenzolar-S-methyl treatment groups were obviously decreased both at 24 and 48 h (data not shown for 48 hours). Since the amount of decrease is similar and adequate for half of cell growth inhibition (IC50) with both 24 h and 48 h incubation, we did not further conduct 72 h experiment. For SH-SY5Y cells, acibenzolar-S-methyl at the concentration of 10 mM caused half of cell growth inhibition (IC50) at 24 h (Figure 1A ***p < 0.001). Therefore, this concentration and this time point were used in all further experiments.

Acibenzolar-S-methyl Inhibited MEK1/2 Signaling in SH-SY5Y Neuroblastoma Cell Line

To investigate the effect of acibenzolar-S-methyl on MEK1/2 signaling, Western blotting was performed with 10 mM acibenzolar-S-methyl -treated SH-SY5Y cells using mouse monoclonal anti- MEK1/2 (sc-81504, Santa Cruz Biotechnology) and mouse monoclonal anti-calnexin (sc-80645, Santa Cruz Biotechnology) as the internal control. Blotting results showed that MEK1/2 signaling was significantly inhibited upon acibenzolar-S-methyl treatment (Figures 2A and 2B, *** p<0.001).

Acibenzolar-S-methyl Induced Caspase-3 Activity in SH-SY5Y Neuroblastoma Cell Line

The MTS assay showed that the viability of SH-SY5Y cells was significantly decreased upon acibenzolar-S-methyl treatment which was consistent with the decrease in MEK1/2 signaling. In order to reveal whether the decrease in cell viability is associated with the activation of a major apoptotic protein, caspase-3, active-caspase 3 expression was analyzed by western blotting using mouse monoclonal anti-caspase-3 (sc-271759, Santa Cruz Biotechnology) and mouse monoclonal anti-calnexin (sc-80645, Santa Cruz Biotechnology) as the internal control. Western blotting results indicated that active-caspase 3 levels significantly increased with acibenzolar-S-methyl treatment (Figures 3A and 3B, *** p<0.001).

DISCUSSION

One of the major underlying mechanisms of diseases such as cancer, autoimmunity, and diabetes is the disruption of intracellular signaling cascades controlling cellular behavior by organizing essential cellular activities in the cell. Thus, it has become the most important focus of cancer biology to better understand the molecular mechanisms of signal transduction deficiency and its relation to cancer development (1). In this regard, numerous studies showed that SA containing low dose aspirin is protective against many cancers such as colorectal, breast, gastric, lung cancers (2-6). The increasing number of evidence indicated that SA has an apoptotic action in cancer and this action may be due to its regulatory effect on mitogenic MEK1/2 signaling cascade (9). In many cancers, inhibiting

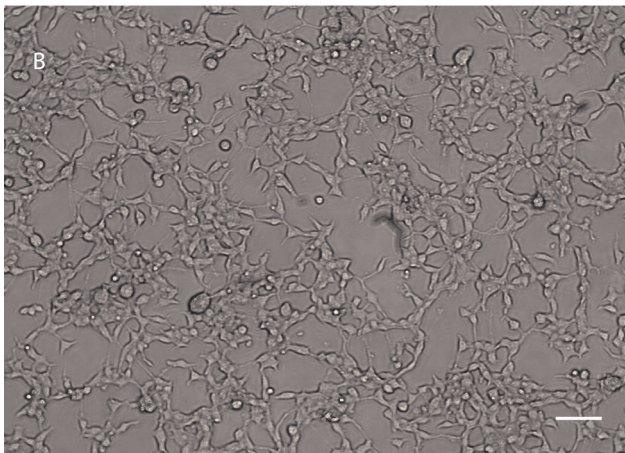
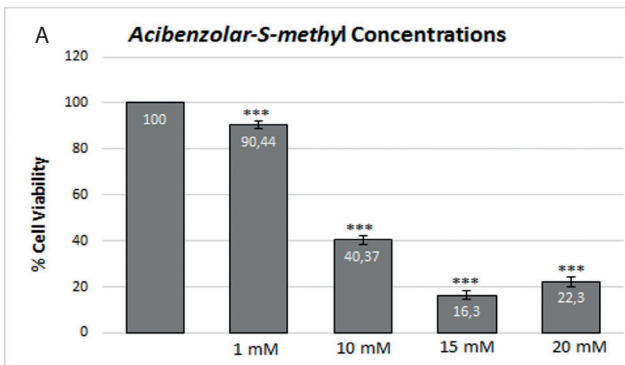


Figure 1. Inhibiting effects of acibenzolar-S-methyl on neuroblastoma cell line SH-SY5Y growth after exposure of 24h. **(A)** Acibenzolar-S-methyl was added to each well of a 96-well plate to yield the final concentrations of 1, 10, 15 and 20 mM. Cell viability was determined by the MTS assay and absorbance was measured at 490 nm using a microplate reader. The graph indicates quantitative analysis of MTS results which were expressed as percentages of proliferation compared to the control. Bar represents mean values \pm SD. *** $p < 0.001$ **(B)** Inverted microscopy image of control SH-SY5Y cells (Magnification: 10X). The scale bar is 50 μ m. **(C)** Inverted microscopy image of 10 mM- Acibenzolar-S-methyl treated SH-SY5Y cells (Magnification: 10X). The scale bar is 50 μ m.

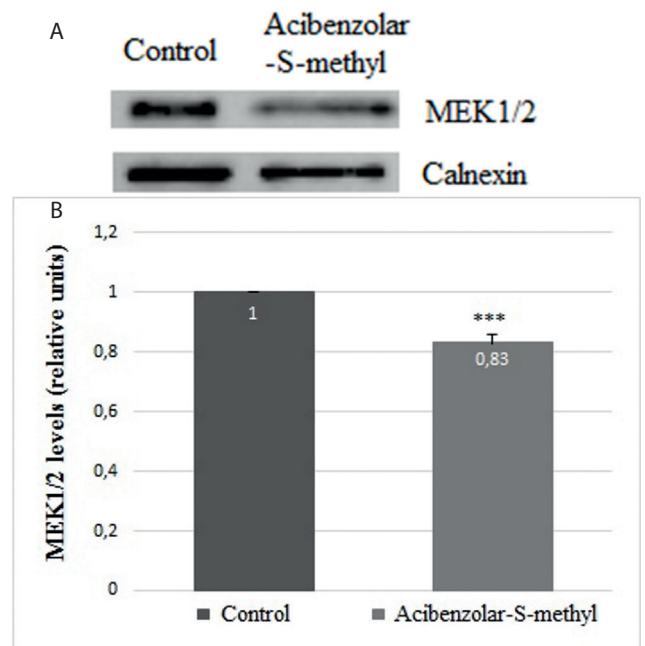


Figure 2. Inhibition effect of acibenzolar-S-methyl on MEK1/2 signaling in SH-SY5Y cells. **(A)** Western blotting membrane was probed with MEK1/2 antibody and calnexin antibody as internal control. **(B)** The graph indicates quantitative analysis of signals in Panel A. Band intensity of MEK1/2 was normalized according to calnexin. Numbers were calculated according to experimental/control ratio of MEK1/2 expression and results were represented as fold change. The bar represents mean values \pm SD. *** $p < 0.001$

MEK1/2 signaling results in apoptotic death, while in certain types of cancers such as melanoma, inhibiting MEK1/2 signaling conversely ends up with resistance to apoptosis (10). However, a limited number of studies have been focused on the effect of this signaling pathway in neuroblastoma cancer. Moreover, there is no study about the effect of SA on MEK1/2 signaling.

In the present study, we investigated the effect of SA analog acibenzolar-S-methyl on the MEK1/2 signaling and correlatively on cell viability in neuroblastoma cells and we showed that acibenzolar-S-methyl inhibited MEK1/2 signaling and this inhibition has the potential to induce the death of SH-SY5Y neuroblastoma cells.

Our results indicated that treating SH-SY5Y cells with 10 mM acibenzolar-S-methyl downregulated MEK1/2 signaling (Figures 2A and 2B) which is consistent with the results of another study conducted in A549 human lung cancer cells demonstrating the suppressing effect of SA on MAPK signaling (9).

Furthermore, we aimed to make a preliminary interpretation about the apoptotic effect of MEK1/2 signaling inhibition and cell viability reducing effect of acibenzolar-S-methyl in SH-SY5Y neuroblastoma cells. For this reason, we analyzed a very strong apoptosis indicator, active caspase-3 protein levels by western

blotting and we showed that there is a significant two-fold increase in active-caspase 3 levels of acibenzolar-S-methyl-treated and MEK1/2 inhibited SH-SY5Y cells (Figures 3A and 3B). This result correlates with the results of the studies performed with human colorectal tumor cell lines and hepatoma cell line showing dose- and time-dependent apoptotic effect of SA (7,8), and also with the results of the study performed with A549 human lung cancer cells demonstrating the suppressing and apoptotic effect of SA on MAPK signaling (9). On the other hand, our result is inconsistent with the results of the study showing that inhibiting MEK1/2 signaling contributes to resistance to apoptosis in melanoma cells (10). This contradiction implies that the molecular basis of cancer may be quite heterogeneous and thereby peculiar to each type of cancer. Thus, all these results strongly emphasize the importance of a better understanding of each cancer type-specific molecular mechanism in order to find an effective way to regulate the right targets for convenient treatment modalities. For this reason, although our active caspase-3 analysis implies that SA may be apoptotic against certain cancers, further apoptosis studies are needed to conclude a causal association between acibenzolar-S-methyl treatment and apoptosis in SH-SY5Y cells.

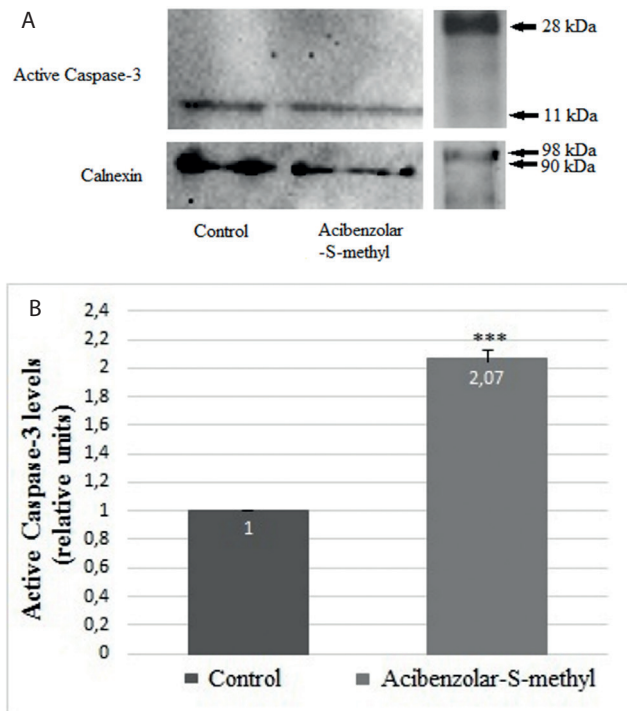


Figure 3. Activation of caspase-3 upon acibenzolar-S-methyl treatment in SH-SY5Y cells. (A) Western blotting membrane was probed with caspase-3 antibody and calnexin antibody as internal control. (B) Graph indicates quantitative analysis of signals in Panel A. Band intensity of caspase-3 was normalized according to calnexin. Numbers were calculated according to experimental/control ratio of caspase-3 expression and results were represented as fold change. The bar represents mean values \pm SD. *** $p < 0.001$

For further studies, investigating the utility of SA or its analogs as anti-cancer agents in neuroblastoma, non-cancerous healthy cell lines may be utilized to clearly analyze and compare the effects and side effects of SA in both cancerous and non-cancerous cells. Besides, *in vitro* studies should be performed with neuroblastoma patient samples as well as *in vivo* studies with disease models to analyze its exact effectiveness in living organisms.

CONCLUSION

In this study, we showed for the first time that SA analog acibenzolar-S-methyl negatively affects MEK1/2 signaling and decreases viability of SH-SY5Y neuroblastoma cells. Since there are studies demonstrating the cancer-promoting anti-apoptotic properties of SA in some cancers such as melanoma, to obtain a preliminary apoptosis data we performed active caspase-3 analysis and showed that it may be pro-apoptotic for SH-SY5Y neuroblastoma cells which needs further exploration. In this regard, considering the heterogeneous and idiosyncratic nature of each cancer type, this study has the potential to enable the selection of appropriate therapeutic targets and the development of effective diagnosis and treatment strategies for many cancers, particularly for neuroblastoma cancer.

Peer-review: Externally peer-reviewed.

Author Contributions: Conception/Design of study: A.Y.; Data Acquisition: A.Y.; Data Analysis/Interpretation: A.Y.; Drafting Manuscript: A.Y.; Critical Revision of Manuscript: A.Y.; Final Approval and Accountability: A.Y.

Conflict of Interest: The author declare that they have no conflicts of interest.

Financial Disclosure: This study was supported by grant to Ayşegül Yıldız from Muğla Sıtkı Kocman University Scientific Research Project Office, Research and Development Projects (Project No: 17/023).

Acknowledgements: I would like to thank Assoc.Prof.Dr. Esin Sakallı ÇETİN from Muğla Sıtkı Koçman University, Faculty of Medicine, Medical Biology Department and Prof. Dr. Arzu KARABAY KORKMAZ from Istanbul Technical University, Faculty of Science and Letters, Molecular Biology and Genetics Department for allowing me to use their laboratory infrastructure. I also would like to thank Prof. Dr. Ömür BAYSAL from Muğla Sıtkı Koçman University, Faculty of Science, Molecular Biology and Genetics Department for his generous gift of acibenzolar-S-methyl (Syngenta).

REFERENCES

1. Çoban ZD, Güran Ş. The role of signal transducing mechanisms in cancer diagnosis and treatment. *Cumhuriyet Medical Journal* 2013; 35: 302-10.
2. Brasky TM, Bonner MR, Moysich KB, Ambrosone CB, Nie J, Tao MH. Non steroidal anti-inflammatory drug use (NSAID) and breast cancer risk in the western New York Exposures and breast cancer (WEB) study. *Cancer Causes Control* 2010; 9: 1503-12.

3. Rothwell PM, Wilson M, Price JF, Belch JF, Meade TW, Mehta Z. Effect of Daily aspirin on risk of cancer metastasis: a study of incident cancers during randomised controlled trials. *Lancet* 2012; 379:1591-601.
4. Elwood PC, Morgan G, Pickering JE, Galante J, Weightman AL, Morris D, Kelson M, Dolwani S. Aspirin in the treatment of cancer: reductions in metastatic spread and in mortality: a systematic review and meta-analyses of published studies. *PLoS One*. 2016; 11(4): e0152402. doi:10.1371/journal.pone.0152402
5. Klessig DF. Newly identified targets of aspirin and its primary metabolite, salicylic acid. *DNA Cell Biol* 2016; 35(4):163-6. doi:10.1089/dna.2016.3260
6. Giampieri R, Restivo A, Pusceddu V, Del Prete M, Maccaroni E, Bittoni A, Faloppi L, Andrikou K, Bianconi M, Cabras F, Berardi R, Zorcolo L, Scintu F, Cascinu S, Scartozzi M. The role of aspirin as antitumoral agent for heavily pretreated patients with metastatic colorectal cancer receiving capecitabine monotherapy. *Clin Colorectal Cancer* 2016;16(1):38-43. doi:10.1016/j.clcc.2016.07.011
7. Liu Y, Wang Y, Li L, Hu Y, Ge S, Li K, Wang S. The apoptotic inducible effects of salicylic acid on hepatoma cell line: relationship with nitric oxide signaling. *J Cell Commun Signal* 2017; 11: 245-53.
8. Elder DJ, Hague A, Hicks DJ, Paraskeva C. Differential Growth Inhibition by the aspirin metabolite salicylate in human colorectal tumor cell lines: Enhanced apoptosis in carcinoma and in vitro-transformed adenoma relative to adenoma cell lines. *Cancer Research* 1996; 56: 2273-76.
9. Pan MR, Chang HC, Hung WC. Non-steroidal anti-inflammatory drugs suppress the ERK signaling pathway via block of Ras/c-Raf interaction and activation of MAP kinase phosphatases. *Cell Signal* 2008; 20(6):1134-41.
10. Haydn JM, Hufnagel A, Grimm J, Maurus K, Scharf M, Meierjohann S. The MAPK pathway as an apoptosis enhancer in melanoma. *Oncotarget* 2014; 5(13): 5040-53.
11. Dhillon AS, Hagan S, Rath O, Kolch W. MAP kinase signalling pathways in cancer. *Oncogene* 2007;26(22):3279-90.
12. Mattingly RR, Milstein ML, Mirkin BL. Down-regulation of growth factor-stimulated MAP kinase signaling in cytotoxic drug-resistant human neuroblastoma cells. *Cell Signal* 2001; 13(7):499-505.
13. Maris JM. Recent advances in neuroblastoma. *N Engl J Med* 2010; 362(23):2002.
14. Lubanska D, Market B, de Carvalho A., Mikkelsen T, Fidalgo da Silva E, Porter LA. The atypical cell cycle regulator Spy1 suppresses differentiation of the neuroblastoma stem cell population. *Oncoscience* 2014; 25: 64-7.

Genetic Diversity of Gazelles (*Gazella marica* and *Gazella gazella*) in Southeast Turkey: A Special Emphasis on Ongoing Conservation Studies of *Gazella marica* in Turkey*

Fikriye Dilan Saatoglu¹ , Melis Denizci Oncu² , Hasan Emir³ , Taner Hatipoglu³ ,
Sinan Can Acan⁴ , Tolga Kankilic⁵ , Inci Togan¹ , Evren Koban Bastanlar^{2,6} 

¹Middle East Technical University, Graduate School of Natural and Applied Sciences, Department of Biological Sciences, Ankara, Turkey

²TUBITAK Marmara Research Center, Genetic Engineering and Biotechnology Institute, Gebze, Kocaeli, Turkey

³Ministry of Agriculture and Forestry, General Directorate of Nature Conservation and National Parks, Wildlife Department, Ankara, Turkey

⁴Middle East Technical University, Computer Center, Ankara, Turkey

⁵Aksaray University, Faculty of Arts and Science, Department of Biology, Aksaray, Turkey

⁶Ege University, Faculty of Science, Department of Biology, Izmir, Turkey

ORCID IDs of the authors: F.D.S. 0000-0003-3936-287X; M.D.O. 0000-0001-9140-1544; H.E. 0000-0002-2563-6545; T.H. 0000-0002-6010-7315; S.C.A. 0000-0002-5534-0024; T.K. 0000-0002-9058-5166; I.T. 0000-0002-2150-772X; E.K.B. 0000-0002-6296-9728

Please cite this article as: Saatoglu FD, Denizci Oncu M, Emir H, Hatipoglu T, Acan SC, Kankilic T, Togan I, Koban Bastanlar E. Genetic Diversity of Gazelles (*Gazella marica* ve *Gazella gazella*) in Southeast Turkey: A Special Emphasis on Ongoing Conservation Studies of *Gazella marica* in Turkey. Eur J Biol 2019; 78(2): 88-102. DOI: 10.26650/EurJBiol.2019.0014

ABSTRACT

Objective: The genetic diversity parameters for gazelle populations sampled in Turkey were estimated to assess the effects of captive breeding on the populations' gene pools and effective population sizes.

Materials and Methods: Four individuals from a recently discovered *Gazella gazella* population in Hatay and two captive gazelle populations were sampled (the Kizilkuyu State Farm (n=48) and the Erikçe State Farm (n=25)) and analyzed using nuclear DNA, mtDNA and Y-chromosome markers.

Results: The mtDNA *cyt-b* partial sequence analysis assigned the Erikçe and Kizilkuyu samples to *Gazella marica*. The structure analysis differentiated significantly between them, and revealed samples originating from wild population. Both, the Y-chromosome INRA126 locus sequences of *Gazella gazella* and *Gazella marica* males and the mtDNA partial *cyt-b* region RFLP analysis from all the samples distinguished the two gazelle species from each other. Based on microsatellites, the estimated effective population sizes were 9.7, 8.9 and 6.4 for the Kizilkuyu, Erikçe and Hatay populations, respectively. When the Kizilkuyu and Erikçe populations (where severe inbreeding depressions seems to be occurring already) were pooled, the estimated Ne was 24.5. All these estimates were too small for the sustainability of either individual or pooled populations in the wild or even in captivity.

Conclusion: The markers used in the study provided information on two of the gazelle species (*Gazella marica*, and *Gazella gazella*): their species identity, degree of divergences, effective population sizes and the presence of admixture within the populations. These results turned out to be invaluable in terms of their contribution to future studies for the conservation of these species.

Keywords: Conservation Genetics, Biodiversity, Phylogeny, Microsatellites, mtDNA, Y-Chromosome, RFLP Analysis

* This article was derived from the MSc Thesis study completed by F. Dilan Saatoğlu in context of the TUBITAK KAMAG 109G016 project and with the contributions from all the co-authors.



Corresponding Author: Evren Koban Bastanlar E-mail: evrenkoban@yahoo.com
Submitted: 24.06.2019 • **Revision Requested:** 28.06.2019 • **Last Revision Received:** 30.06.2019 • **Accepted:** 01.07.2019

© Copyright 2019 by The Istanbul University Faculty of Science • Available online at <http://ejb.istanbul.edu.tr> • DOI: 10.26650/EurJBiol.2019.0014

INTRODUCTION

Gazelles belong to the genus *Gazella* in the Bovidae family. They are the largest and the most diverse family of ungulates (1) in the *Artiodactyla* order, and are distributed from Africa to Northern Asia including South-eastern Anatolia and the Arabian Peninsula (2). Due to the rapid decrease in their population sizes in the wild, many gazelle species are on the IUCN Red List of Threatened Species as reported by the IUCN/SSC Antelope Specialist Group in 2008. For this reason, conservation studies (e.g. captive breeding programs, reintroduction/introduction studies) have been initiated for various gazelle species (3).

The plains of Central and Southeastern Anatolia with hilly geographical structures as well as the climate conditions of the region are highly suitable for gazelle species to inhabit that region. Kasperek (4) reviewed the documents on the existence of gazelles in Anatolia and reported that the first known reports were from Bolvadin (Afyon), in Central Anatolia by the English surgeon William Francis Ainsworth, in 1839. Furthermore, Kasperek (4) provides documents on gazelle observations from the 19th century addressing plains around the Adana region suggesting the existence of two different gazelle species based on their morphological differences. These two species were thought to be *Gazella dorcas* (an African species) and *Gazella subgutturosa* (mainly distributed in the western Asia and the northern Arabian Peninsula). Yet, Kumerloeve et al. (5) suggested that one of these species should have been *Gazella gazella*, a dominant species of the Levantin and the Arabic Peninsula, not the Dorcas Gazelle (*Gazelle dorcas*), as there is no evidence that they spread further than Lebanon. Moreover, Kumerloeve (6, 7) suggested that gazelles were distributed in the area between the border of Turkey-Syria and the Northern plains of Şanlıurfa, and they reported gazelle observations especially around Ceylanpınar. Having worked in the field, Turan (8) defined the distribution of the gazelles from Northern Hatay (Kırıkhan) to Şırnak (Cizre), which corresponds the south-eastern border of Turkey. Although Turan (8) identified the gazelle species he observed as *Gazella subgutturosa*, he had his suspicions about the presence of another gazelle species, *Gazella dorcas*, in the same region. Yet, he did not reject Kumerloeve's view on the distribution of Dorcas gazelles. Lastly, he reported previous sightings of gazelles in Iğdır, Eastern Anatolia.

There are karyotypic (9) and habitat preference studies (10) on gazelles around Şanlıurfa. Morphological studies grouped Anatolian gazelles into *Gazella subgutturosa* species (4, 6-8, 10-14). However, a phylogenetic study based on mitochondrial DNA (mtDNA) cytochrome *b* gene (*cyt-b*) sequence has shown the existence of another gazelle species, the Mountain Gazelle (*Gazella gazella*), in Kırıkhan, Hatay (see Figure 1) (15). Furthermore, based on mtDNA *cyt-b* sequence analysis, they (15) grouped Southeast Anatolian gazelles as *Gazella subgutturosa marica* not as *Gazella subgutturosa*, as suggested by Wronski et al. (16). Throughout the text, we referred to this species as *Gazella marica*, rather than *Gazella subgutturosa marica* since it was shown to be phylogenetically more closely related to the

North-African species (e.g. *Gazella cuvieri* and *Gazella leptoceros*) based on the sequence analyses of the mtDNA cytochrome *b* gene. They emphasized considering *Gazella marica* as a separate species due to the fact that misidentifications in conservation studies would lead to severe consequences (17, 18). For example; studies based on mtDNA *cyt-b* and D-loop sequences pinpointed the possible existence of reciprocally monophyletic lineages of two *Gazella gazella* populations (19, 20). Moreover, one of these populations was found to be confined to a restricted region on the Golan Heights. Therefore, in terms of conservation purposes, this population confined in a small area can be treated as a separate species.

Among the mammal species, there seems to be more complexity in the genus *Gazella*, and the number of studies is low (21, 22). There are still unsolved conflicts in their taxonomy based on morphometric, phenotypic and genetic data (23). Table 1 below describes the common names and the scientific names for the extinct and extant gazelle species present in the literature. It also summarizes the geographical distribution of these gazelle species in the old continents.

Table 1. Distribution and common names of Anatolian gazelles: those which existed in the past or exist currently

Common Name(s)	Scientific Name	Distribution Area
Dorcas Gazelle	<i>Gazella dorcas</i>	Sahelo-Saharan Region, Southern Israel, Syria, Jordan
Mountain Gazelle Idmi Arabian Gazelle	<i>Gazella gazella</i>	Mountains near the Coastal Area of South-eastern Turkey, Lebanon, Palestine, Golan, Western Jordan
Persian Gazelle Goitered Gazelle Black-tailed Gazelle	<i>Gazella subgutturosa</i>	Tigris/Euphrates Basin, Caucasus, Iran, Turkmenistan, China, Mongolia
Sand Gazelle Reem/Rheem Arabian Sand Gazelle	<i>Gazella marica</i> / <i>Gazella s. marica</i>	Iraq, Jordan, Turkey, Syria Oman, Southern Arabia, United Arab Emirates

The population sizes of *Gazella marica* groups are in continuous decline and there are no wild subpopulations whose size exceeds 1000 individuals. Therefore IUCN's Antelope Specialist Group declared them as "Vulnerable" based on the criteria, C2a(i). Despite the law having banned illegal hunting since

1957, the estimated population sizes of gazelles in Ceylanpinar, Şanlıurfa saw a very sharp decline (with only approximately 300 individuals remaining out of 3000) between the years 1968 and 1978 (13, 24). Following this rapid decline, the Ceylanpinar State Farm was founded with 5 individuals from the wild in 1978 ("1" in Figure 1). Then, the Kızılkuyu and Erikçe State Farms ("2" and "3" in Figure 1, respectively) were established (n=24 in 1998 and n=29 in 1999, respectively) with individuals taken from Ceylanpinar State Farm. The last State Farm, Hekimhan ("4" in Figure 1), was founded in 2005 with 8 individuals taken from Kızılkuyu State Farm. Afterwards, Kızılkuyu State Farm received some *Gazella marica* stock from Ceylanpinar in 2009 ("5" in Figure 1). Moreover, Erikçe State Farm received *Gazella marica* stock taken from the wilds of Kızılkuyu in 2009 and 2010 ("6" in Figure 1). Meanwhile, reintroduction studies on the Kızılkuyu wild from the Kızılkuyu State Farm were carried out several times between 2005 and 2014. Based on the records of the Ministry of Agriculture and Forestry (hereafter to be referred to as the Ministry), the death of juveniles can occur especially in the cold winter seasons on the state farms, even though feeding supplements are always provided.

In this study, samples taken from two captive *Gazella marica* populations were analyzed based on 17 autosomal microsatellite loci, partial mtDNA *cyt-b* region and one

Y-chromosome SSR locus (INRA126) sequencing. In addition, four individuals from the *Gazella gazella* population in Kırıkhan, Hatay were analyzed based on the same markers. The study objectives were as follows:

- (i) Estimation of the genetic diversity within and between gazelle populations to evaluate the effects of captive-breeding on both populations in terms of their gene pools and effective population sizes in order to help developing conservation strategies for these populations.
- (ii) To confirm the presence of both species, *Gazella marica* and *Gazella gazella*, in the Southeastern Anatolia based on the mtDNA *cyt-b* sequences of the samples collected independent of the previous studies.
- (iii) To identify the endonucleases to be used in the Restriction Fragment Length Polymorphism (RFLP) analysis of mtDNA *cyt-b* fragments as a quick method to discriminate between the two gazelle species of Anatolia.
- (iv) Analyzing the diversity among two gazelle species based on a Y chromosome SSR locus, to be carried out for the first time in current literature.

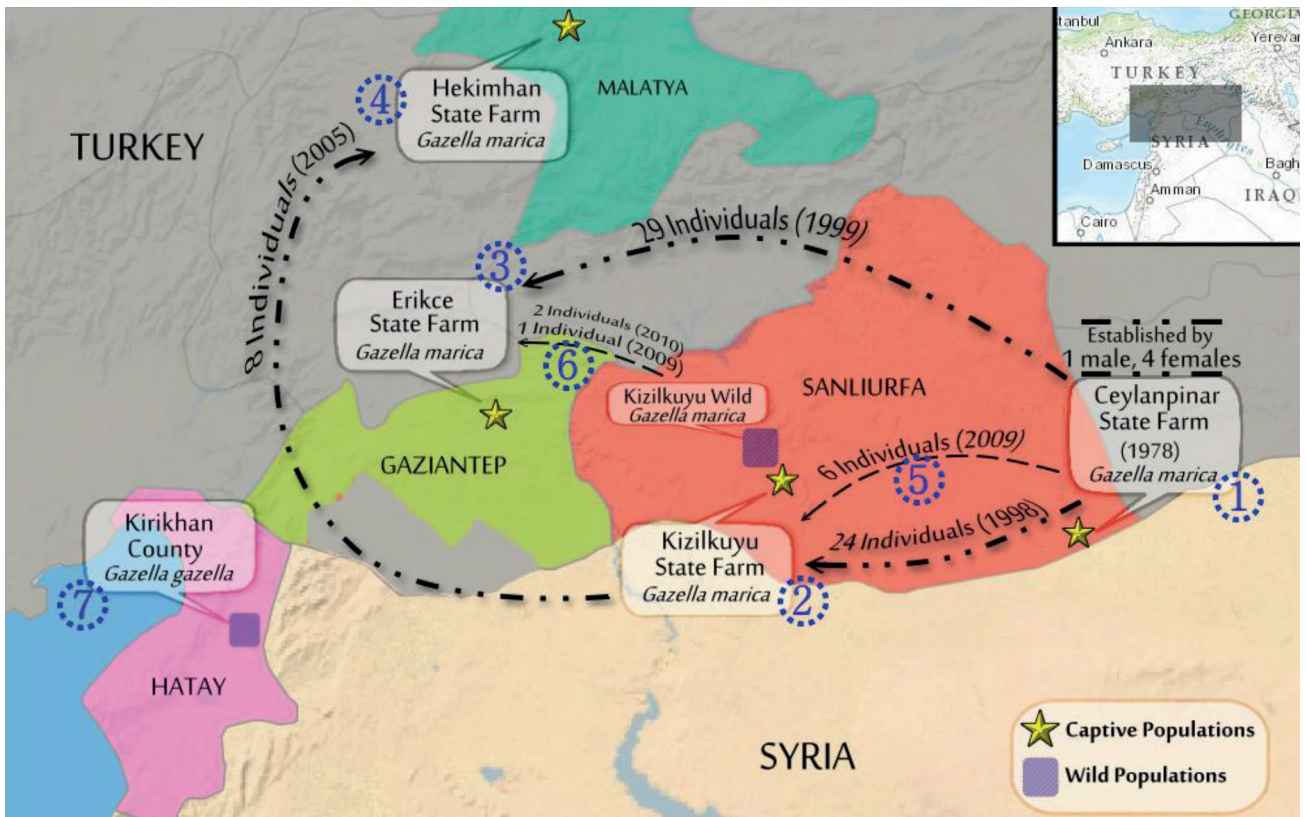


Figure 1. The map showing the locations of *Gazella marica* breeding State Farms, the wild *Gazella marica* population and the wild *Gazella gazella* population. The foundation years for the State Farms, the number of starting individuals and the source populations (the direction is shown by the arrows) are also indicated on the map.

The Ministry's plan for Erikçe State Farm is to transfer all the *Gazella marica* individuals to Aralık and establish a wild self-sustaining *Gazella gazella* population there. All the first group of individuals (n=25) introduced to Aralık (İğdir) were genetically analyzed in the present study. The results of the present study will be the springboard for a long term monitoring study on the re-introduced İğdir population.

MATERIALS AND METHODS

The blood and tissue samples were collected with the approval of the Selçuk University Veterinary Faculty Ethics Committee (permit number: 2009/041) and were collected by the GDNPNP.

Samples and DNA Extraction

A total of 77 individuals were sampled (blood samples collected in 10 ml vacuum tubes containing K₃EDTA and/or tissue samples collected in ethanol) from wild-living *Gazella gazella*, and captive *Gazella marica* populations by the Ministry and sent to our laboratory. *Gazella marica* samples came from two different locations: Kızılkuyu (n=48; State Farm and wild population in total) and Erikçe State Farm (n=25). The samples from the Kızılkuyu wild population were from individuals shot by licensed hunters during hunting seasons. Only four samples in the present study belonged to the *Gazella gazella* species (Kırıkhan, Hatay) provided by

Table 2. The names of the microsatellite loci used in the study, source organisms and related references

Loci	Primer 5'-3'	Source of Loci	Reference
RT1	TGCCTTCTTTCATCCAACAA CATCTTCCCATCCTCTTTAC	Caribou	27
ETH10	GTTCAGGACTGGCCTGCTAACAA CCTCCAGCCCATTCTCTTCTC	Bovine	28
OarFCB304	CCCTAGGAGCTTTCATAAAGAATCGG CGCTGCTGTCAACTGGGTCAGGG	Ovine	29
MM12	CAAGACAGGTGTTTCAATCT ATCGACTCTGGGGATGATGT	Bovine	30
BM848	TGGTTGGAAGGAAAACCTGG CCCTCTGCTCCTCAAGACAC	Bovine	31
BMC1009	GCACCAGCAGAGAGGACATT ACCGGCTATTGTCCATCTTG	Bovine	32
INRA40	TCAGTCTCCAGGAGAGAAAAC CTCTGCCCTGGGGATGATTG	Bovine	33
IDVGA29	CCCACAAGGTATCTATCTCCAG CCAAGAAGGTCCAAAGCATCCAC	Bovine	34
BM4505	TTATCTTGCTTCTGGGTGC ATCTTCACTTGGGATGCAGG	Bovine	31
ETH152	TACTCGTAGGGCAGGCTGCCTG GAGACCTCAGGGTTGGTGATCAG	Bovine	35
INRABERN172	CCACTTCCCTGTATCCTCT GGTGCTCCCATTGTGTAGAC	Goat	36
TGLA122	CCCTCCTCCAGGTAATCAGC AATCACATGGCAAATAAGTACATAC	Bovine	37
ILSTS005	GGAAGCAATGAAATCTATAGCC TGTTCTGTGAGTTTGTAAAGC	Bovine	38
BM757	TGGAACAATGTAACCTGGG TTGAGCCACCAAGGAACC	Bovine	31
BM143	ACCTGGGAAGCCTCCATATC CTGCAGGCAGATTCTTTATCG	Bovine	31
CSSM39	AATCGGAACCTAGAATATTTGAG AGATAAAATGTGAGTGTGGTCTCC	Bovine	39
CSSM43	AAAACCTCTGGGAACCTGAAAATA GTTACAAATTTAAGAGACAGAGTT	Bovine	39

the locals in 2013-2014. The DNAs were extracted from blood samples using the standard phenol:chloroform:isoamyl alcohol method (25:24:1) (25). The DNAs from tissue samples were extracted using the CTAB method adapted from Winnepenninckx et al (26) at TUBITAK MRC laboratories. Stock DNA samples were stored at -20°C, diluted DNA aliquots were stored at +4°C for short-term use.

Microsatellite DNA Analysis

Seventeen microsatellite loci chosen from the literature (Table 2) were PCR amplified. After being checked by agarose gel electrophoresis (1%, 1X TAE), the PCR products were genotyped using the Beckman Coulter CEQ8800 Genetic Analysis System based on capillary electrophoresis.

The genotypic data was first analysed for possible genotyping errors during the experimental stage (e.g. the existence of null alleles, short allele dominance) using MICRO-CHECKER 2.2.3 software (40). In addition, Linkage Disequilibrium (LD) was tested (settings: 10.000 Markov Chain, 1.000 dememorization steps and 5.000 number of batches) using the Arlequin v.3.5.1.3. software (41).

The expected and observed heterozygosity (H_e , H_o) parameters as well as deviations from the Hardy-Weinberg Equilibrium (HWE) were calculated using Arlequin v.3.5.1.3 software (41). The allelic richness per locus was estimated using the FSTAT V.2.9.3 package program (42) and the allelic richness of the populations was tested for significance using the Wilcoxon-Signed rank test (43). The Polymorphism Information Content (PIC) for each locus was estimated using CERVUS 3.0 (44). Moreover, the within and among population differentiations based on F-statistics (45) were analyzed using the FSTAT V.2.9.3 package program (42). For assessing any possible genetic admixture, STRUCTURE v2.3.4 (46) was used (settings: 10.000 burn-in, $K=2-7$ with 10 iterations). Both Evanno et al's (47) and Tapio et al's (48) methods were employed for estimating the most likely K value, representing the number of differing gene pools. Furthermore, similarity coefficients were obtained by CLUMPP v1.1.2 (49) and Distruct v1.1 (50) was used to display the graphic results obtained from STRUCTURE Software. Lastly, Effective Population Size (N_e) was estimated using Ne Estimator V.2.01 (51) for the gazelle populations in the present study.

mtDNA Cytochrome b (cyt-b) Region

The partial *cyt-b* region was amplified by the primers L14724: 5'-CGAAGCTTGATATGAAAAACCATCGTTG-3' (52) and H15149:

5'-AAACTGCAGCCCCTCAGAATGATATTTGCCTCA-3' (53). Then, PCR amplicons were bidirectionally sequenced using the same PCR primers. The sequencing reactions were prepared using Beckman Coulter's GenomeLab Dye Terminator Cycle Sequencing Quick Start Kit. Afterwards, the PCR products were first ethanol precipitated, and then the chromatograms were collected by capillary electrophoresis on the Beckman Coulter CEQ8800 Genetic Analysis System. The sequences were read by the Sequencing Analysis program implemented within the system. The chromatograms were checked and individual contigs were obtained by ChromasPro software (<http://www.technelysium.com.au/ChromasPro.html>). After exporting the consensus sequences obtained from the contigs in FASTA format, the sequences were aligned, edited and trimmed using BioEdit software version 7.2.5 (54) for further statistical analysis. Based on this data, first, the best nucleotide substitution model was detected as Kimura 2 Parameter with gamma distribution ($G=0.23$) and then a Neighbor joining (NJ) tree was constructed with 1000 bootstrap values using software MEGA version 6.06 (55). Finally, after examining the sequences for possible RFLP, these partial mtDNA *cyt-b* gene PCR products were cut by two restriction endonucleases (*HaeIII*, *HinfI*), which had been suggested for distinguishing between the gazelle species (18).

Y-Chromosome Analysis

Two microsatellite loci (Table 3) situated on the Y- chromosome were amplified by PCR and then the purified PCR products were sent to the private RefGen Company (<http://www.refgen.com/>) for Sanger sequencing using the platform ABI PRISM® 3100 Genetic Analyzer System.

Estimating Life Parameters

The birth and death rates for the State farms were estimated using the data provided by the Ministry to gain a general idea about their current trend as both of these parameters are affected by inbreeding in captive populations. The birthing period for gazelles is from April to the end of May. To calculate the birth rate; first the populations' sizes were estimated before and after the birthing period. Then the absolute difference between these population sizes was taken. Finally, this number (the difference) was divided into the number of females present before the birth. Moreover, the death rate was calculated by dividing the number of deaths into the census size of the populations including newborns of that year. The trends in these estimated parameters were compared with the other findings of the present study.

Table 3. The Y-chromosome microsatellite loci used in the study: the primer sequences, the source organism and related references

Loci	Primer 5'-3'	Source Organism	Reference
INRA126	GTTGTTGCCTCTGCAGAGTAGG	Bovine	33
	GACACTCTTTCTATTTTCAAGG		
UMN0103	ACACAGAGTATTACCTGAG	Bovine	56
	ATTACTCTGGGTCAAAGCAC		

RESULTS

Genetic Variation Based on Microsatellite Loci

Among the 17 microsatellite markers, BM143 and CSSM39 had the lowest number of alleles, whereas INRA40 and OarFCB304 had the highest. The observed allele ranges and the number of observed alleles per population for each locus are given in Table 4.

Table 4. The allele ranges for each loci and the number of alleles per locus per population observed in the study

Locus / Pop.	Allele Range	<i>Gazella gazella</i>		<i>Gazella marica</i>	
		Kızilkuyu (n:48)	Erikçe (n:25)	Total	Hatay (n:4)
RT1	196-200	3	3	3	2
ETH10	213-245	10	8	10	6
OARFCB304	144-174	10	9	12	4
MM12	79-81	2	2	2	2
BM848	207-229	5	5	6	2
BMC1009	274-300	8	5	8	4
INRA40	201-297	12	7	12	5
IDVGA29	99-132	3	1	3	5
BM4505	196-254	10	5	10	1
ETH152	192-210	1	1	1	5
INRABERN172	229-251	8	6	9	5
TGLA122	122-126	3	3	3	3
ILSTS005	179-195	5	3	6	6
BM757	159-201	4	2	4	2
BM143	84-114	1	1	1	1
CSSM39	177-183	1	2	2	1
CSSM43	246-264	9	7	9	4

Presence of null alleles and LD

There was a signal indicating the possibility of null allele in the Kızilkuyu population for the locus IDVGA29 when the data was analyzed using MICROCHECKER 2.2.3 software (40). Therefore, this locus was excluded from further analysis. Linkage Disequilibrium analysis with Bonferroni Correction for the pairwise comparisons of the remaining 16 loci within the study populations did not result in a significant deviation. In addition, there was no significant deviation from the HWE detected in any locus in any population.

Diversity Estimates and Allelic Richness

The average expected heterozygosity per locus per population was calculated as 0.69 for the Kızilkuyu *Gazella marica* population, 0.63 for the Erikçe *Gazella marica* population and 0.602 for the Hatay *Gazella gazella* population. The average observed and expected heterozygosity estimates per locus per population and overall averages are given in Table 5.

For the Kızilkuyu population, thirteen out of sixteen allelic richness (AR) estimates were equal to or slightly higher than the Erikçe population, and when tested, a significant difference was detected between the Kızilkuyu and Erikçe populations ($p < 0.05$) using the Wilcoxon-Signed rank test (43) based on AR estimates. The average maximum and minimum mean allelic richness estimates among the loci analysed were 9.338 for OarFCB304, and 1.000 for both ETH152 and BM143. In addition, the most informative locus based on PIC estimates was ETH10 (0.801) and the least informative ones were ETH152 and BM143 (0.000). As larger samples are expected to have more alleles, a rarefaction algorithm was employed in these estimates to correct for sample size differences.

The pairwise F_{ST} measures were estimated for three of the populations (Kızilkuyu, Erikçe and Hatay) and the pairwise genetic differentiation between the study populations was found to be statistically significant ($p < 0.01$, see Table 6) after applying permutation tests with Bonferroni Correction. However, it must be noted that the pairwise F_{ST} estimate for the Kızilkuyu and Erikçe populations (0.0444) is < 0.05 ; therefore, it can be considered as "non-significant" when Wright's scale (57) is applied since it interprets F_{ST} estimates as non-significant for values < 0.05 , significant for values between 0.05 and 0.25, and highly significant for values > 0.25 .

Structure Analysis

The genotypic data was run on STRUCTURE v2.3.4 (46) software using these settings: 10.000 burn-in, $K=2-7$, and 10 iterations. First, the most likely K value was estimated using the Delta K method (47). The results suggested that the most likely number of genetic groups is $K=3$. The similarity test (48) run by CLUMPP software (49) revealed two probable K values (2 and 4) as the constructed graphics revealed two highest peaks for H'. Afterwards, the microsatellite data was run on STRUCTURE software again by setting the K parameter as "2-4", and the resulting graphics were displayed by DISTRUCT software (Figure 2). When $K=2$, the individuals were grouped with respect to their origin of species: *Gazella gazelle* and *Gazella marica*. When $K=3$, a genetic heterogeneity was detected between the individuals of the *Gazella marica* populations. However, differentiation between the two *Gazella marica* populations of Kızilkuyu and Erikçe (Figure 2) are evident with $K=4$. The four major components in the three populations were depicted by blue, purple, red and green. Blue is exclusively associated with the Hatay population (*Gazella gazella*). Kızilkuyu seemed to be represented mainly by purple whereas green is associated mainly with Erikçe.

When $K=4$, there were a few differentiated individuals (depicted in red) present in the *Gazella marica* populations, but mostly in the Kızilkuyu population, which were indicated with numbers (3-10, 12 and 13) (Figure 2). All these individuals (3-10, 12 and 13) have more than 30% of the genetic component displayed in red. According to the records provided by the Ministry, most of these numbered individuals (1 to 8 and 10 to 12) were hunted individuals from the wild Kızilkuyu population. Therefore, it can be anticipated that the red color may, in general, be

Table 5. The average expected and observed heterozygosity (He, Ho) parameters estimated per locus per population and average estimates per population as found in the study

Locus	Kızilkuyu (n:48)		Erikçe (n:25)		Hatay (n:4)	
	He	Ho	He	Ho	He	Ho
RT1	0.516	0.5	0.581	0.64	Monomorphic	
ETH10	0.846	0.813	0.825	0.88	0.857	1
OARFCB304	0.840	0.729	0.786	0.76	Monomorphic	
MM12	0.379	0.375	0.444	0.32	Monomorphic	
BM848	0.654	0.625	0.692	0.64	0.679	0.5
BMC1009	0.803	0.851	0.776	0.88	0.536	0.75
INRA40	0.850	0.792	0.812	0.72	Monomorphic	
BM4505	0.768	0.666	0.573	0.6	Monomorphic	
ETH152	Monomorphic		Monomorphic		0.571	0
INRABERN172	0.719	0.813	0.816	0.96	0.429	0.5
TGLA122	0.651	0.681	0.492	0.64	Monomorphic	
ILSTS005	0.522	0.458	0.605	0.64	0.571	0.5
BM757	0.551	0.583	0.510	0.44	Monomorphic	
BM143	Monomorphic		Monomorphic		0.571	1
CSSM39	Monomorphic		0.115	0.12	Monomorphic	
CSSM43	0.844	0.792	0.802	0.76	Monomorphic	
Population Average	0.69	0.6675	0.6304	0.6429	0.602	0.6071

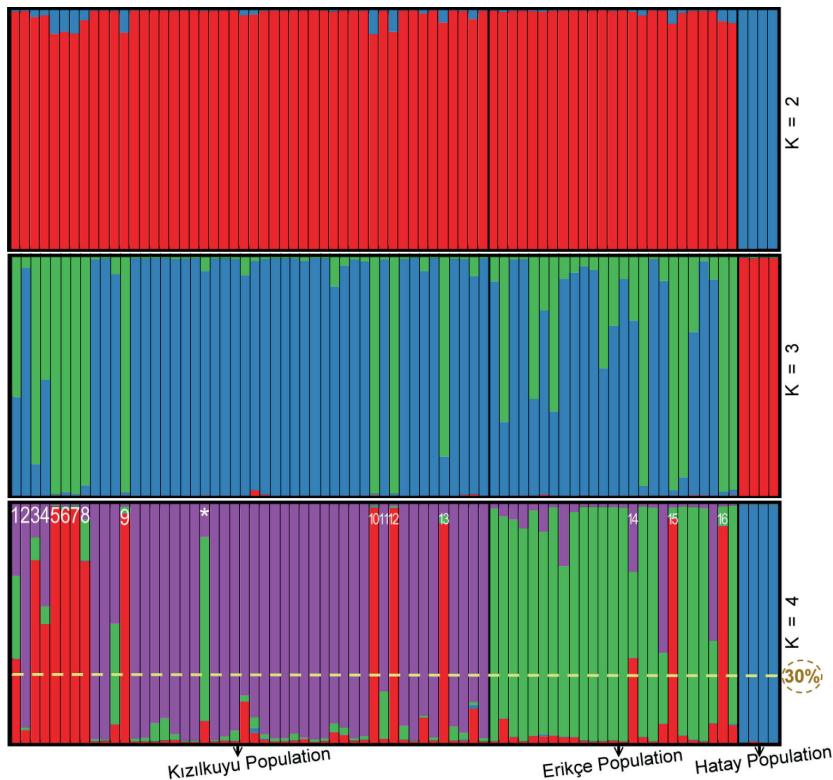


Figure 2. An admixture analysis of the three populations was obtained using the software STRUCTURE v2.3.4 (45). Each individual is represented by a bar plot in the figure above. For K=4, the genetic components within individuals are represented by 4 colors: Purple, green, red and blue. The numbered individuals from 1 to 8 and from 10 to 12 in the Kızilkuyu population are hunted individuals from the wild Kızilkuyu population based on the information provided by the Ministry. The individual from Kızilkuyu population indicated by a star is heavily represented by (~75%) a green color. The numbered individuals from the Erikçe population (14-16) (those exhibiting more than 30% of their genetic component) were depicted in red.

Table 6. Pairwise F_{ST} estimates (above the diagonal) with p values (below the diagonal) based on 3000 permutations and Bonferroni corrections

Pairwise F_{ST}	Kızilkuyu (n:48)	Erikçe (n:25)	Hatay (n:4)
Kızilkuyu (n:48)		**	**
Erikçe (n:25)	0.0444		**
Hatay (n:4)	0.4378	0.4588	

($p^{**}<0.01$)

marking the individuals from the Kızilkuyu wild population. On the other hand, the individual indicated with a star in the Kızilkuyu population exhibited mostly (~75%) a green color. Thus, it seems to be more similar to members of the Erikçe population than to those of the Kızilkuyu population. Moreover, the numbered individuals in the Erikçe population (14-16) had a genetic component (>30%) displayed in red associated with the wild Kızilkuyu members, suggesting that these individuals had their origins in the wild Kızilkuyu population.

Effective Population Size Estimation

The effective population sizes were estimated as 9.7 for the Kızilkuyu population (*Gazella marica*, n=48), 8.9 for the Erikçe population (*Gazella marica*, n=25) and 6.4 for the Hatay population (*Gazella gazelle*, n=4). When we pooled the Kızilkuyu and Erikçe populations, the estimated N_e was 24.5. Furthermore, we re-estimated N_e for the Kızilkuyu population after removing the individuals reported as hunted due to the possibility that they might have originated from the Kızilkuyu wild region rather than from the state farm, which decreased from 9.7 to 8.9.

Sequence Variation at Partial mtDNA Cyt-b Gene

The mtDNA *cyt-b* partial fragments (381 bp long) of 77 individuals were successfully amplified and sequenced. No polymorphisms were found within this 381 bp region based on sequences either within or between the populations of the *Gazella marica* samples; nor were any polymorphisms detected within the *Gazella gazelle* sample (n=4). However, these two species (*Gazella marica* and *Gazella gazelle*) were found to be different at 23 sites out of the 381 bp region that was analyzed. The sequences were employed in the construction of an NJ tree (Figure 3), where sequences of the different gazelle species taken from the GenBank (Table 7) were also included.

According to the phylogenetic tree, reconstructed based on the partial mtDNA *cyt-b* sequences (Figure 3):

1. Hatay samples were included in the *Gazella gazelle* cluster confirming the results of Kankılıç et al. (15).
2. Ceylanpınar State Farm originated individuals were grouped with those individuals once called *Gazella subgutturosa marica*, but now called *Gazella marica* (16).

3. Compared to the present day Arabian Peninsula (Oman and Iraq) samples contained in this phylogenetic tree, some genetic variation was observed among the individuals of the *Gazella marica* species.

As a consequence, based on the mtDNA *cyt-b* sequences analyzed in this study, the existence of two different species (*Gazella marica* and *Gazella gazelle*) within the borders of Turkey was confirmed.

“RFLP Analysis” as a Quick and Cheap Species Identification Method

The restriction enzymes, *HaeIII* and *HinfI* did not exhibit any polymorphism within or between the *Gazella marica* populations nor within the *Gazella gazelle* sample as expected from the sequence analysis. However, both of the enzymes’ restriction profiles discriminated between the *Gazella marica* and *Gazella gazelle* species as shown on the right margin in Figure 4.

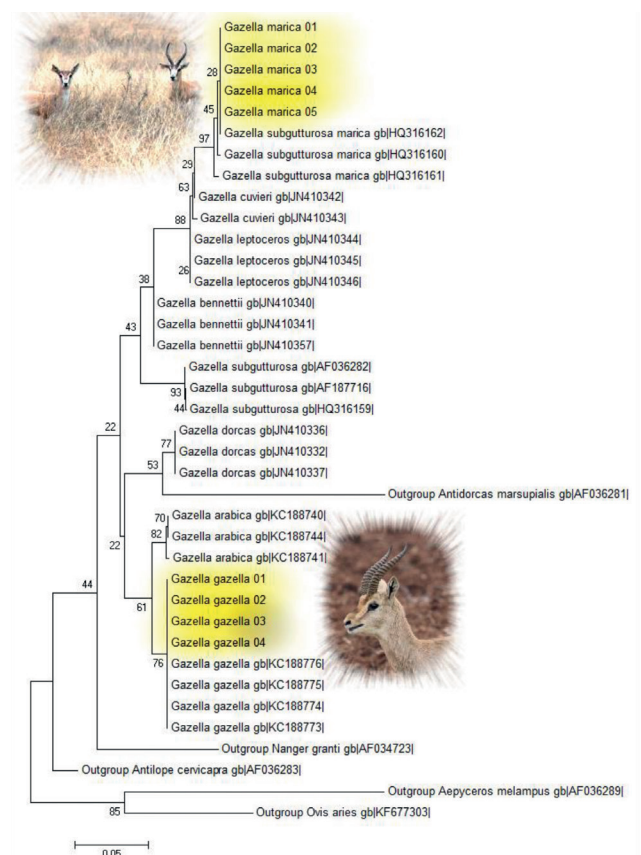


Figure 3. The phylogenetic tree constructed using an NJ algorithm with a 1000 Bootstrap value and employing a K2 nucleotide substitution model with gamma distribution (G=0.23). The GenBank Accession numbers for the samples taken from the literature were given at the end of the sample names. The highlighted samples are those analyzed in the present study. The MEGA v6.06 software (54) was used for the analysis.

Table 7. The summary of information about the samples taken from the literature. Their geographic origins (if available), their captive/wild status, accession numbers and related references are given in the table

Species	Origin	Captive/Wild	Accession Number	Reference
<i>G. arabica</i>	Southern Arava Valley, Israel	Wild	KC188740	60
<i>G. arabica</i>	Southern Arava Valley, Israel	Wild	KC188741	60
<i>G. arabica</i>	Southern Arava Valley, Israel	Wild	KC188744	60
<i>G. bennettii</i>	KKWRC, Thumamah	Captive	JN410340	20
<i>G. bennettii</i>	KKWRC, Thumamah	Captive	JN410341	20
<i>G. bennettii</i>	KKWRC, Thumamah	Captive	JN410357	20
<i>G. cuvieri</i>	EEZA, Almeria	Captive	JN410342	20
<i>G. cuvieri</i>	EEZA, Almeria	Captive	JN410343	20
<i>G. dorcas</i>	KKWRC, Thumamah	Captive	JN410332	20
<i>G. dorcas</i>	KKWRC, Thumamah	Captive	JN410336	20
<i>G. dorcas</i>	Tunisia	Wild	JN410337	20
<i>G. gazella</i>	Central Israel	Wild	KC188773	60
<i>G. gazella</i>	Central Israel	Wild	KC188774	60
<i>G. gazella</i>	Central Israel	Wild	KC188775	60
<i>G. gazella</i>	Central Israel	Wild	KC188776	60
<i>G. leptoceros</i>	Tunisia	Wild	JN410344	20
<i>G. leptoceros</i>	Tunisia	Wild	JN410345	20
<i>G. leptoceros</i>	Western Desert, Egypt	Wild	JN410346	20
<i>G. subgutturosa</i>	MNHN, Paris	Unspecified	AF036282	58
<i>G. subgutturosa</i>	Aksu, Chinese Turkistan	Wild	HQ316159	18
<i>G. subgutturosa</i>	Samarra, Iraq	Wild	AF187716	17
<i>G. s. marica</i>	Ramlat Fasad, Oman	Wild	HQ316160	18
<i>G. s. marica</i>	WA-SWC, United Arab Emirates	Captive	HQ316161	18
<i>G. s. marica</i>	Wadi Abu Al Jir, Iraq	Wild	HQ316162	18
Outgroup				
<i>Antidorcas marsupialis</i>	MNHN, Paris	Unspecified	AF036281	58
<i>Nanger granti</i>	MNHN, Paris	Unspecified	AF034723	58
<i>Antilope cervicapra</i>	MNHN, Paris	Unspecified	AF036283	58
<i>Aepyceros melampus</i>	MNHN, Paris	Unspecified	AF036289	58

Abbreviations: EEZA – Estación Experimental de Zonas Áridas, Spain; KKWRC – King Khalid Wildlife Research Centre, Riyadh, Saudi Arabia; WA-SWC–Wadi Al-Safa Wildlife Center, Dubai; MNHN: Muséum National d’Histoire Naturelle, Paris.

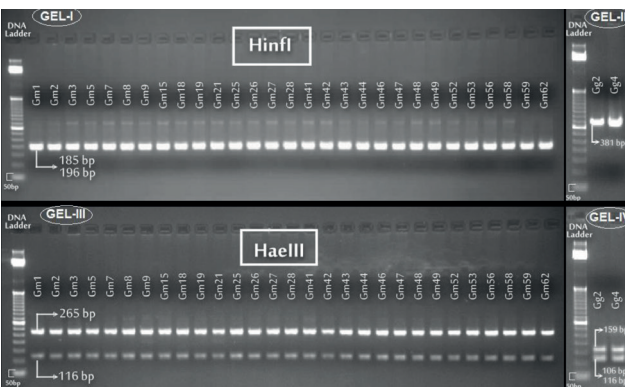


Figure 4. A sample image from the mtDNA partial *cytb* gene RFLP analysis results of the samples from two different gazelle species. The image is composed of views from four different gels as indicated in the figure and the samples are labeled: ‘Gm’ is used for *Gazella marica* from Kızılkuyu (Şanlıurfa) and Erikçe (Gaziantep); ‘Gg’ is used for *Gazella gazella* (Hatay Mountain Gazelle) from Hatay.

Y-Chromosome Analysis

Two microsatellite loci on the Y chromosome (UMN103, INRA126) of gazelle species were amplified. UMN103 did not produce clean sequences, but amplification and sequencing of INRA126 locus produced clean results. Two alleles were observed with a single nucleotide difference at the 216th base (Figure 5), which differentiated between the males of the two gazelle species of the present study (*Gazella gazella* and *Gazella marica*).

Life Parameters

Captivity populations are, in general, closed populations and have low effective population sizes. Therefore, they are prone to suffer from inbreeding depression. We obtained the documents kept by the Ministry on the two captive *Gazella marica* populations (Kızılkuyu and Erikçe). However, there seems to be inconsistency in year-to-year census values. Nevertheless, we used these records to estimate approximate birth and death rates in these captive populations to project

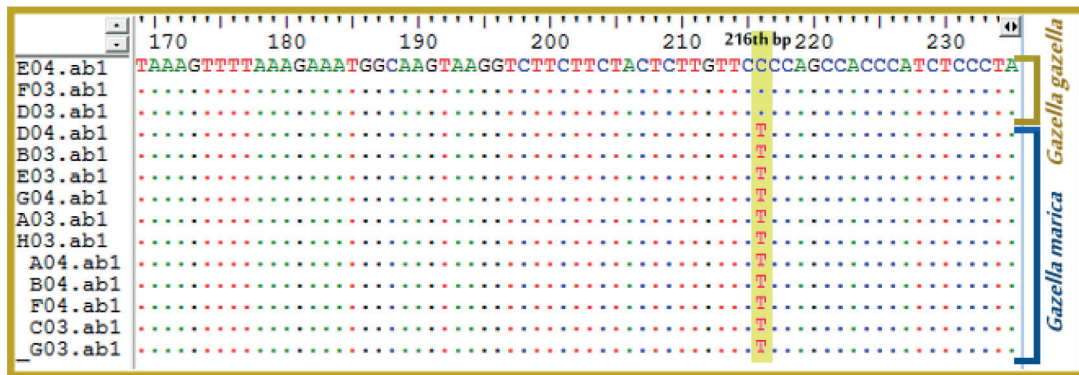


Figure 5. The alignment of the Y chromosome INRA126 locus sequences obtained in the study. Male individuals of *Gazella marica* and *Gazella gazella* showed a single base difference at the 216th bp as highlighted in yellow.

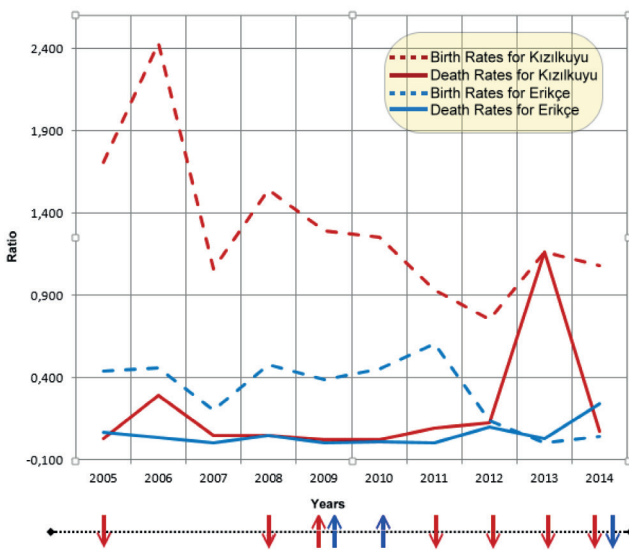


Figure 6. Approximate birth (dashed lines) and death rates (solid lines) of the Kızilkuyu (red) and Erikçe (blue) State Farm populations. The upward arrows indicate the reintroduction/introduction practices where the individuals were taken from the state farms, whereas the downward arrows indicate those years when new individuals were introduced into the state farms.

the present trend in these populations and this graphic is presented in Figure 6.

Estimations of the life parameters for the Kızilkuyu and Erikçe populations revealed that, in general, there has been a decrease in birth rates and an increase in death rates in both of these captive populations over time. Moreover, the estimates proposed that, the Erikçe population has lower birth rates and higher death rates than the Kızilkuyu population.

DISCUSSION

Gazelles and its close relatives are contained within the *Antilopinae* subfamily. One of the most commonly used markers for this subfamily is the mtDNA *cyt-b* region (2, 15,

18-20, 59, 60). This enables comparative studies within and between *gazella spp.* Employing this marker in our analyses confirmed the existence of both *Gazella marica* and *Gazella gazella* species and confirmed their taxonomic status. Additionally, *HaeIII* and *HinI* endonucleases used for the RFLP analysis of mtDNA *cyt-b* fragments (18) produced different haplotypes and separated the *Gazella marica* and *Gazella gazella* species from each other (Figure 4). Furthermore, we retrieved the *Gazella subgutturosa* mtDNA *cyt-b* sequences from the GenBank and identified their RFLP haplotypes with respect to the two endonucleases used in the study. Then, we compared the restriction profiles of the three gazelle species (Table 8).

Table 8. The restriction sites for the two restriction endonucleases; *HaeIII* and *HinI*, on the partial mtDNA *cyt-b* sequences of the three gazelle species are given

RFLP Enzyme	Species	Restriction Site
<i>HaeIII</i>	<i>Gazella marica</i>	116 th bp
	<i>Gazella subgutturosa</i>	116 th and 275 th bp
	<i>Gazella gazella</i>	116 th and 275 th bp
<i>HinI</i>	<i>Gazella marica</i>	185 th bp
	<i>Gazella subgutturosa</i>	185 th and 302 nd bp
	<i>Gazella gazella</i>	None

The *HinI* enzyme distinguished the three gazelle species from each other, whereas *HaeIII* could only make a distinction between the *Gazella marica* and *Gazella subgutturosa* species. Wachter et al. (18) employed these enzymes to discriminate between *Gazella marica* and *Gazella subgutturosa*. Our results have further shown that *Gazella gazella* can be differentiated from the other two gazelle species based on the mtDNA *cyt-b* RFLP analysis with *HaeIII* endonuclease. It has been reported that some individuals may look exactly like *Gazella subgutturosa* but carry *Gazella marica* type of mtDNA (59). For this reason, we propose employing L14724 and H15149 primers for the amplification of mtDNA *cyt-b* region and then analyzing the RFLP profile of this region (using *HaeIII* and *HinI* restriction endonucleases) as a quick and cheap method. This can solve

the conflict differentiating between *Gazella marica* and *Gazella subgutturosa*. Furthermore, an unknown tissue sample can be analyzed using these two endonucleases for species identification if it belongs to one of these three species.

To reveal sex-linked introgression in populations, mtDNA and Y-chromosome markers should be analyzed as well as autosomal markers. The Y chromosome locus, INRA126 (33), was sequenced from both *Gazella gazella* and *Gazella marica* species for the first time in literature by this study. The INRA 126 locus was chosen as it showed high polymorphism in different bovid species (61, 62). The results suggested that this locus can differentiate the males of these two gazelle species. However, the high number of wild samples from both of the species must be tested to confirm the discriminatory power of this sequence.

Populations with low N_e may show wild fluctuations in their allele frequencies and are expected to lose variability due to genetic drift; especially in mtDNA and Y chromosome on the account of their haploid nature. We have observed one Y chromosome haplotype (INRA126) and one mtDNA haplotype in the Ceylanpinar State Farm population. Since this farm started with one male, a single Y chromosome haplotype was expected. However, there were more than one female in the starting population, and may be more than one mtDNA haplotype. Yet, as the founding population size was very small, with a low N_e under random drift, it might have resulted in a single haplotype for mtDNA. Twenty years after the foundation of the Ceylanpinar State Farm, individuals transferred to the Kizilkuyu and the Erikçe State Farms as founders most probably had little or no genetic variation. Therefore, it can be presumed that these two farms must have started with a very low N_e . Moreover, they probably had the same single haplotypes for both Y chromosome and mtDNA present in Ceylanpinar. Therefore, it is not surprising that no variation was observed either in the mtDNA or in the Y chromosome sequences in these captive populations.

During the preparation stage of our study, we could not find in the literature any genetic diversity study on gazelle species based on microsatellite loci analyses. Therefore, we have analyzed 17 polymorphic loci randomly chosen among the previously studied loci of different species (bovine, ovine, goat and caribou), which were available in the literature (Table 2). Since then, six studies have been published concerning the captive and wild populations of different gazelle species, and they all utilized bovine, ovine and goat originated microsatellite loci. Among these studies, we have one common locus (OarFCB304) out of seven with Zachos et al. (63); eight common loci (BMC1009, CSSM43, BM4505, OARFCB304, BM848, INRA040, IDVGA29, CSSM39) out of twenty with Ruiz-Lopez et al. (64); four common loci (BM4505, CSSM043, INRA40, OarFCB304) out of eleven with Lerp et al. (65); four common loci (ETH10, INRA40, BM4505, TGLA122) out of nine with Hadas et al. (66); one common locus (OarFCB304) out of twelve with Duo et al. (67); two common loci (OarFCB304, CSSM043) out of ten with Okada et al. (68). We have compared our results with this recently

published data. The population sample sizes varied from 11 (Acacia gazelle, 66) to 138 (Mongolian gazelle, 68) in these studies and the average number of observed alleles across the analyzed microsatellite loci changed between 3.3 (*Gazella dama* captive population, $n=112$, 64) and 15 (Mongolian gazelle wild population, $n=138$, 68). Our sample sizes were $n=4$ (*Gazella gazella*, Hatay wild population), $n=48$ (*Gazella marica*, Kizilkuyu captive and wild samples), $n=25$ (*Gazella marica*, Erikçe captive population) and the average number of observed alleles were 3.4, 5.6 and 4.1, respectively. Moreover, the average observed heterozygosity in the above-mentioned literature ranged between 0.335 (*Gazella arabica* Farasan Islands wild population, 65) and 0.91 (Przewalskii's gazelle Sand Island wild population, 67), whereas the average expected heterozygosity ranged between 0.353 (Acacia gazelle, 66) and 0.854 (Mongolian gazelle, 68). In our study, the average observed heterozygosity values were 0.67, 0.64 and 0.61; and the average expected heterozygosities were 0.69, 0.63 and 0.60 for the Kizilkuyu and Erikçe *Gazella marica* samples and Hatay *Gazella gazella* sample, respectively. Comparatively, Hadas et al. (66) reported the average H_e within a wild *Gazella gazella* population in Southern Levant as 0.616 and the average H_e for a wild Acacia gazelle population suffering from inbreeding depression in the same region as 0.35 based on nine microsatellite loci. Furthermore, the average H_e estimate based on seven microsatellite loci for a captive population of Arabian oryx was reported as 0.57 (69). Consequently, it can be said that the gene diversity (H_e) observed within the populations of the present study is as high as that of the wild gazelle populations found in the literature.

Allelic richness takes variations in the sample sizes into account, measures the genetic diversity (in terms of allele numbers at a locus) and provides information on the population's long-term potential for adaptability and persistence. The Polymorphic Information Content (PIC) parameter is estimated based on the number of alleles and their relative frequencies at a locus, which predicts the informativeness of that locus. PIC values between 0.4 and 0.7 are interpreted as being moderately informative; whereas, PIC values higher than 0.7 can be interpreted as highly informative (70). According to this information, we can state that the most informative locus was ETH10 (0.801), 6 out of 16 loci were highly informative, and 6 out of 16 loci were moderately informative. In total, twelve loci (RT1, ETH10, OARFCB304, BM848, BMC1009, INRA40, BM4505, INRABERN172, TGLA122, ILSTS005, BM757 and CSSM43) were found to be informative. Therefore, one can select from these twelve loci in future studies on gazelles to assess their genetic diversity of populations or perform pedigree analysis.

Observing a low genetic variability is not surprising in small and/or captive populations. We assessed the genetic diversity based on expected heterozygosity (H_e) and allelic richness parameters, which are not affected significantly by low sample sizes. For both of the parameters the Erikçe population exhibited slightly lower estimates (average H_e : 0.63 and allelic richness: 4.31) than the Kizilkuyu captive population (average H_e : 0.69, allelic richness: 5.05). The Wilcoxon-Signed rank test

(43) based on the allelic richness estimates found a statistically significant ($p < 0.05$) difference between the Kızilkuyu and Erikçe populations. For the Hatay population, allelic richness was not considered due to its low sample size and the heterozygosity was estimated as 0.6. Subsequently, a random subpopulation of size $n=4$ (the same size as the Hatay population) was drawn from Kızilkuyu. For this subpopulation; the estimated H_e (0.68) was found to be higher than the H_e (0.6) estimate of the Hatay population. This results should be interpreted with care. It might be indicative of a lower genetic diversity in the Hatay population (*Gazella gazella*) than either of the two captive *Gazella marica* populations.

Gene pools of small and isolated populations can easily diverge from their source populations. The genetic drift occurring in small populations can quickly result in big changes. Kızilkuyu and Erikçe captive populations were sourced by the same population and established about 20 years ago. They may not be strictly isolated, but they must have diverged due to random drift, for about 10-12 generations (generation time of gazelle was assumed as 1 or 2 years). That is why, we have observed a significant ($p < 0.01$) pairwise F_{ST} value (0.044) between them.

Testing the three different K values, suggested by the two methods (47, 48), revealed that the gazelle population (*Gazella gazella*) from Hatay had a completely different gene pool than those of Erikçe and Kızilkuyu. This result was expected, as the two captive populations belonged to a different gazelle species than the Hatay population. Before carrying out the analyses, the Kızilkuyu samples were considered as one group of captive population. After the structure analysis, the Ministry was asked about the origins of the distinct individuals (represented by red in the structure plot), and it was understood that some of the samples were obtained from licensed hunters and they were from the wild population of Kızilkuyu (the samples numbered from 1 to 8 and from 10 to 12 in Figure 2). Thus, the power of the admixture analysis is attested by unraveling the fact that some individuals in the population had different source populations. However, a few hunted (wild) individuals, such as the two samples labeled 2 and 11 in Figure 2, seemed to originate from the captive Kızilkuyu population's gene pool (largely purple). It can be speculated that these two individuals might have been released from the Kızilkuyu farm into the wild, before they were hunted. We know that the Ministry had periodically released some individuals from this farm before the hunting seasons. In addition, two individuals (numbered 9 and 13 in Figure 2) of the Kızilkuyu state farm exhibited a different genetic structure than the rest of the Kızilkuyu samples. Presumably, we might label them as the Kızilkuyu wild type. It is possible that, they might have originated from those wild individuals introduced to the Kızilkuyu captive population. As explained in Figure 1, there are individuals taken from the Kızilkuyu wild site and introduced into the Erikçe State Farm, too. The genetically differentiated individuals found in the Erikçe State Farm (labeled 14-16 in Figure 2) could have originated from these introduced wild individuals.

Microsatellite-based N_e estimations for both the Kızilkuyu and Erikçe populations revealed low numbers (9.7 for Kızilkuyu and 8.9 for Erikçe). These low numbers are observed despite the fact that they are not completely closed populations. Firstly, the state farms are open for individuals found wounded or illegally captured. This results in gene flow into the captive populations from other sources, most probably from the wild populations. Secondly, it is known that three individuals were transported from the Kızilkuyu wild population to the Erikçe farm and six individuals from Ceylanpınar were transported to the Kızilkuyu farm. This also supports the view that they are not totally closed populations. If these estimations are approximately correct, the estimated N_e (which is 24.5 when we pool the populations) is still much lower than 50, which is an indicator of a small population size according to the 50/500 rule by Franklin (71) and Soulé (72). This rule claims that a minimum N_e of 50 is necessary to avoid inbreeding and a minimum N_e of 500 is necessary to reduce genetic drift. Finally, for the Hatay population, N_e was estimated as 6.4, which is very low. This might be due to the low number of individuals ($n=4$) sampled in this study, or alternatively, this population might indeed have a small N_e . In order to understand the underlying reason, more samples should be analyzed and this estimation should be repeated. The *Gazella gazella* population in Hatay is the only one existing in Turkey. Therefore, the present diversity must be analyzed before taking conservation actions.

The decreasing birth rates and increasing death rates, observed in the Kızilkuyu and Erikçe populations from the estimated life parameters, probably resulted from inbreeding depression, which is expected when N_e values are very low. Furthermore, in the Erikçe population, lower birth rates and higher death rates than those of the Kızilkuyu population are a good match for the lower genetic diversity (allelic richness and heterozygosity) observed in the Erikçe population. As can be seen from the graph (Figure 6) for Kızilkuyu, birth and death rates had peaks at the same time after reintroduction/introduction practices (indicated by upward arrows) were carried out. Possibly, after transporting individuals from the state farms, intraspecific competition decreased and therefore the birth rate increased and the death rate decreased. Intraspecific competition might be due to the available space in the state farms rather than the food supply as limited physical space (or crowding) may also cause decreased fecundity, increased mortality in juveniles and post-reproductives due to upsets induced in the endocrine system (73). Furthermore, the introduction of wild Kızilkuyu individuals into the Erikçe State Farm in 2010 and 2011 may have delayed the population collapse until 2014.

The results that should be considered for the conservation studies of Anatolian *Gazella marica* populations can be summarized as follows: (i) Both of the captive populations have low effective population sizes, and (ii) there is significant divergence between them. (iii) whether the two captive populations' gene pool diverged from the Kızilkuyu wild population must be checked in future studies, urgently), (iii) Both of the captive populations presented signals of inbreeding

depression, and iv) possibly, they might both be suffering from intraspecific competition. If a corridor is established between the populations (both wild and state farm) of *Gazella marica* species, it may slow down the diversity loss and genetic drift and thus decrease differentiation from each other. Furthermore, the reason for the possible intraspecific competition can be analyzed and intraspecific competition can be reduced. However, even then, chances are slim that the populations of the present study can ever be used to establish sustainable populations in the wild. Perhaps a better strategy would be to consider exchanges of individuals between the populations of different countries.

CONCLUSION

The markers employed in this study provides a good means of assessing populations of gazelle species for their species identity, degree of divergences, effective population sizes and for the presence of admixture within the populations. This data would certainly contribute to the development of better strategies in future studies for the conservation of the species.

Peer-review: Externally peer-reviewed.

Author Contributions: Conception/Design of study: E.K.B., H.E., T.H., T.K.; Data Acquisition: F.D.S., M.D.O. E.K.B.; Data Analysis/ Interpretation: F.D.S., M.D.O., E.K.B., S.C.A., I.T., H.E., T.H., T.K.; Final Approval and Accountability: F.D.S., M.D.O., E.K.B., S.C.A., I.T., H.E., T.H., T.K.; Drafting Manuscript: F.D.S., M.D.O., E.K.B.; Critical Revision of Manuscript: E.K.B., I.T.; Technical or Material Support: E.K.B., H.E., T.H.; Supervision: E.K.B., I.T.

Conflict of Interest: The authors declare that they have no conflicts of interest.

Financial Disclosure: The project was financially supported by the Scientific and Technological Research Council of Turkey (Project no: KAMAG 109G016).

Acknowledgment: No conflicts of interest related to this study.

References

1. Groves CP, Grubb P. Ungulate taxonomy. Baltimore, Md.: JHUP; 2011.
2. Lerp H, Wronski T, Plath M, Schröter A, Pfenninger M. Phylogenetic and population genetic analyses suggest a potential species boundary between Mountain (*Gazella gazella*) and Arabian Gazelles (*Gazella arabica*) in the Levant. *Mamm Biol* 2013; 78(5): 383-86.
3. Mallon DP. *Gazella subgutturosa*. IUCN Red List of Threatened Species. Version 2011.2; 2008.
4. Kasperek M. On the historical distribution and present situation of gazelles, *Gazella* spp., in Turkey. *Zool Middle East* 1986; 1: 11-5.
5. Kumerloeve, H. Die Säugetiere (Mammalia) Syriens und des Libanon. *Spixiana* 1975b; 18, 159-225.
6. Kumerloeve, H. Bemerkungen zum Gazellen Vorkommen im südöstlichen Kleinasien. *Z. Säugetierkd.* 1969; 34, 113-20.
7. Kumerloeve, H. Die Säugetiere (Mammalia) der Türkei. *Spixiana* 1975a; 18, 69-158.
8. Turan N. Game and wildlife of Turkey mammals. *Ongun Kardeşler Matbaacılık Sanayii*, Turkey; 1984.
9. Tez C, Akalın H, Erkekkaş M. Additional karyological data on goitered gazelle, *Gazella subgutturosa*, from Turkey. *Arch Biol Sci* 2009; 61(1):45-8.
10. Durmuş M. Determination of home range size and habitat selection of gazelles (*Gazella subgutturosa*) by GPS Telemetry in Şanlıurfa. Middle East Technical University Graduate School of Natural and Applied Sciences, MSc Thesis. 2010.
11. Kumerloeve H. Zur Verbreitung kleinasiatischer Raub- und Huftiere sowie einiger Großnager. *Säugetierkd Mitt* 1967; 15: 337-409.
12. Turan N. Report on the protection and restoration of gazelle (*Gazella subgutturosa*) in Turkey. Turkish Department of Game-Wildlife: 7; 1977.
13. Ölçer SY. Chapter 20: Turkey. Mallon DP, Kingswood SC, compilers. *Antelopes Part 4: North Africa, the Middle East, and Asia Global survey and regional action plans SSC Antelope Specialist Group IUCN, Gland, Switzerland and Cambridge, UK; 2001. p.112-13.*
14. Çobanoğlu AE. Identification Of Demographic Structure and Population Viability Analysis of *Gazella subgutturosa* in Şanlıurfa. Middle East Technical University Graduate School of Natural and Applied Sciences, MSc Thesis. 2010.
15. Kankılıç T, Özü D, Gürlü Ş, Kence M, Bozkaya F, Kence A. Rediscovery of a new mountain gazelle population and clarification of taxonomic status of the genus *Gazella* in Turkey using mtDNA sequencing. *Folia Zool* 2012; 61(2): 129-37.
16. Wronski T, Sandouka M, Plath M, Cunningham P. Differences in sexual dimorphism among four gazelle taxa (*Gazella* spp.) in the Middle East. *Anim Biol* 2010; (60) 395-412.
17. Hammond RL, Macasero W, Flores B, Mohammed OB, Wachter T, Bruford MW. Phylogenetic Reanalysis of the Saudi Gazelle and Its Implications for Conservation. *Conserv. Biol.* 2001; 15:1123-33.
18. Wachter T, Wronski T, Hammond RL, Winney B, Blacket MJ, Hundertmark KJ, et al. Phylogenetic analysis of mitochondrial DNA sequences reveals polyphyly in the goitered gazelle (*Gazella subgutturosa*). *Conserv Genet* 2011; 12:827-31.
19. Wronski T, Wachter T, Hammond RL, Winney B, Hundertmark KJ, Blacket MJ, et al. Two reciprocally monophyletic mtDNA lineages elucidate the taxonomic status of Mountain gazelles (*Gazella gazella*). *Syst Biodivers* 2010; 8(1): 119-29.
20. Lerp H, Wronski T, Pfenninger M, Plath M. A phylogeographic framework for the conservation of Saharan and Arabian Dorcas gazelles (Artiodactyla: Bovidae). *Org Divers Evol* 2011; 11(4): 317-29.
21. Groves CP, Harrison DL. The taxonomy of the gazelles (genus *Gazella*) of Arabia. *J Zool London* 1967; 152:381-7.
22. Groves CP. On the smaller gazelles of the Genus *Gazella* de Blainville, 1816. *Z. Säugetierkd.* 1969; 37:38-60.
23. Lerp H, Wronski T, Butynski T, Plath M. Speciation of Arabian gazelles. In: Michalak P (ed.) *Speciation: Natural Processes, Genetics and Biodiversity*. Nova Science Publishers, Hauppauge, NY pp. 59-82; 2013.
24. Oğurlu I. Wild ungulates of Turkey. *Ongulés/Ungulates* 1992; 91:575-7.
25. Sambrook J, Fritsch EF, Maniatis T. *Molecular Cloning: A Laboratory Manual*, 2nd ed. Vol. 3, Cold Spring Harbor Laboratory, New York, USA; 1989.
26. Winnepeninckx B, Backeljau T, de Wachter R. Extraction of high molecular weight DNA from molluscs. *Trends in Genet* 1993; 9 (12): 407.
27. Wilson GA, Strobeck C, Wu L, Coffin JW. Characterization of microsatellite loci in caribou Rangifer tarandus, and their use in other artiodactyls. *Mol Ecol* 1997; 6: 697-9.

28. Toldo S, Fries SR, Steffen P, Neibergs HL, Barendse W. Physically mapped cosmid-derived microsatellite markers as anchor loci on the bovine chromosome. *Mamm Genome* 1993; 4:720-7.
29. Buchanan FC and Crawford AM. Ovine microsatellites at the OarFCB11, OarFCB128, OarFCB193, OarFCB266 and OARFCB304 loci. *Anim Genet* 1993; 24: 145.
30. Mommens GW, Coppieters A. Dinucleotide repeat polymorphism at the bovine MM12E6 and MM8D3 loci. *Anim Genet* 1994; 25: 368.
31. Bishop MD, Kappes SM. A genetic linkage map for cattle. *Genetics* 1994; 136:619-39.
32. Kappes SM, Keele JW, Stone RT, McGraw RA, Sonstegard TS, Smith TP, et. al. A second-generation linkage map of the bovine genome. *Genome Res* 1997; 7(3): 235-49.
33. Vaiman D, Mercier D. A set of 99 cattle microsatellites: characterisation, synteny mapping, and polymorphism. *Mamm Genome* 1994; 5:288-97.
34. Mezzelani A, Zhang Y, Redaelli L, Castiglioni B, Leone P, Williams JL, et. al. Chromosomal localization and molecular characterization of 53 cosmid-derived bovine microsatellites. *Mamm Genome* 1995; 6(9): 62935.
35. Steffen P, Eggen A. Isolation and mapping of polymorphic microsatellites in cattle. *Anim Genet* 1993; 24: 121-4.
36. Saitbekova N, Gaillard C, Obexer-Ruff G, Dolf G. Genetic diversity in Swiss goat breeds based on microsatellite analysis. *Anim Genet* 1999; 30 (1): 36-41.
37. Georges M, Massey J. Polymorphic DNA markers in Bovidae. *J World Intellect Prop Publ No* 92:13120, 1992
38. Kemp SJ, Brezinsky L, Teale AJ. ILSTS002: a polymorphic bovine microsatellite. *Anim Genet* 1992; 23: 184.
39. Moore SS, Byrne K. Characterisation of 65 bovine microsatellites. *Mamm Genome* 1994; 5: 84-90.
40. Oosterhout C, Hutchinson WF, Wills DPM, Shipley PF. Micro-Checker: software for identifying and correcting genotyping errors in microsatellite data. *Mol Ecol Notes* 2004; 4:535-8.
41. Excoffier L, Laval G, Schneider S. ARLEQUIN version 3.01: an integrated software package for population genetics data analysis. University of Bern, Institute of Zoology, Switzerland. Available from <http://cmpg.unibe.ch/software/arlequin3> 2006.
42. Goudet J (2001) FSTAT, A Program to Estimate and Test Gene Diversities and Fixation Indices, Version 2.9.3. <http://www.unil.ch/izea/software/fstat.html>
43. Sokal RR, Rohlf FJ. *Biometry* (3rd edn). WH Freeman and company: New York; 1995.
44. Kalinowski ST, Taper ML, Marshall TC. Revising how the computer program CERVUS accommodates genotyping error increases success in paternity assignment. *Mol Ecol* 2007; 16(5): 1099-106.
45. Wright S. The Interpretation of Population Structure by F-Statistics with Special Regard to Systems of Mating. *Evolution* (N Y) 1965; 19(3):395-420.
46. Pritchard JK, Stephens M, Donnelly P. Inference of population structure using multilocus genotype data. *Genetics* 2000; 155:945-59.
47. Evanno G, Regnaut S, Goudet J. Detecting the number of clusters of individuals using the software structure: a simulation study. *Mol Ecol* 2005; 14:2611-20.
48. Tapio M, Ozerov M, Tapio I, Toro M, Marzanov N, Cinkulov M, et. al. Microsatellite-based genetic diversity and population structure of domestic sheep in northern Eurasia. *BMC Genetics* 2010; 11:76.
49. Jakobsson M, Rosenberg NA. CLUMPP: a cluster matching and permutation program for dealing with label switching and multimodality in analysis of population structure. *Bioinformatics* 2007; 23: 1801-6.
50. Rosenberg NA. DISTRUCT: a program for the graphical display of population structure. *Mol. Ecol. Notes* 2004; 4: 137-8.
51. Do C, Waples RS, Peel D, Macbeth GM, Tillett BJ, Ovenden JR. Ne Estimator V2: re-implementation of software for the estimation of contemporary effective population size (Ne) from genetic data. *Mol Ecol Resour* 2014; 14(1): 209-14.
52. Kocher TD, Thomas WK, Meyer A, Edwards SV, Pääbo S, Villablanca FX, et. al. Dynamics of mitochondrial DNA evolution in animals: amplification with conserved primers. *PNAS USA* 1989; 86: 6196-200.
53. Irwin D, Kocher T, Wilson A. Evolution of the cytochrome-b gene of mammals. *J Mol Evol* 1991; 32: 128-44.
54. Hall TA (2013) BioEdit v 7.2. 3. Biological sequence alignment editor for Win 95/98/NT/2K/XP7.
55. Tamura K, Stecher G, Peterson D, Filipski A, Kumar S. MEGA6: molecular evolutionary genetics analysis version 6.0. *Mol Biol and Evol* 2013; 30(12): 2725-9.
56. Liu WS, Mariani P, Beattie CW, Alexander LJ, De León FAP. A radiation hybrid map for the bovine Y Chromosome. *Mamm Genome* 2002; 13(6): 320-6.
57. Wright S. Vol. 4: Variability within and among natural populations. Chicago, University of Chicago Press; 1978.
58. Hassanin A, Douzery EJ. The tribal radiation of the family Bovidae (Artiodactyla) and the evolution of the mitochondrial cytochrome b gene. *Mol Phylogenet Evol* 1999; 13(2): 227-43.
59. Murtskhvaladze M, Gurielidze Z, Kopaliani N, Tarkhnishvili D. Gene introgression between *Gazella subgutturosa* and *G. marica*: limitations of maternal inheritance analysis for species identification with conservation purposes. *Acta Theriol* 2012; 57: 383-6.
60. Lerp, H., Wronski, T., Plath, M., Schröter, A., & Pfenninger, M. Phylogenetic and population genetic analyses suggest a potential species boundary between Mountain (*Gazella gazella*) and Arabian Gazelles (*Gazella arabica*) in the Levant. *Mamm Biol* 2013b; 78(5): 383-86.
61. Hanotte O, Okomo M, Verjee Y, Rege JEO, Teale A. A polymorphic Y chromosome microsatellite locus in cattle. *Anim Genet* 1997; 28(4): 318-9.
62. Edwards CJ, Dolf G, Looft C, Loftus RT, Bradley DG. Relationships between the endangered Pustertaler-Sprinzen and three related European cattle breeds as analysed with 20 microsatellite loci. *Anim Genet* 2000; 31: 329-32.
63. Zachos FE, Karami M, Ibenouazi Z, Hartl GB, Eckert I, Kirschning J. First genetic analysis of a free-living population of the threatened goitered gazelle (*Gazella subgutturosa*). *Mamm Biol* 2010; 5:277-82.
64. Ruiz-Lopez MJ, Roldan ER, Espeso G, Gomendio M. Pedigrees and microsatellites among endangered ungulates: what do they tell us? *Mol Ecol* 2009; 18(7): 1352-64.
65. Lerp H, Plath M, Wronski T, Bärman EV, Malczyk A, Resch RR, et al. Utility of island populations in re-introduction programmes-relationships between Arabian gazelles (*Gazella arabica*) from the Farasan Archipelago and endangered mainland populations. *Mol Ecol* 2014; 23(8): 1910-22.
66. Hadas L, Hermon D, Boldo A, Arieli G, Gafny R, King R, et. al. Wild Gazelles of the Southern Levant: genetic profiling defines new conservation priorities. *PLoS One* 2015; 10(3).
67. Duo H, Na L, Hong Y, Zhang Y, Li D. Genetic diversity of Przewalski's gazelle using noninvasive DNA and its implications for conservation. *AJB* 2015; 14(13): 1107-13.

68. Okada A, Ito TY, Buuveibaatar B, Lhagvasuren B, Tsunekawa A. Genetic structure in Mongolian gazelles based on mitochondrial and microsatellite markers. *Mamm Biol* 2015; 80(15): 303-11
69. Arif IA, Khan HA, Shobrak M, Homaidan AAA, Sadoon MA, Farhan AHA. Measuring the genetic diversity of Arabian Oryx using microsatellite markers: implication for captive breeding. *Genes Genet Syst.* 2010; 85(2): 141-5.
70. Hildebrand CE, David C, Torney C, Wagner P. Informativeness of polymorphic DNA markers. *The Human Genome Project: deciphering the blueprint of heredity.* University Science Books, CA, USA,; 1994. p 100-2.
71. Franklin IR. Evolutionary change in small populations. Soulé ME and Wilcox BA, editors. *Conservation Biology: an evolutionary-ecological perspective,* Sunderland: Sinauer; 1980. p 135-50.
72. Soulé ME. Thresholds for survival: maintaining fitness and evolutionary potential, in *Conservation Biology: An Evolutionary-Ecological Perspective,* M. E. Soule and A. Wilcox, Eds., Sinauer Associates, Sunderland, UK, 1980 p. 151-69
73. Fischer MS and Schliemann H. Volume VIII Mammalia. founded by Kükenthal W, edited by Schmidt-Rhaesa, Andreas W de Gruyter. *Handbuch der Zoologie/Handbook of Zoology: Natural History of the Phyla of the Animal Kingdom,* Berlin; 2005.

First Report on the Occurrence of Invasive Macrophyte *Elodea canadensis* Michx. in Sapanca Lake

Sezgi Ersoy¹ , Yelda Aktan Turan¹ 

¹Istanbul University, Faculty of Aquatic Sciences, Department of Marine and Inland Water Resources Management, Istanbul, Turkey

ORCID IDs of the authors: S.E. 0000-0002-1081-5719; Y.A.T. 0000-0001-7920-8979

Please cite this article as: Ersoy S, Aktan Turan Y. First Report on the Occurrence of Invasive Macrophyte *Elodea canadensis* Michx. in Sapanca Lake. Eur J Biol 2019; 78(2): 103-107. DOI: 10.26650/EurJBiol.2019.0018

ABSTRACT

Objective: *Elodea canadensis* Michx. is a common invasive aquatic macrophyte that has successfully spread along European, Asian and Australian inland waters. The aim of this study is to evaluate the presence and distribution of an alien and invasive species, *E. canadensis*, in Sapanca Lake (Turkey) for the first time.

Materials and Methods: Sampling for macrophytes and main environmental parameters was carried out seasonally between the years 2016 and 2017 along the coasts of Sapanca Lake. Macrophytes samples were taken from bounded areas. Morphological observations were made on both unfixed-living and dried materials, and morphological details were observed under a light microscope.

Results: *Elodea canadensis* Michx. was reported for the first time in Sapanca Lake during the spring period of 2016 with water temperatures of $20.9 \pm 0.9^\circ\text{C}$. A total of six submerged macrophytes species were recorded together with *E. canadensis*.

Conclusion: The first record of this species in Sapanca Lake is important for contributing to the changing biodiversity dynamics of the lake and also contributes to the assessment of the possible ecological and economic risks of the region in terms of lake management.

Keywords: Invasive macrophytes, *Elodea canadensis*, Sapanca Lake

INTRODUCTION

Aquatic macrophytes play an important role in both structuring and functioning communities in aquatic environments (1). They contribute significantly to the productivity and biodiversity in the littoral region by representing a suitable habitat for micro and macro flora and fauna as well as a significant number of ecological and economical species. Moreover, they have an important role in ensuring nutrient dynamics, protecting against coastal erosion and in stabilising the sediments by reducing the negative effect of the wave (2). Moreover, recent studies have indicated that the invasion of alien aquatic macrophytes introduced by natural or anthropogenic means has been a highlighted issue. Hussner (3) reported findings of 96 alien aquatic plant species from European inland waters, and *Elodea*

canadensis Michx. was reported to be the most widely distributed alien aquatic plant in Europe.

E. canadensis is a submerged aquatic plant belonging to Hydrocharitales (Magnoliophyta) (4). The native distribution of this species is reported to be from North American and Canadian Inland waters (4-6) but it is a common invasive species in Europe, Asia and Australia (4, 6). The first record of the plant in European waters came from Ireland in 1836 (6) and later studies indicated that it successfully spread and rapidly colonised in north and central European shallow lakes and streams (3, 7-12) and then extended to Asian fresh waters (13). *E. canadensis* has been defined as a "catastrophic phenomenon" in Baikal Lake (14) due to forming fast and uncontrolled thriving populations in a very short space of time. The species has been categorized as



Corresponding Author: Yelda Aktan Turan E-mail: yaktan@istanbul.edu.tr

Submitted: 04.07.2019 • **Revision Requested:** 02.10.2019 • **Last Revision Received:** 14.10.2019 • **Accepted:** 21.10.2019

© Copyright 2019 by The Istanbul University Faculty of Science • Available online at <http://ejb.istanbul.edu.tr> • DOI: 10.26650/EurJBiol.2019.0018

a least concern (LC) species by the International Union for Conservation of Nature (IUCN) (15). Recent studies indicate that *E. canadensis* is now widespread globally with the exception of Iceland, Greenland, the Faroe Islands and the Norwegian islands (16) and is reported to be a noxious weed in freshwaters (4).

In Turkey, *E. canadensis* was first reported in the Thrace Region (North-western part of Turkey) by Davis (17). Later, the presence of the species was noted in Gala Lake (18) and also in some drainage channels in the surrounding areas (19). In 2005, the first record of the species was given from western Anatolia (Eğirdir Lake, South-western part of Turkey) and in the following years its spreading to the entire lake area was reported (20). The presence of this invasive species poses an ecological, sociological and economic threat in freshwater ecosystems (21, 22). *Elodea* has high invasion success, considering the advantage such as the high tolerance to changing environmental factors, fast vegetative reproduction ability by fragments and easy dispersion vectors (irrigation canal, animals, fishing activities and recreational use of waters). Increasing nutrient input and eutrophication process also promote its mass development and spread. Considering its widespread appearance and rapid colonization success in European waters, research scientists need to know its spreading areas and to make an evaluation of its effects on the biodiversity of the lake ecological status. This study reports the presence of an alien and invasive species, *E. canadensis*, in Sapanca Lake for the first time.

Sapanca Lake, located in the north-western part of Turkey (40°43'N and 30°15'E) is a tectonic lake, with a surface area of 47 km² and maximum depth of 55 m. At a local level, the lake is an important freshwater source of drinking water and is used for domestic water and industrial needs, besides commercial and sport fisheries. The catchment area consists of small towns, villages and forests and the lake is used for tourism and various recreational activities. This lake is fed by several creeks and partly by groundwater. The shallow shores are covered by a wide vegetation belt. Sapanca Lake with its winter overturn is a typical warm-monomictic lake. The lake water is mixed thoroughly from top to bottom in February-March, providing enrichment of the surface layer with nutrients from deep waters as well as ventilation of bottom waters (23). Though there is no direct discharge of waste into the lake, chemical pollutants of both domestic and agricultural origin find their way into the lake through surface-runoff (24). Before 1980, a few studies of its principal limnological properties showed the lake to contain low concentrations of dissolved inorganic ions and the water to be adequate for drinking, industrial usage and irrigation. Recently there has been some impact of pollutants, particularly sewage effluent. Towards the end of the 1990s some colour changes indicating water-blooms were occasionally observed and routine studies revealed that a cyanobacterium, *Planktotrix rubescens* (De Candolle ex Gomont) Anagnostidis&Komarek was responsible (23, 25). In recent years, cyanobacterial blooms frequently occur as a result of degradation of water quality and the eutrophication in the lake.

MATERIALS AND METHODS

Field observation and sampling for macrophytes and main environmental parameters was carried out seasonally between the years 2016 and 2017 along the coasts of Sapanca Lake (Figure 1). Moreover, short time-scale samplings (weekly) along the coast of the Lake were conducted from July to August in summer periods. Aquatic plants were observed along the coast by means of a viewing tube and collected using a rake. Macrophytes samples were taken from bounded areas with three replicates and their relative abundance was estimated based on their dry-wet weight in each sampling area. Morphological observations were made on both unfixed-living and dried materials and morphological details were observed under a light microscope in the laboratory.

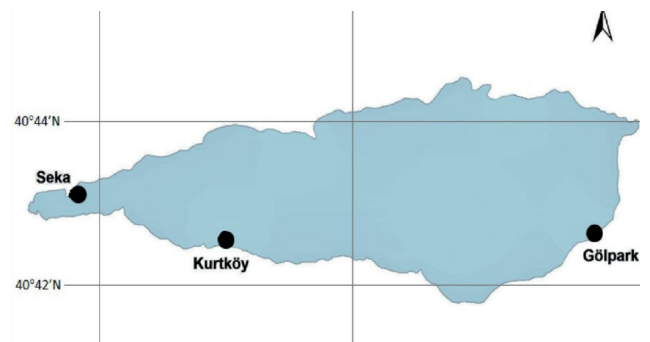


Figure 1. Map of Sapanca Lake showing sites where *Elodea canadensis* Michx. was found

The identification of *Elodea* was made according to Casper and Krausch (5), Bowmer et al. (4) and Simpson (26). Moreover, main environmental parameters influencing the presence/absence of the species were recorded. Water temperature, dissolved oxygen, conductivity and pH were measured *in situ* with a multiparameter prob and transparency with a Secchi disc. Water samples for nutrients and chlorophyll *a* were taken from surface. For chlorophyll *a* analysis, water was filtered through a glass fiber filter (Whatman GF/C) and Chlorophyll *a* concentration was determined spectrophotometrically (27). Nutrients (reactive phosphorus, nitrate and nitrite nitrogen, and silicate) were analysed in the laboratory according to standard analytical techniques (28). Measured environmental parameters and chlorophyll *a* results of Lake Sapanca surface water were given by the mean with standard deviations.

RESULTS

The first observation of *E. canadensis* Michx. was recorded in the spring of 2016 at water temperatures of 20.9±0.9°C during the preliminary study for a project on aquatic macrophytes of Sapanca Lake. In the routine sampling which was on-going during 2017, the species was observed again from a depth of 1-3 meters at the Seka and Kurtköy regions of the Lake during the summer. When the presence of the species was monitored

Table 1: Measured environmental parameters and chlorophyll *a* means with standard deviations (SD) of Lake Sapanca surface water

Parameters	Range	Mean±SD
Water temperature (°C)	5.8-28.0	17.6±0.4
pH	6.9-8.2	7.5±0.1
Dissolved oxygen (mg l ⁻¹)	6.6-10.4	8.6±0.4
Conductivity µs cm ⁻¹	248-286	265±5
Water transparency (m)	max	max
(NO ₂ +NO ₃)-N (mg l ⁻¹)	2.16-12.10	4.54±0.17
PO ₄ -P (mg l ⁻¹)	2.25-3.35	2.34±0.10
Chlorophyll <i>a</i> (mg l ⁻¹)	1.62-22.73	8.9±3.4

seasonally, it was observed that its spreading area extended to the inner western shore of the lake during the summer period (from June to August) at temperatures of 27.4±0.5°C. Measured environmental parameters and chlorophyll *a* means with standard deviations of Lake Sapanca surface water are given in Table 1. The species had the highest biomass during the autumn period (209 g/m² in dry weight) with temperatures of 15.8±0.3°C, and in addition to these areas it was also recorded

at Gölpark region along the eastern shore of the lake. During the study period, a total of six submerged macrophytes species (*Myriophyllum spicatum* L., *Ceratophyllum demersum* L., *Najas minor* All., *Chara* sp., *Potamogeton perfoliatus* L. and *Potamogeton lucens* L.) were reported together with *E. canadensis*.

Elodea is a perennial aquatic submerged plant measuring 20-30 cm in length. The identification of *E. canadensis* is based

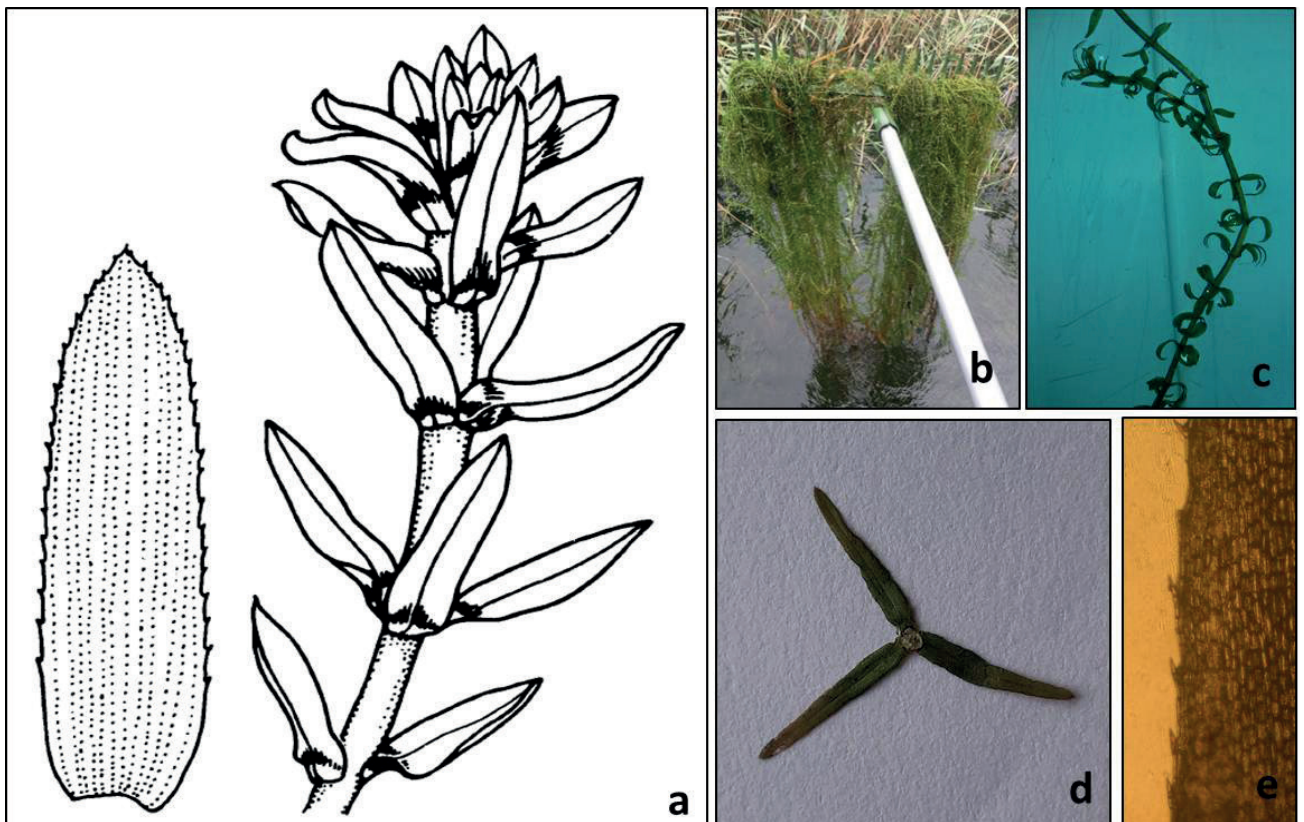


Figure 2. *Elodea canadensis* Michx., (a) morphological illustration of leaves, from Bowner et al (4) (Illustration by Christine Payne, from Sainty and Jacobs, 1988), (b-c) during the sampling from Sapanca Lake by rake, and (d-e) detailed photos of leaves.

on leaf characteristics. Towards the stem apex leaves usually overlap in regular rows and lie along the stem (4). In collected samples from Sapanca Lake, *E. canadensis* is identified with its three oblong linear leaves in whorls, the size of leaves being 8.96 ± 1.89 mm in length and 1.86 ± 0.38 mm in width at the mid-point (Figure 2).

DISCUSSION

Macrophytes are key elements of the lake ecosystem, contributing significantly to the productivity of littoral areas. However, during the last decades, the degradation of natural balance as a result of increased human activities has led to the destruction of habitats, loss of biodiversity and/or excessive increase in some species with a decrease in water quality. Several studies have focussed on alien species and the impact of invasive macrophytes on aquatic systems, and these studies have revealed that this problem is one of the major environmental problems in inland water (3, 29, 30).

In this study, *Elodea canadensis* Michx., is recorded for the first time in Sapanca Lake. *Elodea* is a flowering plant but vegetative reproduction by fragments is also very common (9). Earlier studies showed that the species has high ecological tolerance with temperatures of 10-25°C and pH 6.5-10, and it can be rapidly dominant in waters with average nutrient content, especially ranging from mesotrophic to eutrophic waters (8, 31). These ecological and biological characteristics of *Elodea* contribute to its success at being invasive. In the present study, the total biomass of *Elodea* recorded during the summer and autumn periods ranged between 95 and 209 g/m² in dry weight. Its distribution was limited to the southern part of the lake, and its relative abundance did not exceed 3% in the total macrophytes biomass. However, considering its widespread appearance in European waters (3, 12) as a result of global change caused by humans (29), and considering the colonization success of this species, the importance of monitoring studies on alien species is clear.

Alien species may have been introduced by natural or anthropogenic means. The origin of the population on the lake remains uncertain. The number of alien aquatic macrophytes in inland waters is much lower compared to the marine and terrestrial ecosystems due to geographical and climatic limitation and less introduction vector. More than 400 aquarium plants are used commercially and they considered as potential invaders to European inland waters (3). The commercial use of these species has also played an important role in the introduction of *E. canadensis* (3, 32). The presence and uncontrolled spread of these plants could cause important ecological and socio-economic losses in the future. Intervention against alien and invasive species is considerably difficult and costly. In addition, these interventions, which are mechanical, chemical and biological, have many disadvantages. The latest studies show that aquatic biosecurity is an important issue (30, 32-34). Biosecurity management in environmental and fishery policies, and raising awareness of the local people who

use the lake for fishing, tourism and sporting activities play an important role in preventing the entrance and spread of alien species.

CONCLUSION

This study presents the appearance of *Elodea canadensis* Michx., an alien and invasive species, in Lake Sapanca and contributes to a new data on its distribution in inland water of Turkey. The first record of this species in Sapanca Lake is important as a contribution to the changing biodiversity dynamics of the lake and also contributes to assessing the possible ecological and economic risks of the region in terms of lake management.

Peer-review: Externally peer-reviewed.

Author Contributions: Conception/Design of study: Y.A.; Data Acquisition: S.E.; Data Analysis/Interpretation: Y.A., S.E.; Drafting Manuscript: Y.A., S.E.; Critical Revision of Manuscript: Y.A.; Final Approval and Accountability: Y.A, S.E.

Conflict of Interest: The authors declare that they have no conflicts of interest.

Financial Disclosure: This study was financially supported by the Research Fund of Istanbul University (Project number: FLY-2016-20468).

Acknowledgements: The authors thank Captain Harun UMUTLU and Mr. Mustafa ÖZDEMİR for his support during fieldwork and all members of the Sapanca Inland Fish Culture Research and Application Unit.

REFERENCES

1. Søndergaard M, Johansson SL, Lauridsen TL, Jørgensen TB, Liboriussen L, Jeppesen E. Submerged macrophytes as indicators of the ecological quality of lakes. *Freshwater Biol* 2010; 55: 893–908.
2. Barko JW, James WF. Effects of submerged aquatic macrophytes on nutrient dynamics, sedimentation, and resuspension. Jeppesen, E. Søndergaard, M., Søndergaard, M., Christoffersen K. editors, *The Structuring role of submerged macrophytes in lakes. Ecological Studies (Analysis and Synthesis)*, 131. Springer, New York; 1998, 423pp.
3. Hussner A. Alien aquatic plant species in European countries. *Weed Res* 2012; 52: 297-306.
4. Bowmer HK, Jacobs SWL, Saintry GR. Identification, biology and management of *Elodea canadensis*, Hydrocharitaceae. *J Aquat Plant Manage* 1995; 33: 13-9.
5. Casper SJ, Krausch HD. Süßwasserflora von Mitteleuropa, Pteridophyta und Anthophyta, 1. Teil. Band 23. Gustav Fischer Verlag, Stuttgart; 1980, 403 pp.
6. Simpson DA. A short history on the introduction and spread of *Elodea* Michx. in the British Isles. *Watsonia* 1984; 15: 1–9.
7. Spicer KW, Catling PM. The biology of Canadian weeds, *Elodea canadensis* Michx. *Can J Plant Sci* 1988; 68: 1035-51.
8. Heikkinen RK, Leikola N, Fronzek S, Lampinen R, Toivonen H. Predicting distribution patterns and recent northward range shift of an invasive aquatic plant: *Elodea canadensis* in Europe. *BioRisk* 2009; 2, 1–32.

9. Kočić A, Horvatić J, Jelaska SD. Distribution and morphological variations of invasive macrophytes *Elodea nuttallii* (Planch.) H. St. John and *Elodea canadensis* Michx in Croatia. Acta Bot Croat 2014; 73(2): 437–46.
10. Hilt S, Gross EM, Hupfer M, Morscheid H, Mahlmann J, Melzer A et al. Restoration of submerged vegetation in shallow eutrophic lakes – A guideline and state of the art in Germany. Limnologica 2006; 36: 155–71.
11. Tokarska-Guzik B, Zaja CM, & Zaja, CA. Geographical and ecological aspects of the spread of alien plant species in Poland. Rabbitsh W, Essl F, Klingenstein F editors, Biological Invasions—from Ecology to Conservation, 7. Neobiota 2008, pp. 143–52.
12. Hussner A, van de Weyer K, Gross EM, Hilt, S. Comments on increasing number and abundance of nonindigenous aquatic macrophyte species in Germany. Weed Res 2010; 50: 519–26.
13. Kolada A, Kutyla S. *Elodea canadensis* (Michx.) in Polish Lakes: A non-aggressive addition to native flora. Biol Invasions 2016;18(11): 3251–64.
14. Kozhova OM, Izhboldina LA. Spread of *Elodea canadensis* in Lake Baikal. Hydrobiologia 1992; 239: 43-52.
15. Maiz-Tome L. *Elodea canadensis*. The IUCN red list of threatened species. 2016 Available from URL: <http://dx.doi.org/10.2305/IUCN.UK.2016-1.RLTS.T13506646A13506651.en>.
16. Josefsson M. NOBANIS-Invasive species fact sheet–*Elodea canadensis*, *Elodea nuttallii* and *Elodea callitrichoides*. Available from Online Database of the European Network on Invasive Alien Species; 2011.
17. Davis PH. Flora of Turkey and the East Aegean Islands. Vol. 8, First Edition, Edinburgh: Edinburgh University Press; 1984.
18. Altınayar G. Su yabancı otları. Bayındırlık ve İskan Bakanlığı, DSİ Genel Müdürlüğü İşletme ve Bakım Dairesi Başkanlığı, Ankara; 1988, 239 pp.
19. Seçmen Ö, Leblebici E. Türkiye Sulak Alan Bitkileri ve Bitki Örtüsü. Ege Üniversitesi Fen Fakültesi Yayınları No:158, Bornova, İzmir;1997, 870 pp.
20. Kesici E, Gülle İ, Turna İ. Eğirdir Gölü'nde *Elodea canadensis* Michaux'in ilk bildirimi ve istilası üzerine bir araştırma. SDÜ Fen Dergisi 2009; 4(2):120-8.
21. Huotari T, Korpelainen H, Leskinen E, Kostamo K. Population genetics of the invasive water weed *Elodea canadensis* in Finnish waterways. Plant Syst Evol 2011; 294: 27–37.
22. Zehnsdorf A, Hussner A, Eismann F, Rönicke H, Melzer A. Management options of invasive *Elodea nuttallii* and *Elodea canadensis*. Limnologica 2015; 51: 110-7.
23. Aykulu G, Albay M, Akçaalan R, Tüfekçi H, Aktan Y. Species composition, abundance and seasonality of phytoplankton in a moderately deep Turkish Lake. Nova Hedwigia 2006; 130: 325-38.
24. Morkoç E, Tuğrul S, Öztürk M, Tüfekçi H, Egesel L, Tüfekçi V et al. Trophic characteristics of the Sapanca Lake (Turkey). Croat Chem Acta 1998; 71(2): 303-22.
25. Albay M, Akçaalan R, Matthiensen A, Beattie KA. Some biochemical features of two filamentous algae isolated from Lake Sapanca, Turkey. J Fish Aqua Sci 2001; 18(1): 149-60.
26. Simpson DA. Taxonomy of *Elodea* Michx. in the British Isles. Watsonia 1986; 16: 1–14.
27. Golterman, HL, Clyno, RS, Ohnstad MAM. Methods for physical and chemical analysis of freshwaters. 2 nd ed. Blackwell, Oxford 1978; 315 pp.
28. APHA, AWWA, WEF. Standard methods for examination of water and wastewater. 22nd ed. Washington, American Public Health Association 2012; 1360 pp.
29. Vitousek PM, D'antonio CM, Loope LL, Rejmanek M, Westbrooks R. Introduced species: A significant component of human-caused global change. New Zeal J Ecol 1997; 21: 1–16.
30. Caffrey JM, Gallagher C, Dick JTA, Lucy F. Aquatic invasive alien species–top issues for their management. EIFAAC Occasional Paper No. 50, Rome, FAO; 2015, 63 pp.
31. Ceglowska A, Jusik S, Samecka-Cymerman A, Klink A, Szoszkiewicz K. Habitat requirements of *Elodea canadensis* Michx. in Polish Rivers. Oceanol Hydrobiol St 2017; 46(4): 363-78.
32. Champion PD, Clayton JS, Hofstra DE. Nipping aquatic plant invasion in the bud: weed risk assessment and the trade. Hydrobiologia 2010; 656:167–72.
33. Champion PD. Knowledge to action on aquatic invasive species: Island biosecurity – the New Zealand and South Pacific Story. Manag Biol Invasion 2018; 9(4): 383–94.
34. Coughlan NE, Cuthbert RN, Dickey JWE, Crane K, Caffrey JM, Lucy FE, et al. Better biosecurity: spread-prevention of the invasive Asian clam, *Corbicula fluminea* (Müller, 1774). Manag Biol Invasion 2019; 10(1): 111–26.

Karyotypes of Southeastern Turkish Scorpions *Hottentotta saulcyi* and *Buthacus macrocentrus* (Scorpiones: Buthidae)

Halil Koc¹ , Ersen Aydin Yagmur² , Frantisek Štáhlavský³ 

¹Sinop University, Faculty of Arts and Science, Department of Biology, Sinop, Turkey

²Celal Bayar University, Alaşehir Vocational School, Manisa, Turkey

³Charles University in Prague, Faculty of Science, Department of Zoology, Prague, Czech Republic

ORCID IDs of the authors: H.K 0000-0003-0429-2824; E.A.Y. 0000-0002-0396-3975; F.Š. 0000-0002-8520-9166

Please cite this article as: Koc H, Yagmur EA, Štáhlavský F. Karyotypes of Southeastern Turkish Scorpions *Hottentotta saulcyi* and *Buthacus macrocentrus* (Scorpiones: Buthidae). Eur J Biol 2019; 78(2): 108-113. DOI: 10.26650/EurJBiol.2019.0008

ABSTRACT

Objective: The species *Hottentotta saulcyi* is widely distributed from Mardin to Hakkari while the distribution of *Buthacus macrocentrus* is limited to the south-east of Turkey (only Şanlıurfa). The aim of this study is to analyze the cytogenetic structure of *Hottentotta saulcyi* and *Buthacus macrocentrus*.

Materials and Methods: The specimens were collected during the night from Şırnak and Şanlıurfa using a UV lamp. The male *Hottentotta saulcyi* were collected from Şırnak and male and female *Buthacus macrocentrus* from Şanlıurfa. Chromosome preparations were made using cells from the male testes and the female ovaries of the species studied. Chromosome preparations were made using the classical spreading method.

Results: The diploid chromosome number for *Hottentotta saulcyi* was $2n=14$, and $2n=28$ for *Buthacus macrocentrus*.

Conclusion: The karyotypes of *Hottentotta saulcyi* and *Buthacus macrocentrus* have been presented for the first time. Both analyzed species have holocentric chromosomes that gradually decrease in size. Quadrivalent and hexavalent were observed during the first meiotic division in males of *Buthacus macrocentrus*.

Keywords: Karyotype, *Hottentotta saulcyi*, *Buthacus macrocentrus*

INTRODUCTION

Currently, 213 genera and 2433 scorpion species are classified under 17 families (1). Although scorpions are widely distributed in the tropics and subtropics and all types of terrestrial habitats all over the continents (except Antarctica) (2), our present knowledge of their karyotypes is still scarce. Chromosome data on 155 scorpions belonging to 11 families have thus far been determined. Among them, 91 species of Buthidae have been studied, limited to some geographic regions-especially Brazil and Africa (3). Karyotypes of these scorpions are composed of holocentric chromosomes without a localized centromere region (4).

Cytogenetic studies have been carried out on *Leiurus abduhbayrami* Yağmur, Koç&Kunt, 2009 and *Compsobuthus matthiesseni* (Birula, 1905) present a karyotype with $2n=22$ (5), *Androctonus crassicauda* (Olivier, 1807) has a karyotype of $2n=24$ (6), *Aegaeobuthus gibbosus* (Brullé, 1832) shows $2n=28$, *Mesobuthus eupeus* (C.L. Koch, 1839) has $2n=20$ (Buthidae) and *Euscorpis aladaglarenis* Tropea&Yağmur, 2016 (7) shows $2n=88$ (Euscorpiidae), which are distributed in Turkey.

The present knowledge of the cytogenetics of Turkish scorpions is scarce and fragmented. The aim of this paper is to report the first chromosomal data of two species (*Hottentotta saulcyi* and *Buthacus macrocentrus*) from



Corresponding Author: Halil Koc E-mail: koc.halil@hotmail.com

Submitted: 16.05.2019 • **Revision Requested:** 17.07.2019 • **Last Revision Received:** 09.09.2019 • **Accepted:** 17.09.2019

© Copyright 2019 by The Istanbul University Faculty of Science • Available online at <http://ejb.ibul.edu.tr> • DOI: 10.26650/EurJBiol.2019.0008

Turkey. The genus *Hottentotta* Birula, 1908 is widespread throughout Africa, the Middle East and Asia (8, 9). This genus comprises almost 51 species (10). *H. judaicus* (Simon, 1872) (11), *H. tamulus* (Fabricius, 1798) (12-14) and *H. trilineatus* (Peters, 1861) (15) have been analyzed in cytogenetic studies up to present day. *Hottentotta saulcyi* (Simon, 1880) was firstly recorded in Mardin (10) and then reported in Batman, Şırnak, and Hakkâri in Turkey (9). Meanwhile, the genus *Buthacus* Birula, 1908 is distributed across northern and western Africa, Israel, Palestine, Jordan, Syria, Turkey, the Arabian Peninsula, Iraq, Iran, Afghanistan, and Pakistan. 23 species belonging to *Buthacus* have thus far been described (1, 10, 16-19). In Turkey, *Buthacus macrocentrus* (Ehrenberg, 1828) is known only from Şanlıurfa (10, 18, 20). Cytogenetic analyses have been performed for only one species namely *Buthacus stockmanni* Kovraik, Lowe&Stahlavsky, 2016 having $2n=20$ (21).

MATERIALS AND METHODS

The scorpions were collected using a UV lamp during the night from Şırnak and Şanlıurfa respectively (Figure 1). The collected specimens were transferred to the laboratory in individual plastic containers. In total, six specimens of *Hottentotta saulcyi* and seven of *Buthacus macrocentrus* were analyzed (for detailed information, see "Material examined" below).

The gonads were used from both males and females. The specimens were killed by ventral puncture to the prosomal area. Under a stereomicroscope, the gonads were removed by dissection in the presence of physiological salt solution for invertebrates. The gonads were then kept in a hypotonic solution (0.075 M KCl) for 20 min. The gonads were fixed in a freshly prepared fixative (3: 1, methanol: acetic acid) for 20 min. A few drops of 60% acetic acid were then dropped on a slide and then shredded with a tungsten needle. The drop on the slide was placed on the heating plate and spread with tungsten needles (22). The prepared slides were stained with 5% Giemsa in Sørensen's phosphate buffer. The chromosome preparations were analyzed under a Leica DM 500 microscope with a 100x objective. Images were taken with a Leica camera using Leica Application LAZ software. The measurements were analyzed using software ImageJ 1.47 (23) with the plugin Levan (24). The relative length of the chromosomes was calculated as a percentage of the diploid set and it based on seven mitotic metaphases in *Hottentotta saulcyi* and on seven postpachytene in *Buthacus macrocentrus*. The preparations were kept in a slide box and the remains of the specimens were fixed in a solution of 96% alcohol and stored in a refrigerator at 4 °C at the Zoological Museum of Sinop University, Turkey (ZMSU).

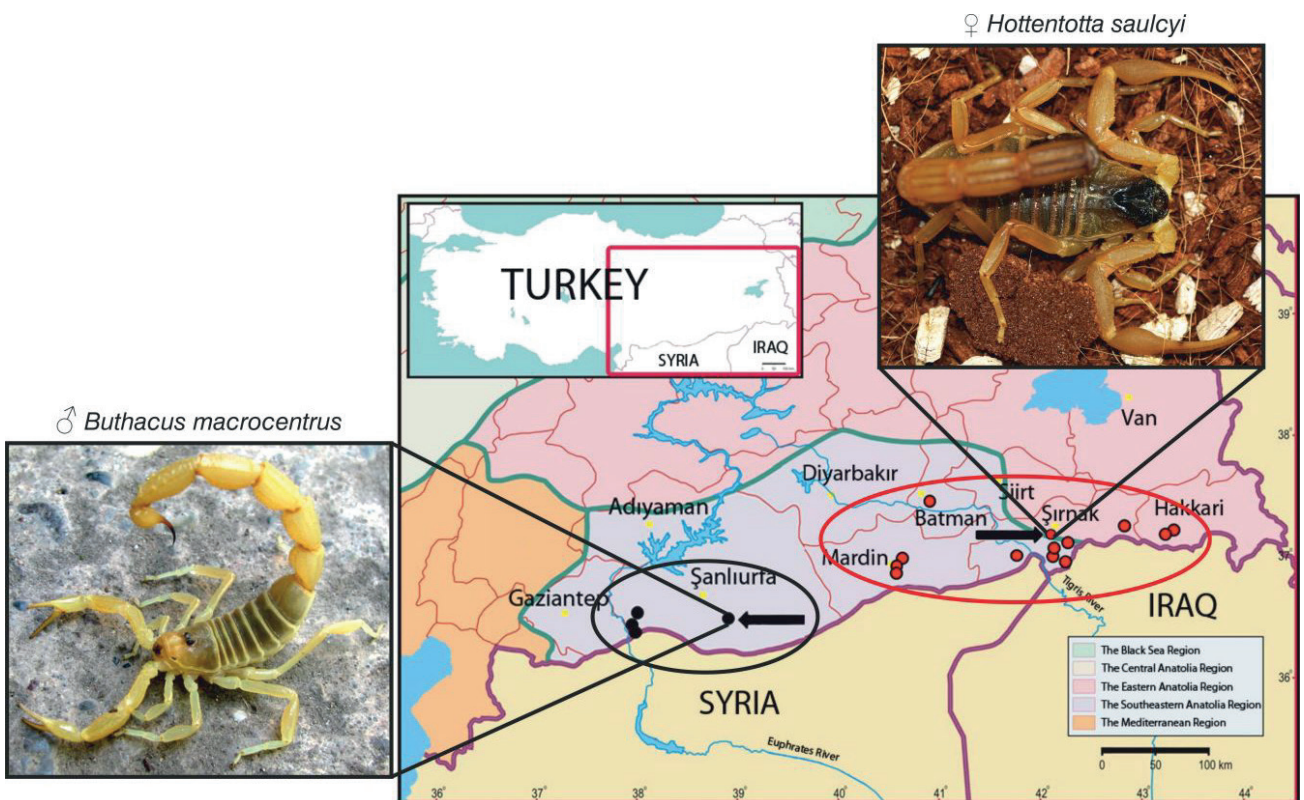


Figure 1. Distribution of *Hottentotta saulcyi* (red circle) and *Buthacus macrocentrus* (black circle) in south-eastern Turkey. Arrows show the localities of examined materials.

RESULTS

Family : Buthidae C.L. Koch, 1837

Genus-1 : *Hottentotta* Birula, 1908

Species-1 : *Hottentotta saulcyi* (Simon, 1828) (Figures 2 and 3)

Material examined: 2♂ 3♀ and 1♂ subadult, Şırnak, 2.5 km SW of Şırnak, 37°29'57.3"N; 42°26'32.7"E, 1024 m, 17.07.2014, leg. E. A. Yağmur (Figure 1).



Figure 2. Male *Hottentotta saulcyi*, dorsal and ventral views. Scale=1cm.



Figure 3. Female *Hottentotta saulcyi*, dorsal and ventral views. Scale=1cm.

Karyotype Investigation

The chromosome complement of *Hottentotta saulcyi* consisted of 14 chromosomes (Figure 4). We observed only the mitotic phases for this species. The relative chromosome length gradually decreased from 11.65 to 4.39% of the diploid set (Figure 4a).

Genus-2 : *Buthacus* Birula, 1908

Species-2 : *Buthacus macrocentrus* (Ehrenberg, 1828) (Figures 5 and 6)

Material examined: 4♂, Şanlıurfa, Birecik District, 2 km S of Mezra Village, 36°56'50.1"N; 38°01'20.3"E, 375 m, 08.07.2013, leg. E. A. Yağmur. 3♀, Şanlıurfa, Birecik District, 2 km S of Mezra Village, 36°57'35"N; 38°00'43"E, 387 m, 27.07.2014, leg. E. A. Yağmur (Figure 1).



Figure 5. Male *Buthacus macrocentrus*, dorsal and ventral views. Scale=1cm.

Karyotype Investigation

The number of diploid chromosomes in all male and female *Buthacus macrocentrus* specimens examined was 28 (Figure 7a). The relative chromosome length of the first chromosome (6.31%) was slightly larger than the remaining chromosomes which

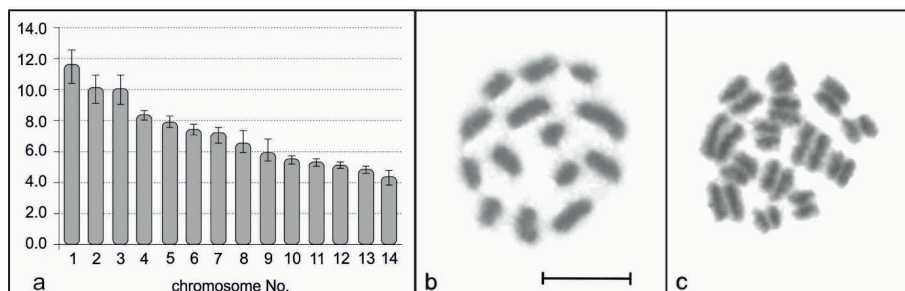


Figure 4. Ideogram and chromosomes of male *Hottentotta saulcyi*, $2n=14$. a. ideogram based on mitotic metaphases (y axis - % of the diploid chromosome length, lines indicate min.-max. values); b. mitotic metaphase; c. early mitotic anaphase. Scale=10 µm.



Figure 6. Female *Buthacus macrocentrus*, dorsal and ventral views. Scale=1cm.

gradually decreased from 5.14 to 1.95% of the diploid set (Figure 7a). Achiasmatic bivalents were detected in males during the first meiotic division. In the female, mitotic metaphases were obtained (Figure 7b). A distinct quadrivalent or hexavalent association of chromosomes were found in all individuals and observed in four males during meiosis (Figures 7c and d). The size of the detected multivalent chromosomes gradually

reduced. The chromosomes forming quadrivalent or hexavalent were different in size (Figure 7a). During the first meiosis division phase (anaphase, pachytene, postpachytene, metaphase-I), no indication of crossing-over was observed. In the polar view of metaphase I (Figures 7b and c), the majority of these bivalents presented parallel-arranged homologous chromosomes. In pachytene (Figure 7e), bivalents were all strip-shaped.

DISCUSSION

The present study provides the first cytogenetic analysis of the *Hottentotta saulcyi* and *Buthacus macrocentrus*, species of the Buthidae family. The karyotypes of these species consist of 14 and 28 chromosomes (Table 1). 91 species of Buthidae have been cytogenetically studied thus far, and which show the lowest chromosome numbers within scorpions. This family has a diploid chromosome number varying from $2n=5$ [*Tityus bahiensis* (Perty, 1833)] to $2n=36$ [*Barbaracurus somalicus* (Hirst, 1907) and *Parabuthus mossambicensis* (Peters, 1861)], excluding dubious information (see 3). Buthidae family, as well as the entire order Scorpiones, is characterized by achiasmatic meiosis in males (25). In contrast to other scorpions, the examined species of buthids usually possess a relatively low chromosome number and all of them have holocentric organization (4).

Although there are several faunistic and taxonomic studies on the genus *Hottentotta*, there is a paucity of cytogenetic studies.

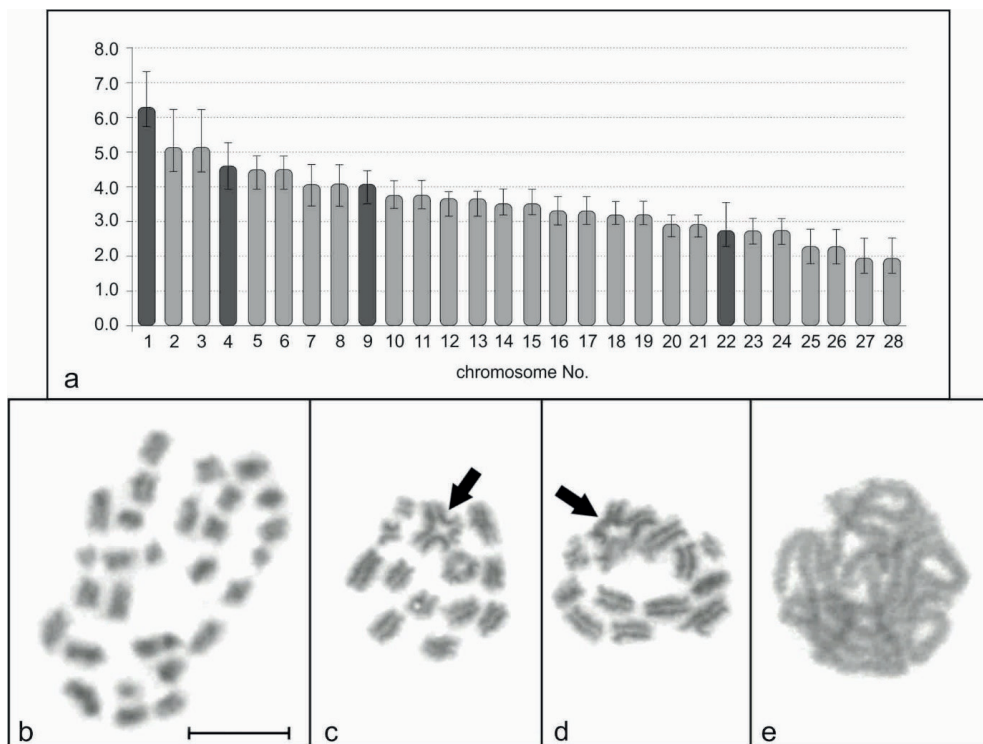


Figure 7. Ideogram (a) and chromosomes of female (b) and male (c-e) *Buthacus macrocentrus*, $2n=28$. a. ideogram based on postpachytene with quadrivalent (dark grey) (y axis - % of the diploid chromosome length, lines indicate min.-max. values); b. mitotic metaphase of female; c. metaphase I of male, arrow shows quadrivalent; d. metaphase I of male, arrow shows hexavalent; e. pachytene of male. Scale = 10 μ m.

Table 1: Number of diploid chromosomes in eight species of scorpions from Turkey.

Taxon	2n	Sampling locality	Reference
Buthidae			
<i>Androctonus crassicauda</i> (Olivier, 1807)	24	Turkey: Şanlıurfa Province	(6)
<i>Buthacus macrocentrus</i> (Ehrenberg, 1828)	28	Turkey: Şanlıurfa Province	the present study
<i>Compsobuthus matthiesseni</i> (Birula, 1905)	22	Turkey: Gaziantep Province	(5)
<i>Hottentotta saulcyi</i> (Simon, 1880)	14	Turkey: Şırnak Province	the present study
<i>Leiurus abduallahbayrami</i> Yağmur, Koç & Kunt, 2009	22	Turkey: Gaziantep Province	(5)
<i>Mesobuthus eupeus</i> (C. L. Koch, 1839)	20	Turkey: Niğde Province	(7)
<i>Aegaeobuthus gibbosus</i> (Schenkel, 1947)	28	Turkey: Niğde Province	(7)
Euscorpiidae			
<i>Euscorpius aladaglarensis</i> Tropea & Yağmur, 2016	88	Turkey: Niğde Province	(7)

Chromosomal data are known for only three of the total of 51 currently recognized species of the genus *Hottentotta* species (10), were included in cytogenetic studies (11-15). *Hottentotta tamulus* species possesses 2n=22, 24 or 20-28 chromosomes forming a continuous series (12-14). But, Venkatanarasimhiah and Rajasekarasetty (13) stated that the chromosome number of same species have 2n=23 stable chromosome number in India. Sharma et al. (12) observed the tetravalent formation which is very common in *H. tamulus*. The diploid number was given as 2n=24 for *Hottentotta trilineatus* by Newlands and Martindale (15). Qumsiyeh et al. (11) reported diploid chromosomes as 2n=16 for *Hottentotta judaicus* specimens from the Palestinian Territories. We obtained diploid chromosomes as 2n=14 for *Hottentotta saulcyi*. Our results supported that genus *Hottentotta* displays interspecific karyotype differences with 2n ranging from 14 (this study) to 24. However, we could not observe multivalent in *H. saulcyi* as previously documented in *H. tamulus*.

The genus *Buthacus* was studied cytogenetically for the first time by Kovařík et al. (21). The karyotype of *B. stockmanni* has 2n=20 chromosomes with holocentric and achiasmatic meiotic complement (21). According to cytological observation of *B. stockmanni*, the first pair of chromosomes are distinctively larger (13.41% of the diploid set) than the other chromosomes that gradually decrease from 5.84 % to 2.69 % of the diploid set. The cytogenetic analyses revealed that *Buthacus macrocentrus* consisted of 2n=28. The chromosomes are holocentric and achiasmatic meiotic complement as Kovařík et al. (21). The ideogram show that chromosomes of 1, 4, 9 and 22 are involving the arrangement of quadrivalent chromosome. These findings confirm the results of Shanahan and Hayman (26) who stated that multivalent formations involve during the achiasmatic meiosis of buthid. The first chromosome is significantly longer (6.31%) than the remaining chromosomes that gradually decrease from 5.14% to 1.95% of the diploid set.

In our present study, it is interesting to note that the presence of quadrivalents and hexavalents seems to be frequent in *B. macrocentrus* species.

CONCLUSION

Our analysis of karyotype data provides a first step towards understanding the chromosome numbers and the structure of chromosomes in one of the most important and dangerously venomous members of the family Buthidae. In general, our findings support that buthids have a low chromosome number with holocentric chromosomes. In the present study, the karyotype of two buthids, *Hottentotta saulcyi* and *Buthacus macrocentrus*, was identified for the first time as 2n=14 and 2n=28 respectively. The genus *Hottentotta* possess interspecific karyotype differences in a continuous series of the chromosomal number with 2n ranging from 14 to 24. As far as we know, this is the second karyological analysis of the genus *Buthacus*, thus our study is a significant contribution to the description of the chromosomal features of *Buthacus macrocentrus*. Our data highlights that the frequency of the multivalent is very high in this species. The chromosomes were arranged and numbered according to their total length in a gradually decreasing size order and their ideogram was developed (see Fig. 4a and Fig. 7a). Nevertheless, the results show that chromosome numbers are not a useful character in some buthids, and are therefore not effective for taxonomic purposes. Moreover, more detailed analysis of the karyotype of the buthid species is required for comparative cytotaxonomy of the Buthidae.

Peer-review: Externally peer-reviewed.

Author Contributions: Conception/Design of study: H.K.; Data Acquisition: H.K., E.A.Y.; Data Analysis/Interpretation: H.K., F. Ş.; Drafting Manuscript: H.K.; Critical Revision of Manuscript: H.K., F. Ş., E.A.Y.; Final Approval and Accountability: H.K.

Conflict of Interest: The authors declare that they have no conflicts of interest.

Financial Disclosure: The project was financially supported by the Sinop University BAP Unit (FEF 1901-13-03).

REFERENCES

1. Rein JO. The Scorpion Files. Trondheim: Norwegian University of Science and Technology. [Accessed 2019.01.23]. Available from <https://www.ntnu.no/ub/scorpion-files> 2019.
2. Dunlop JA, Penney D. Fossil Arachnids. Monograph Series Volume 2. Siri Scientific Press, Manchester 2012; 192 pp.
3. Schneider MC, Mattos VF, Cella DM. The scorpion cytogenetic database. Available in www.arthropodacytogenetics.bio.br/scorpiondatabase 2019.
4. Mattos VF, Cella DM, Carvalho LS, Candido DM, Schneider MC. High chromosome variability and the presence of multivalent associations in buthid scorpions. *Chrom Res* 2013; 21:121–36.
5. Šťáhlavský F, Koç H, Yağmur EA. The first record of karyotypes in *Leiurus abduallahbayrami* and *Compsobuthus matthiesseni* (Scorpiones: Buthidae) from Turkey. *North-West J Zool* 2014; 10 (2): 355-8.
6. Sadılek D, Nguyen P, Koç H, Kovarik F, Yağmur EA, Šťáhlavský F. Molecular cytogenetics of *Androctonus* scorpions: an oasis of calm in the turbulent karyotype evolution of the diverse family Buthidae. *Biol J Linn Soc* 2015; 115: 69-76.
7. Karataş Ay, Uçak M, Karataş Ah, Eroğlu O. Records of chromosomal data of some scorpions (Arachnida: Scorpiones) from Turkey. *Haceteppe J Biol&Chem* 2019; 47(1): 1-6.
8. Kovařík F. A revision of the genus *Hottentotta* Birula, 1908, with descriptions of four new species (Scorpiones, Buthidae). *Euscorpius* 2007; 58: 1–109.
9. Yağmur EA, Koç K, Yalçın M. Distribution of *Hottentotta saulcyi* (Simon 1880) (Scorpiones: Buthidae) in Turkey. *Euscorpius* 2008; 76: 1– 8.
10. Crucitti P, Vignoli V. Gli scorpioni (Scorpiones) dell'Anatolia sudorientale (Turchia). *Boll Mus Reg Sci Nat* 2002; 19 (2): 433-80.
11. Qumsiyeh MB, Salman INA, Salsaa' M, Amr ZS. Records of scorpions from the Palestinian Territories, with the first chromosomal data (Arachnida: Scorpiones). *Zool Middle East* 2013; 59: 70–6.
12. Sharma GP, Parshad R, Joneja MG. Chromosome mechanism in the males of three species of scorpions (Scorpiones–Buthidae). *Res Bull Panjab Uni* 1959; 10: 197-207.
13. Venkatanarasimhiah CB, Rajasekarasetty MR. Contributions to the cytology of Indian scorpions. *Experientia* 1964; 21: 154.
14. Gupta AKD, Sarker SK. A study of the meiotic chromosomes of the scorpion *Buthus tamulus* Fabr. *Curr Sci* 1965; 2: 54-5.
15. Newlands G, Martindale CB. The buthid scorpion fauna of Zimbabwe-Rhodesia with checklists and keys to the genera and species, distributions and medical importance (Arachnida: Scorpiones). *South African Ins Med Res* 1980; 67: 51-77.
16. Levy G, Amitai P. Scorpiones, In: Fauna Palaestina, Arachnida I., Israel Acad. Sci. Human., Jerusalem 1980; 130 pp.
17. Fet V, Lowe G. Family Buthidae. pp. 54-286. In: Fet V, Sissom WD, Lowe G, Braunwalder ME. Catalog of the Scorpions of the World (1758-1998). The New York Entomological Society, New York 2000; 690 pp.
18. Kovařík F. Taxonomic position of species of the genus *Buthacus* Birula, 1908 Described by Ehrenberg and Lourenço, and description of a new species (Scorpiones: Buthidae). *Euscorpius* 2005; 28: 1–13.
19. Lourenço WR. Further considerations on the genus *Buthacus* Birula, 1908 (Scorpiones, Buthidae), with a description of one new species and two new subspecies. *Bol SEA* 2006; 38: 59-70.
20. Yağmur EA, Yalçın M, Çalıřır G. Distribution of *Androctonus crassicauda* (Olivier, 1807) and *Buthacus macrocentrus* (Ehrenberg, 1828) (Scorpiones: Buthidae) in Turkey. *Serket* 2008; 11(1): 13-8.
21. Kovařík F, Lowe G, Šťáhlavský F. Review of northwestern African *Buthacus*, with description of *Buthacus stockmanni* sp. n. from Morocco and western Sahara (Scorpiones, Buthidae). *Euscorpius* 2016; 236: 1-18.
22. Traut W. Pachytene mapping in the female silkworm, *Bombyx mori* L. (Lepidoptera). *Chromosoma* 1976; 58: 275-84.
23. Schneider C.A., Rasband W.S., Eliceiri K.W. NIH Image to ImageJ: 25 years of image analysis. *Nat Meth* 2012; 9: 671–5.
24. Sakamoto, Y., Zacaro A.A. LEVAN, an ImageJ plugin for morphological cytogenetic analysis of mitotic and meiotic chromosomes. <http://rsbweb.nih.gov/ij/plugins/levan/levan.html> 2009.
25. Shanahan C. Cytogenetics of Australian scorpions. I. Interchange polymorphism in the family Buthidae. *Genome* 1989; 32:882–9.
26. Shanahan C., Hayman, D. Synaptonemal complex formation in male scorpions exhibiting achiasmate meiosis and structural heterozygosity. *Genome* 1990; 33: 914–26.

Investigation of Antimicrobial, Antibiofilm, and Cytotoxic Effects of Straight-Chained Sulfanyl Members of Arylamino-1,4-naphthoquinones as Potential Antimicrobial Agents

Emel Mataraci Kara¹ , Ayse Tarbin Jannuzzi² , Nilufer Bayrak³ , Hatice Yildirim³ ,
Mahmut Yildiz⁴ , Amac Fatih Tuyun⁵ , Buket Alpertunga² , Berna Ozbek Celik¹ 

¹Istanbul University, Faculty of Pharmacy, Department of Pharmaceutical Microbiology, Istanbul, Turkey

²Istanbul University, Faculty of Pharmacy, Department of Pharmaceutical Toxicology, Istanbul, Turkey

³Istanbul University-Cerrahpasa, Engineering Faculty, Chemistry Department, Istanbul, Turkey

⁴Gebze Technical University, Faculty of Science, Department of Chemistry, Kocaeli, Turkey

⁵Istanbul University-Cerrahpasa, Engineering Faculty, Engineering Sciences Department, Istanbul, Turkey

ORCID IDs of the authors: E.M.K. 0000-0003-4541-1893; A.T.J. 0000-0003-0578-6893; N.B. 0000-0002-0777-4012; H.Y. 0000-0003-3988-6120; M.Y. 0000-0001-6317-5738; A.F.T. 0000-0001-5698-1109; B.A. 0000-0001-6043-7560; B.O.C. 0000-0001-8909-8398

Please cite this article as: Mataraci Kara E, Jannuzzi AT, Bayrak N, Yildirim H, Yildiz M, Tuyun AF, Alpertunga B, Ozbek Celik B. Investigation of Antimicrobial, Antibiofilm, and Cytotoxic Effects of Straight-Chained Sulfanyl Members of Arylamino-1,4-naphthoquinones As Potential Antimicrobial Agents. Eur J Biol 2019; 78(2): 114-120. DOI: 10.26650/EurJBiol.2019.0017

ABSTRACT

Objective: Naphthoquinone derivatives are known to have antibacterial activity and are likely to succeed a new class of compound that can be applied as antimicrobial agents.

Materials and Methods: The purpose of this experiment was to evaluate the potential antimicrobial, antibiofilm, anticancer, and cytotoxic activities of six naphthoquinone compounds previously reported in the literature.

Results: According to our studies, 2-(4-(trifluoromethyl)phenylamino)-3-(propylthio)naphthalene-1,4-dione (5a) and 2-(4-(trifluoromethyl)phenylamino)-3-(pentylthio)naphthalene-1,4-dione (5b) were found to have good antimicrobial activity against *Staphylococcus aureus* ATCC 29213 with 1.22 and 19.53 µg/mL MIC values, respectively. When we carried out the test against biofilm, the most effective agent, 5a, showed up to 40% inhibition of the *S. aureus*'s biofilm at the 1 x MIC concentration. However, when we investigated the cytotoxic effect of 5a on the cancer and non-cancer cell lines, we found that 5a showed higher toxicity to cancer cell lines.

Conclusion: The findings of our study suggest that further studies to develop these compounds and investigate its pharmacological properties could be useful to define the functionality of them as antimicrobial or anticancer agents.

Keywords: Sulfanyl 1,4-naphthoquinone, Arylamine, Antimicrobial activity, Cytotoxicity, Biofilm

INTRODUCTION

Discovering the potential of naphthoquinone compounds as antimicrobial agents increased the efforts towards synthesis new molecules and investigation of their antimicrobial properties by scientists (1, 2). Structure-

activity relationship studies performed to determine structural features or functional groups of the naphthoquinone derivatives that increase or decrease antimicrobial activity pointed out that the incorporation of substituted aromatic ring and sulphur (S) atom in the quinone skeleton was an important factor for enhancing



Corresponding Author: Emel Mataraci Kara E-mail: emelmataraci@hotmail.com

Submitted: 23.07.2019 • **Revision Requested:** 19.08.2019 • **Last Revision Received:** 16.10.2019 • **Accepted:** 18.10.2019

© Copyright 2019 by The Istanbul University Faculty of Science • Available online at <http://ejb.ibilistanbul.edu.tr> • DOI: 10.26650/EurJBiol.2019.0017

the biological activities (3). The increase in the number of studies on this subject is not surprising. In this context, it is no surprise that recent studies contain these activity increasing substituents (4, 5). Recently Errante et al. reported that some thio derivatives of naphthoquinones exhibited better activities than amphotericin B against some fungi (6). In a previous study, phenylamino derivatives of naphthoquinone that also bear straight chain thiol groups in the structure as substituents were obtained. Infrared, NMR (^1H , ^{13}C), and mass spectrometry were first used by Bayrak to identify their structures as original compounds (Figure 1) (7).

In the present study, we evaluated the potential antimicrobial, antibiofilm, and bactericidal efficacies of previously synthesized (7) thio derivatives of phenylamino-naphthoquinones against several pathogen microorganisms. Moreover, the cytotoxic activity of compound **5a** (which has the strongest antimicrobial activity in diverse cancer cell lines in comparison to non-cancerous cell lines) was examined.

MATERIALS AND METHODS

Microorganisms

The proposed routine quality control strains used in order to screen test performance with synthesized compounds in test panels are shown in Table 1. *Staphylococcus aureus* (ATCC 25923) was included in the experiment as a reference strain to confirm the biofilm forming bacteria to ensure antibiofilm activity of the

Table 1. The proposed routine quality control strains used to screen test performance with synthesized compounds in test panels.

Organisms	Culture Collection Numbers
<i>Escherichia coli</i>	ATCC 25922
<i>Staphylococcus aureus</i>	ATCC 29213
<i>Staphylococcus epidermidis</i>	ATCC 12228
<i>Enterococcus faecalis</i>	ATCC 29212
<i>Pseudomonas aeruginosa</i>	ATCC 27853
<i>Proteus mirabilis</i>	ATCC 14153
<i>Klebsiella pneumoniae</i>	ATCC 4352
<i>Candida albicans</i>	ATCC 10231
<i>Candida parapsilosis</i>	ATCC 22019
<i>Candida tropicalis</i>	ATCC 750

ATCC: American Type Culture Collection, 12301, Parklawn Drive, Rockville, MD 20852, USA.

compound. Inoculums of bacteria and yeasts were prepared with overnight cultures to cultivate a concentration of 1×10^8 colony forming units (CFU/mL) and 1×10^7 CFU/mL, respectively.

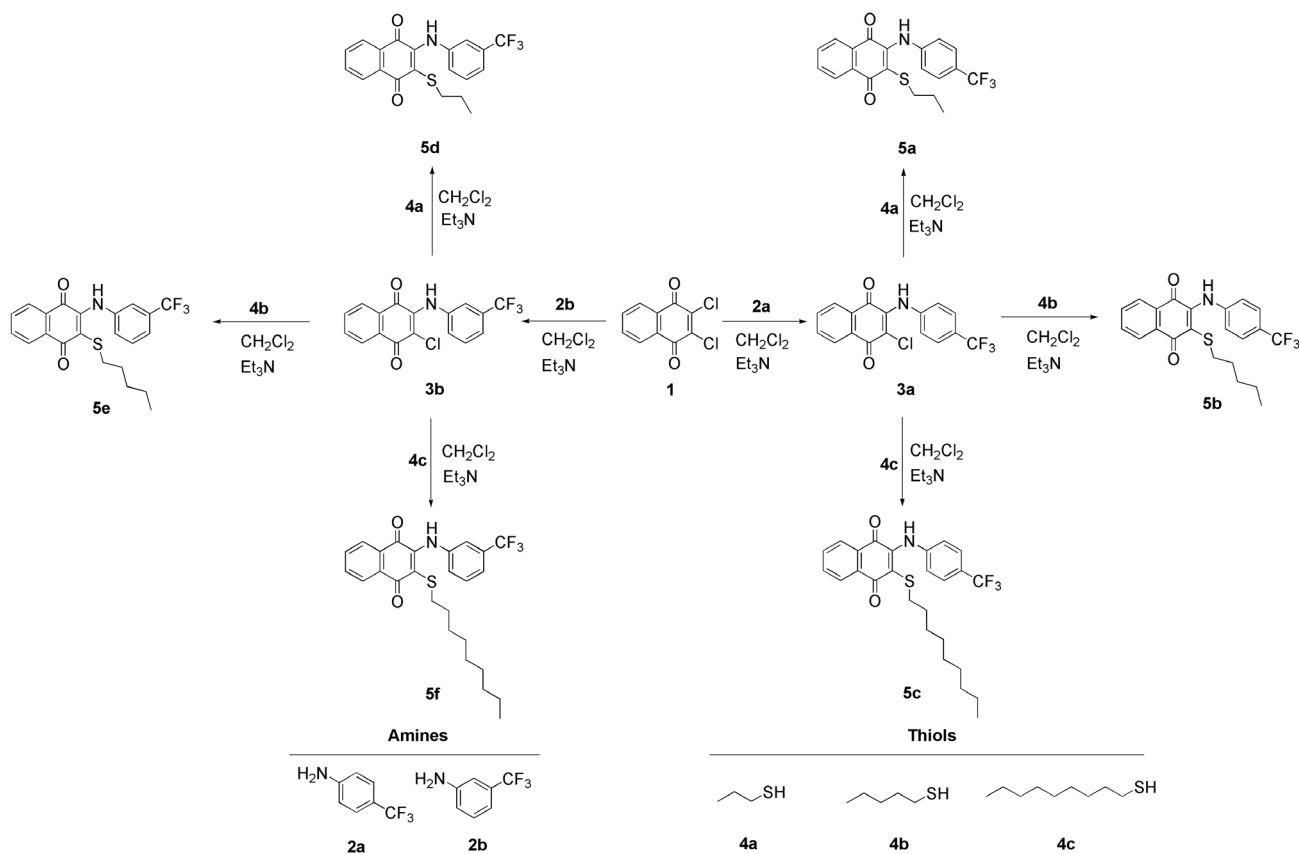


Figure 1. Straight-chained thio phenylamino-1,4-naphthoquinone derivatives.

Media

Tryptic soy broth (TSB- Difco Laboratories) plus 1% glucose was used for the biofilm production and antibiofilm activities assays. Mueller-Hinton broth (MHB, Oxoid) was used to identify the minimum inhibitory concentration (MIC) and time-kill curve; and Tryptic Soy agar (TSA, Difco Laboratories) was used for vital growth colony counts.

Antimicrobial Activity Assessment

Minimum Inhibitory Concentration Assay

This assay comprises of the determination of the synthesized compounds' spectrum of antimicrobial susceptibility in compliance with the resistance of studied Gram positive/negative bacteria and yeasts by the CLSI broth microdilution reference method (8, 9). The MIC was defined as the lowest concentration of the molecules causing complete inhibition in visible growth. The antimicrobial effect of the solvents was determined as a control and the test results were evaluated accordingly.

The conclusion from the antimicrobial activity tests prompted our research to investigate in vitro antimicrobial activities of compound **5a** contrary to 20 clinically obtained strains of *Staphylococcus aureus* by the CLSI broth microdilution reference method (8).

Antibiofilm Activity Assessment

The initial biofilm attachment assay and inhibition of biofilm formation tests were performed by using a slightly modified version of the method by Mataraci et al. (10) that was previously explained. 1/10 x MICs of the compound **5a** were appended to the 24 h biofilm and the plates were incubated for 1, 2 and 4 h for *S. aureus* ATCC 25923 (biofilm forming bacteria) at 37°C; molecules at 1x, 1/10x and 1/100 x MIC concentrations were appended to the 24 h biofilm and the wells were incubated for 24 h at 37 °C, respectively. Six wells were used for the tested compound. Sterile TSB-glucose was used for the positive controls. Then the plates were washed with PBS and evaluated at OD595 nm (BioTek EON Microplate Reader).

Determination of Bactericidal Effects by Time-Kill Curves

Time-kill curve analyses were performed by culturing *S. aureus* ATCC 29213 in MHB medium, in the presence of **5a** at 1 x MIC. An assessment of the dynamic bactericidal activity of compound **5a** was made with the time-kill curve method by testing at 1x times the MIC against *S. aureus* ATCC 29213 as described previously. Solvent containing the control was included in the test for the tested strain. The inoculum was quantified spectrophotometrically and added to the flasks. The antimicrobial amount was checked by the inhibition of viable colony growth at the site of the initial inoculum in accordance with NCCLS recommendations (11). Bactericidal activity was described as a decrease of $\geq 3 \log_{10}$ CFU/mL from the initial inoculum at 24 h.

Cell Cultures

Three non-cancer cell lines were used in this study: Mouse embryonic fibroblast (BALB/3T3), human umbilical vein endothelial cell (HUVEC), and human keratinocyte (HaCaT). The three cancer cell lines used were human hepatocellular carcinoma (HepG2),

human neuroblastoma (SH-SY5Y), and human prostate cancer cell (PC-3). All cells were grown with DMEM medium containing 10% fetal bovine serum and 1% antibiotic-antimycotic solution in a 37 °C, 5% CO₂ humidified incubator. The cells were passaged routinely at a confluence of 90% by trypsinization.

Cell Treatments and Cytotoxicity Assay

For the cytotoxicity assay, the cells were seeded in 96 well plates 1x10⁴ cells/well and incubated overnight for cell attachment. Subsequently, the media were replaced with fresh media and the cells were treated with compound final concentrations 100-6.25 µg/mL and vehicle control 1% DMSO for 24 h at 37 °C. After 24 hours, cell viability was measured using the 3-(4,5-dimethylthiazol-2-yl)-2,5-diphenyltetrazolium bromide (MTT) assay. The final volume of the 5 mg/mL MTT reagent was added to the wells and the plates were incubated in the dark for 3 h.

The media was then removed and the formazan precipitates were dissolved in 100 µL DMSO. Optical density was measured using a microplate reader (Biotek Instruments, Inc., Vermont, USA) at 590 nm. Cell viability was expressed as a percentage of the absorbance recorded for vehicle control.

Statistical Analysis

All tests were performed in three independent assays. One-way ANOVA, Bonferroni's multiple comparison test was used to compare the differences between the control and compound-treated biofilms and time-kill kinetics. A *p* value < 0.001 was considered as statistically significant.

RESULTS

Molecules

In this study, we used six molecules (2-(4-(trifluoromethyl)phenylamino)-3-(propylthio)naphthalene-1,4-dione (**5a**), 2-(4-(trifluoromethyl)phenylamino)-3-(pentylthio)naphthalene-1,4-dione (**5b**), 2-(4-(trifluoromethyl)phenylamino)-3-(nonylthio)naphthalene-1,4-dione (**5c**), 2-(3-(trifluoromethyl)phenylamino)-3-(propylthio)naphthalene-1,4-dione (**5d**), 2-(3-(trifluoromethyl)phenylamino)-3-(pentylthio)naphthalene-1,4-dione (**5e**), 2-(3-(trifluoromethyl)phenylamino)-3-(nonylthio)naphthalene-1,4-dione (**5f**)) that had been previously synthesized by Bayrak (7). Bayrak reported that the thiol derivatives of phenylamino-1,4-naphthoquinones (**5a-f**) were obtained by a substitution reaction with phenylamino-chloro-1,4-naphthoquinone derivatives (**3a-b**) that synthesized by the chemical reaction of 2,3-dichloro-1,4-naphthoquinone with trifluoro substituted phenyl amines and the appropriate straight-chained thiol in dichloromethane were mixed at room temperature by applying Et₃N (7). The reactions of 2-(4-(trifluoromethyl)phenylamino)-3-chloronaphthalene-1,4-dione (**3a**) and 2-(3-(trifluoromethyl)phenylamino)-3-chloronaphthalene-1,4-dione (**3b**) with aliphatic thiol compounds (propane, pentane, and nonane thiol) proceeded via the substitution of a chlorine atom with a sulfur atom to form phenylamino-1,4-naphthoquinones with straight chain thio group (**5a-f**). The structures of **5a-f** were also clarified by IR, ¹H NMR, ¹³C NMR, and MS data (Figure 1).

Antimicrobial Activity

The *in vitro* antimicrobial activity of six thio phenylamino-1,4-naphthoquinone derivatives (**5a-f**) against three Gram-positive bacteria, four Gram-negative bacteria, and three fungi by the microbroth dilutions technique using the CLSI recommendations (8, 9).

The antimicrobial experiment results of all the six sulfanyl derivatives of phenylamino-1,4-naphthoquinone (**5a-f**) are given in Table 2. The test-cultures *E. coli*, *P. mirabilis*, and *K. pneumoniae* appeared to be resistant to the all synthesized compounds. None of the studied molecules showed any antibacterial activity against the Gram-negative bacteria except for **5f**. Concerning the antibacterial activity, the Gram-positive bacteria were more susceptible to the sulfanyl derivatives of phenylamino-1,4-naphthoquinone than the Gram-negative ones. Generally, the findings showed that some compounds displayed varying effects on the growth of the tested Gram-positive bacterial strains. The results showed that all thio-phenylamino-1,4-naphthoquinone derivatives exhibited antimicrobial activity against *S. aureus*. **5a** and **5b** showed good activity against *S. aureus* with an MIC value of 1.22 and 19.53 µg/mL, respectively. Notably, **5a** had the same inhibitory activity against *S. aureus* as that of Cefuroxime-Na (MIC = 1.22µg/mL). An evaluation of the antifungal activity of the thio- phenylamino-1,4-naphthoquinone derivatives exhibited no antifungal activity against *C. albicans*, *C. parapsilosis*, and *C. tropicalis* except **5d**. The **5d** was active analog against *C. tropicalis* (MIC = 312.5µg/mL) (Table 2). According to our results, **5a** was found active against the standard *S. aureus*, so we investigated the potential antimicrobial activity of this compound against 20 clinically obtained *Staphylococcus aureus* (Table 3). Susceptibility testing demonstrated that the MIC ranges for **5a** were 1250- >2500 µg/mL, for these clinically obtained strains.

Antibiofilm Activities

Because of the its potent activity, only **5a** was used in the antibiofilm activities assays. When we carried out these tests, the agent inhibited the biofilm attachment according to time, and it showed an important inhibitor activity against biofilm formation at 24 h depending on concentration (Figure 2).

Time-kill Kinetics

Time-kill kinetic studies showed that the naphthoquinone compounds used in this study displayed concentration-dependent bactericidal activity. When **5a** was used at 1 × MIC, bactericidal activity was not seen for the studied strain *S. aureus* ATCC 29213 at 24 h (Figure 3). However, in our study **5a** only showed approximately 2 log₁₀ reduction in bacterial cell count at the 1 × MIC concentration used.

Cytotoxicity Assay

The cytotoxicity of **5a** was screened in three different non-cancer cell lines, mouse embryonic fibroblast (BALB/3T3), human umbilical vein endothelial cell (HUVEC), and human keratinocyte (HaCaT), together with three cancer cell lines, human hepatocellular carcinoma (HepG2), human neuroblastoma (SH-SY5Y), and human prostate cancer cell (PC-3). In all cell lines **5a**

Table 2. *In vitro* antimicrobial activity results of thio-phenylamino-1,4-naphthoquinone derivatives (5a-f).

ID	Microorganisms									
	Gram-negative Bacteria (MIC, µg/mL)				Gram-positive Bacteria (MIC, µg/mL)				Yeast (MIC, µg/mL)	
	<i>P. aeruginosa</i>	<i>E. coli</i>	<i>K. pneumoniae</i>	<i>P. mirabilis</i>	<i>S. aureus</i>	<i>S. epidermidis</i>	<i>E. faecalis</i>	<i>C. albicans</i>	<i>C. parapsilosis</i>	<i>C. tropicalis</i>
5e	-	-	-	-	625	1250	-	-	-	-
5f	625	-	-	-	1250	1250	-	-	-	-
5b	-	-	-	-	19.53	1250	-	-	-	-
5c	-	-	-	-	1250	-	-	-	-	-
5d	-	-	-	-	312,5	-	-	-	-	312.5
5a	-	-	-	-	1.22	1250	625	-	-	-
Reference antimicrobials	2.4	4.9	4.9	2.4	1.2	9.8	128	4.9	0.5	1
	Ceftazidime	Cefuroxime-Na	Cefuroxime-Na	Cefuroxime-Na	Cefuroxime-Na	Cefuroxime	Amikacin	Clotrimazole	Amphotericin B	Amphotericin B

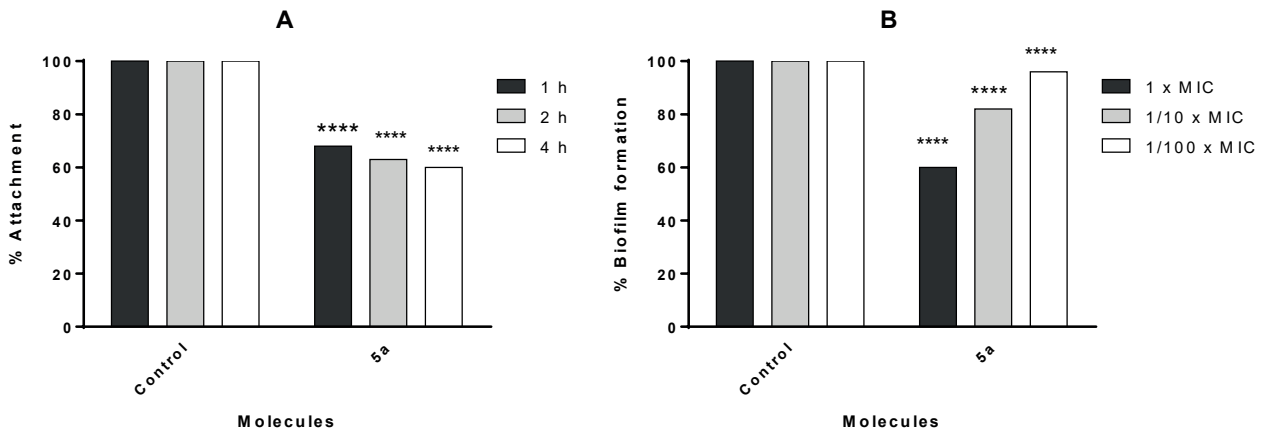


Figure 2. Inhibition of *S. aureus*. **A**: surface attachment to the wells contained 1/10 x MIC of molecule and an inoculum of 1×10^7 CFU/200 μ l, incubated for 1, 2, or 4 h at 37°C; **B**: biofilm formation in each well contained 1 x, 1/10 x, or 1/100 x MIC of molecule and an inoculum of 5×10^5 CFU/200 μ l, incubated for 24 h at 37°C. Control bars indicate bacterium without molecule accepted as 100%. Six wells were used for the tested molecule. Each experiment is representative of three independent tests. All differences between the control and molecule treated biofilms were statistically significant ($p < 0.001$).

decreased cell proliferation significantly after 24 h. The most significant effect was seen in the HepG2 cell line with an IC_{50} value of 21.96 μ g/mL. **5a** showed a similar cytotoxic effect in the SH-SY5Y and PC-3 cells with IC_{50} values of 31.94 μ g/mL and 31.95 μ g/mL, respectively (Figure 4). **5a** had IC_{50} values of 60.72 μ g/mL, 5727 μ g/mL, and 38.8 μ g/mL against non-cancer cells, HaCaT, 3T3, and HUVEC cells respectively (Figure 5), implies that higher concentrations of compound exhibit toxicity to non-cancer cells.

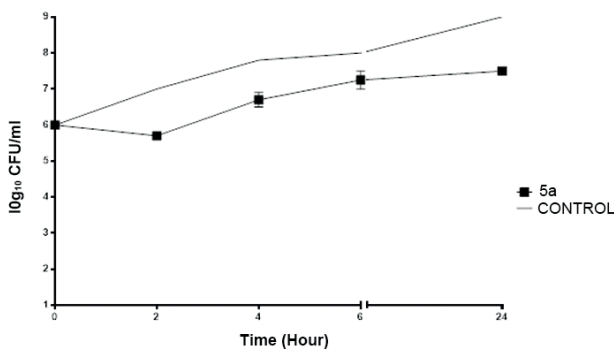


Figure 3. Time kill determinations for *S. aureus* ATCC 29213 strain after treatment with **5a** alone at 1 x MIC. The x-axis represents the killing time, and the y-axis represents the logarithmic *S. aureus* survival.

Table 3. *In vitro* activities of **5a** against 20 clinically obtained strains of *S. aureus*.

Molecule	Staphylococcus aureus		
	MIC range	MIC50	MIC90
5a	1250- >2500	1250	2500

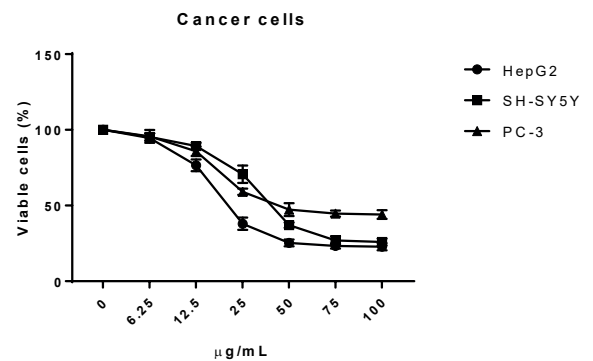


Figure 4. Cytotoxic effect of **5a** against HepG2, SH-SY5Y and PC-3 cells determined by MTT assay. Each point representing the mean of three separate biological experiments \pm S.D.

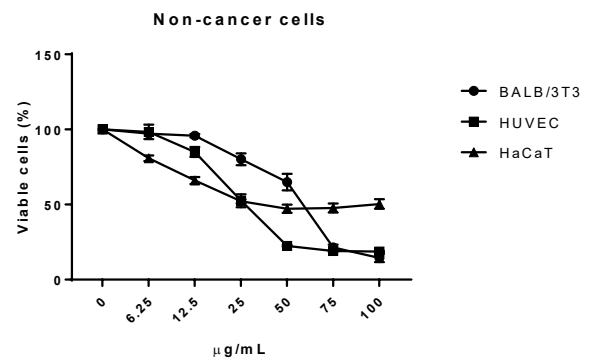


Figure 5. Cytotoxic effect of **5a** against BALB/3T3, HUVEC and HaCaT cells determined by MTT assay. Each point representing the mean of three separate biological experiments \pm S.D.

DISCUSSION

The increase and spread of antimicrobial resistance among the various microorganisms is now one of the world's major health problems. Antibiotic resistance is increasing both in the community and in hospitals, multidrug resistant (MDR) and even pan resistant strains (resistant to all common antibiotic groups for therapeutic use), which lead to failure of antibiotic treatment, increased mortality and morbidity and have a huge increase on the cost of medical treatment and prevention of bacterial infectious diseases (12, 13). For these reasons, researchers have produced many synthetic or semi-synthetic molecules as candidates for new and beneficial drugs (13-15). The discovery of new antibacterial agents or multidrug agents for reversing is critical as we may not have any effective medicines to treat bacterial infections caused by the emerging superbugs that are resistant to the majority of clinically available antibiotics (16).

In our present study, the *in vitro* antimicrobial activities of known phenylamino derivatives of naphthoquinone having straight chain thiol groups were evaluated and two molecules (**5a** and **5b**) were found to have a potent antibacterial efficacy against *S.aureus* human-pathogenic strains and causes not only community acquired but also immortal nosocomial infections (10).

The communities of microorganisms attached to a surface were termed 'biofilm'. Bacteria within the biofilm require a 100 to 1000 times greater antibiotic concentration to achieve destruction versus planktonic bacteria. Standard intravenous therapy does not reach a high enough concentration to reduce the bacterial burden within the biofilm. It is a fact that this is the case for up to 60% of the infections which are usually associated with microorganisms that have settled in the microbial biofilms. Not all antimicrobial agents are the same in terms of biofilm eradication. The agent's mechanism of action, its interaction with the biofilm matrix and the effect of biofilm related parameters such as oxygen concentration, biofilm and growth rate should be considered (17-19). To this end, we researched the inhibition of surface bacterial adhesion and the inhibition of biofilm production by MIC or sub-MIC values of the **5a** compound. **5a** significantly inhibited the attachment of bacteria at 1/10 x MIC in 1-4 h and 24 h biofilm formation up to 40%, in particular at 1 x MIC ($p < 0.001$). Although the inhibition of mature biofilm is very difficult, the inhibition of biofilm formation seems to be more applicable in early critical stages.

Although **5a** has limited bactericidal activity against *S. aureus* at 1 x MIC, it could be considered for future studies since its combination with antibiotics as an adjuvant could cause synergism, thus lowering **5a**'s potential toxic effects and preventing the development of resistance. Moreover, comparing the cytotoxic effect of the compound on non-cancer and cancer cell lines, we noticed that **5a** showed higher toxicity to cancer cell lines. Human hepatocellular cancer HepG2 cells in particular were the most effected cells. This result may suggest potential anticancer use against human hepatocellular cancer.

HaCaT cells are immortalized human keratinocytes and it is a useful model for studying dermal toxicity. **5a** showed the least toxicity to

the HaCaT cells and IC_{50} value was over 60 $\mu\text{g/mL}$. Also, increasing doses of the compound did not cause more cytotoxic effect in the HaCaT cells. Additionally, the compound showed a 2-fold higher IC_{50} value to the mouse embryonic fibroblast BALB/3T3 cells than the cancer cells. These results may indicate potential antibacterial dermal use of the compound in low concentrations without causing significant dermal toxicity. Follow-up research is essential to understand the compound's mechanism of action and define detailed the activity-structure relationship.

CONCLUSION

With respect to the antimicrobial, anticancer, and cytotoxic activities of the phenylamino derivatives of naphthoquinone that contain straight chain thiol groups in the structure as substituents which had been previously synthesized, further studies to establish their pharmacological properties would be helpful to define their functionality as antimicrobial or anticancer agents.

Peer-review: Externally peer-reviewed.

Author Contributions: Conception/Design of study: E.M.K., A.T.J., N.B., B.O.C., B.A., M.Y., A.F.T., H.Y.; Data Acquisition: E.M.K., A.T.J., N.B., B.O.C., B.A., H.Y.; Data Analysis/Interpretation: E.M.K., A.T.J., N.B., B.O.C., B.A., M.Y., A.F.T., H.Y.; Drafting Manuscript: B.O.C., B.A., M.Y., B.O.C., B.A., M.Y.; Critical Revision of Manuscript: E.M.K., A.T.J., N.B., B.O.C., B.A., M.Y., A.F.T., H.Y.; Final Approval and Accountability: E.M.K., A.T.J., N.B., B.O.C., B.A., M.Y., A.F.T., H.Y.; Technical or Material Support: E.M.K., A.T.J., N.B., B.O.C., B.A., M.Y., A.F.T., H.Y.; Supervision: E.M.K., A.T.J., N.B., B.O.C., B.A., M.Y., A.F.T., H.Y.

Conflict of Interest: The authors declare that they have no conflicts of interest.

Financial Disclosure: There are no funders to report for this submission.

REFERENCES

1. Ryu CK, Shim JY, Chae MJ, Choi IH, Han JY, Jung OJ, et al. Synthesis and antifungal activity of 2/3-arylthio- and 2,3-bis(arylthio)-5-hydroxy-/5-methoxy-1,4-naphthoquinones. *Eur J Med Chem* 2005; 40 (5): 438-44.
2. Bayrak N, Yildirim H, Tuyun AF, Mataraci-Kara E, Ozbek-Celik B, Gupta GK, et al. Synthesis, computational study, and evaluation of *in vitro* antimicrobial, antibiofilm, and anticancer activities of new sulfanyl aminonaphthoquinone derivatives. *Lett Drug Des Discov* 2016; 13 (999).
3. Ryu CK, Lee JY, Jeong SH, Nho JH. Synthesis and antifungal activity of 1H-pyrrolo[3,2-g]quinoline-4,9-diones and 4,9-dioxo-4,9-dihydro-1H-benzo[f]indoles. *Bioorg Med Chem Lett* 2009; 19: 146-8.
4. Yildirim H, Bayrak N, Tuyun AF, Mataraci-Kara E, Ozbek-Celik B, Gupta GK. 2,3-disubstituted-1,4-naphthoquinones containing an arylamine with trifluoromethyl group: synthesis, biological evaluation, and computational study. *Rsc Adv* 2017; 7: 25753-64.
5. Kacmaz A, Acar ET, Atun G, Kaya K, Sigirci BD, Bagcigil F. Synthesis, electrochemistry, DFT calculations, antimicrobial properties and X-ray crystal structures of some NH- and/or S- substituted-1,4-quinones. *Chemistryselect* 2018; 3: 8615-23.

6. Errante G, Motta GL, Lagana C, Wittebolle V, Sarciron MÉ, Barret R. Synthesis and evaluation of antifungal activity of naphthoquinone derivatives. *Eur J Med Chem* 2006; 41: 773–8.
7. Bayrak N. Novel straight-chained sulfanyl members of arylamino-1,4-naphthoquinones: synthesis and characterization. *JOTCSA* 2017; 4(2): 597-606.
8. Clinical and Laboratory Standards Institute (CLSI), Methods for dilution antimicrobial susceptibility tests for bacteria that grow aerobically, in, Wayne, PA, USA, 2006.
9. Clinical and Laboratory Standards Institute (CLSI), Reference Method for Broth Dilution Antifungal Susceptibility Testing of Yeasts; Approved Standard–Second Edition, in, Wayne, PA, USA, 1997.
10. Mataracı E, Döşler S. In vitro activities of antibiotics and antimicrobial cationic peptides alone and in combination against methicillin resistant *Staphylococcus aureus* biofilms. *Antimicrob Agents Chemother* 2012; 56: 6366-71.
11. National Committee for Clinical Laboratory Standards. Methods for Determining Bactericidal Activity of Antimicrobial Agents-Approved Guideline M26 A. Wayne NCCLS, 1999.
12. Cepas V, López Y, Muñoz E, Rolo D, Ardanuy C, Martí S, et al. Relationship between biofilm formation and antimicrobial resistance in gram-negative bacteria. *Microb Drug Resist* 2019; 25(1): 72-9.
13. Döşler S, Mataracı-Kara E, Başpınar Küçük H, Yusufoglu AS. Antibacterial and anti-biofilm activities of new chiral and racemic 1,3-dioxolanes. *Istanbul J Pharm* 2015; 45(1): 19-28.
14. Calderone R, Sun N, Gay-Andrieu F, Groutas W, Weerawarna P, Prasad S, et al. Antifungal drug discovery: the process and outcomes. *Future Microbiol* 2014; 9: 791-805.
15. Nigam A, Gupta D, Sharma A. Treatment of infectious disease: Beyond antibiotics. *Microbiol Res* 2014; 169: 643-51.
16. Mosolygó T, Kincses A, Csonka A, Tönki ÁS, Witek K, Sanmartín C, et al. Selenocompounds as novel antibacterial agents and bacterial efflux pump inhibitors. *Molecules* 2019; 24: 1487.
17. Jamal M, Ahmad W, Andleeb S, Jalil F, Imran M, Nawaz MA, et al. Bacterial biofilm and associated infections. *J Chin Med Assoc* 2018; 81(1): 7-11.
18. Donlan RM, Costerton JW. Biofilms: survival mechanisms of clinically relevant microorganisms. *Clin Microbiol Rev* 2002; 15: 167-93.
19. Hoiby N, Bjarnsholt T, Moser C, Bassi GL, Coenye T, Donelli G, et al. ESCMID guideline for the diagnosis and treatment of biofilm infections 2014. *Clin Microbiol Infect* 2015; 21(S1): S1-S25.

Antioxidant Effects of Epigallocatechin Gallate in Cerulein-Induced Pancreatitis

Elif Karacaoglu¹ , Gozde Girgin² , Guldeniz Selmanoglu¹ , Terken Baydar² 

¹Hacettepe University, Faculty of Science, Department of Biology, Ankara, Turkey

²Hacettepe University, Faculty of Pharmacy, Department of Toxicology, Ankara, Turkey

ORCID IDs of the authors: E.K. 0000-0003-3426-4584; G.G. 0000-0002-7051-0490; G.S 0000-0001-6565-736X; T.B 0000-0002-5497-9600

Please cite this article as: Karacaoglu E., Girgin G., Selmanoglu G., Baydar T. Antioxidant Effects of Epigallocatechin Gallate in Cerulein-Induced Pancreatitis. Eur J Biol 2019; 78(2): 121-128. DOI: 10.26650/EurJBiol.2019.0035

ABSTRACT

Objective: Acute pancreatitis (AP) is an inflammatory disease of the pancreas resulting from auto-activation of digestive enzymes and damage to the pancreatic parenchyma. Reactive oxygen species (ROS) play an important role in the progression of AP. In the present study, we aimed to evaluate epigallocatechin-3 gallate (EGCG) in reducing the inflammatory reaction and tissue damage in experimental AP rat model.

Materials and Methods: Amylase, tumor necrosis factor-alpha (TNF- α) and interleukin-6 (IL-6) levels were measured. Histopathological, immunohistochemical analyses of apoptotic cells, CD-8 α and CD-68 were performed. Superoxide dismutase (SOD), catalase (CAT) and glutathione S-transferase (GST) were determined in hemolysates.

Results: Cerulein+EGCG treatment did not cause decreases in the amylase levels. IL-6 levels decreased in cerulein+EGCG group, however, TNF- α levels increased. No changes were observed in SOD activity by EGCG treatment, CAT and GST activities increased. EGCG treatment caused severe edema, inflammation and fat necrosis after cerulein-induced pancreatitis. Apoptosis in pancreas, CD8- α and CD-68 positive cells increased in EGCG treatment after pancreatitis induction.

Conclusion: It may be suggested that EGCG showed a pro-oxidant effect, in contrast to the expected in the pancreatitis model when compared to a positive control. It can be concluded that overconsumption of EGCG should be avoided in pancreatitis conditions.

Keywords: Acute Pancreatitis, Reactive Oxygen Species, Epigallocatechin-3 Gallate, N-acetylcysteine, Antioxidant Effect

INTRODUCTION

Acute pancreatitis (AP) is an inflammatory disease of the pancreas resulting from the auto-activation of digestive enzymes and damages to the pancreatic parenchyma as the result of auto-digestion. Various causative factors underlie the disease process, including gallstone disease, alcohol abuse, hyperlipidemia, drugs (azathioprine, sulphonamides, estrogens), autoimmune diseases etc. (1). Eighty per cent of the cases are mild/edematous pancreatitis, and resolve completely with proper treatment modalities (2). On the other hand, the remaining one fifth of the cases progress to severe AP (SAP), and

have a mortality rate of 20-30% (1-3). The main pathophysiologic event in the initiation and progression of pancreatitis is the digestive enzyme auto-activation and acinar cell damage leading to inflammation (2). Trypsin is the main pancreatic enzyme that is activated, and is responsible for the parenchymal damage and also for activation of the inflammatory cascade (2,3). It activates the kallikrein and kinin systems, and also activates the coagulation and/or fibrinolysis cascade (4). Inflammation and acinar cell damage is actually an overlapping event. Local inflammation causes an up-regulation in the expression of the adhesion molecules in the capillary endothelium, leading to the increased



Corresponding Author: Elif Karacaoglu E-mail: elifkush@hacettepe.edu.tr

Submitted: 01.10.2019 • **Revision Requested:** 28.10.2019 • **Last Revision Received:** 01.11.2019 • **Accepted:** 06.11.2019

© Copyright 2019 by The Istanbul University Faculty of Science • Available online at <http://ejb.istanbul.edu.tr> • DOI: 10.26650/EurJBiol.2019.0035

migration of the leukocytes to the region (4). The migrating neutrophils will be activated in the pro-inflammatory milieu, and start degranulation (2-6). This leads to the production and release of various mediators, such as phospholipase A2, nitric oxide and oxygen radicals. All those result in an increase in the severity of the inflammation, and it is usually seen with SAP (5, 6). Elucidation of the factors that cause the progression of the potent inflammatory response and furthermore, modulation of this response, have been the subject of current pancreatitis research. In pancreatitis, once the disease process progresses to SAP, various organ systems are affected by this systemic inflammatory process (2,5,7, 8).

Reactive oxygen species (ROS) seem to play a crucial role in the pathogenesis of AP (9). The leukocytes isolated from the patients with pancreatitis showed enhanced capabilities for production and release of ROS (9,10). The enhanced production of ROS, not only leads to severe organ damage, but also causes activation of nuclear factor kappa-light-chain-enhancer of activated B cells (NF- κ B) pathway activation (10,11). Since ROS causes both tissue damage that potentiates the inflammatory process, and enhanced pro-inflammatory cytokine production through certain cellular pathways, blocking the ROS may be a valid treatment strategy for the treatment of AP (10).

Experimental models for AP provide the exact mechanism of the disease and developing new therapeutic strategies. Recently, several animal models have been produced for AP, including non-invasive and invasive methods (12). In the present study, we used the hormone-induced model (cerulein as a cholecystokinin-pancreozymin analogue), which is one of the non-invasive methods for induction of AP. This experimental method was chosen due to several advantages, such as being an easy simple method to perform. Additionally, the cerulein-induced AP model was reported to be a useful method, due to healing process which begins after the disease induction agent is discontinued (12).

Epigallocatechin-3 gallate (EGCG) is a naturally occurring polyphenol that belongs to the broad family of chemical compounds called the flavonoids (13, 14). Flavonoids are abundant in various foods such as apples, grapes, cherries, berries, while EGCG is a polyphenol that is mainly found in cacao and its products, and especially in green tea (13, 14). EGCG, like all polyphenols acts through antioxidant and non-antioxidant mechanisms. Antioxidant mechanisms aim to restore the redox balance and counteract the ROS activity in organisms, and repair oxidant-induced injury (15-17). However, non-antioxidant mechanisms include the oestrogen receptor signalling, cell signalling cascade and cell cycle control pathways (18). Green tea polyphenols have high antioxidant capacity, and these phenolic compounds proved to exert pro-oxidant effects and, by means of their pro-oxidant effect, they were suggested as a potential prevention mechanism for cancer (19). Studies from cancer research have shown that EGCG inactivates the signal transduction and transcription (STAT) pathways (20). Furthermore, it also plays a role in the inactivation of anti-tumour immunity.

Persistent STAT3 activation causes a tumour promoting inflammation through the activation of NF- κ B, interleukin-6 (IL-6) family of cytokines and gp130, Janus Kinase (JAK) pathway (21). Additionally, EGCG binds the p65 subunit of NF- κ B and inhibits the pathway, and causes a reduction in the pro-inflammatory cytokine production. The above mentioned action mechanism of EGCG emphasizes its capability to reduce inflammation (22). Therefore, it can reduce the main pathophysiologic event, inflammation in AP, and reduce tissue damage and hence, can decrease the morbidity and mortality resulting from this serious illness. On the other part, N-acetylcysteine (NAC), which plays a crucial role in the formation of glutathione as a powerful antioxidant in the body, has been shown to prevent the increase in the cytosolic calcium status, and reduce the accumulation of enzymes in acinar cells during AP (23). Green tea has been demonstrated as a polyphenol-rich extract with a high content of catechins, including epicatechin, epicatechin-3-gallate, EGCG and epigallocatechin (24), and EGCG was known to have potent antioxidant properties among other catechins (25). Although effects of green tea extract on cerulein-induced pancreatitis was studied in a mice model previously (11), in that study, the authors evaluated the whole green tea extract rather than a flavonoid. So, it is necessary to study which flavonoids in the green tea extract caused ameliorative effects. So, we intended to evaluate EGCG which is the most abundant flavonoid found in the green tea. The main aim of this study was to evaluate EGCG in reducing the inflammatory reaction and tissue damage in an experimental AP rat model.

MATERIALS AND METHODS

Animals

All experiments were performed in accordance with the protocols approved by the veterinarian. This study was performed by the official permission of the Hacettepe University Ethical Committee for the Protection of Animals in Research (#2008/54). Male Wistar rats (approximately weighing 300-350 g) were housed in polycarbonate cages in a controlled environment with 12:12-hours light-dark cycles. The rats were given standard laboratory chow and water ad libitum.

Chemicals

Cerulein ($\geq 95\%$) was provided by Sigma-Aldrich (St. Louis, MO, USA). Both of EGCG, and NAC were obtained from Sigma-Aldrich (St. Louis, MO, USA), and each stock solution with a 100 mg/kg concentration was prepared in water. All other chemicals and reagents were provided by Sigma-Aldrich (St. Louis, MO, USA).

Induction of Acute Pancreatitis

Rats were injected intramuscularly with ketamine (50 mg/kg) and xylazine (5 mg/kg) for anesthesia. After anesthesia, an intravenous catheter was placed into right jugular vein. Rats were injected twice into the catheter at a 1-h interval, with a supra-maximally stimulating dose of cerulein to elicit AP. Rats in the control group received similar injections of saline solution. The animals were injected with saline following the induction of AP.

Experimental Groups

The treatment was started with EGCG and NAC following the induction of AP in order to simulate the actual clinical scenario. Therefore, 20 animals were randomized into 4 groups including 5 animals in each group.

Pancreatitis was induced by cerulein at a dose of 5µg/kg/h, established following intravenous infusion from the catheter inserted into the internal jugular vein as standard (13). Rats with cerulein-induced pancreatitis were treated with EGCG or NAC at doses of 100 mg/kg i.p. at 6 and 18 hours. The dose selection of EGCG was based on the previous study (26). NAC was used as a positive control. Laparotomy was performed in all groups, including the control group at 24 hours. Groups were as follows:

The control group consisted of the sham group; rats were injected with saline in two doses 1 hour apart. The cerulein group was the AP group, induced by Cerulein. The cerulein+NAC group consisted of the NAC treated pancreatitis group and the cerulein+EGCG group consisted of the EGCG treated pancreatitis group. At the end of the experiment, the animals were sacrificed under anaesthesia by opening the thoracic cavity and also drawing blood via the inferior vena cava.

Management and Harvest of the Samples

Venous blood samples and pancreatic tissues were dissected from the animals. Pancreatic tissues were fixed in 10% neutral buffered formalin for immunohistochemistry and Bouin's solution for histopathology. Blood samples were taken and placed in heparinized tubes, and centrifuged at 3500 rpm for 15 min. Erythrocytes were washed with PBS, and hemolysates were prepared with the addition of cold deionized water, and samples were centrifuged for the removal of cellular debris. The supernatants were used for the enzyme assays. All supernatant samples were stored at -20°C until further analyses.

Histopathology

Pancreas tissues of each rat were dissected, then observed grossly and weighed. Relative organ weights (organ weight/body weight) were calculated. Pancreas tissues were fixed in Bouin's solution, dehydrated in increasing alcohol degrees and embedded in paraffin blocks. 5 µm-thick sections were obtained, and were tissues stained with H&E for the light microscopy. Histological evaluation was performed according to Schmidt criteria (Table 1).

Immunohistochemistry of CD8-α and CD68

Immunohistochemical analyses were principally performed by the streptavidin-biotin amplification method. Monoclonal antibodies were against formalin fixed CD8-α (Santa Cruz Biotechnology, INC, 6A242) and CD68 (Santa Cruz Biotechnology, INC, 6A324) transmembrane proteins. Briefly, portion of the pancreas tissues were fixed in 10% neutral buffered formalin, dehydrated in increasing alcohol degrees and embedded in paraffin blocks. Then 5 µm-thick sections were replaced on poly-L-lysine coated slides. After sections were deparaffinized, tissue sections were treated with citrate buffer at 95°C for 20 min for antigen retrieval. Sections were washed with PBS with 0.01% Triton X-100 and treated with 0.3% hydrogen peroxidase for 15 min at room temperature, then incubated with ultra V block for 10 min. The sections were incubated with mouse CD8-α against rat (1:50 dilution), and with mouse CD68 against rat (1:25 dilution) at +4°C overnight. Peroxidase labelling was carried out using the Ultravision Polyvalent (Rabbit-Mouse) HRP kit (Thermo Scientific/Lab Vision), and the positive stainings were visualized by using DAB kit (Thermo Scientific/Lab Vision) to display the reaction product with a brown colour. Then, counterstaining was performed by Haematoxylin staining. Ten random areas were selected at x100 magnification, and CD8-α and CD68 positive cells were counted. CD8-α, and CD68 were expressed as positive cell numbers per square millimetre.

TUNEL Assay

10% neutral buffered formalin fixed sections were deparaffinised and dehydrated. Then, sections were digested by Proteinase K for 15 minutes at room temperature. The endogenous peroxidase was quenched in 3% hydrogen peroxide. Apoptotic nuclei of the pancreas were performed by in situ terminal deoxynucleotidyl transferase (TdT)-mediated deoxyuridine triphosphate (dUTP)-biotin nick end-labelling (TUNEL) using Apoptag®Plus kit (Millipore, S7100 EMD Millipore). Counterstain was performed by 0.5% methyl green. Apoptotic cells were quantified by counting the number of TUNEL positive cells per square millimeter. For each section, 10 areas were randomly selected at x100 magnification per animal and then, the numbers of apoptotic cells were calculated per one square millimeter.

Enzyme Assays

Catalase (CAT) and superoxide dismutase (SOD) enzyme specific activities were performed as previously described (27). Briefly, blood samples were centrifuged, and separated erythrocytes were washed with PBS. Supernatant samples of hemolysates

Table 1. Schmidt Criteria for histopathological scoring

Pathological Grade	0	1	2	3
Edema	None	Interlobular	Intralobular	Inter acinus
Acinar cell degeneration	None	Focal (<5%)	Sublobular (5%-20)	Lobular (>20%)
Inflammation	None	Mild	Moderate	Severe
Hemorrhage	None	Mild	Moderate	Severe

were used for the experiments for SOD, CAT and glutathione-S-transferase (GST) antioxidant enzyme activity measurements. Total protein component was measured in order to calculate the specific enzyme activities. Amylase, IL-6 and tumour necrosis factor alpha (TNF- α) in serum samples were measured with commercial ELISA kits.

Statistical Analysis

All results were expressed as mean \pm standard error. Differences between groups were analysed by non-parametric Kruskal-Wallis variance analyses. Mann-Whitney U-test was performed for independent groups with $p \leq 0.05$ significance levels.

RESULTS

Plasma serum amylase activities were shown in Figure 1A. According to the amylase activity results, the amylase activity in cerulein, cerulein+NAC and cerulein+EGCG groups was statistically increased when compared to control group ($p < 0.05$).

Serum inflammatory cytokine levels were measured, and the results were shown in Figure 1B-1C. While IL-6 levels statistically decreased, TNF- α levels of cerulein+EGCG group were statistically increased when compared to the control group ($p = 0.009$, $p = 0.009$). Additionally, TNF- α levels of cerulein+EGCG group were also significantly increased compared to the cerulein and cerulein+NAC groups (respectively, $p = 0.04$, $p = 0.02$).

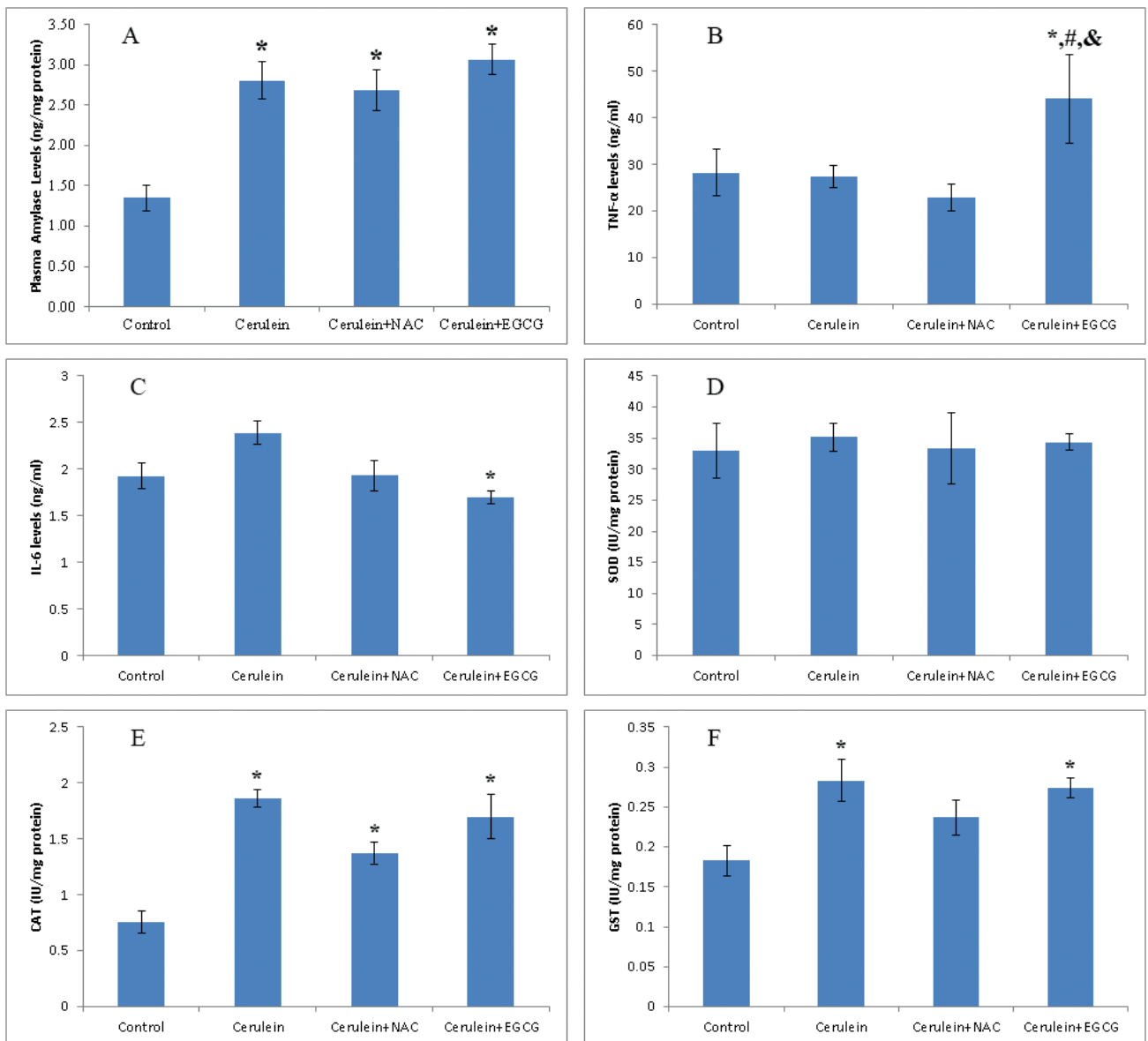


Figure 1. Enzyme activity and inflammatory cytokine results of rats belong to all groups. **A)** Plasma amylase activity, **B)** Serum TNF- α levels, **C)** Serum IL-6 levels, **D)** SOD activities, **E)** CAT activities, **F)** GST activities. *Statistically significant from control group, #Statistically significant from cerulein group, &Statistically significant from cerulein+NAC group ($p \leq 0.05$). Each bar represents mean \pm standard error.

Activities of antioxidant enzymes, including SOD, CAT and GST were performed, and results were shown in Figures 1D-F. SOD activities did not differ among groups. CAT activities increased in the cerulein group, as well as in the cerulein+NAC and cerulein+EGCG groups compared to control group. GST activities of the cerulein group, as well as the cerulein+EGCG group were found significantly increased compared to the control group (respectively, $p = 0.03$ and $p = 0.01$).

Pancreases of the rats in all groups were evaluated histopathologically to determine the pancreatitis severity according to Schmidt criteria. Pancreas tissues were evaluated for the severity of edema, inflammation and fat necrosis. Histopathological results were shown in Figures 2-3A. The control group had no pathological findings. Edema in cerulein (Figure 2B) and cerulein+EGCG groups was found statistically increased compared to the cerulein+NAC group (Figure 3A). Groups were also compared in terms of inflammation and fat necrosis (Figure 3A). Both the cerulein and cerulein+EGCG groups were statistically increased compared to the cerulein+NAC group.

According to TUNEL assay results, apoptotic cells increased significantly in the cerulein+EGCG group compared with the cerulein+NAC group (Figure 3). CD8- α positive cells in the cerulein+EGCG group increased statistically compared with the cerulein+NAC ($p = 0.035$). Results were shown in Figure 3B. Although CD68 positive cells increased in the cerulein+EGCG, no statistical significance was found between groups.

DISCUSSION

In recent decades, studies on oxidative stress, which plays a crucial role in the development of several pathologies, have drawn attention of scientists to understand the relationship between oxidative stress and diseases, and the struggles to develop new treatment strategies. AP is a complex disease that brings about several complications, and associated with a high mortality rate (28). Pathophysiology of AP was mainly attributed to oxidative stress and therefore, trials of several antioxidant agents came into prominence for therapy.

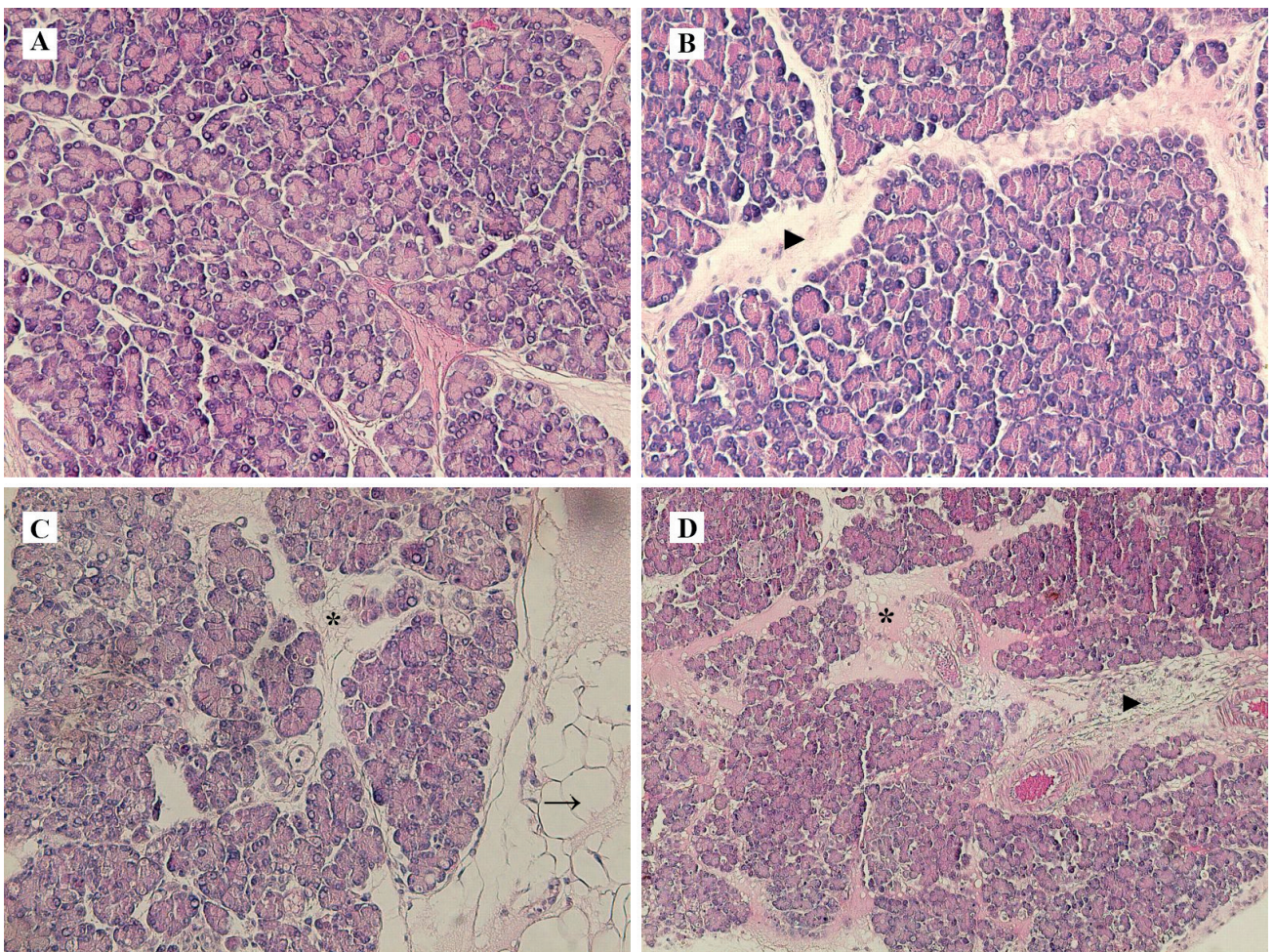


Figure 2. Histopathological findings according to Schmid criteria, H&E staining. **A)** Control group, x100; **B)** Cerulein group, interlobular edema (▶), x100; **C)** Cerulein+EGCG, intralobular edema (*), and fat necrosis (→), x100; **D)** Cerulein+EGCG, intralobular edema (*) and inflammation (▶), x50.

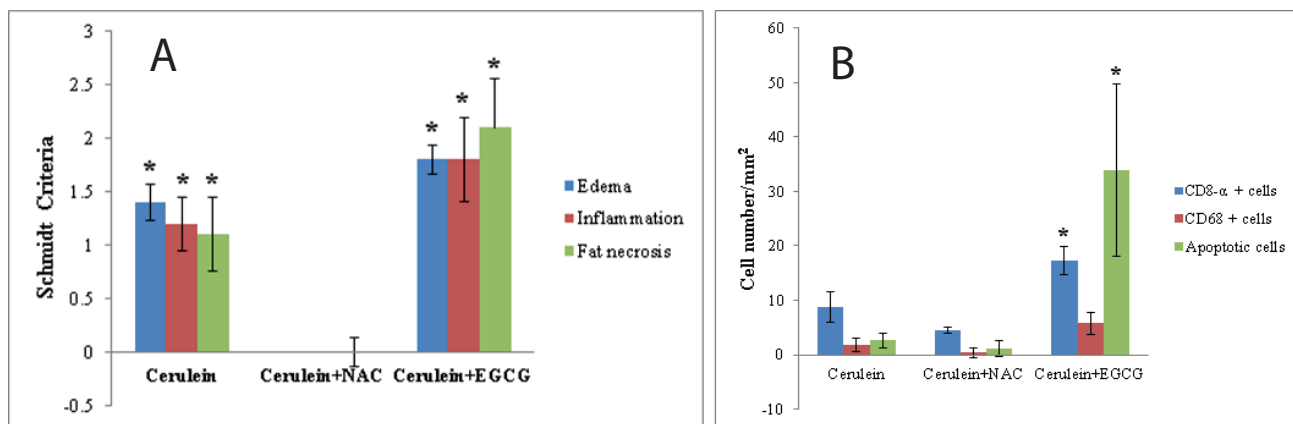


Figure 3. A) Graph of histopathological evaluations according to Schmidt criteria. *Statistically significant from Cerulein+NAC group, ($p \leq 0.05$). Each bar represents mean \pm standard error. B) Graphical analysis of immunohistochemical stainings, #Statistically significant from Cerulein+NAC group, ($p \leq 0.05$). Each bar represents mean \pm standard error.

Cerulein-induced pancreatitis was proven to be one of the alternative experimental pancreatitis models, and best characterized by exerting similar pathophysiological characteristics (29). In normal physiological conditions, digestive enzymes are known to be stored in acinar cells as proenzymes in zymogen granules. When animals were exposed to high dose cerulein which is a cholecystokinin (CCK) analogue, it was shown to cause induction of exocytosis of zymogen granules and consequently, excessive secretion of digestive enzymes. However, after stimulation by excessive CCK when bound to low affinity CCK receptor, digestion enzyme secretion is inhibited (30). In previous studies, it was indicated that induction of pancreatic enzyme activated by cerulein in 30 min after intravenous injection. Hyperamylasaemia, as well as common histopathological changes, including inflammatory cell infiltration, active digestive enzyme in pancreas and edema are the major findings of the cerulein-induced pancreatitis model (30). In the present study, cerulein caused increases in serum amylase levels, as well as histopathological changes, indicating that the AP model was successful. In the present study, while serum amylase level decreased in the cerulein+NAC group, it increased in the cerulein+EGCG treatment groups compared to the cerulein group. Although NAC seemed to be protective effects against pancreatitis, EGCG treatment worsened the pancreatitis scenario.

Oxidative stress is caused by the impairment of the balance between ROS and the antioxidant system of the body (31). Oxidative stress has been reported to play an important role in the pathophysiology of several diseases, resulting in high mortality such as in AP, endotoxic shock as well as sepsis. Besides, the body has a defence mechanism that scavenges the excess free radicals. Increases in SOD and CAT activities are consistent with ROS, and it was shown that SOD and CAT activities elevated in SAP (32). GST is an antioxidant enzyme and plays important role in oxidative stress situations (33). In the present study, SOD activities did not change between groups. However, CAT and GSH enzyme activities in the cerulein+NAC and cerulein+EGCG groups were found higher than in the control group. It should be stated that NAC treatment

may lower the cerulein-induced pancreatitis. On the other hand, considering CAT and GST activities, EGCG was as effective as NAC in reducing oxidative stress.

Interaction between oxidative stress and cytokine release plays an important role in the systemic response of AP (34). In AP, it was known that pro-inflammatory cytokine levels, including TNF- α , IL-1 and IL-6 increase, and these pro-inflammatory cytokines may play pivotal role in initiating the systemic response (35). The results of the present study showed that pro-inflammatory cytokine levels increased in response to pancreatitis induction. NAC treatment as an antioxidant agent caused decreases in serum IL-6 levels. Additionally, EGCG treatment seemed to be more effective in balancing IL-6 levels. However, serum TNF- α results showed a statistically significant increase in serum TNF- α level at a higher degree, compared to the results of the EGCG treatment group, relative to pancreatitis. It has been mentioned previously that when the AP is induced, pancreas inflammation begins in 3 hours and leukocyte recruitment, and pro-inflammatory cytokines are released by activated macrophages as a result of pancreatic damage (34). Increased levels of pro-inflammatory cytokines were reported to be correlated with the pancreatic inflammation stage (36). TNF- α and IL-1 β are two of the cytokines that initiate the systemic inflammatory response in AP, and they are known to amplify cascades of inflammatory response (37). In our cerulein-induced pancreatitis model, histopathological results were consistent with the model. However, while NAC treatment ameliorated the inflammatory response, the inflammatory response in the EGCG treated group seemed to be more severe than in the pancreatitis group. As well, in the inflammation sites of the pancreas, it was known that T cells take place in a smaller number in addition to macrophages. In the present study, increased number of CD8- α positive cells, which is a marker of cytotoxic T cells, were observed in the cerulein-induced pancreatitis group, but EGCG treatment made the situation worsen by increased number of cytotoxic T cells. Similar results could be seen for macrophages with staining of CD68+ cells. EGCG treatment caused increases in macrophage

numbers. Recently, it was indicated that activated macrophages have an important role in decreasing the inflammation, and prompting wound healing, fibrosis as well as tumorigenesis. Fibrosis is reported to be regulated mainly by macrophages (38). Additionally, increases in the serum TNF- α level in EGCG groups were consistent with increased numbers of apoptotic cells. Accordingly, in several cells it was proved that TNF- α stimulate apoptotic/necrotic cell death (39). The results of previous studies conducted with cerulein-induced pancreatitis model, TNF- α mediated apoptosis was one of the main findings (39). Moreover, in the present study it may be suggested that EGCG treatment may be the aggravating factor, and may worsen pancreatitis for the cerulein-induced pancreatitis model.

EGCG, which is one of the most effective catechin compounds, mainly found in green tea leaves, has numerous health benefits, and these were attributed to having free radical scavenging properties, as well as being highly antioxidant. Green tea extract, which has numerous polyphenols, has been reported to ameliorate cerulein-induced male mice by inactivation of NF- κ B inactivation and the oxidative stress pathway (11). However, in our study we aimed to evaluate especially EGCG, and our results were not consistent with the previous study. Although having beneficial effects, previous studies concluded that green tea extracts, such as EGCG, might have toxic and pro-oxidant effects (40). It was claimed that EGCG may induce apoptosis by the production of H₂O₂ in human cancer cell line H661 (41). EGCG was reported to induce apoptosis in pancreatic cancer by caspase activation and mitochondrial membrane depolarization (42). Catechins are antioxidants that scavenge the free radicals, but also they were reported to induce oxidative stress, and such pro-oxidant effects were reported to induce apoptosis in cancer cells (19). One of previous studies declared that EGCG had strong ROS scavenging activity and protective effects at 2-30 mM concentrations; however, it was found that in concentrations higher than 60 mM, EGCG increased the oxidative damage on DNA. It was suggested that, EGCG had protective effects at lower concentrations; on the contrary, it was reported that at higher concentrations, EGCG exerted pro-oxidant effects on DNA by increased ROS (43, 44). In summary, in the cancer therapy, green tea polyphenols may be a good alternative for consumption. Although, its protective effects were proved for cancer treatment strategies, the present study suggests that it is not an alternative treatment for AP.

CONCLUSION

In conclusion, although pro-oxidant effects of EGCG may induce apoptosis in tumorigenic cells and used for cancer therapy, when it comes to pancreatitis, EGCG may worsen the degree of pancreatitis. That may be attributed to the use of higher doses of EGCG. It can be concluded that overconsumption of polyphenols having pro-oxidant effects, including EGCG, may worsen pancreatitis conditions. Further analyses need to be performed in order to exert the pro-oxidant mechanisms and the dose dependency of action of EGCG for AP.

Peer-review: Externally peer-reviewed.

Author Contributions: Conception/Design of study: T.B.; Data Acquisition: T.B., G.G., E.K., G.S.; Data Analysis/Interpretation: E.K., G.G.; Drafting Manuscript: E.K., G.G.; Critical Revision of Manuscript: G.S., T.B.; Final Approval and Accountability: T.B., G.G., E.K., G.S.

Conflict of Interest: The authors declare that they have no conflicts of interest.

Financial Disclosure: This study was financially supported by the Hacettepe University Research Projects Coordination Unit (Project no: 09 D03 301 001).

REFERENCES

1. Lei QC, Wang XY, Xia XF, Zheng HZ, Bi JC, Tian F, et al. The role of omega-3 fatty acids in acute pancreatitis: A meta-analysis of randomized controlled trials. *Nutrients* 2015; 7(4): 2261-73.
2. Jha RK, Ma Q, Sha H, Palikhe M. Acute pancreatitis: a literature review. *Med Sci Mon* 2009; 15(7): RA147-RA56.
3. Aranda-Narváez JM, González-Sánchez AJ, Montiel-Casado MC, Titos-García A, Santoyo-Santoyo J. Acute necrotizing pancreatitis: surgical indications and technical procedures. *World J Clin Cases* 2014; 2(12): 840.
4. Elfar M, Gaber LW, Sabek O, Fischer CP, Gaber AO. The inflammatory cascade in acute pancreatitis: relevance to clinical disease. *Surg Clin North Am* 2007; 87(6): 1325-40.
5. Saruç M, Yuçeyar H, Turkel N, Ozutemiz O, Tuzcuoglu I, Ayhan S, et al. The role of heme in hemolysis-induced acute pancreatitis. *Med Sci Mon* 2007; 13(3): BR67-BR72.
6. Wei M, Gong Y-J, Tu L, Li J, Liang Y-H, Zhang Y-H. Expression of phosphatidylinositol-3 kinase and effects of inhibitor wortmannin on expression of tumor necrosis factor- α in severe acute pancreatitis associated with acute lung injury. *World J Emerg Med* 2015; 6(4): 299.
7. De Campos T, Deree J, Coimbra R. From acute pancreatitis to end-organ injury: mechanisms of acute lung injury. *Surgical Infect* 2007; 8(1): 107-20.
8. Mokra D, Kosutova P. Biomarkers in acute lung injury. *Respir Physiol Neurobiol* 2015; 209: 52-8.
9. Tsuji N, Watanabe N, Okamoto T, Niitsu Y. Specific interaction of pancreatic elastase and leucocytes to produce oxygen radicals and its implication in pancreatitis. *Gut* 1994; 35(11): 1659-64.
10. Yu JH, Kim H. Oxidative stress and inflammatory signaling in cerulein pancreatitis. *World journal of gastroenterology: WJG* 2014; 20(46): 17324.
11. Babu BI, Malleo G, Genovese T, Mazzon E, Di Paola R, Crisafulli C, et al. Green tea polyphenols ameliorate pancreatic injury in cerulein-induced murine acute pancreatitis. *Pancreas* 2009; 38(8): 954-67.
12. Su KH, Cuthbertson C, Christophi C. Review of experimental animal models of acute pancreatitis. *HPB (Oxford)*. 2006; 8(4): 264-86.
13. Pandey KB, Rizvi SI. Plant polyphenols as dietary antioxidants in human health and disease. *Oxid Med Cell Longev* 2009; 2(5): 270-8.
14. Shay J, Elbaz HA, Lee I, Zielske SP, Malek MH, Hüttemann M. Molecular mechanisms and therapeutic effects of (-)-epicatechin and other polyphenols in cancer, Inflammation, Diabetes, and Neurodegeneration. *Oxid Med Cell Longev* 2015; 2015.
15. Erguder IB, Avci A, Devrim E, Durak I. Effects of cooking techniques on antioxidant enzyme activities of some fruits and vegetables. *Turk J Med Sci* 2007; 37(3): 151-6.

16. Mekiňová D, Chorvathova V, Volkovova K, Staruchova M, Graňičová E, Klvanova J, et al. Effect of intake of exogenous vitamins C, E and B-carotene on the antioxidative status in kidneys of rats with streptozotocin-induced diabetes. *Mol Nutr Food Res* 1995; 39(4): 257-61.
17. Sülođlu AK, Girgin G, Selmanođlu G, Balcı S, Baydar T. Possible effects of lycopene and silymarin on rat liver functions and oxidative stress markers. *Turk J Biochem/Turk Biyokim Derg* 2014; 39(3):344-50.
18. Sureda A, Tejada S, Del Mar Bibiloni M, Antoni Tur J, Pons A. Polyphenols: well beyond the antioxidant capacity: polyphenol supplementation and exercise-induced oxidative stress and inflammation. *Curr Pharm Biotechnol* 2014; 15(4): 373-9.
19. Lambert JD, Elias RJ. The antioxidant and pro-oxidant activities of green tea polyphenols: a role in cancer prevention. *Arch Biochem Biophys* 2010; 501(1): 65-72.
20. Lin C-H, Chao L-K, Hung P-H, Chen Y-J. EGCG inhibits the growth and tumorigenicity of nasopharyngeal tumor-initiating cells through attenuation of stat3 activation. *Int J Clin Exp Pathol* 2014; 7(5): 2372.
21. Yu H, Pardoll D, Jove R. Stats in cancer inflammation and immunity: a leading role for stat3. *Nat Rev Cancer* 2009; 9(11): 798-809.
22. Mukherjee S, Siddiqui MA, Dayal S, Ayoub YZ, Malathi K. Epigallocatechin-3-gallate suppresses proinflammatory cytokines and chemokines induced by toll-like receptor 9 agonists in prostate cancer cells. *J Inflamm Res* 2014; 7: 89.
23. Ramudo L, Manso MA. N-acetylcysteine in acute pancreatitis. *World J Gastrointest Pharmacol Ther* 2010; 1(1): 21.
24. Muià C, Mazzon E, Di Paola R, Genovese T, Menegazzi M, Caputi AP, et al. Green tea polyphenol extract attenuates ischemia/reperfusion injury of the gut. *Nannyn-Schmiedeberts Arch Pharmacol* 2005; 371(5): 364-74.
25. Senthil Kumaran V, Arulmathi K, Srividhya R, Kalaiselvi P. Repletion of antioxidant status by EGCG and retardation of oxidative damage induced macromolecular anomalies in aged rats. *Exp Gerontol* 2008; 43(3): 176-83.
26. Meng M, Li Y-Q, Yan M-X, Kou Y, Ren H-B. Effects of epigallocatechin gallate on diethyldithiocarbamate-induced pancreatic fibrosis in rats. *Biol Pharm Bull* 2007; 30 (6): 1091-6.
27. Abdallah MF, Karacaoglu E, Girgin G, Kilicarslan B, Selmanoglu G, Baydar T. Influence of subacute melatonin treatment on antioxidant factors in the liver of female rats. *J Exp App Anim Sci* 2015; 1(3): 359-68.
28. Yagci G, Gul H, Simsek A, Buyukdogan V, Onguru O, Zeybek N, et al. Beneficial effects of N-acetylcysteine on sodium taurocholate-induced pancreatitis in rats. *J Gastroenterol* 2004; 39(3): 268-76.
29. Kim H. Cerulein pancreatitis: oxidative stress, inflammation, and apoptosis. *Gut Liver* 2008; 2(2): 74-80.
30. Hyun JJ, Lee HS. Experimental models of pancreatitis. *Clin Endosc* 2014; 47(3): 212-6.
31. Rodrigo R, Gil-Becerra D. Chapter 17 - Implications of polyphenols on endogenous antioxidant defense systems in human diseases. *Polyphenols in Human Health and Disease*. San Diego: Academic Press; 2014. p. 201-17.
32. Fukui M, Kanoh M, Takamatsu Y, Arakawa Y. Analysis of serum catalase activities in pancreatic diseases. *J Gastroenterol* 2004; 39(5): 469-74.
33. Rahman SH, Ibrahim K, Larvin M, Kingsnorth A, McMahon MJ. Association of antioxidant enzyme gene polymorphisms and glutathione status with severe acute pancreatitis. *Gastroenterology* 2004; 126(5): 1312-22.
34. Pérez S, Pereda J, Sabater L, Sastre J. Redox Signaling in acute pancreatitis. *Redox Biol* 2015; 5: 1-14.
35. Gomez-Cambronero LG, Sabater L, Pereda J, Cassinello N, Camps B, Vina J, et al. Role of cytokines and oxidative stress in the pathophysiology of acute pancreatitis: therapeutical implications. *Curr Drug Targets Inflamm Allergy* 2002; 1(4): 393-403.
36. Mayer J, Rau B, Gansauge F, Beger HG. Inflammatory mediators in human acute pancreatitis: clinical and pathophysiological implications. *Gut* 2000; 47(4): 546-52.
37. Javier E, Javier P, Alessandro A, Juan S, Luis S, Luis A, et al. Role of redox Signaling, protein phosphatases and histone acetylation in the inflammatory cascade in acute pancreatitis: therapeutic implications. *Inflamm Allergy Drug Targets* 2010; 9(2): 97-108.
38. Xue J, Sharma V, Hsieh MH, Chawla A, Murali R, Pandol SJ, et al. Alternatively activated macrophages promote pancreatic fibrosis in chronic pancreatitis. *Nat Commun* 2015; 6: 7158.
39. Gukovskaya AS, Gukovsky I, Zaninovic V, Song M, Sandoval D, Gukovsky S, et al. Pancreatic acinar cells produce, release, and respond to tumor necrosis factor-alpha. Role in regulating cell death and pancreatitis. *J Clin Invest* 1997; 100(7): 1853-62.
40. Elbling L, Weiss R-M, Teufelhofer O, Uhl M, Knasmueller S, Schulte-Hermann R, et al. Green tea extract and (-)-epigallocatechin-3-gallate, the major tea catechin, exert oxidant but lack antioxidant activities. *The FASEB J* 2005; 19(7): 807-09.
41. Yang G-Y, Liao J, Li C, Chung J, Yurkow EJ, Ho C-T, et al. Effect of black and green tea polyphenols on c-Jun phosphorylation and H₂O₂ production in transformed and non-transformed human bronchial cell lines: possible mechanisms of cell growth inhibition and apoptosis induction. *Carcinogenesis* 2000; 21(11): 2035-9.
42. Qanungo S, Das M, Haldar S, Basu A. Epigallocatechin-3-gallate induces mitochondrial membrane depolarization and caspase-dependent apoptosis in pancreatic cancer cells. *Carcinogenesis* 2005; 26(5): 958-67.
43. Hayakawa F, Ishizu Y, Hoshino N, Yamaji A, Ando T, Kimura T. Prooxidative activities of tea catechins in the presence of Cu²⁺. *Biosci Biotechnol Biochem* 2004; 68(9): 1825-30.
44. Preedy VR. *Tea in health and disease prevention*: Academic Press; 2012.

Larvicidal Activities of Essential Oils Extracted from Five Algerian Medicinal Plants against *Culiseta longiareolata* Macquart. Larvae (Diptera: Culicidae).

Ismahane Nabti¹ , Mustapha Bounechada¹ 

¹University Ferhat Abbas, Faculty of Nature and Life Sciences, Department of Biology and Animal Physiology, Laboratory Research LADPVA, Setif, Algeria

ORCID IDs of the authors: I.N. 0000-0001-5192-5626; M.B. 0000-0002-3237-5769

Please cite this article as: Nabti I, Bounechada M. Larvicidal Activities of Essential Oils Extracted from Five Algerian Medicinal Plants against *Culiseta longiareolata* Macquart. Larvae (Diptera: Culicidae). Eur J Biol 2019; 78(2): 129-135. DOI: 10.26650/EurJBiol.2019.0015

ABSTRACT

Objective: The use of essential oils in mosquito control is considered as a potential alternative of synthetic insecticides. The current study aimed to assess the larvicidal activity of the essential oils extracted from five medicinal plants collected from northeastern Algeria against the *Culiseta longiareolata* larvae, a vector of the *Plasmodium* species in birds and one of the most abundant mosquito species in Algeria.

Materials and Methods: The essential oils extracted from: *Thymus vulgaris*, *Artemisia herba-alba*, *Juniperus phoenicea*, *Rosmarinus officinalis*, and *Eucalyptus globulus* were tested against the 3rd and 4th instar *Culiseta longiareolata* larvae. The larvae were exposed to a series of concentrations of the tested essential oils for 24h. The concentrations that caused between 10% and 90% mortality were replicated four times, and the entire test was repeated three times. The collected data were used to determine the LC₅₀ and LC₉₀ values,

Results: The tested oils revealed an efficient larvicidal activity. *T. vulgaris* showed 100% mortality at 80ppm final concentration, while the other tested oils showed 100% mortality at 200ppm. Furthermore, the lethal concentrations that caused 50% and 90% mortality (LC₅₀ and LC₉₀) were varying. *T. vulgaris* was the most efficient essential oil (LC₅₀=25.64ppm, LC₉₀=50.53ppm), followed by *J. Phoenicea* (LC₅₀=59.83ppm, LC₉₀=137.68ppm), *R. officinalis* (LC₅₀= 64.18ppm, LC₉₀= 96.55ppm), *A. herba-alba* (LC₅₀=86.67ppm, LC₉₀=139.55ppm), then *E. globules* (LC₅₀=95.83ppm, LC₉₀= 168.25ppm).

Conclusion: The use of essential oils or their principal active components as α -pinene, 1,8-cineole and Camphor may serve as an eco-friendly method to control mosquito larvae. Nevertheless, the field application of essential oils and their principal components remains a fundamental step to evaluate the field efficacy of these botanic extracts and to note their possible secondary effects on non-targeted organisms.

Keywords: Aromatic medicinal plants, *Culiseta longiareolata*, Essential oil, Larvicidal activity, Mosquitoes

INTRODUCTION

Culicidae, or mosquitoes as commonly known, is a family of Diptera insects that reproduce quickly and abundantly. Simultaneously, this family includes major vectors for many deadly and dangerous diseases. Therefore, the importance of the mosquito family in terms of public health makes mosquito control an important initiative to minimize the negative effects

of mosquito-borne diseases. Mosquito control may depend on various strategies; the most common in the past decades was the use of synthetic insecticides as inexpensive and available products. However, the use of synthetic insecticides has over time created environment pollution and resistance problems (1, 2).

Recently, eco-friendly methods were developed to control mosquitoes. For instance, the enhancement



Corresponding Author: Ismahane Nabti E-mail: ismahanenabti@univ-setif.dz

Submitted: 17.09.2019 • **Revision Requested:** 01.10.2019 • **Last Revision Received:** 06.10.2019 • **Accepted:** 16.10.2019

© Copyright 2019 by The Istanbul University Faculty of Science • Available online at <http://ejb.istanbul.edu.tr> • DOI: 10.26650/EurJBiol.2019.0015

of behavior-based control tools and the development of repellent and toxic products based on botanic components can target different mosquito life stages (3, 4). Essential oils (EOs) extracted from different parts of plants were frequently tested for their mosquitocidal activity (5). These primary botanic materials present various biological activities. They can act as insecticides where they can affect the oviposition, survival, larval duration, pupation and insect emergence (6, 7). However, the larvae stage appears to be more appropriate to control mosquito populations because of the high reproduction rates and larvae food mechanisms that allow a high number of mosquito individuals to be targeted simultaneously. Therefore, the assessment of the larvicidal efficacy of various plant derivatives was the main objective of many research papers (8-11).

Culiseta longiareolata (Macquart 1838) constitutes with the *Culex pipiens* (Linnaeus 1758) complex the most abundant species in Algeria. It usually breeds near human habitations, however, the females prefer to feed on bird blood (12). *Cs longiareolata* has uniquely adaptive and survivor features. Kiflawi et al. (13) have confirmed that the females of this species showed an adaptive response against the risk of predation and negative density effects where they avoid laying their eggs in predator pools. Further, *Cs longiareolata* is considered as a primary vector of *Plasmodium (Giovannolaia) circumflexum* (Kikuth 1931), *Plasmodium relictum* (modified from Garnham 1966) and *Plasmodium polare* (Manwell 1934) in birds, and its capacity to transmit *P. relictum* in Algeria was proven experimentally (14, 15). In this context, we have assessed the larvicidal activity of EOs extracted from five aromatic medicinal plants, harvested from Northeastern Algeria, against *Cs longiareolata* larvae. The efficacy of the tested EOs will be evaluated by calculating the LC_{50} and LC_{90} values and by comparing them with the LC_{50} and LC_{90} values of the same EOs tested previously against other targeted mosquito species.

MATERIALS AND METHODS

Mosquito Collection

Culiseta longiareolata larvae were collected regularly from three clean fixed and controlled pools in Algeria, where the mosquitoes were not exposed to any insecticides. Larvae of the third and fourth instar were used directly in the test; eggs, first and second instar larvae were reared in room temperature ($27^{\circ}C \pm 2^{\circ}C$), in a 12 h light: 12 h dark photoperiod, until the fourth instar was reached.

Essential Oils Extraction

The aerial parts of the tested plants were collected from different regions in the Mediterranean and semi-arid climate northeastern Algeria: *Thymus vulgaris* L. from Guelma, *Artemisia herba-alba* Asso from M'Sila, *Juniperus phoenicea* L. from Jijel, *Rosmarinus officinalis* Linn from Bouira and *Eucalyptus globules* L. from Batna. The plants' collection started at the beginning of the summer (June) in 2018. The samples were air-dried at room temperature. The dried plants were

submitted to classical steam distillation for 3-6 h. The samples were exposed to the water vapor produced in the flask crosses, the vapor was charged with the EO, and then was condensed in the condenser. The EO floated on the water surface was then recuperated. The yield of the EOs was between 0.8 and 1.5%.

Larvicidal Bioassay

According to WHO guidelines for laboratory and field testing of mosquito larvicides (16), we tested the larvicidal activity of EOs extracted from the leaves of five aromatic medicinal plants *T. vulgaris*, *A. herba-alba*, *J. phoenicea*, *R. officinalis*, *E. globulus* against *Culiseta longiareolata* larvae under laboratory conditions. The EOs were extracted by steam distillation, they were next serially diluted in ethanol to obtain 10%, 1%, 0.1% and 0.01% of stock solution, and 0.1-1ml of the previous dilutions were added to 100ml of water to obtain the final concentrations. A series of concentrations and controls were applied on 25 mosquito larvae distributed in five cups containing 100ml of water. A total of 8925 larvae were tested. We started the test with the lowest concentrations. The concentrations that showed less than 10% mortality were excluded. Concentrations that showed 10% mortality or more were replicated 4 times, and each test was run three times. After 24h of exposure, moribund and dead larvae were counted. We have chosen four concentrations which caused between 10% and 90% mortality to determine the LC_{50} and LC_{90} values. The data obtained from the four replicates in the three tests were pooled for analysis.

Statistical Analyses

Data were subjected to probit analysis using SPSS software V25 (Using probit model because of the normal distribution of data); and final concentrations were transformed to \log_{10} . Lethal concentration LC_{50} and LC_{90} with a 95% confidence limit (CL) suspected of killing 50% and 90% of the population respectively, were calculated and presented with the regression equations ($Y = a + b \cdot x$) and regression coefficients (R^2).

RESULTS

Five plant EOs were tested to evaluate their larvicidal activity, and the tested oils revealed various mortality percentages at different concentrations (Table 1). The majority of the tested oils showed 100% mortality at 200ppm final concentration, except for *T. vulgaris* that showed 100% mortality at 80ppm. Further, the oils started to affect the larvae life at different concentrations; the lowest concentration that caused equal or more than 10% mortality was 20ppm for *T. vulgaris*, 40ppm for *J. phoenicea*, 50ppm for *A. herba-alba* and *R. officinalis* and 70ppm for *E. globules* (Table1). The 24h LC_{50} and LC_{90} estimate, upper and lower values obtained from the larvicidal activity test of EOs extracted from the five plants in addition to the regression equations and regression coefficients are presented in Table 2. *T. vulgaris* was the most efficient with 25.64 (16.58-32.03) LC_{50} and 50.53 (40.15-82.43) LC_{90} , while *A. herba-alba* was the least efficient. Likewise, the influence degree of increasing one unit of EOs concentration on their larvicidal activity was

different. Among the tested EOs, the augmentation of one unit of *R. officinalis* concentration showed the highest influence in increasing the LC₅₀ and LC₉₀ (b=7.16). The R² was close to 1 in

all probit analysis, the minimal residuals obtained between the observed and expected values was shown by *E. globulus* EO (R²=0.99) (Table 2; Figures 1-5).

Table 1: The mortality observed to the *Culiseta longiareolata* larvae, caused by the application of the tested essential oils at different concentrations, with the arithmetic mean (AM) and standard error (SE).

Dead in a total of 300 larvae (AM±SE)							
IC (%)	Aliquot (ml)	FC (ppm)	<i>Thymus vulgaris</i>	<i>Juniperus phoenicea</i>	<i>Artemisia herba-alba</i>	<i>Rosmarinus officinalis</i>	<i>Eucalyptus globules</i>
1	0,2	20	93 (7.75±1.53)	-	-	-	-
	0,4	40	253 (21.08±1.97)	94 (7.83±1.23)	-	-	-
	0,5	50	257 (21.42±1.59)	103 (8.58±1.23)	24 (2±0.75)	75 (6.25±1.54)	-
	0,6	60	286 (23.83±0.42)	156 (13±1.58)	57 (4.75±1.52)	106 (8.83±1.56)	-
	0,7	70	-	-	-	-	68 (5.67±1.1)
	0,8	80	300 (7.75±1.53)	176 (14.67±1.91)	89 (8.17±1.36)	236 (19.67±0.85)	107 (8.92±1.02)
	0,9	90	-	-	-	-	134 (11.17±1.6)
	1	100	300 (25±0.0)	255 (21.25±1.55)	216 (18±2.03)	274 (22.83±1.21)	159 (13.25±1.69)
10	0,2	200	300 (25±0.0)	300 (25±0.0)	300 (25±0.0)	300 (25±0.0)	300 (25±0.0)

IC(initial concentration), FC (final concentration)

Table 2: The LC₅₀ and LC₉₀ values of essential oils extracted from *T. vulgaris*, *A. herba-alba*, *J. phoenicea*, *R. officinalis* and *E. globules* against the 3rd and 4th instar larvae of the *Culiseta longiareolata*, after 24 hours exposure period; with regression equations and regression coefficients (R²).

Essentialoils	LC50 (ppm) 95% CI			LC90 (ppm) 95% CI			Sig (df)	Regression equation	R2
	Estimate	Lower	Upper	Estimate	Lower	Upper			
<i>Thymus vulgaris</i>	25.64	16.58	32.03	50.53	40,15	82.43	p>0.05 (2)	y=-6.15+4.36*x	0.97
<i>Juniperus phoenicea</i>	59.83	45.36	75.81	137.68	97.21	<250	p>0.05 (3)	y=-6.49+3.66*x	0.9
<i>Artemisia herba-alba</i>	86.67	66.59	<250	139.55	98.03	<250	p>0.05 (2)	y=-11.77+6.08*x	0.93
<i>Rosmarinus officinalis</i>	64.18	55.41	72.56	96.55	82.73	139.84	p>0.05 (2)	y=-12.93+7.16*x	0.98
<i>Eucalyptus globules</i>	95.83	92.27	101.09	168.25	146.59	201.87	p>0.05 (2)	y=-10.45+5.28*x	0.99

Sig (significance level), df (degrees of freedom)

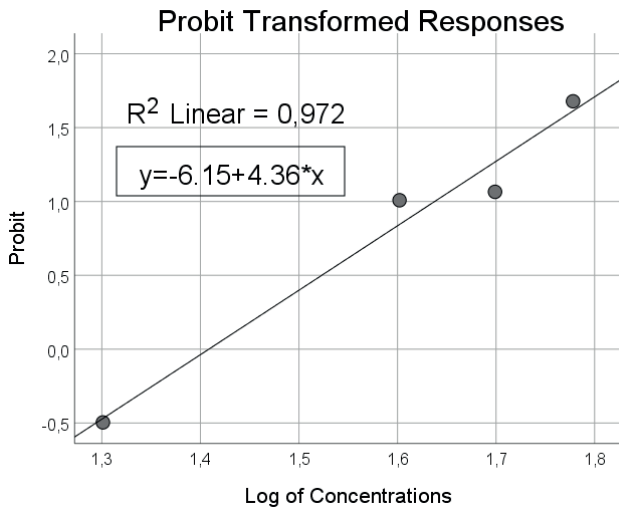


Figure 1. Probit transformed responses with equation regression and coefficient of determination R^2 for *Thymus vulgaris* essential oil tested on 3rd and 4th instars larvae of *Culiseta longiareolata* for 24 h.

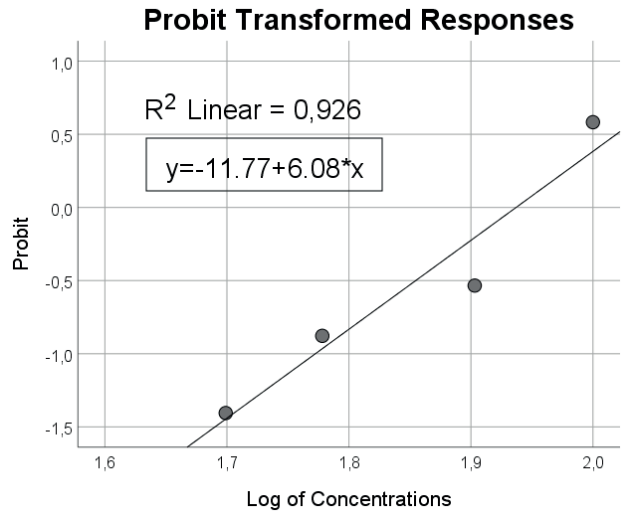


Figure 3. Probit transformed responses with equation regression and coefficient of determination R^2 , for *Artemisia herba-alba* essential oil tested on 3rd and 4th instars larvae of *Culiseta longiareolata* for 24 h.

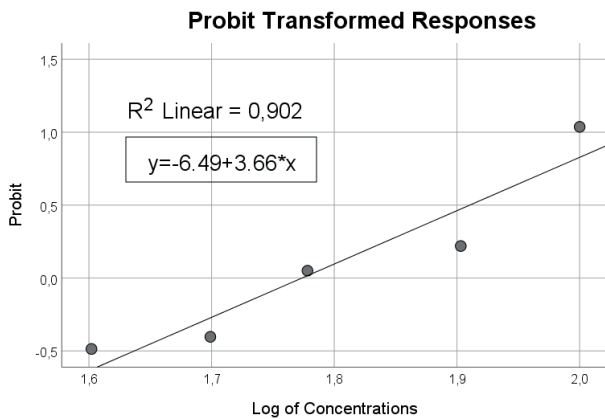


Figure 2. Probit transformed responses with equation regression and coefficient of determination R^2 for *Juniperus Phoenicia* tested on 3rd and 4th instars larvae of *Culiseta longiareolata* for 24 h.

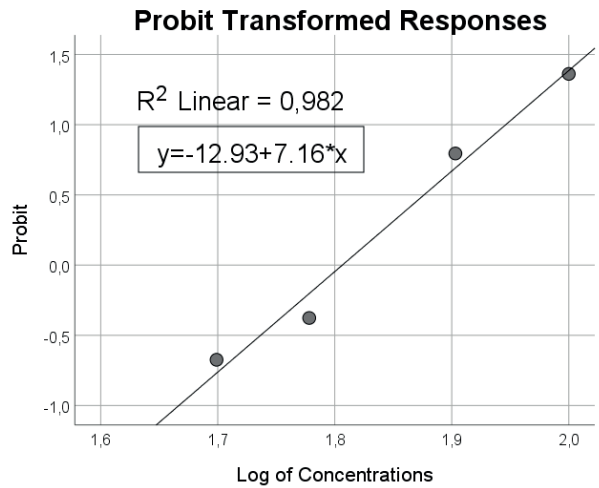


Figure 4. Probit transformed responses with equation regression and coefficient of determination R^2 for *Rosmarinus officinalis* essential oil tested on 3rd and 4th instars larvae of *Culiseta longiareolata* for 24 h.

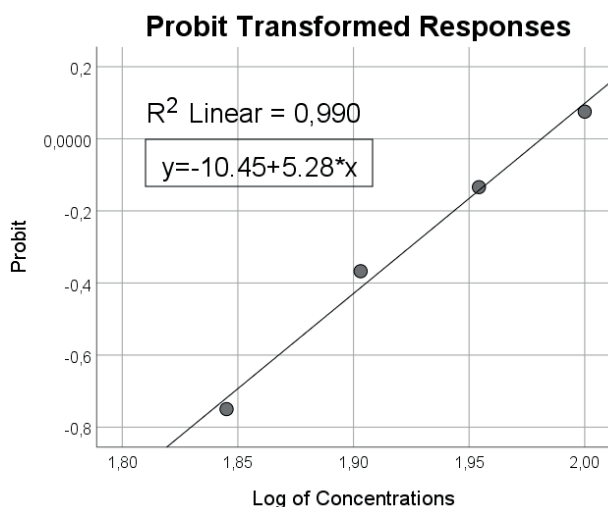


Figure 5. Probit transformed responses with equation regression and coefficient of determination R^2 for and *Eucalyptus globulus* essential oil tested on 3rd and 4th instars larvae of *Culiseta longiareolata* for 24 h.

DISCUSSION

The current study has confirmed that the EOs extracted from the aromatic medicinal plants *T. vulgaris*, *A. herba-alba*, *J. phoenicea*, *R. officinalis* and *E. globulus* present an efficient larvicidal activity against the *Culiseta longiareolata* larvae; however, the mortality responses obtained were varying.

T. vulgaris is a flowering herb that has a worldwide distribution (17). From the total of the tested oils, the *T. vulgaris* EO was the most efficient. This EO was previously assessed by Knio et al. (18) against the *Ochlerotatus caspius* (Pallas 1771) larvae; however,

its toxicity against *Oc caspius* (LC_{50} =33.65ppm; LC_{90} =50.85ppm) was less than that shown by our *T. vulgaris* EO. Likewise, the larvicidal activity of the EOs extracted from the *Juniperus* species was tested in previous studies: *J. Phoenicea* against *Aede salbopictus* (Skuse 1894) (LC_{50} = 55.5ppm; LC_{90} = 77ppm), and *J. virginiana* L. against *Ae aegypti* (Linnaeus 1762) and *Cx pipiens* (19, 20). Comparing our results, our *J. phoenicea* EO showed lower larvicidal activity against *Cs longiareolata*. Moreover, the larvicidal activity of *R. officinalis* EO was assessed against *Ae albopictus* (LC_{50} <250ppm; LC_{90} = 211.53ppm) and *Anopheles subpictus* Grassi (LC_{50} = 64.5ppm; LC_{90} = 113.74ppm) (21, 22). The *R. officinalis* EOs tested against *Ae albopictus*, *Cx tritaeniorhynchus* and *An subpictus* in the previous researches showed lower values than the toxicity results that we obtained by testing the same EO against *Cs longiareolata*.

The other EOs *E. globules* and *A. herba-alba* were less efficient; however, their lethal concentrations were notable. *E. grandis* L. EO and its major components were assessed for their larvicidal activity against *Aedes aegypti* by Lucia et al. (23). The EO showed 32.4ppm LC_{50} and the principal components α -pinene (52.71%) and 1,8-cineole (18.38%) showed 15.4ppm and 57.2ppm LC_{50} respectively. The principal leaf oil components of *E. globules* harvested from Algeria are α -pinene and 1,8-cineole, according to Samir et al. (24). However, our *E. globules* EO tested against *Cs longiareolata* was less efficient (LC_{50} = 95.83ppm). Furthermore, EOs extracted from *Artemisia* genus were assessed for their larvicidal activity against various mosquito species. Our *A. herba-alba* EO tested against *Cs longiareolata* larvae was more efficient (LC_{50} = 86.67ppm) than *A. vulgaris* L. that was tested by Ilahi and Ullah (25) against *Cx quinquefasciatus* (LC_{50} = 803.2ppm), but less efficient than *A. absinthium* L. tested by Govindarajan and Benelli (26) against *An stephensi* (Liston 1901), *An subpictus*, *Ae aegypti*, *Ae albopictus*, *Cx quinquefasciatus* (Say 1823), and *Cx*

Table 3: Principal component percentages of *T. vulgaris*, *A. herba-alba*, *J. Phoenicea*, *R. officinalis* and *E. globules* harvested from Algeria, according to previous works.

Principal components	<i>T. vulgaris</i> (29)	<i>J. phoenicea</i> (30)	<i>A. herba-alba</i> (31)	<i>R. officinalis</i> (32)	<i>E. globules</i> (24)
Carvacrol	11.41	-	-	-	-
Thymol	25.57	-	-	-	-
α -Pinene	12.1	34.5	Tr	5.4	8.8
α -Terpinylacetate	-	14.7	-	-	-
p-Cymene	26.36	-	-	-	-
Thymoquinone	10.5	-	-	-	-
β -Phellandrene	-	22.4	-	-	-
Camphor	-	-	19.4	14.6	-
1,8-Cineole	-	-	Tr	12.2	71.3
β -Caryophyllene	-	-	-	10.9	-
Borneol	-	-	-	10.6	-
γ -terpinene	-	-	23.8	-	-
β -thujone	-	-	15.0	-	-
chrysanthenone	-	-	15.8	-	-
trans-pinocarveol	-	-	16.9	-	-

tritaeniorhynchus (LC_{50} =41.85, 52.02, 46.33, 57.57, 50.57, and 62.16 ppm respectively). Various mosquito species were targeted in the previous researches to assess the larvicidal activity of EOs. However, *Cs longiareolata* was not previously targeted by EOs, but by the lichen metabolites evaluated by Cetin et al. (27), that showed high larvicidal activity against *Cs longiareolata*.

The results obtained confirm the previous studies; the use of EOs can serve as an eco-friendly method to control mosquito larvae. However, the noted variability in the efficacy level of the tested oils may be due to their chemical composition and the percentages of their principal components as α -Pinene, Camphor and 1,8-Cineole (Table 3); whereas, the direct use of the principal components of EOs may produce a higher efficacy in mosquito control. This hypothesis was proven in the study conducted by Lucia, Gonzalez-Audino (23), where the principal components of Turpentine and *E. grandis* EO showed lower LC_{50} than that obtained by the use of the entire *E. grandis* EO. Moreover, the repellency effect of the thyme EO compounds against *Culex pipiens* mosquito evaluated by Park et al. (28) showed higher repellent efficacy of α -Terpinene and Carvacrol than the commercial formulation diethyltoluamide (DEET), and an equal efficacy between the Thymol component and the DEET.

CONCLUSION

The EOs extracted from the aromatic medicinal plants and their principal components may serve as safe products to control the *Culiseta longiareolata* larvae in Algeria; nevertheless, their practical application remains a fundamental step to evaluate their field efficacy and to note their possible secondary effects on non-targeted organisms.

Peer-review: Externally peer-reviewed.

Author Contributions: Conception/Design of study: I.N., M.B.; Data Acquisition: I.N.; Data Analysis/Interpretation: I.N.; Drafting Manuscript: I.N.; Critical Revision of Manuscript: I.N., M.B.; Final Approval and Accountability: I.N., M.B.; Supervision: M.B.

Conflict of Interest: The authors declare that they have no conflicts of interest.

Financial Disclosure: There are no funders to report for this submission.

REFERENCES

1. Mossa ATH, Mohafra SM, Chandrasekaran N. Safety of Natural Insecticides: Toxic Effects on Experimental Animals. BioMed Research International. 2018; 2018: 1-17.
2. Hemingway J, Ranson H. Insecticide resistance in insect vectors of human disease. Annu Rev Entomol. 2000; 45(1): 371-91.
3. Benelli G. Research in mosquito control: current challenges for a brighter future. Parasitol Res. 2015; 114(8): 2801-5.
4. Benelli G, Jeffries C, Walker T. Biological control of mosquito vectors: past, present, and future. Insects. 2016; 7(4): 52.
5. Pavela R. Essential oils for the development of eco-friendly mosquito larvicides: a review. Industrial crops and products. 2015; 76: 174-87.
6. Bakkali F, Averbeck S, Averbeck D, Idaomar M. Biological effects of essential oils—a review. Food Chem Toxicol. 2008; 46(2): 446-75.
7. Bessah R, Benyoussef E-H. La filière des huiles essentielles Etat de l'art, impacts et enjeux socioéconomiques. Revue des Energies Renouvelables. 2015; 18(3): 513-28.
8. Elimam AM, Elmaliq KH, Ali FS. Efficacy of leaves extract of *Calotropis procera* Ait.(Asclepiadaceae) in controlling *Anopheles arabiensis* and *Culex quinquefasciatus* mosquitoes. Saudi J Biol Sci. 2009; 16(2): 95-100.
9. Park IK, Lee SG, Shin SC, Park JD, Ahn YJ. Larvicidal activity of isobutylamides identified in *Piper nigrum* fruits against three mosquito species. J Agric Food Chem. 2002; 50(7): 1866-70.
10. Ghosh A, Chowdhury N, Chandra G. Plant extracts as potential mosquito larvicides. The Indian journal of medical research. 2012; 135(5): 581.
11. Markouk M, Bekkouche K, Larhsini M, Bousaid M, Lazrek H, Jana M. Evaluation of some Moroccan medicinal plant extracts for larvicidal activity. J Ethnopharmacol. 2000; 73(1-2): 293-7.
12. Al-Jaran TK, Katbeh-Bader AM. Laboratory studies on the biology of *Culiseta longiareolata* (Macquart)(Diptera: Culicidae). Aquat Insects. 2001; 23(1): 11-22.
13. Kiflawi M, Blaustein L, Mangel M. Predation-dependent oviposition habitat selection by the mosquito *Culiseta longiareolata*: a test of competing hypotheses. Ecol Lett. 2003; 6(1): 35-40.
14. Valkunas G. Avian malaria parasites and other haemosporidia: CRC press; 2004.
15. Santiago-Alarcon D, Palinauskas V, Schaefer HM. Diptera vectors of avian Haemosporidian parasites: untangling parasite life cycles and their taxonomy. Biological Reviews. 2012; 87(4): 928-64.
16. Organization WH. Guidelines for laboratory and field testing of mosquito larvicides. Geneva: World Health Organization. 2005.
17. Hosseinzadeh S, Kukhdan AJ, Hosseini A, Armand R. The application of *Thymus vulgaris* in traditional and modern medicine: a review. Global J Pharmacol. 2015; 9: 260-6.
18. Knio K, Usta J, Dagher S, Zournajian H, Kreydiyyeh S. Larvicidal activity of essential oils extracted from commonly used herbs in Lebanon against the seaside mosquito, *Ochlerotatus caspius*. Bioresource technology. 2008; 99(4): 763-8.
19. Lee H-S. Mosquito larvicidal activity of aromatic medicinal plant oils against *Aedes aegypti* and *Culex pipiens pallens*. J Am Mosq Control Assoc. 2006; 22(2): 292-6.
20. Giatropoulos A, Pitarokili D, Papaioannou F, Papachristos DP, Koliopoulos G, Emmanouel N, et al. Essential oil composition, adult repellency and larvicidal activity of eight Cupressaceae species from Greece against *Aedes albopictus* (Diptera: Culicidae). Parasitol Res. 2013; 112(3): 1113-23.
21. Conti B, Canale A, Bertoli A, Gozzini F, Pistelli L. Essential oil composition and larvicidal activity of six Mediterranean aromatic plants against the mosquito *Aedes albopictus* (Diptera: Culicidae). Parasitol Res. 2010; 107(6): 1455-61.
22. Govindarajan M. Larvicidal and repellent properties of some essential oils against *Culex tritaeniorhynchus* Giles and *Anopheles subpictus* Grassi (Diptera: Culicidae). Asian Pac J Trop Med. 2011; 4(2): 106-11.
23. Lucia A, Gonzalez-Audino P, Seccacini E, Licastro S, Zerba E, Masuh H. Larvicidal effect of *Eucalyptus Grandis* essential oil and turpentine and their major components on *Aedes Aegypti* larvae. J Am Mosq Control Assoc. 2007; 23(3): 299-303.
24. Samir B, Benayache F, Benyahia S, Chalchat J-C, Garry R-P. Leaf Oils of some *Eucalyptus* Species Growing in Algeria. Journal of Essential Oil Research. 2001; 13(3): 210-3.

25. Ilahi I, Ullah F. Larvicidal activities of different parts of *Artemisia vulgaris* Linn. against *Culex quinquefasciatus* Say.(Diptera: Culicidae). *International Journal of Innovation and Applied Studies*. 2013; 2(2): 189-95.
26. Govindarajan M, Benelli G. *Artemisia absinthium*-borne compounds as novel larvicides: effectiveness against six mosquito vectors and acute toxicity on non-target aquatic organisms. *Parasitol Res*. 2016; 115(12): 4649-61.
27. Cetin H, Tufan-Cetin O, Turk A, Tay T, Candan M, Yanikoglu A, et al. Larvicidal activity of some secondary lichen metabolites against the mosquito *Culiseta longiareolata* Macquart (Diptera: Culicidae). *Natural product research*. 2012; 26(4): 350-5.
28. Park B-S, Choi W-S, Kim J-H, Kim K-H, Lee S-E. Monoterpenes from thyme (*Thymus vulgaris*) as potential mosquito repellents. *J Am Mosq Control Assoc*. 2005; 21(1): 80-3.
29. Giordani R, Hadeif Y, Kaloustian J. Compositions and antifungal activities of essential oils of some Algerian aromatic plants. *Fitoterapia*. 2008; 79(3): 199-203.
30. Mazari K, Bendimerad N, Bekhechi C. Chemical composition and antimicrobial activity of essential oils isolated from Algerian *Juniperus phoenicea* L. and *Cupressus sempervirens* L. *Journal of Medicinal Plants Research*. 2010; 4(10): 959-64.
31. Dob T, Benabdelkader T. Chemical composition of the essential oil of *Artemisia herba-alba* Asso grown in Algeria. *Journal of Essential Oil Research*. 2006; 18(6): 685-90.
32. Djeddi DS, Bouchenah N, Settar I, Skaltsa H. Composition and antimicrobial activity of the essential oil of *Rosmarinus officinalis* from Algeria. *Chemistry of Natural Compounds*. 2007; 43(4): 487-90.

Isolation, Identification and Pathogenicity of *Flavobacterium columnare* SGM4 in Catfish *Clarias batrachus* (Linnaeus 1758)

Sudeshna Sarker¹ , Thangapalam Jawahar Abraham¹ 

¹West Bengal University of Animal and Fishery Sciences, Faculty of Fishery Sciences, Department of Aquatic Animal Health, West Bengal, India

ORCID IDs of the authors: S.S. 0000-0002-0984-9671; T.J.A. 0000-0003-0581-1307

Please cite this article as: Sarker S, Abraham TJ. Isolation, Identification and Pathogenicity of *Flavobacterium columnare* SGM4 in Catfish *Clarias batrachus* (Linnaeus 1758). Eur J Biol 2019; 78(2): 136-143. DOI: 10.26650/EurJBiol.2019.0027

ABSTRACT

Objective: This study assessed the pathogenicity of *Flavobacterium columnare* isolated from the gill-rot of catfish, *Clarias batrachus* in West Bengal, India.

Materials and Methods: The diseased catfish were examined as per standard laboratory practices. *F. columnare* SGM4 was identified based on the morphological, phenotypic and genotypic characterization. Abrasion-immersion and agar-disc diffusion methods were followed to assess the pathogenicity and antibiotic sensitivity of *F. columnare*, respectively.

Results: The diseased catfish had white gills, tail rot, body discoloration, saddle-back, peeled skin, emaciation, and inflamed kidney. The yellow-pigmented rhizoid colonies from the gills of catfish were identified as *F. columnare*. Phylogenetically, *F. columnare* SGM4 branched with *F. columnare* strains. In abrasion-immersion challenge experiments, *F. columnare* SGM4 induced considerable mortalities (45%) in *C. batrachus* at 7.2×10^6 cells/mL at 24-30 °C. In challenged catfish, it caused cutaneous lesions, tail rot, white patches on the gills and degeneration of internal organs. *F. columnare* strains were highly sensitive to broad-spectrum antibiotics except for sulphafurazole.

Conclusion: Adoption of good nursery practices and appropriate health management measures would help to minimize the development and spread of columnaris disease.

Keywords: *Clarias batrachus*, Gill-rot, *Flavobacterium columnare*, Pathogenicity, Antibiotic susceptibility

INTRODUCTION

Columnaris disease is the most common disease of cultured catfish globally. It is caused by a Gram-negative bacillus *Flavobacterium columnare*, an acute to chronic bacterial infection, that affects virtually all species of warm water fish (1,2). *F. columnare* is ubiquitous in the freshwater environment and can cause tragic mortalities in both wild as well as cultured species. The catfish are especially vulnerable to *F. columnare* infections (3). Mortalities in farmed catfish from columnaris can be as high as 50-60% (2). It is one of the important bacterial pathogens of freshwater fish and can be of economic

importance in catfish farming, particularly in the intensive channel catfish *Ictalurus punctatus* farming. In the United States catfish industry, it caused an estimated annual loss of US\$ 30 million (2,4). The gills, skin and fins of fish are normally affected by *F. columnare* with varying degrees of clinical manifestation and virulence (2,4,5). The disease is often initiated as an external infection on the body surface, fins or gills, and subsequently developed into yellow-orange lesions along the dorsal midline leading to a condition called saddleback (2).

F. columnare is usually of low pathogenicity and infects fish under stressful conditions. Several authors demonstrated



Corresponding Author: Thangapalam Jawahar Abraham E-mail: abrahamtj1@gmail.com
Submitted: 17.09.2019 • **Revision Requested:** 11.10.2019 • **Last Revision Received:** 02.11.2019 • **Accepted:** 21.11.2019

© Copyright 2019 by The Istanbul University Faculty of Science • Available online at <http://ejb.istanbul.edu.tr> • DOI: 10.26650/EurJBiol.2019.0027

divergence in the virulence of *F. columnare* (2,6-8). The columnaris disease outbreaks are heavily dependent on the environmental factors such as the temperature, pH and hardness of water (3). In aquaculture, the risk for the columnaris is associated with environmental stress. The risk increases with temperature fluctuation, higher feeding rates, more organic loads as well as the increasing stocking densities (2,8). Some strains of this bacterium are highly pathogenic and may cause disease in the absence of documented stress (2). Columnaris disease has been confirmed by molecular characterization of *F. columnare* in carps such as *Catla catla* (9), *Labeo rohita* and *Ctenopharyngodon idella* (10), goldfish *Carassius auratus* (11) and climbing perch *Anabas testudineus* (10) cultured in Indian conditions. The present study aimed at the characterization of *F. columnare* associated with the gill-rot of diseased *Clarias batrachus* by phenotypic and molecular means, and the pathogenic potential in *C. batrachus* fingerlings.

MATERIALS AND METHODS

Isolation and Phenotypic Characterization of Bacteria

In February 2015, extensive mortalities in catfish, *C. batrachus* (Linnaeus, 1758) of 13-14 cm in length and 40-50 g weight were reported from a nursery in Ramchandrapur (Lat. 22°52' N; Long. 88°28' E), North 24 Parganas district, West Bengal, India. About 1000 catfish juveniles were stocked in cemented tanks (10 m × 10 m × 0.5 m, water depth). The nursery experienced chronic mortalities with 10-20 catfish dying daily. The water temperature fluctuated from 16 to 23°C during the mortality period. The morbidity and cumulative mortality were about 65 and 43%,

respectively. Water exchange and benzalkonium chloride (50%) application (0.5 ppm) were attempted thrice. The examination of diseased catfish for gross and clinical signs was done at the site as per Heil (1). The morbid catfish with clinical manifestation of columnaris disease (n=15) were transported to the laboratory in oxygen-filled polythene bags and within 3 hours of collection. Following rinsing in sterile saline and wiping with sterile paper towels, inocula from the catfish gill-rot (n=5) were aseptically streaked onto selective cytophaga agar [SCA] (12) and incubated at 30 °C for 48 h. Yellow-pigmented rhizoid colonies of 2 mm size were predominant in all the plates. From all diseased fish, one each of representative yellow-pigmented colony was arbitrarily picked (n=5), purified and characterized on the basis of cell morphology, phenotypic (13,14) and genotypic (14) characters. The genotypic characterization was done for only one rhizoid strain SGM4 (Figure 1).

Molecular and Phylogenetic Characterization

The 16S rRNA of the rhizoid strain SGM4 was amplified as per the conditions and protocols described in our earlier study (14) using the universal prokaryotic forward (8F) and reverse (1492R) primers (15). The phylogenetic tree was constructed using 30 16S rRNA gene sequences that included the consensus sequence of the present study (strain SGM4), one type strain and seven non-type strains of *F. columnare*, 14 type strains of *Flavobacterium* spp., one each of *Chryseobacterium indologenes* and *Tenacibaculum maritimum*. As out-group, the type strains *Flectobacillus roseus* (n=1), *Sphingobacterium thalpophilum* (n=1) and *Pseudomonas* spp. (n=3) were included. The 16S rRNA gene sequences for



Figure 1. Yellow-pigmented rhizoid colonies of *Flavobacterium columnare* SGM4 on cytophaga agar

phylogenetic analysis were collected from the NCBI GenBank and EzBioCloud database (Figure 2). ClustalW 1.6 was followed for the data analysis and multiple alignments. Evolutionary analyses were as per MEGA6 (16).

Pathogenicity of *Flavobacterium columnare* SGM4

F. columnare SGM4 cell suspension was prepared and the cell counts determined as described in Sarker et al. (14). Healthy hatchery-raised *C. batrachus* fingerlings (n=125) of weight 3.83±0.28 g were procured from a reputed hatchery and transported to the laboratory in oxygen-filled polythene bags. The fingerlings were disinfected in 5 ppm potassium permanganate solution for 5 min and transferred to 500-L capacity fibreglass reinforced plastic

(FRP) tanks containing 300-L borewell water. The fingerlings were acclimatized for 20 days under optimal conditions and fed twice daily with pellet feed at 4% of body weight. On alternate days, the faecal matter and other wastes were removed by siphoning and 40-50% water exchanged.

Pathogenicity of *F. columnare* SGM4 was tested in *C. batrachus* fingerlings by the abrasion-immersion method as described in Sarker et al. (14). In brief, healthy fingerlings were stocked at 10 fish/tank (58 × 45 × 45 cm) and acclimatized in the aerated tank for 3 days at 24-30 °C. The catfish were divided into five groups, viz., A, B, C, D and E in duplicate. Prior to the challenge, the scales of catfish from each tank of groups A, B and D were

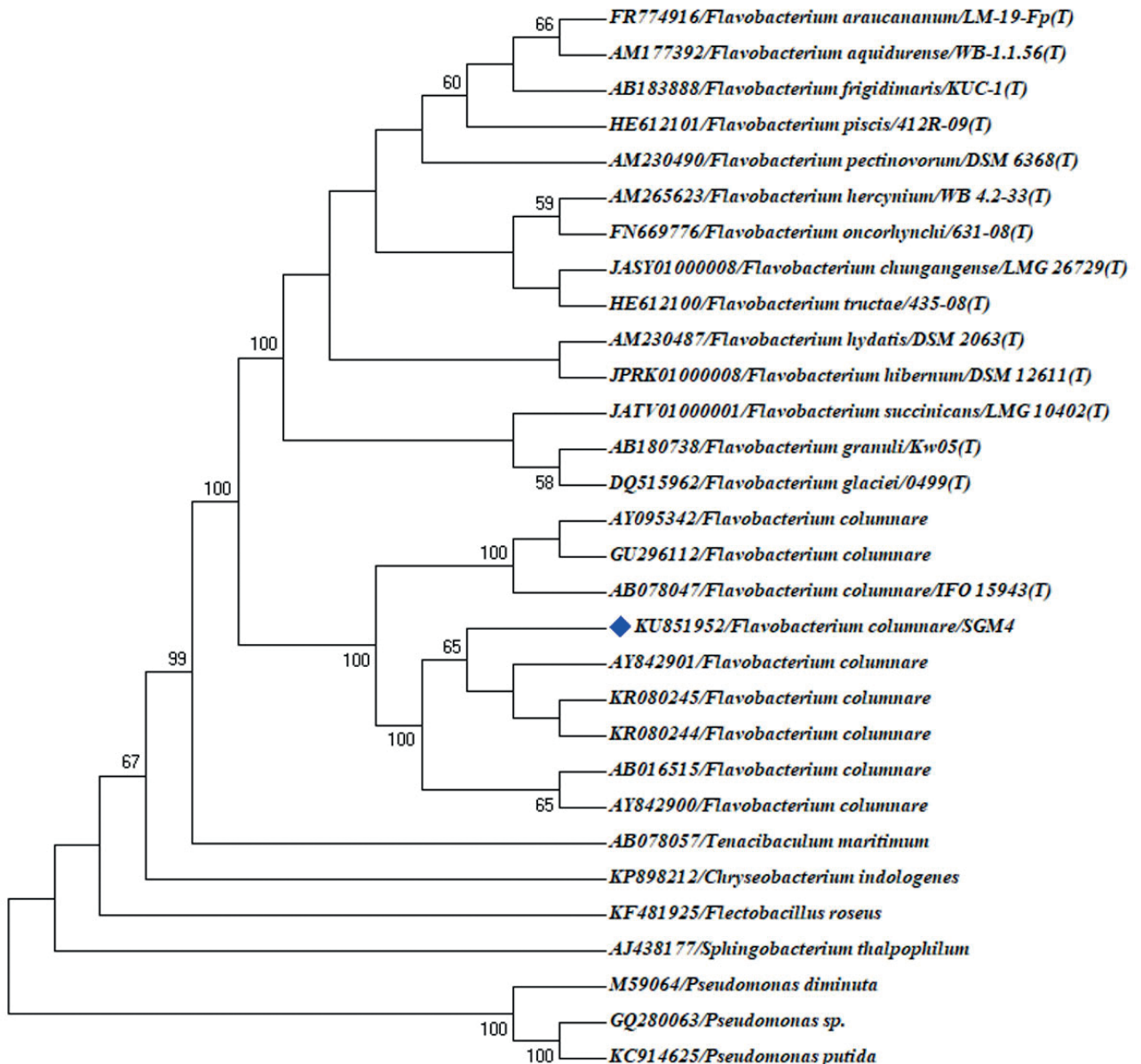


Figure 2. Phylogenetic tree based on the 16S rRNA sequence analysis by Neighbor-Joining method. Numbers at nodes indicate bootstrap confidence values (1000 replicates). The GenBank accession number is provided for each species.

scrapped off gently on one side with a scalpel 1.0 cm from caudal peduncle towards the pectoral fin (abraded). The abraded catfish of groups A and B were then immersed in *F. columnare* SGM4 suspensions containing 7.2×10^6 cells/mL, 7.2×10^5 cells/mL for 30 min, respectively. The group C was non-abraded and immersed in *F. columnare* SGM4 suspensions containing 7.2×10^6 cells/mL for 30 min. The group D abraded fish was served as a positive control after immersion in 0.85% saline for 30 min. The fish of all groups were then transferred to the respective tanks. No abrasion or challenge was done to the catfish of group E, which served as a negative control. The challenged and control fish groups were observed for the behavioural abnormalities, external signs of infection and mortality for 28 days. Re-isolation of the challenged bacterium from freshly dead catfish was on SCA followed by phenotypic confirmation.

Antibiotic Sensitivity of *Flavobacterium columnare*

F. columnare strains (n=5) were screened for their sensitivity to ten broad-spectrum antibiotics, viz., amoxyclav (30 µg), chloramphenicol (30 µg), ciprofloxacin (5 µg), co-trimoxazole (25 µg), erythromycin (15 µg), gatifloxacin (5 µg), gentamicin (10 µg), nitrofurantoin (300 µg), oxytetracycline (30 µg) and sulphafurazole (300 µg) by Kirby Bauer agar-disc diffusion technique (17) on cytophaga agar at 30 °C. The antibiotic impregnated discs were procured from HiMedia, India. Interpretation of sensitivity was based on the zone size interpretation chart for Gram-negative bacteria (18).

RESULTS

Isolation and Phenotypic Characterization of Bacteria

Inocula from the catfish gill-rot on SCA yielded yellow-pigmented rhizoidal growth within 48 h. The rhizoid colonies were Gram-negative long rods. Five rhizoid strains were characterized phenotypically by conventional biochemical tests, which identified them as *F. columnare* (Table 1). The strains were, however, identified as *Aeromonas salmonicida* by the Vitek 2 compact system with a 93% probability. Minor variation in L-Proline arylamidase activity was noted in one of the strains.

Molecular and Phylogenetic Characterization

The amplified 16S rRNA gene (≈1500 bp) of the strain SGM4 was edited to a sequence length of 1432 bp. Phylogenetic analysis confirmed the strain as a member of the family Flavobacteriaceae. Phylogenetically, the members of the genus *Flavobacterium* clustered together as a separate clade, distinctly different from other bacteria. The strain SGM4 branched with the type strain *F. columnare* IFO 15943(T) [NCBI accession number AB078047] and the non-type strains of *F. columnare* with high node value. The 16S rRNA gene sequence of *F. columnare* SGM4 (accession number KU851952) was deposited in NCBI GenBank.

Pathogenicity of *Flavobacterium columnare* SGM4

The abraded and immersion challenged *C. batrachus* fingerlings were sluggish, erratic, hanging and anorectic. In challenged catfish, white patches on the gills, excessive mucus secretion, saddleback, caudal peduncle lesions, tail rot, cutaneous haemorrhages, ulceration in the abraded area, skin discolouration, skin peeling, pale and discoloured kidney and liver, and haemorrhages in

the internal organs were observed. About $45 \pm 5\%$ and $10 \pm 0\%$ mortalities were noted in abraded groups when challenged at 7.2×10^6 cells/mL and 7.2×10^5 cells/mL levels, respectively. The internal organs of challenged catfish were haemorrhagic in the later stage (Table 2).

Antibiotic Sensitivity of *Flavobacterium columnare*

All *F. columnare* strains were highly sensitive to amoxyclav, chloramphenicol, ciprofloxacin, gatifloxacin, gentamicin and oxytetracycline. Few strains were resistant to co-trimoxazole (n=2), erythromycin (n=2), nitrofurantoin (n=1) and sulphafurazole (n=4) (Table 3).

DISCUSSION

The emaciated and diseased catfish had white hues on the gills, gill-rot, tail rot, discoloured skin, saddleback, peeled skin and swollen kidney. Gross and clinical signs observed in diseased catfish signified columnaris disease (2,5,13). The isolation of *F. columnare* from the gill-rot of diseased *C. batrachus* indicated the opportunistic potential of this bacterium in immunosuppressed catfish during the winter season. The rhizoid type colonies were reportedly virulent to fish (7,19). The low levels of mortalities with 10-20 fish dying daily suggested chronic columnaris disease in catfish at temperatures in the range of 16-23 °C. Vitek 2 compact system identified the tested strains as *A. salmonicida* as the software contained only the database on clinical isolates. Unlike our earlier study (14), this identity also contradicted with the conventional and molecular diagnosis. The Vitek-2 records were, therefore, used for characterizing the strains phenotypically. The phenotypic characteristics of all the *F. columnare* strains, as shown in Table 1, were almost the same. The Vitek-2 results indicated only minor phenotypic variations among the *F. columnare* strains of diseased catfish. The phylogeny of the strain SGM4 confirmed the bacterium as *F. columnare*, a member of the family Flavobacteriaceae. It branched with the type strain *F. columnare* IFO 15943(T) [NCBI accession number AB078047] along with other *F. columnare* strains with high node value.

Though various challenge routes to induce columnaris disease are available, we chose to follow abrasion and immersion challenge as it gave consistently better results in our earlier study (14). About $45 \pm 5\%$ and $10 \pm 0\%$ mortalities were noted in abraded groups when challenged at 7.2×10^6 cells/mL and 7.2×10^5 cells/mL levels, respectively. No mortalities were noted in non-abraded and immersion challenged catfish and other groups at 24-30 °C. While in the naturally infected population about 65% morbidity and 43% cumulative mortalities were recorded at 16-23°C in tropical Indian condition. Likewise, in temperate condition, Durborow et al. (20) found that columnaris disease commonly occurs in channel catfish when water temperatures are in the range of 25-32 °C. Columnaris epidemics reportedly occur in water temperatures below 25 °C; even as low as 15 °C, but mortalities and acuteness of disease are significantly less than in higher temperatures (2,3,8). Further, the experiments of Holt et al. (21) revealed that temperatures in excess of 12.2 °C are required for *F. columnare* induced mortalities in trout and salmon.

Table 1. Phenotypic characteristics of *Flavobacterium columnare* strains (n=5) as assessed by conventional biochemical tests and VITEK 2 compact system (bioMérieux, France)

Biochemical characteristics	Reaction	Biochemical characteristics	Reaction
Conventional biochemical tests		Vitek 2-Compact system	
Colony colour	Yellow	D-Mannose (dMNE)	-
Rhizoid colony	+	D-Sorbitol (dSOR)	-
Gram reaction	-	D-Tagatose (dTAG)	-
Cell morphology, Long rod	+	D-Trehalose (dTRE)	-
Gliding motility	+	Ellman (ELLM)	-
Oxidase	-	Fermentation/ glucose (OFF)	-
Oxidative/Fermentative reaction	-/-	Gamma-glutamyl transferase (GGT)	-
Casein hydrolysis	+	Glu-Gly-Arg-arylamidase (GGAA)	-
Chondroitin sulphate degradation	-	Glutamyl arylamidase pNA (AGLTp)	-
Congo red reaction	+	Glycine arylamidase (GlyA)	-
Fibrinogen hydrolysis	-	H ₂ S production (H ₂ S)	-
Flexirubin pigment presence	-	L Pyrrolydonyl-arylamidase (PyrA)	-
Gelatin hydrolysis	-	L-Arabitol (IARL)	-
Growth in selective cytophaga agar#	+	L-Histidine assimilation (IHISa)	-
Vitek 2 Compact system		Lipase (LIP)	-
5-Keto D-gluconate (5KG)	-	L-Lactate alkalinisation (ILATk)	-
Adonitol (ADO)	-	L-Lactate assimilation (ILATa)	-
Ala-Phe-Pro-arylamidase (APPA)	-	L-Malate assimilation (IMLTa)	-
Alpha-galactosidase (AGAL)	-	L-Proline arylamidase (ProA)	(-)*
Alpha-glucosidase (AGLU)	-	Lysine decarboxylase (LDC)	-
Beta-alanine arylamidase pNA (BALap)	-	Malonate (MNT)	-
Beta-galactosidase (BGAL)	-	O/129 Resistance (O129R)	-
Beta-glucuronidase (BGUR)	-	Ornithine decarboxylase (ODC)	-
Beta-glucosidase (BGLU)	-	Palatinose (PLE)	-
Beta-xylosidase (BXYL)	-	Phosphatase (PHOS)	-
Citrate (sodium) (CIT)	-	Saccharose/Sucrose (SAC)	-
Coumarate (CMT)	+	Succinate alkalinisation (SUCT)	-
D-Cellobiose (dCEL)	-	Tyrosine arylamidase (TyrA)	-
D-Glucose (dGLU)	-	Urease (URE)	-
D-Maltose (dMAL)	-	β-N-acetyl-galactosaminidase (NAGA)	-
D-Mannitol (dMAN)	-	β-N-Acetyl-glucosaminidase (BNAG)	-

VITEK 2 compact system identified the strains as *Aeromonas salmonicida*. *: One strain exhibited a weak reaction.

Table 2. Pathogenicity of *Flavobacterium columnare* SGM4 by abrasion and immersion challenge

Treatment group and the challenge dose	Mortality (%)
Group A: Abraded and immersion challenged at 7.2×10^6 cells/mL	45.00±5.00
Group B: Abraded and immersion challenged at 7.2×10^5 cells/mL	10.00±0.00
Group C: Non-abraded and immersion challenged at 7.2×10^6 cells/mL	0.00±0.00
Group D: Abraded and immersion in 0.85% saline	0.00±0.00
Group E: Neither abraded nor challenged	0.00±0.00

Table 3. Antibiotic-resistance in *Flavobacterium columnare* strains (n=5) isolated from columnaris diseased catfish *Clarias batrachus*

Antibiotic (µg/disc)	Interpretation of zone size (in mm)		Numbers resistant	Numbers sensitive
	Resistant (≤)	Sensitive (≥)		
Amoxyclav (30)	13	18	0	5
Chloramphenicol (30)	12	18	0	5
Ciprofloxacin (5)	15	21	0	5
Co-trimoxazole (25)	10	16	1	4
Erythromycin (15)	13	23	1	4
Gatifloxacin (5)	14	18	0	5
Gentamicin (10)	12	15	0	5
Nitrofurantoin (300)	14	17	1	4
Oxytetracycline (30)	11	15	0	5
Sulphafurazole (300)	12	17	4	1

With the increase in water temperature, the mortalities reduced and fish became almost normal. These findings indicated that temperature can have a strong effect on the virulence of *F. columnare* in the culture environment and presumably on disease progression. In other fish pathogens also the growth of bacteria at higher-than-optimal temperature resulted in decreased virulence (8). Abrasion and low temperature exacerbated the rate of infection, which endorse the findings of Moyer and Hunnicutt (22) in zebrafish *Danio rerio*. In abrasion-bath treatment with *F. columnare*, they recorded LD₅₀ values in the range of 1.1×10^6 - 1.1×10^7 cfu/mL. In another study, Nayak et al. (23) recorded the LD₅₀ values of *F. columnare* in *Cirrhinus mrigala* fry in the range of 3.0×10^5 - 9.0×10^6 cfu/mL by immersion assay. In contrast, Swain et al. (24) recorded no mortalities in non-abraded *L. rohita* fingerlings at a challenge dose of 10^6 - 10^8 cfu/mL in immersion challenge study with *F. branchiophilum*. The experimental challenge results of this study displayed that the gill associated *F. columnare* SGM4 can induce mortalities in catfish in conjunction with skin damages. In later stages, the development of haemorrhages in the internal

organs of challenged catfish indicated a septicemic condition, which supported the study of Decostere et al. (6).

All *F. columnare* strains were highly sensitive to most of the tested antibiotics. Likewise, Sarker et al. (25) recorded highly sensitive *Flavobacterium* spp. in carps of sewage-fed farms in West Bengal, India. They also recorded *Flavobacterium* spp. resistant to erythromycin, co-trimoxazole, oxytetracycline and nitrofurantoin with multidrug resistance index ranging from 0.000 to 0.667. Contrarily, 97 and 100% of the *F. columnare* strains were regarded as susceptible to sulfadimethoxine and ormetoprim (5:1) and oxytetracycline, respectively (12). Many earlier studies also reported no exceptional resistance to antimicrobial drugs among the environmental *Flavobacterium* strains (23,26,27).

CONCLUSION

In tropical Indian condition, water temperature and challenge mode induced variations in mortalities due to *F. columnare* infection were noted. Though the *F. columnare* strains were

highly sensitive to antibiotics, with the emergence of antibacterial resistance, the effective preventive measures are warranted. Management measures such as maintenance of optimal stocking densities and water quality parameters, physical removal of biofilm on tank surfaces, adoption of good nursery hygiene, sanitation, and other health management measures would help to minimize the development and spread of columnaris disease.

Peer-review: Externally peer-reviewed.

Author Contributions: Concept:T.J.A.; Design:T.J.A.; Supervision:T.J.A.; Resource:T.J.A., S.S.; Materials:T.J.A., S.S.; Data Collection and/or Processing:S.S.; Analysis and/or Interpretation:S.S.,T.J.A.; Literature Search:S.S.; Writing:S.S., T.J.A.; Critical Reviews:T.J.A.

Ethics Committee Approval: All the experimental protocols with catfish as an experimental animal were approved by the Ethical Committee, WBUAFS, Kolkata, India.

Conflict of Interest: The authors have no conflict of interest to declare.

Financial Disclosure: The research work was supported by the Indian Council of Agricultural Research (Grant F. 10(12)/2012-EPD dated 23.03.2012), Government of India, New Delhi under the Niche Area of Excellence program.

Acknowledgement: The authors thank the Vice-Chancellor, West Bengal University of Animal and Fishery Sciences, Kolkata for providing necessary facilities to carry out the work.

REFERENCES

1. Heil N. National wild fish health survey—laboratory procedures manual. US Fish and Wildlife Service. Warm Springs, GA. 2009.
2. Declercq AM, Haesebrouck F, Van den Broeck W, Bossier P, Decostere A. Columnaris disease in fish: a review with emphasis on bacterium-host interactions. *Vet Res* 2013; 44(1): 1-7.
3. Zhou T, Yuan Z, Tan S, Jin Y, Yang Y, Shi H et al. A review of molecular responses of catfish to bacterial diseases and abiotic stresses. *Front Physiol* 2018; 9:1113.
4. Shoemaker CA, Olivares-Fuster O, Arias CR, Klesius PH. *Flavobacterium columnare* genomovar influences mortality in channel catfish (*Ictalurus punctatus*). *Vet Microbiol* 2008; 127(3-4): 353-9.
5. Loch TP, Faisal M. Emerging flavobacterial infections in fish: a review. *J Adv Res* 2015; 6(3): 283-300.
6. Decostere A, Ducatelle R, Haesebrouck F. *Flavobacterium columnare* (*Flexibacter columnaris*) associated with severe gill necrosis in koi carp (*Cyprinus carpio* L). *Vet Rec* 2002; 150(22): 694-5.
7. Kunttu HM, Jokinen EI, Valtonen ET, Sundberg LR. Virulent and non-virulent *Flavobacterium columnare* colony morphologies: characterization of chondroitin AC lyase activity and adhesion to polystyrene. *J Appl Microbiol* 2011; 111(6): 1319-26.
8. Ashrafi R, Bruneaux M, Sundberg LR, Pulkkinen K, Valkonen J, Ketola T. Broad thermal tolerance is negatively correlated with virulence in an opportunistic bacterial pathogen. *Evol Appl* 2018; 11(9): 1700-14.
9. Verma DK, Rathore G. Molecular characterization of *Flavobacterium columnare* isolated from a natural outbreak of columnaris disease in farmed fish, *Catla catla* from India. *J Gen Appl Microbiol* 2013; 59(6): 417-24.
10. Patra A, Sarker S, Banerjee S, Adikesavalu H, Biswas D, Abraham TJ. Rapid detection of *Flavobacterium columnare* infection in fish by species-specific polymerase chain reaction. *J Aquacult Res Development* 2016; 7: 9.
11. Verma DK, Rathore G, Pradhan PK, Sood N, Punia P. Isolation and characterization of *Flavobacterium columnare* from freshwater ornamental goldfish *Carassius auratus*. *J Environ Biol* 2015; 36(2): 433-9.
12. Hawke JP, Thune RL. Systemic isolation and antimicrobial susceptibility of *Cytophaga columnaris* from commercially reared channel catfish. *J Aquat Ani Health* 1992; 4(2): 109-13.
13. Austin B, Austin DA. Bacterial fish pathogens: disease of farmed and wild fish. Fifth ed. Chichester, UK: Springer-Praxis in Aquaculture in Fisheries, Praxis Publication Ltd; 2012.
14. Sarker S, Abraham TJ, Banerjee S, Adikesavalu H, Patra A. Characterization, virulence and pathology of *Flavobacterium* sp. KG3 associated with gill rot in carp, *Catla catla* (Ham.). *Aquaculture* 2017; 468: 579-84.
15. Eden PA, Schmidt TM, Blakemore RP, Pace NR. Phylogenetic analysis of *Aquaspirillum magnetotacticum* using polymerase chain reaction-amplified 16S rRNA-specific DNA. *Int J Syst Evol Microbiol* 1991; 41(2): 324-5.
16. Tamura K, Stecher G, Peterson D, Filipksi A, Kumar S. MEGA6: molecular evolutionary genetics analysis version 6.0. *Mol Biol Evol* 2013; 30(12): 2725-9.
17. Bauer AW, Kirby WM, Sherris JC, Turck M. Antibiotic susceptibility testing by a standardized single disk method. *Am J Clin Pathol* 1966; 45: 493-6.
18. CLSI, Performance Standards for Antimicrobial Disk Susceptibility Tests, Approved Standard, Seventh ed. CLSI document M02-A11. Clinical and Laboratory Standards Institute, 950 West Valley Road, Suite 2500, Wayne, Pennsylvania 19087, USA. 2012.
19. Kunttu HM, Suomalainen LR, Jokinen EI, Valtonen ET. *Flavobacterium columnare* colony types: connection to adhesion and virulence? *Microb Pathog* 2009; 46(1): 21-7.
20. Durborow R, Thune R, Hawke J, Camus A. Columnaris disease: a bacterial infection caused by *Flavobacterium columnare*. Southern Regional Aquaculture Center, Publication No. 479. Stoneville, Mississippi, US Department of Agriculture, Stoneville, Mississippi. 1998.
21. Holt R, Sanders J, Zinn J, Fryer J, Pilcher K. Relation of water temperature to *Flexibacter columnaris* infection in steelhead trout (*Salmo gairdneri*), coho (*Oncorhynchus kisutch*) and chinook (*O. tshawytscha*) salmon. *J Fish Res Board Can* 1975; 32(9):1553-59.
22. Moyer TR, Hunnicutt DW. Susceptibility of zebrafish *Danio rerio* to infection by *Flavobacterium columnare* and *F. johnsoniae*. *Dis Aquatic Org* 2007; 76(1): 39-44.
23. Nayak KK, Pradhan J, Das BK. Characterization, pathogenicity, antibiotic sensitivity and immune response of *Flavobacterium columnare* isolated from *Cirrhinus mrigala* and *Carassius auratus*. *Int J Curr Microbiol Appl Sci* 2014; 3(11): 273-87.
24. Swain P, Mishra S, Dash S, Nayak SK, Mishra BK, Pani KC, Ramakrishna R. Association of *Flavobacterium branchiophilum* in bacterial gill disease of Indian major carps. *Indian J Anim Sci* 2007; 77(7): 646-9.

25. Sarker S, Abraham TJ, Patra A. Prevalence of diseases caused by *Flavobacterium* spp. and other opportunistic bacteria in carps of sewage-fed farms in West Bengal, India. *J Fish* 2019; 7(1): 663-70.
26. Saha P, Chakrabarti T. *Flavobacterium indicum* sp. nov., isolated from warm spring water in Assam, India. *Int J Syst Evol Microbiol* 2006; 56(11): 2617-21.
27. Park M, Ryu SH, Vu TH, Ro HS, Yun PY, Jeon CO. *Flavobacterium defluvii* sp. nov., isolated from activated sludge. *Int J Syst Evol Microbiol* 2007; 57(2): 233-7.

Effects of Tempol in Lipopolysaccharide-Induced Liver Injury

Perihan Sinem Serin¹ , Asli Kandil² , Huri Bulut³ , Tugba Kaskavalci⁴ ,
Erman Caner Bulut⁴ , Cihan Demirci-Tansel² 

¹Yeditepe University Specialty Hospital, Adult Bone Marrow Transplantation Unit, Istanbul, Turkey

²Istanbul University, Faculty of Science, Department of Biology, Istanbul, Turkey

³Bezmialem Vakif University, Faculty of Medicine, Department of Medical Biochemistry, Istanbul, Turkey

⁴Istanbul University, Institute of Graduate Studies in Sciences, Department of Biology, Istanbul, Turkey

ORCID IDs of the authors: P.S.S. 0000-0001-6404-5687; A.K. 0000-0001-8408-2610; H.B. 0000-0003-2706-9625; T.K. 0000-0002-4938-9702; E.C.B. 0000-0001-8674-0947; C.D.T. 0000-0001-7926-3089

Please cite this article as: Serin PS, Kandil A, Bulut H, Kaskavalci T, Bulut EC, Demirci-Tansel C. Effects of Tempol in Lipopolysaccharide-Induced Liver Injury. Eur J Biol 2019; 78(2): 144-152. DOI: 10.26650/EurJBiol.2019.0034

ABSTRACT

Objective: Sepsis leads to conditions such as inflammatory and anti-inflammatory process, circulatory abnormalities, cellular and humoral reactions. Endotoxin-induced oxidative stress causes injury in the liver. The aim of this study was to evaluate the effects of a radical scavenger Tempol in lipopolysaccharide (LPS)-induced liver injury in rats.

Materials and Methods: Male Wistar rats were divided into four groups: Control, LPS (15 mg/kg), LPS + Tempol group (100 mg/kg Tempol, three hours after LPS administration) and Tempol (100 mg/kg). Blood glucose and body temperature were measured during the experiment. Superoxide dismutase (SOD), aspartate aminotransferase (AST), alanine aminotransferase (ALT) and C-reactive protein (CRP) levels were measured in plasma or liver tissue. Furthermore, histopathological changes and myeloperoxidase-stained leukocytes infiltration were assessed in liver tissue.

Results: LPS caused tissue damage and leukocytes infiltration, increased AST, ALT and CRP levels, and decreased body temperature, blood glucose and SOD levels. Tempol reduced AST and ALT levels and increased SOD levels. Tempol did not prevent tissue damage, leukocytes infiltration and increment of CRP levels. There were no changes in body temperature and blood glucose levels.

Conclusion: The present study suggests that tempol may have antioxidant properties in LPS-induced liver injury. These results may contribute to a better understanding of the role of tempol and basic mechanisms of underlying oxidative stress-related liver injury for further investigations.

Keywords: Lipopolysaccharide, Liver, Tempol

INTRODUCTION

Sepsis is characterized by hypotension, vascular hyporeactivity to vasoconstrictor agents, distribution of organ blood flow and myocardial dysfunction (1, 2). Sepsis is caused by gram negative and gram positive bacteria (2, 3). It is known to cause the release of cytokines, activation of pro- and anti-inflammatory pathways, coagulation and endothelial activation, and then lead to multiple organ failure (1-4). The liver has an important role in the initiation and progression of multiple organ failure in sepsis and shock (5-8). Pathophysiology of liver injury is complex,

and not yet fully understood. Liver dysfunction occurs depending on hepatic blood flow perfusion deterioration and hypoxia in relation to systemic and microvascular circulation failures (6, 9, 10), direct damage of endotoxins such as lipopolysaccharide (LPS) (6), inflammation and cytokines (9-14).

The liver which contains hepatocytes, Kupffer cells and sinusoidal endothelial cells regulates both metabolic and immunological signal pathways, and has a critical role in the inflammatory responses in infection (6, 15). Kupffer cells are the primary defenders of the liver, and prevent



Corresponding Author: Asli Kandil E-mail: aslikandil@istanbul.edu.tr

Submitted: 20.09.2019 • **Revision Requested:** 30.10.2019 • **Last Revision Received:** 28.11.2019 • **Accepted:** 29.11.2019

© Copyright 2019 by The Istanbul University Faculty of Science • Available online at <http://ejb.istanbul.edu.tr> • DOI: 10.26650/EurJBiol.2019.0034

the entry of bacteria and endotoxins into the portal vein from systemic circulation (9, 10, 15-17). Kupffer cells are activated by LPS which causes the production of cytokines, nitric oxide and reactive oxygen species (ROS) (10, 13, 18). Kupffer cells stimulate neighbouring cells including endothelial cells, polymorphonuclear leukocytes, thrombocytes, lymphocytes, Ito cells and hepatic parenchymal cells to secrete various pro-inflammatory cytokines and chemical agents which induce endothelial cell and hepatocyte damage (2, 6, 10, 13, 18). In addition to hepatocytes damage, leukocytes, thrombocytes, Kupffer and other inflammatory cells because activated endothelial cells causes damage in sinusoids and leads to fibrin microthrombin formation (14). The increase and aggregation of these inflammatory cells into sinusoids cause occlusion and lead to the decrease of blood flow in sinusoids (14, 19). This gives rise to structural changes in the sinusoidal endothelial cells, hepatocytes and bile canaliculi membranes, and expansion of the Disse areas.

The increased level of endotoxin in circulation has a key role in the release of cytokines and systemic inflammatory response. The formation of free radicals and ROS can also be a trigger in the case of the inflammatory response resulting from the endotoxin such as LPS (3). These free radicals are neutralized by complex antioxidant systems in the normal physiological station (3, 20). Antioxidant enzymes are superoxide dismutase (SOD), glutathione peroxidase catalase, hydroperoxidase and cytochrome C oxidase. SOD catalyzes superoxide free radical to water and oxygen, and mainly detoxifies ROS in cells (3, 20, 21).

Tempol (4-hydroxy-2,2,6,6-tetramethylpiperidine-1-oxyl) is a scavenger eliminating the formations and effects of many free radicals such as superoxide anions, peroxynitrite and hydroxyl radicals. Tempol is a low molecular weight, stable nitroxide and cell membrane-permeable SOD mimetic compound (22). Moreover, tempol is widely studied in the experimental animal models (23-27). Many previous studies have shown the beneficial effects of tempol in endotoxemia and sepsis (27-31). It has been suggested that tempol protected renal blood flow and glomerular filtration rate (28, 29), inhibited damages in kidney and liver, maintained blood flow and metabolism (30, 31) and improved mesenteric blood flow (32) in experimental shock models.

The aim of this study was to evaluate the effects of tempol on oxidative stress, tissue damage and inflammation in LPS-induced liver injury.

MATERIALS and METHODS

Animals

The present study was approved by Istanbul University Local Committee on animal Research Ethics. Care and handling of animals were in accordance with the Institute for Laboratory Animal Research Guide for Care and Use of Laboratory Animals. Experiments were performed on 24 Wistar albino male rats (Bezmialem Vakif University, Istanbul, Turkey) with body weight of 300-350g.

Experimental Protocol

The animals were divided into 4 groups (n=6).

Control group: Isotonic saline solution was administered intraperitoneally (ip).

LPS group: 15 mg/kg LPS (*E. coli*, serotype 026: B6, Sigma, Missouri, USA) was administered ip.

LPS + Tempol group: 100 mg/kg Tempol (4-hidroksi-TEMPO), Sigma, Missouri, USA) was injected ip 3 hours after LPS injection.

Tempol group: 100 mg/kg Tempol was administered ip 3 hours after isotonic saline solution injection.

The animals were anesthetized with intraperitoneal injection of sodium pentothal (90 mg/kg, I.E ULAGAY, Istanbul, Turkey). Blood samples were collected by cardiac puncture. Liver samples were taken for histological, immunohistochemical and biochemical analyses.

Body Temperature and Blood Glucose Measurement

Blood samples were taken from the tail vein to measure blood glucose level at three time points 1) the beginning of experiment (baseline, T0); 2) third hour of experiment (the middle of experiment, T1); 3) sixth hour of experiment (the end of experiment, T2). In addition, the body temperature of animals in each group was measured by rectal Probe for rats (ADInstruments, Sidney, AUS) at T0, T1 and T2 time points.

Biochemical Analyses

Blood samples were centrifuged to collect plasma at 4000xg for 10 minutes, at 4°C. The plasma samples were stored at -20°C until biochemical analyses. Liver samples were weighed (wet weight) and homogenized in Sorensen's phosphate buffer (pH 7.4) with homogenizer (Sartorius, Goettingen, Germany). Homogenates were diluted 1/10 (w/v) and then centrifuged at 4000 rpm for 7 minutes at 4°C. Supernatants were stored at -20°C until analysis.

SOD, aspartate aminotransferase (AST), alanine aminotransferase (ALT) and C-reactive protein (CRP) levels were measured in plasma and/or liver tissue using ELISA kits for rats (Uscn Life Science Inc., Qingdao, Shandong, China) according to the manufacturer's protocol.

Histological Analysis

Liver samples were fixed in 10% neutral formalin and embedded in paraffin. Liver sections (4µm) were taken with a Rotary microtome and stained with hematoxylin-eosin (HE). Histopathological changes in liver tissue were examined under a light microscope. Photographs of the sections were taken with Image Pro-Plus (Kameram 390CU, Istanbul, Turkey).

Immunohistochemical Analysis

Liver samples were fixed in 10% neutral formalin, embedded in paraffin and prepared as described previously (33). Myeloperoxidase (MPO)-staining was performed on the liver sections with anti-MPO antibodies (RB-373-A, Thermo Scientific,

Fremont, CA, USA) (34). The distribution of MPO reaction was evaluated in the liver sections. MPO-stained leukocytes were counted in 10 randomly selected areas of liver section taken from each animal of the experimental groups under a light microscope at X40 magnification. Photographs were taken with Image Pro-Plus (Kameram 390CU, Istanbul, Turkey).

Statistical Analysis

Significant differences within groups were estimated using one-way ANOVA with Tukey's multiple comparison test, and differences between groups were estimated using two-way ANOVA with Bonferonni posttest. p<0.05 was considered significant. Statistical analyses were performed with GraphPad Prism version 5.0 for Windows (GraphPad Software, San Diego, CA, USA).

RESULTS

Blood Glucose Results

Blood glucose levels are presented on Table 1. Blood glucose levels in LPS injected animals were decreased at the end of experiment (T2) compared with the control group (p<0.001). Treatment of tempol did not change the glucose level compared with the LPS group. Blood glucose level in LPS + Tempol group was still lower than the control group (p<0.001).

Blood glucose levels decreased during the experiment (T1 and T2) compared with the beginning of experiment (T0) in LPS (p<0.05, p<0.001) and LPS + Tempol groups (p<0.05, p<0.001). Blood glucose levels remained stable during the experiment in the control and tempol groups and also were similar at all three time points.

Body Temperature Results

The body temperature values are presented on Table 2. Body temperatures in LPS injected animals decreased at T2 compared with the control group (p<0.01). Treatment of tempol did not prevent the reduction of body temperature and it was still lower than the control group (p<0.001).

The body temperature decreased during experiment (T1 and T2) compared with the beginning of experiment (T0) in LPS (p<0.01, p<0.01) and LPS + Tempol groups (p<0.05, p<0.001). Body temperatures in the control and tempol groups were similar at three time points.

Biochemical Results

LPS administration increased both AST (p<0.001) and ALT levels (p<0.001) in the plasma and tissue. Tempol reduced AST (p<0.001; p<0.05) and ALT (p<0.001; p<0.05) levels in plasma and tissue of LPS injected rats. In the tempol group, while AST in plasma was similar to the control group, AST in the tissue was lower than the control group (p<0.001). In this group, ALT in tissue was similar to the control group, however, ALT in the plasma was higher than in the control group (p<0.001) (Figures 1, 2).

LPS also caused a decrease in the plasma and tissue levels of SOD compared with the control group (p<0.001; p<0.05). Tempol administration increased SOD levels in the plasma and tissue of LPS injected animals (p<0.001). In the tempol group, SOD levels in the plasma was similar to the control group, with increasing levels of SOD in liver tissue (p<0.001) (Figure 3).

CRP, which is synthesized in liver in response to a wide variety of inflammatory stimuli, increased in the liver tissue of LPS

Table 1. Blood glucose levels (mg/dl) in the experimental groups at the three time points: T0 (the beginning of experiment), T1 (the middle of experiment) and T2 (the end of experiment). *p<0.05, ***p<0.001 vs. Control group. # p<0.05, ### p<0.001 vs. T0 baseline level.

	T0	T1	T2
Control group	104.50 ± 2.69	101.00 ± 4.35	97.50 ± 3.88
LPS group	126.57 ± 3.44*	95.13 ± 9.26#	66.38 ± 9.26***###
LPS + Tempol group	123.67 ± 3.86	100.43 ± 5.07#	60.86 ± 7.68***###
Tempol group	122.33 ± 3.77	109.714 ± 4.89	114.86 ± 3.91

Table 2. The body temperature values in experimental groups at three time points: T0 (the beginning of experiment), T1 (the middle of experiment) and T2 (the end of experiment). **p<0.01, ***p<0.001 vs. Control group. #p<0.05, ##p<0.01, ###p<0.001 vs. T0 baseline level.

	T0	T1	T2
Control group	38.0 ± 0.12	37.57 ± 0.08	37.83 ± 0.24
LPS group	38.50 ± 0.2	36.94 ± 0.14##	36.67 ± 0.48***##
LPS + Tempol group	38.7 ± 0.23	37.30 ± 0.18#	36.31 ± 0.51***###
Tempol group	37.77 ± 0.19	37.47 ± 0.11	37.7 ± 0.15

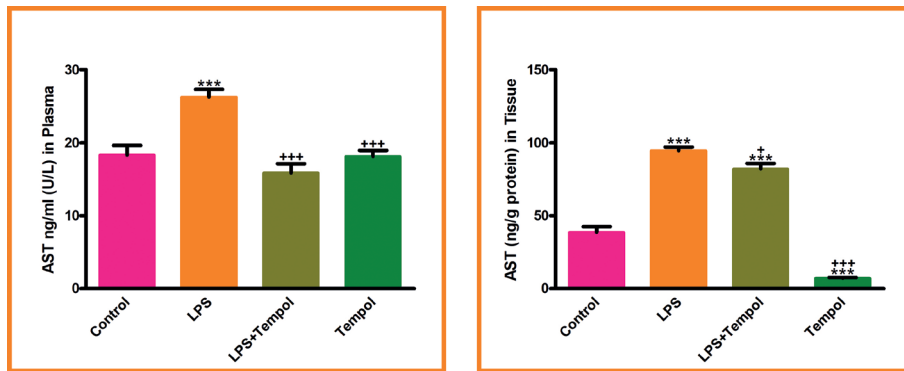


Figure 1. Aspartate aminotransferase (AST) levels in plasma and tissue of Control, LPS, LPS + Tempol and Tempol groups. ***p<0.001 vs. Control group. *p<0.05, ***p<0.001 vs. LPS group.

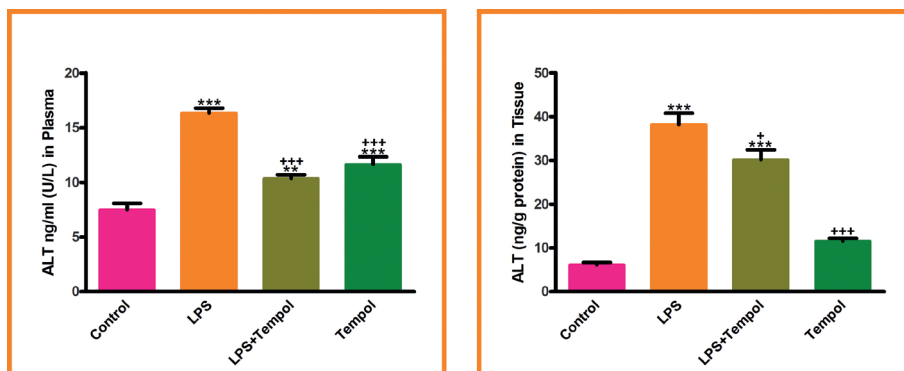


Figure 2. Alanine aminotransferase (ALT) levels in plasma and tissue of Control, LPS, LPS + Tempol and Tempol groups. **p<0.01, ***p<0.001 vs. Control group. *p<0.05, ***p<0.001 vs. LPS group.

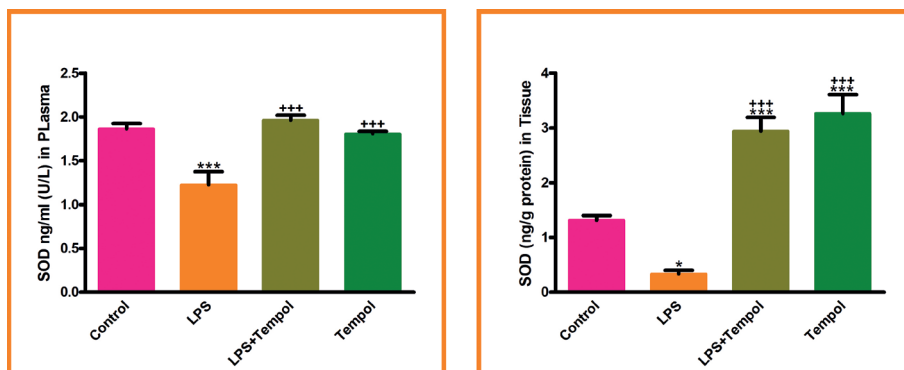


Figure 3. Superoxide dismutase (SOD) levels in plasma and tissue of Control, LPS, LPS + Tempol and Tempol groups. *p<0.05, ***p<0.001 vs. Control group. ***p<0.001 vs. LPS group.

administrated animals ($p<0.001$). Tempol did not prevent the increase of CRP levels in LPS injected rats. In the Tempol group, CRP was similar to the control group (Figure 4).

Histological Results

Histopathological changes were shown in HE-stained sections of LPS injected animals. Dilatation of sinusoids, leukocyte infiltration, loss of outlines of hepatic plates and damage to the endothelium of central veins were seen in the LPS group. LPS leads to severe inflammatory reaction in liver parenchyma. Infiltration of many

inflammatory cells was observed in liver parenchyma especially in sinusoids and vessel lumens. These inflammatory cells caused sinusoidal occlusions. In addition to these changes, structural changes in portal areas were seen in this group. Many of these results were determined in LPS + Tempol group. Tempol did not prevent inflammation and sinusoidal dilatation in the liver tissue of LPS treated animals. The histological structure of liver tissue in the group which was only given tempol was similar to the control group (Figure 5).

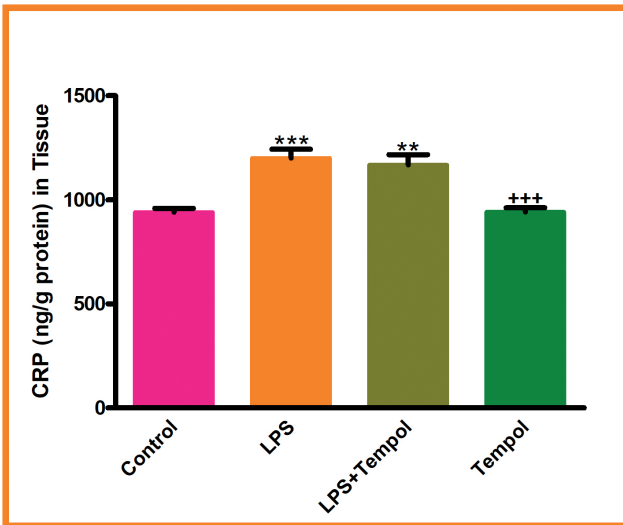


Figure 4. C-reactive protein (CRP) levels in tissue of Control, LPS, LPS + Tempol and Tempol groups. ** $p < 0.01$, *** $p < 0.001$ vs. Control group. *** $p < 0.001$ vs. LPS group.

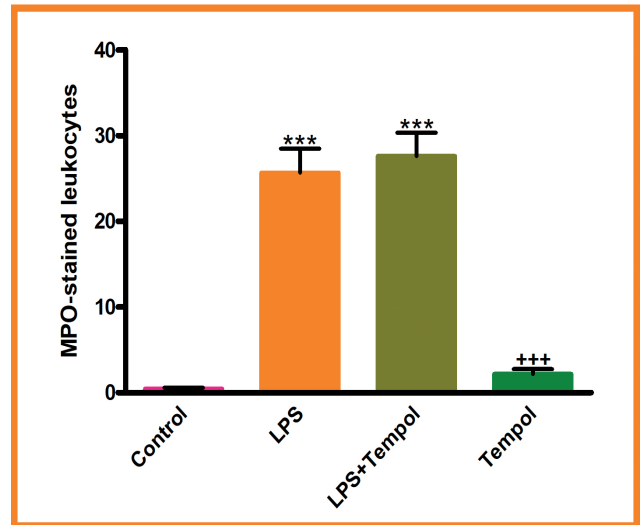


Figure 6. MPO-stained leukocytes distributions in liver tissue of Control, LPS, LPS + Tempol and Tempol groups. *** $p < 0.001$ vs. Control group. *** $p < 0.001$ vs. LPS group.

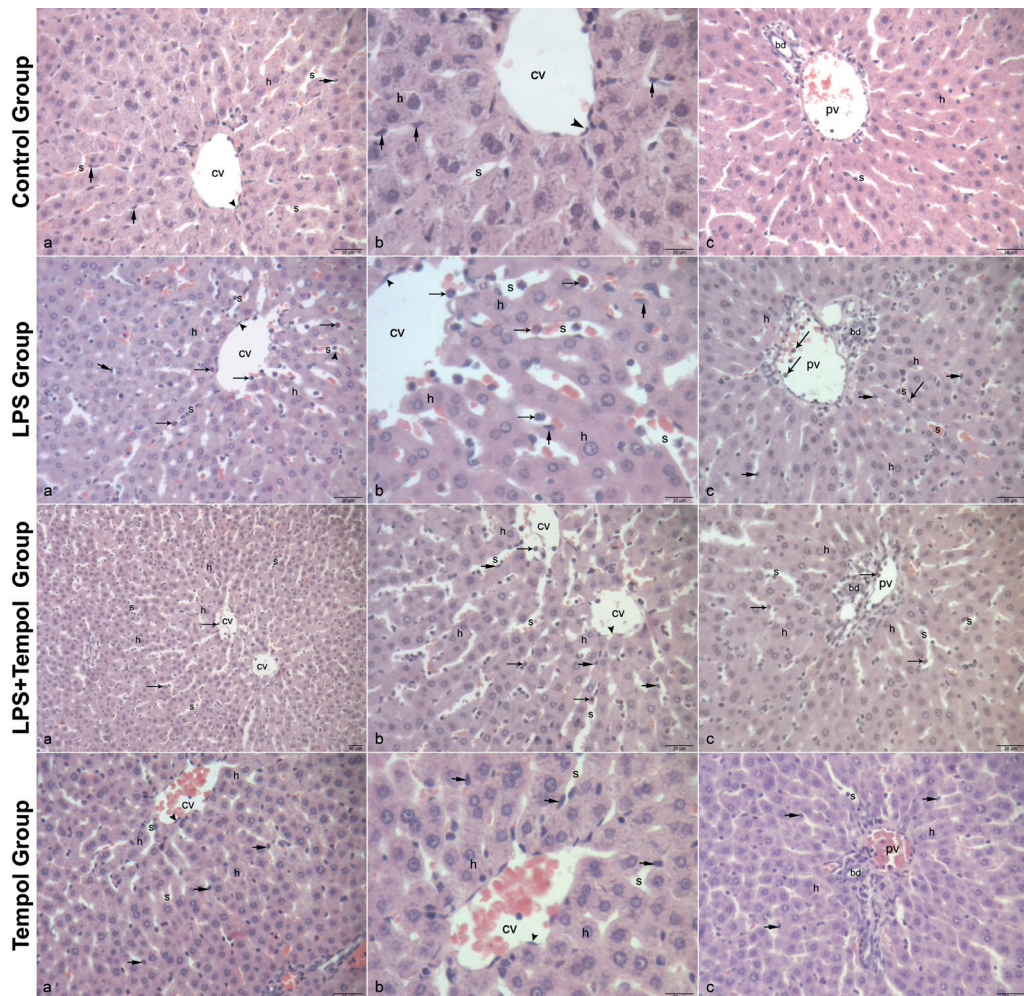


Figure 5. Central vein (cv), sinusoid (s), endothelium (\blacktriangleright), hepatocyte (h), Kupffer cell (\blacktriangleright), leukocyte (\blacktriangleright), portal vein (pv) and bile duct (bd) on liver tissue of Control, LPS, LPS + Tempol and Tempol groups. a-c) Bar: 20 μ m, HE.

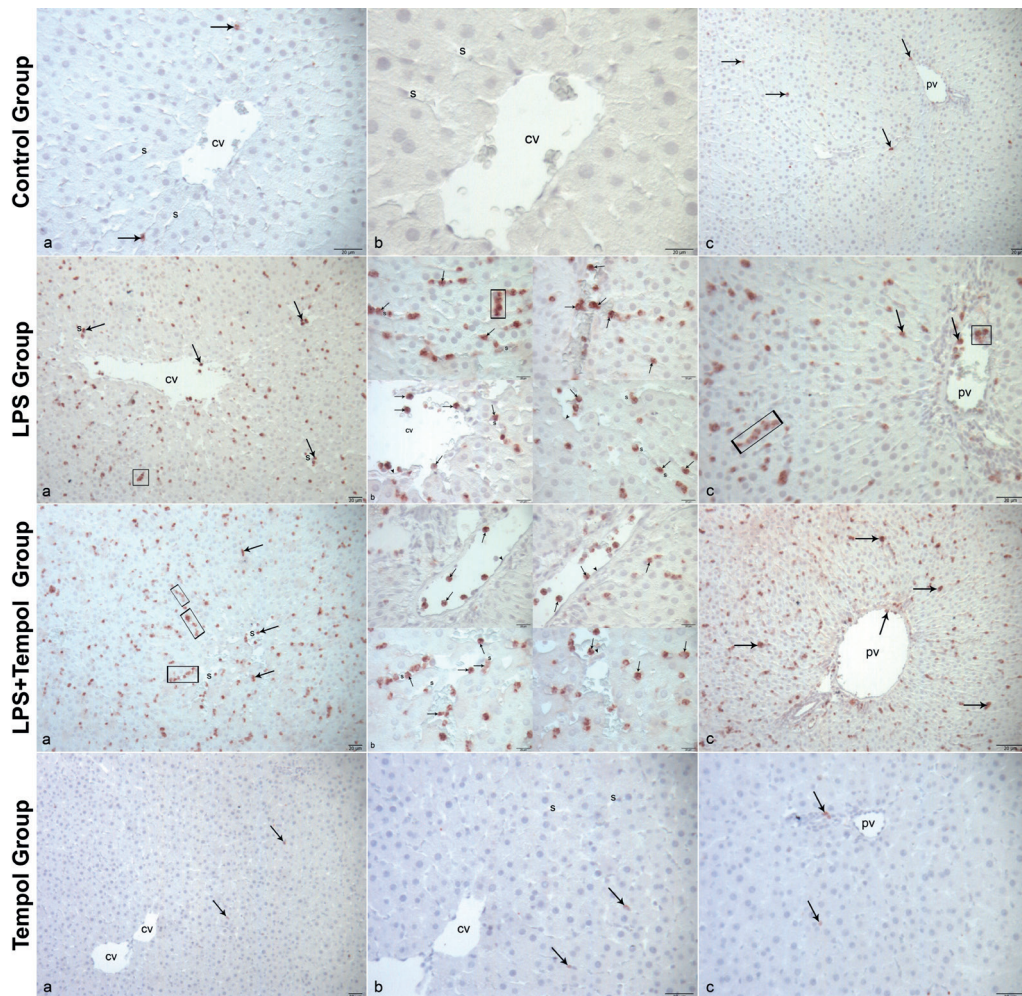


Figure 7. MPO-stained leukocytes (→, □) in liver tissue of Control, LPS, LPS + Tempol and Tempol groups. Central vein (cv), sinusoid (s), endothelium (▶) and portal vein (pv). a-c Bar: 20 μm.

Immunohistochemical Results

MPO-stained leukocytes in liver tissue increased in the LPS group ($p < 0.001$) in comparison with the control. However, tempol administration did not change the distribution of MPO-stained leukocytes in LPS injected animals. MPO-stained leukocytes were seen in sinusoids, central veins and portal areas of the liver parenchyma. Infiltration of neutrophils in sinusoids led to micro abscesses formation MPO staining in tempol group was similar to control group (Figures 6, 7).

DISCUSSION

The pathophysiology of liver dysfunction in sepsis is not clearly understood (5). Liver injury in sepsis occurs not only from hypoperfusion, but also from the spread of bacteria or endotoxins, release of inflammatory cytokines and other mediators during infection (6, 9-14). Liver injury in sepsis or shock has been studied in many animal models (35). Many studies have reported that sepsis leads to liver damage, change in glucose metabolism, and increase in aminotransferase enzymes and CRP levels (6, 31, 36-48)

Cecum ligation and puncture (CLP)-induced sepsis leads to pathological changes such as necrosis, inflammation, portal inflammation in the liver of rats (36). In LPS/D-galactosamine-induced liver injury model, the liver was observed hemorrhagic necrosis and severe hepatocyte damage (37). LPS administration resulted in pathological abnormalities including hepatic edema, inflammatory cell aggregation in sinusoids and central veins at 6 hours (38). LPS-induced histopathological changes including necrosis, inflammatory cell infiltration and vacuolar degeneration were observed in the liver 4 hours after LPS injection (39). In our study, LPS administration resulted in histological changes such as hepatocytes and endothelium damage, dilatation of sinusoids, leukocyte infiltration and inflammation. The liver damage can directly contribute to liver dysfunction. It is known that AST and ALT levels in plasma and tissue are the most important markers in assessing of liver functions during experimental and clinical liver injury (31, 40). Many studies have reported that LPS resulted in significant elevation of ALT and AST levels (31, 38-41). In this study, LPS administration resulted in significant elevation of ALT and

AST in plasma and liver. These results show that LPS induced liver injury and dysfunction in the experimental sepsis model.

Endotoxin causes enhanced peripheral glucose utilization, depletion of hepatic glycogen and an increase in gluconeogenesis (42). Bacterial infections influence glucose metabolism. Endotoxin results in hyperglycemia, followed by hypoglycemia (43-45). LPS causes blood glucose levels to decrease to hypoglycemic level (43, 46). The blood glucose level and liver glycogen decreased at 3h after LPS injection. The glucose levels increased at 3h after cecal incision, however, they decreased at 6h after cecal incision (47). CLP caused a time-dependent increase in rectal temperature which reached the maximal at 15h after CLP and then declined, whereas it caused a biphasic change in blood glucose such as hyperglycemia in the early stage (3h) and hypoglycemia in the late stage (15-18h) (27). In the present study, it was observed that LPS resulted in a decrease in the blood glucose levels at 3h and 6h after LPS injection. Also, body temperature decreased at the same time point in LPS treated animals.

CRP is an acute phase protein synthesized from the liver. Bacterial infections result in increases in CRP levels in a few hours. CRP levels are used in the diagnosis and prognosis of infection and also sepsis (6, 48). In this study, LPS caused an increase in the CRP level in the liver. The increase in CRP and leukocytes infiltration indicated the inflammatory response and oxidative stress in LPS-induced experimental sepsis model. Furthermore, LPS administration decreased SOD levels in the liver and plasma.

Our findings including liver damage, leukocytes infiltration, the elevation of aminotransferases enzymes and CRP, and the decrease of SOD level indicated LPS-induced liver injury and oxidative stress in the experimental sepsis models.

The role of oxidative stress in the pathophysiology of many diseases leads to a focus on drugs that prevent the formation of ROS and to the development of treatment strategies including antioxidant enzymes such as SOD, catalase and radical scavengers. It is known that tempol prevents the formation of hydroxyl radicals by sweeping intracellular superoxide radicals and other radicals (22). Tempol is a cell membrane permeable, a radical scavenger and a SOD mimetic agent (22, 23). Because of these abilities and properties, tempol has been studied in animal models associated with oxidative stress (23-32). The effects of tempol on hypertension were investigated in the experimental model (23, 24). Schnackenberg et al., (1998) suggested that short- and long-term administration of the stable, membrane-permeable SOD mimetic tempol significantly reduces mean arterial pressure in spontaneously hypertensive rats (24). It has been shown that tempol treatment ameliorates oxidative damage in liver tissue in methotrexate-induced liver injury. Therefore, it has been suggested that tempol may be useful in protecting the liver from injury in these experimental models (25). Many previous studies have shown the beneficial effects of tempol in endotoxemia and sepsis (27-31). Liaw et al., (2005) reported that tempol (30 mg/kg injected 90 min after CLP and then continuously infused for 18 h) not only ameliorated the deterioration of hemodynamic

changes, renal and liver injuries but also attenuated neutrophil infiltration in the lung in the sepsis induced by CLP. In addition, tempol improved the survival in CLP-induced septic rats (27). It has been demonstrated that LPS caused hypotension, hepatocellular and pancreatic injury and renal dysfunction at the sixth hour of injection, and pre-treatment of tempol (100 mg/kg infusion, 15 min prior to 30 mg/kg LPS infusion) could not affect the circulatory failure, but reduced liver injury caused by LPS (31).

In our study, tempol administration reduced the AST and ALT levels in the LPS induced sepsis rats, although, these values were still higher in the tissue. These results indicated that tempol has a role in LPS-induced liver injury, but could not prevent oxidative stress and its effects. While tempol could not attenuate histological damage and leukocytes infiltration, and also did not cause any change in CRP levels, blood glucose levels and body temperature, tempol significantly increased SOD levels both in LPS-induced sepsis and in the control animals. In addition, tempol did not cause histological damage in liver tissue of the control animals. Therefore, it could be suggested that tempol may have an antioxidant effect as SOD mimetic agent. It was thought that tempol would be more effective to apply before LPS or extended to the administration time of tempol administrated 3 hours after LPS.

CONCLUSION

Results of the present study indicated that LPS induced liver injury is associated with oxidative stress and inflammation and that tempol has an antioxidant role. However, the effects of tempol were limited in this study. Therefore, further experimental studies are needed to determine the role of tempol in sepsis and shock models.

Peer-review: Externally peer-reviewed.

Author Contributions: Conception/Design of study: P.S.S., A.K., C.D.T.; Data Acquisition: P.S.S., A.K., C.D.T., T.S., H.B.; Data Analysis/ Interpretation: P.S.S., A.K., C.D.T., T.K., H.B.; Drafting Manuscript: A.K., C.D.T., E.C.B.; Critical Revision of Manuscript: A.K., C.D.T., E.C.B.; Final Approval and Accountability: P.S.S., A.K., C.D.T., E.C.B., H.B.; Technical or Material Support: P.S.S., A.K., C.D.T., T.K., H.B.; Supervision: A.K., C.D.T.

Conflict of Interest: The authors declare that they have no conflicts of interest.

Financial Disclosure: This study was funded by Scientific Research Projects Coordination Unit of Istanbul University (Project no: 27021 and 33876).

REFERENCES

1. Levy MM, Fink MP, Marshall JC, Abraham E, Angus D, Cook D, et al. 2001 SCCM/ESICM/ACCP/ATS/SIS International Sepsis Definitions Conference. *Intensive Care Med* 2003; 29(4): 530-8.
2. Annane D, Bellissant E, Cavaillon JM. Septic shock. *Lancet* 2005; 365(9453): 63-78.
3. Minasyan H. Sepsis and septic shock: Pathogenesis and treatment perspectives. *J Crit Care* 2017; 40: 229-42.

4. Angus DC, van der Poll T. Severe sepsis and septic shock. *N Engl J Med* 2013; 369(9): 840-51.
5. Nesselser N, Launey Y, Aninat C, Morel F, Mallédant Y, Seguin P. Clinical review: The liver in sepsis. *Crit Care* 2012; 16(5):235.
6. Woźnica EA, Inglot M, Woźnica RK, Łysenko L. Liver dysfunction in sepsis. *Adv Clin Exp Med* 2018; 27(4): 547-51.
7. Koch A, Horn A, Dücker H, Yagmur E, Sanson E, Bruensing J, et al. Increased liver stiffness denotes hepatic dysfunction and mortality risk in critically ill non-cirrhotic patients at a medical ICU. *Crit Care* 2011; 15(6): 266.
8. Recknagel P, Gonnert FA, Westermann M, Lambeck S, Lupp A, Rudiger A, et al. Liver dysfunction and phosphatidylinositol-3-kinase signalling in early sepsis: experimental studies in rodent models of peritonitis. *PLoS Med* 2012; 9(11): e1001338.
9. Wang P, Ayala A, Ba ZF, Zhou M, Perrin MM, Chaudry IH. Tumor necrosis factor-alpha produces hepatocellular dysfunction despite normal cardiac output and hepatic microcirculation. *Am J Physiol* 1993; 265(1 Pt 1): G126-32.
10. Dhainaut JF, Marin N, Mignon A, Vinsonneau C. Hepatic response to sepsis: interaction between coagulation and inflammatory processes. *Crit Care Med* 2001; 29(7 Suppl): 42-7.
11. Garofalo AM, Lorente-Ros M, Goncalvez G, Carriedo D, Ballén-Barragán A, Villar-Fernández A, et al. Histopathological changes of organ dysfunction in sepsis. *Intensive Care Med Exp* 2019; 7(Suppl 1):45.
12. Mannaa, FA, Abdel-Wahhab, KG. Physiological potential of cytokines and liver damages. *Hepatoma Res* 2016; 2: 131-43.
13. Szabo G, Romics L Jr, Frenzl G. Liver in sepsis and systemic inflammatory response syndrome. *Clin Liver Dis* 2002; 6(4): 1045-66.
14. Strnad P, Tacke F, Koch A, Trautwein C. Liver - guardian, modifier and target of sepsis. *Nat Rev Gastroenterol Hepatol* 2017; 14(1): 55-66.
15. Ring A, Stremmel W. The hepatic microvascular responses to sepsis. *Semin Thromb Hemost* 2000; 26(5): 589-94.
16. Wong CH, Jenne CN, Petri B, Chrobok NL, Kubes P. Nucleation of platelets with blood-borne pathogens on Kupffer cells precedes other innate immunity and contributes to bacterial clearance. *Nat Immunol* 2013; 14(8): 785-92.
17. Komine S, Akiyama K, Warabi E, Oh S, Kuga K, Ishige K, et al. Exercise training enhances *in vivo* clearance of endotoxin and attenuates inflammatory responses by potentiating Kupffer cell phagocytosis. *Sci Rep* 2017; 7(1): 11977.
18. Koo DJ, Chaudry IH, Wang P. Kupffer cells are responsible for producing inflammatory cytokines and hepatocellular dysfunction during early sepsis. *J Surg Res* 1999; 83(2): 151-7.
19. McCuskey RS, Nishida J, McDonnell D. Effect of immunoglobulin G on the hepatic microvascular inflammatory response during sepsis. *Shock* 1996; 5 (1): 28-33.
20. Fridovich I. Superoxide radical and superoxide dismutases. *Annu Rev Biochem* 1995; 64: 97-112.
21. Fridovich I. Superoxide dismutases. An adaptation to a paramagnetic gas. *J Biol Chem* 1989; 264(14): 7761-4.
22. Samuni A, Krishna CM, Riesz P, Finkelstein E, Russo A. A novel metal-free low molecular weight superoxide dismutase mimic. *J Biol Chem* 1988; 263(34): 17921-4.
23. Wilcox CS. Effects of tempol and redox-cycling nitroxides in models of oxidative stress. *Pharmacol Ther* 2010; 126(2): 119-45.
24. Schnackenberg CG, Welch WJ, Wilcox CS. Normalization of blood pressure and renal vascular resistance in SHR with a membrane-permeable superoxide dismutase mimetic: role of nitric oxide. *Hypertension* 1998; 32(1): 59-64.
25. Pinar N, Kaplan M, Özgür T, Özcan O. Ameliorating effects of tempol on methotrexate-induced liver injury in rats. *Biomed Pharmacother* 2018; 102: 758-64.
26. Ergin B, Bezemer R, Kandil A, Demirci-Tansel C, Ince C. TEMPOL has limited protective effects on renal oxygenation and hemodynamics but reduces kidney damage and inflammation in a rat model of renal ischemia/reperfusion by aortic clamping. *J Clin Transl Res* 2015; 1(2): 1-13.
27. Liaw WJ, Chen TH, Lai ZZ, Chen SJ, Chen A, Tzao C, et al. Effects of a membrane-permeable radical scavenger, Tempol, on intraperitoneal sepsis-induced organ injury in rats. *Shock* 2005; 23(1): 88-96.
28. Wang W, Zolty E, Falk S, Summer S, Zhou Z, Gengaro P, et al. Endotoxemia-related acute kidney injury in transgenic mice with endothelial overexpression of GTP cyclohydrolase-1. *Am J Physiol Renal Physiol* 2008; 294(3): F571-6.
29. Wang W, Jittikanont S, Falk SA, Li P, Feng L, Gengaro PE, et al. Interaction among nitric oxide, reactive oxygen species, and antioxidants during endotoxemia-related acute renal failure. *Am J Physiol Renal Physiol* 2003; 284(3): F532-7.
30. Zacharowski K, Olbrich A, Cuzzocrea S, Foster SJ, Thiernemann C. Membrane-permeable radical scavenger, tempol, reduces multiple organ injury in a rodent model of gram-positive shock. *Crit Care Med* 2000; 28(6): 1953-61.
31. Leach M, Frank S, Olbrich A, Pfeilschifter J, Thiernemann C. Decline in the expression of copper/zinc superoxide dismutase in the kidney of rats with endotoxic shock: effects of the superoxide anion radical scavenger, tempol, on organ injury. *Br J Pharmacol* 1998; 125(4): 817-25.
32. Yuksel BC, Serdar SE, Tuncel A, Uzum N, Ataoglu O, Atan A, et al. Effect of tempol, a membrane-permeable radical scavenger, on mesenteric blood flow and organ injury in a murine cecal ligation and puncture model of septic shock. *Eur Surg Res* 2009; 43(2): 219-27.
33. Demirci C, Gargili A, Kandil A, Cetinkaya H, Uyaner I, Boynuegri B, et al. Inhibition of inducible nitric oxide synthase in murine visceral larva migrans: effects on lung and liver damage. *Chin J Physiol* 2006; 49(6): 326-34.
34. Legrand M, Almac E, Mik EG, Johannes T, Kandil A, Bezemer R, et al. L-NIL prevents renal microvascular hypoxia and increase of renal oxygen consumption after ischemia-reperfusion in rats. *Am J Physiol Renal Physiol* 2009; 296(5): F1109-17.
35. Lilley E, Armstrong R, Clark N, Gray P, Hawkins P, Mason K, et al. Refinement of animal models of sepsis and septic shock. *Shock* 2015; 43(4): 304-16.
36. Muftuoglu MA, Aktekin A, Ozdemir NC, Saglam A. Liver injury in sepsis and abdominal compartment syndrome in rats. *Surg Today* 2006; 36(6): 519-24.
37. Li G, Liu Y, Tzeng NS, Cui G, Block ML, Wilson B, et al. Protective effect of dextromethorphan against endotoxic shock in mice. *Biochem Pharmacol* 2005; 69(2): 233-40.
38. Liu X, Liu R, Dai Z, Wu H, Lin M, Tian F, et al. Effect of Shenfu injection on lipopolysaccharide (LPS)-induced septic shock in rabbits. *J Ethnopharmacol* 2019; 234: 36-43.
39. Sha J, Zhang H, Zhao Y, Feng X, Hu X, Wang C, et al. Dexmedetomidine attenuates lipopolysaccharide-induced liver oxidative stress and cell apoptosis in rats by increasing GSK-3 β /MKP-1/Nrf2 pathway activity via the α 2 adrenergic receptor. *Toxicol Appl Pharmacol* 2019; 364: 144-52.
40. Zhou R, Chen SH, Li G, Chen HL, Liu Y, Wu HM, et al. Ultralow doses of dextromethorphan protect mice from endotoxin-induced sepsis-like hepatotoxicity. *Chem Biol Interact* 2019; 303: 50-6.

41. Thiemermann C, Ruetten H, Wu CC, Vane JR. The multiple organ dysfunction syndrome caused by endotoxin in the rat: attenuation of liver dysfunction by inhibitors of nitric oxide synthase. *Br J Pharmacol* 1995; 116(7): 2845-51.
42. Mészáros K, Lang CH, Bagby GJ, Spitzer JJ. Contribution of different organs to increased glucose consumption after endotoxin administration. *J Biol Chem* 1987; 262(23): 10965-70.
43. Engin A, Zemheri M, Bukan N, Memiş L. Effect of nitric oxide on the hypoglycaemic phase of endotoxaemia. *ANZ J Surg* 2006; 76(6): 512-7.
44. Wallington J, Ning J, Titheradge MA. The control of hepatic glycogen metabolism in an in vitro model of sepsis. *Mol Cell Biochem* 2008; 308(1-2): 183-92.
45. Yelich MR, Witek-Janusek L. Glucose, lactate, insulin and somatostatin responses to endotoxin in developing rats. *Shock* 1994; 2: 438-44.
46. Anavi S, Hahn-Obercyger M, Margalit R, Madar Z, Tirosh O. A novel antihypoglycemic role of inducible nitric oxide synthase in liver inflammatory response induced by dietary cholesterol and endotoxemia. *Antioxid Redox Signal* 2013; 19(16): 1889-901.
47. Chang CK, Gatan M, Schumer W. Efficacy of anti-tumor necrosis factor polyclonal antibody on phosphoenolpyruvate carboxykinase expression in septic and endotoxemic rats. *Shock* 1996; 6(1): 57-60.
48. Rello J, Valenzuela-Sánchez F, Ruiz-Rodríguez M, Moyano S. Sepsis: A review of advances in management. *Adv Ther* 2017; 34(11): 2393-411.

CRISPR-Cas: Removing Boundaries of the Nature

Nicat Cebrailoglu¹ , Ali Burak Yildiz¹ , Ozlem Akkaya¹ , Yelda Ozden Ciftci¹ 

¹Gebze Technical University, Department of Molecular Biology and Genetics, Kocaeli, Turkey

ORCID IDs of the authors: N.C. 0000-0002-2770-5049; A.B.Y. 0000-0002-9982-7109; O.A. 0000-0003-0473-1417; Y.O.C. 0000-0002-9799-3648

Please cite this article as: Cebrailoglu N, Yildiz AB, Akkaya O, Ozden Ciftci Y. CRISPR-Cas: Removing Boundaries of the Nature. Eur J Biol 2019; 78(2): 153-160. DOI: 10.26650/EurJBiol.2019.0024

ABSTRACT

The CRISPR-Cas 9 system, which is known as a natural way of bacteria to defend against phage infection and plasmid transfer, has been re-purposed as a RNA-guided DNA targeting strategy for genome editing. Together with the advances gained in DNA sequencing technology, this platform opened a new era in molecular biology since its recognition was specified by 20-nt single-guide RNA which made technique easier, efficient and simple for application in any organism. Thus, many studies have discussed and performed the applications of CRISPR-Cas systems on different organisms for genome editing. Moreover, targeted gene regulations, epigenetic modulation, chromatin imaging and manipulation could also be applied with this system. Besides all its potential promising aspects, this tool might have some side effects like off-target mutations. In addition, unexpected results have also been reported after some gene editing applications. Thus, this review provides a brief history of gene editing tools together with the overview of the latest applications, regulations and ethical/structural aspects of the CRISPR Cas system.

Keywords: Gene editing, Gene therapy, Meganucleases, TALEN, ZFN, New breeding technologies

INTRODUCTION

Investigations on natural protection ways of bacteria against phages resulted in tremendous turning points in recombinant DNA technology. Starting with the discovery of restriction enzymes in the late 1970s that enabled scientists to manipulate DNA in test tubes (1), it allowed many opportunities of genetic manipulations in many organisms including bacteria, plants, animals and even humans. The key developments on the precise alteration of DNA in living eukaryotic cells, which is termed as “gene editing” (GE), started with Rothstein’s report in 1983 on yeast cells. Afterwards, Smithies and co-workers (1985) followed by Capecchi (2) demonstrated that it was possible to incorporate an exogenous copy of DNA into the mammalian cells genome through homologous recombination (HR). Although these studies resulted in the characterization of functional roles of many genes in model organisms, they have the following limitations, such as i) the rate

of spontaneous integration was too low (1 in 10³-10⁹ cells, Capecchi, 1989), ii) type and the state of the cell affected the integration rate, iii) the possibility of random integration of exogenous copy to undesired site was similar or even higher than the target site (3).

To overcome these obstacles, scientists started to use different approaches among which the construction of a double-strand break (DSB) at a target site provided the best alternative for the elevation of targeted gene integration frequency. Thus, natural rare cutting meganucleases (i.e., I-SceI) and then re-engineered ones were utilized to achieve targeted DSBs. Even though these attempts resulted in some improvements, these enzymes had several disadvantages listed in Table 1. Afterwards, zinc fingers, that are zinc ion-regulated small proteins that recognize and bind a 3 bp DNA sequence (4), were fused with the DNA cleavage domain of the Fok I endonuclease which is isolated from *Flavobacterium okeanokoites* to create a programmable



Corresponding Author: Yelda Ozden Ciftci E-mail: ozden@gtu.edu.tr

Submitted: 20.06.2019 • **Revision Requested:** 04.07.2019 • **Last Revision Received:** 23.07.2019 • **Accepted:** 29.07.2019

© Copyright 2019 by The Istanbul University Faculty of Science • Available online at <http://ejb.ibul.edu.tr> • DOI: 10.26650/EurJBiol.2019.0024

nucleases (5). Zinc finger nucleases (ZFN) then increased the capability to edit genomes at the targeted sites enabling the usage of this technique for therapeutic applications (6). Likewise, Fok I DNA cleavage domain is also combined with TALE modules in order to be utilized as an effective programmable nuclease (TALEN, transcription activator-like effector nucleases) (7). In contrast to ZFN that recognize a 3 bp, TALE proteins from *Xanthomonas* bacteria can recognize one single base. By using these nucleases, a DSB can be introduced in any site of the genome with known recognition sites of the DNA-binding domains. However, it should also be noted that TALEN nuclease sites require T before the 5'-end of the target sequence which could limit its application.

Although "Nature Methods" announced ZFN and TALEN as the method of the year for precise GE tools (<https://www.nature.com/articles/nmeth.1852.pdf>), their disadvantages indicated in Table 1 made researchers seek alternative approaches such as the **Clustered Regularly Interspaced Short Palindromic Repeats** (CRISPR)-associated protein 9 (Cas9) system. CRISPR-Cas9 system, which is known as a natural way of bacteria to defend against phage infection and plasmid transfer, has been repurposed as a RNA-guided DNA targeting strategy for genome editing and opened a new era in molecular biology since its recognition was specified by 20-nt single-guide RNA (sgRNA) (8).

This recent platform not only mimics the natural trans-activating CRISPR RNA (tracrRNA) and CRISPR RNA (crRNA) structure, but also in contrast to ZFN and TALEN, there is no need for tedious protein engineering of DNA-recognition domains for each target site which make the design easy, simple to use and efficient (9).

CRISPR-Cas: STRUCTURE AND FUNCTION

CRISPR-Cas systems are based on two molecules, guide RNA (gRNA) and Cas protein which are responsible of binding on a specific target at the genome and cutting the target point, respectively. The most applied and discussed one is the CRISPR-Cas9 system, which causes a DSB at the specific target area on the genome and silencing of the gene. This DSB might be repaired by either homology directed repair (HDR) or non-homologous end joining (NHEJ) systems. During the repairing of the gene via these two different types of systems, some indels might occur. Except triple insertion or deletions, other nucleotide changes cause frameshift mutations on the gene. Even though *Streptococcus pyogenes* (SpCas9) is the most used and studied one, there are more types of Cas proteins which are parts of immune metabolisms of archaea and bacteria. In order to function properly, those proteins require some specific short nucleotide sequences near the target area, which is called the protospacer adjacent motif (PAM) that may vary between different Cas proteins (10).

Table 1: The advantages and disadvantages of gene editing tools.

Gene Editing Techniques	Advantages	Disadvantages
Meganucleases	-its ability to recognize long stretches of 14-40 bp DNA increased previously the genome editing efficiency	-As each enzyme has a unique recognition sequence, the possibility of finding a right meganuclease to make a precious target was low. -Since the majority of induced DSBs are repaired through NHEJ, this mechanism may randomly insert or delete DNA pieces at the break site (100)
ZFNs	-increased targeted homologous recombination in model organisms and human cells.	-DNA recognition is specified by protein -Require tedious protein engineering of DNA-recognition domains for each target site
TALENs	-The recognition ability of one base instead of 3 bp of TALE proteins together with fusion of the Fok I DNA cleavage domain served it as an efficient gene editing tool.	-DNA recognition is specified by protein -Require tedious protein engineering of DNA-recognition domains for each target site
CRISPR/CAS9	-Ease of design, simplicity in use and highly efficient	-Off-target and unexpected mutations
	-Can be used not only for genome editing, but also transcriptional perturbation, epigenetic, modulation and genome imaging	

Newly discovered CasX protein has a great potential of human GE since it has a small size and the transformation of this protein to human cells is much easier than other Cas proteins. In addition to that, unlike some Cas9 proteins, CasX proteins are not found in bacteria which live in the human body and CasX proteins do not have any common ancestors with Cas9 proteins. Because of this reason, human immune systems are not capable of showing a strong response against CasX proteins (11). Similar to CasX, Cas14 also has a small size and does not require PAM sequence to generate single strand DNA break (12). Another Cas protein is Cas12a, also known as Cpf1, causes sticky DSB which makes easier the gene insertion into target loci (13).

Depending on the purpose, the Cas protein might be used single or as a fusion protein. For instance, Cas9 protein with an inactivated catalytic side (dCas9) is fused with cytidine deaminase to convert cytidines to uridines without causing any DSB on the target side (14). This method might be used for opposite change, uridines to cytidines with adenosine deaminase (15). CRISPR-Cas system is also utilized for generating epigenetic changes. There are three types of epigenetic changes generated by the CRISPR-Cas system: i) single or multiple gRNAs can manipulate dCas9 fused to a VP64 transcriptional activation domain to enhance the expression of endogenous human genes (16), ii) dCas9-KRAB fusions block the binding or progressing of DNA polymerase, resulting in repression of transcription (17), iii) targeted DNA methylation editing by using dCas9-TET1 catalytic domain fusions (18).

Since DNA editing causes permanent changes on the genome, off-target brings some huge risks for the future of the organism. This situation gives researchers a reason to use the CRISPR-Cas system on RNA editing to prevent these risks, as these types of changes stay at the transcriptional level. For RNA editing, researchers use two types of Cas proteins, Cas13a and Cas13b. Cas13a is used for mRNA degradation, on the other hand dCas13b-ADAR fusion is used for base editing on mRNA (19).

There are several methods for delivering components of the CRISPR-Cas system to an organism. These methods are classified as physical (electroporation) (20), viral (adenovirus, lentivirus, tobacco rattle virus) (21-23) and non-viral methods (lipid nano particles, agrobacterium) (24, 25). After delivery, for the screening of the changes on cell or organisms, several methods are used. Screening of large-scale mutation requires sequencing or determination of the DNA band size with electrophoresis (26). For screening of small-scale mutation T7 endonuclease assay or restriction enzyme assay might be used (27, 28).

As discussed before, CRISPR is a mechanism of bacterial immune system against phages. On the other hand, phages also developed inhibitor proteins against this bacterial mechanism. Those proteins are called anti-CRISPR proteins, which allow us the control application of CRISPR and make clinical trials safer (29).

RECENT APPLICATIONS

In order to use this technology as a gene therapy tool, CRISPR needs to be delivered to the right cells in the human body. There are two different applications: *in vivo* and *in vitro*. Genome editing via *cas-9 in vivo* has been used to correct alleles associated with genetic diseases in animal models. In order to lead to cataract-free progeny, *CRYGC* gene, causing dominant-negative cataract, mutated by injecting Cas9 mRNA into the zygote of the mouse heterozygote and a sgRNA targeting only in the mutant allele (30). Furthermore, in case of this technique was applied to a *mdx* mouse which had a mutation in the gene encoding dystrophin, phenotypic correction was observed between 2% to %100 percent when Cas9, sgRNA and donor template were injected into mouse zygotes (31). All of these studies showed promising advances in the treatment of genetic diseases.

Streptococcus pyogenes Cas9 (SpCas9) promises great potential for curing hereditary disorders including muscle dystrophy, HIV, vision disorders and many others. However, for all these applications to be possible, the dose and timing of SpCas9 activity should be adjusted to reduce the effects of off-targets. If SpCas9 activity can be controlled in these aspects; editing of DNA in model organisms can be successfully achieved. As an example, gene drives in genetically altered mosquitoes can prevent the spread of malaria and similar diseases transmitted by mosquitoes. The demand for the control of SpCas9 activity has raised a requirement for anti-CRISPR molecules. Although the anti-CRISPR proteins target SpCas9 are large and cannot pass through the cells, which can break down by proteases and cause the formation of an adverse immune reactions in the body. Whereas small molecule inhibitors are proteolytically stable and generally do not produce an immune response since they can diffuse through the cells. Future studies are needed to identify the mechanisms of action of the inhibitors on SpCas9: gRNA binding domains (32).

Although many studies have focused on the Cas9 protein so far; in recent years, the CRISPR-Cpf1 protein, also known as Cas12a, has been shown to be more effective than Cas9. As a matter of fact, companies like Mammoth Biosciences have already started using Cas12a technology. Patents containing the Cas12a-RNA complex are supported by the Berkeley and the Broad Institute. Recently CasX, which was originally discovered in Jennifer Doudna's laboratory in 2017, is much smaller than other Cas proteins and has the ability to shade both Cas9 and Cas12a. Since its sources are from bacteria that are not found in humans, the human immune system is more likely to accept it than Cas9 (32, 33). Differently, the newly developed Cas13-based SHERLOCK, which targets RNA, allows us to diagnose multiple diseases with one test and gives us a hundred times more sensitive results. Following the bonding of Cas13 with the viral genome, Cas13 starts to cut free specific RNAs, and these RNA cuttings trigger the formation of signals.

Currently, CRISPR gene-editing technology has been started to be used for human clinical trials: β -thalassemia [Vertex Pharmaceutical/CRISPR Therapeutics], Cancer (melanoma, sarcoma, myeloma) [U Penn/Parker Institute] and HIV [Affiliated Hospital to Academy of Military Medical Sciences]. The earlier studies led by Feng Zhang (MIT) and George Church (Harvard University) showed that the CRISPR system could be used to edit eukaryotic mammalian cells, including human cells. Later, a lot of researches were performed in this field. In November 2018 the Chinese researcher He Jiankui made the world's first genetically edited babies. He used CRISPR to mutate the gene called *CCR5*. Disabling this gene would prevent the HIV virus from entering and destroying Helper T cells. If everything had been gone as planned, children with an immune response to AIDS would have been born. However, it was shown that the growing CRISPR babies may face earlier deaths (average of 1.9 years) (34) a the genetic mutation that protects against HIV causes the babies to have a shorter life span.

Moreover, CRISPRi in which dCas9 is fused to a transcriptional repressor domain [Kruppel associated box (KRAB)] for repression of transcription and CRISPRa in which dCas9 is fused to a sequence (SunTag) containing multiple copies of the activator recruitment domain of the general control protein (GCN4) to activate transcription are also used to elucidate the non-coding genome (35-37). Genome editing by this method allows for efficient disorder of regulatory elements without causing DNA mutations. To sum up, dCas9-based methods enable to clarify the roles of regulatory sequences within the natural genomic structure and can elucidate long non-facilitating RNAs that can be altered by indels generated with Cas9 nucleases (38).

The chromatin structure modulates the genome. However, elucidation of the basis of this modification depends on a limited number of methods used to study chromatin-protein interactions. To identify proteins that interact with a specific genome locus; the chromatin may be precipitated with an antibody against a dCas9-tag fusion protein expressed together with gRNA targeting the desired DNA sequence, which is called 'engineered DNA-binding molecule-mediated chromatin immunoprecipitation' (enChIP). Later on, locus-associated proteins can be identified by mass spectrometry (39). enChIP is used in living cells for biochemical analysis of transcription and epigenetic regulation (40).

CRISPR-based tools can create a new guide RNA, enabling easier genome-wide screening. Many researchers have reported that screening with this method is more specific and more efficient than RNAi, and yields more robust and trustable results (41). In these experiments, sgRNA libraries and Cas9 cells are introduced into the cell, and selection of the treated cells was conducted according to those showing the targeted phenotypic result (42). Such screenings have been used to identify genes that are involved in cancer progression (43), drug resistance (44), immune response (45) susceptibility to bacterial toxins (46) and the emergence of other biomedically important phenotypes.

The ability to screen multiple loci in the human genome at the same time by performing a single experiment via Cas9 (47) enables the identification of complex cell signaling pathways, gene functions, drug targets for therapeutic purposes, and predicting drug side effects.

PLANT CRISPR EDITING

In plant biotechnology, CRISPR is used for both improving and gaining features on plants, such as yield and quality (48-52), herbicide tolerance (53, 54), biotic and abiotic tolerance (26, 55-57). Along with those, CRISPR is also used for functional genomic (58, 59) studies. High mutation frequency of CRISPR is especially important for creating homozygote mutant lines on polyploid plants such as wheat, potato and strawberry. In regards to potato, researchers established a single base change in the ALS gene of the tetraploid plants by using Cas9-Cytidine deaminase fusion, and made the plant resistant to the chlorsulfuron herbicide. This mutation prevents the acetolactate synthase enzyme from inhibition by chlorsulfuron binding (60). Furthermore, CRISPR has made it easy to target multiple genes in a single organism. For instance, researchers mutated different genes in cultivated tomatoes with a single CRISPR application to ensure recovery of stress tolerance since tomato has lost its tolerance to stress due to domestication for a long time. As a result, tomatoes with a bigger fruit size, number and nutritional value were obtained (61). In another study, the *Fad 2.1* gene, responsible for the conversion of oleic acid to less stable linoleic acid, was knocked-out by Calytx Inc. to increase the oleic acid content of the soybean and ultimately the shelf life of the soybean oil. This first commercial GE plant, which was developed for the first time with TALEN, was later achieved by the CRISPR technique (62).

BACTERIAL GENOME EDITING WITH CRISPR

Since there are other effective methods for genome editing in microorganisms such as HR; few studies have been reported on the development of CRISPR-Cas genome editing in various bacteria (i.e., *E. coli*, Cyanobacteria, *Streptomyces*, *Riemerella anatipestifer*, *Clostridium*, *Corynebacterium*, *Bacillus*, *Salmonella*, *Pseudomonas putida*, *Lactobacillus casei*) (63-72). Identification of strains (73), detection of natural or engineered immunity against mobile genetic elements (74, 75), manipulation of microbial consortium (76), and programmable transcriptional regulation (77) are some issues that have been tried to be solved using CRISPR. Moreover, patent studies in this field focused on the growth of microorganisms, preventing antibiotic resistance, biofuel production and enhanced synthesis of desired metabolites (78). The development of this method will enable efficient screening and selection of targeted mutations in microorganisms.

ETHICS AND SAFETY REGULATIONS

Since the first publication in 2012 (79) that reported CRISPR-Cas9 usage for genome editing; this method has been described by different names such as "revolutionary", a "groundbreaking" and

Table 2: Regulatory decisions of different countries for GE crops.

Countries	Regulation Decisions	References
Australia	Most genome editing techniques will be explicitly regulated. But the technique known as SDN-1 [generation of small deletions or insertions (indels) at a precisely defined location] will be excluded* / WTO Statement	92; 93
Argentina, Brazil, Canada, Chile, Colombia, USA	Non-transgenic GE crops are not GMO / WTO Statement	94; 93
Dominican Republic, Guatemala, Honduras, Jordan, Paraguay, Uruguay, Vietnam, Economic Community of West African States (ECOWAS)	WTO Statement	93
Japan	There is little difference between traditional breeding methods and gene editing in terms of safety (Japan Governmental Advisory Committee)	96
Russia	GE technologies as equivalent to conventional breeding methods.	95
The European Court of Justice (ECJ)	Using recombinant nucleases cause GMO	97
Belgium, Sweden, UK	Calling to update EU GMO laws / Gave permission for field trials before ECJ ruling	99; 98
Cyprus, Estonia, Finland, France, Germany, Greece, Netherlands, Italy, Portugal, Slovenia, Spain	Calling to update EU GMO laws	99

*WTO: World Trade Organization

“game changer”, since it provided the opportunity of crossing species boundaries. Naturally, this facility seemed to be very promising at first glance for many researchers.

Clinical trials using CRISPR system for efficient genome editing of various mammalian cells have already started and give promise to the treatment of some major diseases (80-83). In fact, these clinical applications also highlighted the presence of certain risks. Ihry et al. (84) revealed that DSBs generated by Cas9 could be toxic, and it created an obstacle for high genome-editing efficiency of CRISPR/Cas9 in human pluripotent stem cells. This study implied that using CRISPR in human cell lines increased the risk of cancer. Moreover, unexpected mutations resulting from CRISPR editing are another issue that needs improvement (85). Since these mutations can cause various genetic disorders or cancer, some social and ethical doubts about this genome engineering tool have appeared. Editing the unborn child to have the desired eyes or hair color (86), building an army with genetically edited soldiers (87) could be a few of the future applications of this unlimited technology. Despite all these possible risks and ethical considerations, the US and China are the countries that have allowed researchers to apply CRISPR editing on human CAR-T cells (88, 89). In addition to that, as it stated above, an illegal experiment was reported in China to make HIV resistant babies (90). However, it was later showed that HIV-resistant babies with CCR5 mutations were also sensitive to dangerous flu and West Nile Virus (91). All those present studies

suggest that even though CRISPR is a very powerful technique, it is not always the first option in curing diseases.

Likewise, all these ethical and social aspects should also be discussed for gene-editing applications in agriculture. Since CRISPR provides gene editing without any DNA integration, in many countries, engineered plants using this technique have been accepted as a non-transgenic product that is allowed to enter the market freely without the need for regulation (92-97). Only the European Union decided that edited crops should be considered as GMOs (Table 2). However, in some European countries, field trials of altered plants using this approach are still ongoing. It is also expected that after “Brexit” the UK might remove the regulations for CRISPR-edited crops. Recently, 14 European Union (EU) countries have already made a call for updating the laws of GMOs according to New Plant Breeding Technologies (98,99).

CONCLUSIONS

Although CRISPR-Cas system offers tremendous opportunities for clinical and biotechnological applications, it might cause some unexpected results which reveals that the technique needs to be improved and further tested. Besides, ethical issues and regulatory aspects should also be discussed in scientific consortia to have a common decision on GE applications prior to large-scale clinical and field applications.

Peer-review: Externally peer-reviewed.

Author Contributions: Conception/Design of study: Y.A.C., Ö.A., N.C.; Data Acquisition: Y.A.C., Ö.A., N.C., A.B.Y.; Data Analysis/Interpretation: Y.A.C., Ö.A., N.C.; Final Approval and Accountability: Y.A.C., Ö.A., N.C., A.B.Y.; Drafting Manuscript: Y.A.C., Ö.A., N.C., A.B.Y.; Critical Revision of Manuscript: Y.A.C., Ö.A., N.C.; Supervision: Y.A.C.

Conflict of Interest: The authors declare that they have no conflicts of interest.

Financial Disclosure: There are no funders to report for this submission

REFERENCES

- Adli M. The CRISPR tool kit for genome editing and beyond. *Nat Commun* 2018; 9(1): 1911.
- Capecchi MR. Altering the genome by homologous recombination. *Sci* 1989; 244(4910): 1288-92.
- Lin FL, Sperle K, Sternberg N. Recombination in mouse L cells between DNA introduced into cells and homologous chromosomal sequences. *Proc Natl Acad Sci USA* 1985; 82: 1391-95.
- Klug A, Rhodes D. 'Zinc fingers': a novel protein motif for nucleic acid recognition. *Trends Biochem Sci* 1987; 12: 464-69.
- Kim YG, Cha J, Chandrasegaran S. Hybrid restriction enzymes: zinc finger fusions to Fok I cleavage domain. *PNAS* 1996; 93(3): 1156-60.
- Urnov FD, Miller JC, Lee YL, Beausejour CM, Rock JM, Augustus S, et al. Highly efficient endogenous human gene correction using designed zinc-finger nucleases. *Nature* 2005; 435(7042): 646.
- Christian M, Cermak T, Doyle EL, Schmidt C, Zhang F, Hummel A, Targeting DNA double-strand breaks with TAL effector nucleases. *Genetics* 2010; 186(2): 757-761.
- Doudna JA, Charpentier E, The new frontier of genome engineering with CRISPR-Cas9. *Sci* 2014; 346(6213): 1258096.
- Hsu PD, Lander ES, Zhang F. Development and applications of CRISPR-Cas9 for genome engineering. *Cell* 2014; 157(6), 1262-78.
- Leenay RT, Maksimchuk KR, Slotkowski RA, Agrawal RN, Gomaa AA, Briner AE, Barrangou R, Beisel CL. Identifying and visualizing functional PAM diversity across CRISPR-Cas systems. *Mol Cell* 2016, 62(1): 137-47.
- Liu JJ, Orlova N, Oakes BL, Ma E, Spinner HB, Baney KL, Al-Shayeb B. CasX enzymes comprise a distinct family of RNA-guided genome editors. *Nature* 2019; 566(7743): 218.
- Harrington LB, Burstein D, Chen JS, Paez-Espino D, Ma E, Witte IP, Doudna JA. Programmed DNA destruction by miniature CRISPR-Cas14 enzymes. *Sci* 2018; 362(6416): 839-42.
- Li SY, Cheng QX, Liu JK, Nie XQ, Zhao GP, Wang J. CRISPR-Cas12a has both cis- and trans-cleavage activities on single-stranded DNA. *Cell Res* 2018; 28(4): 491.
- Komor AC, Kim YB, Packer MS, Zuris JA, Liu DR. Programmable editing of a target base in genomic DNA without doublestranded DNA cleavage. *Nature* 2016; 533:420-24.
- Gaudelli NM, Komor AC, Rees HA, Packer MS, Badran AH, Bryson DI, Liu DR. Programmable base editing of A*T to G*C in genomic DNA without DNA cleavage. *Nature* 2017; 551:464-71.
- Maeder ML, Linder SJ, Cascio VM, Fu Y, Ho QH, Joung JK. CRISPR RNA-guided activation of endogenous human genes. *Nat Methods* 2013; 10(10): 977.
- Gilbert LA, Larson MH, Morsut L, Liu Z, Brar GA, Torres SE, Lim WA. CRISPR-mediated modular RNA-guided regulation of transcription in eukaryotes. *Cell* 2013; 154(2): 442-51.
- McDonald JI, Celik H, Rois LE, Fishberger G, Fowler T, Rees R, Challen GA. Reprogrammable CRISPR/Cas9-based system for inducing site-specific DNA methylation. *Biol Open* 2016; 5(6): 866-74.
- Cox DB, Gootenberg JS, Abudayyeh OO, Franklin B, Kellner MJ, Joung J, Zhang F. RNA editing with CRISPR-Cas13. *Sci* 2017; 358(6366), 2017; 1019-27.
- Chen S, Lee B, Lee AYF, Modzelewski AJ, He L. Highly efficient mouse genome editing by CRISPR ribonucleoprotein electroporation of zygotes. *J Biol Chem* 2016; 291(28): 14457-67.
- Fakhiri J, Nickl M, Grimm D. Rapid and Simple Screening of CRISPR Guide RNAs (gRNAs) in Cultured Cells Using Adeno-Associated Viral (AAV) Vectors. In *CRISPR Gene Editing, 2019*; (pp. 111-126). Humana Press, New York, NY.
- Malcolm T, Khalili K. U.S. Patent Application, 2018; No. 15/873,483.
- Ali Z, Abul-Faraj A, Li L, Ghosh N, Piatek M, Mahjoub A, Dinesh-Kumar S. Efficient virus-mediated genome editing in plants using the CRISPR/Cas9 system. *Mol Plant* 2015; 8(8): 1288-91.
- Li L, Hu S, Chen X. Non-viral delivery systems for CRISPR/Cas9-based genome editing: Challenges and opportunities. *Biomaterials* 2018; 171: 207-18.
- Veillet F, Perrot L, Chauvin L, Kermarrec MP, Guyon-Debast A, Chauvin JE, Mazier M. Transgene-Free Genome Editing in Tomato and Potato Plants Using Agrobacterium-Mediated Delivery of a CRISPR/Cas9 Cytidine Base Editor. *Int J Mo. Sci* 2019; 20(2): 402.
- Nekrasov V, Wang C, Win J, Lanz C, Weigel D, Kamoun S. Rapid generation of a transgene-free powdery mildew resistant tomato by genome deletion. *Sci Rep* 2017; 7(1): 482.
- Woo JW, Kim J, Kwon SI, Corvalán C, Cho SW, Kim H, Kim JS. DNA-free genome editing in plants with preassembled CRISPR-Cas9 ribonucleoproteins. *Nat Biotechnol* 2015; 33(11): 1162.
- Liang Z, Zhang K, Chen K, Gao C. Targeted mutagenesis in Zea mays using TALENs and the CRISPR/Cas system. *J Genet Genomics* 2014; 41(2): 63-68.
- Bondy-Denomy J, Garcia B, Strum S, Du M, Rollins MF, Hidalgo-Reyes Y, Davidson AR, Multiple mechanisms for CRISPR-Cas inhibition by anti-CRISPR proteins. *Nature* 2015; 526(7571): 136.
- Wu Y, Liang D, Wang Y, Bai M, Tang W, Bao S, Yan Z, Li D, Li J. Correction of a Genetic Disease in Mouse via Use of CRISPR-Cas9. *Cell Stem Cell* 2013; 13:659-62.
- Long C, McAnally JR, Shelton JM, Mireault AA, Bassel-Duby R, Olson EN. Prevention of muscular dystrophy in mice by CRISPR-Cas9-mediated editing of germline DNA. *Sci* 2014; 345:1184-88.
- Maji B, Gangopadhyay SA, Lee M, Shi M, Wu P, Heler R, Mok B, Lim D, Siriwardena SU, Paul B, Dančik V. A high-throughput platform to identify small-molecule inhibitors of CRISPR-Cas9. *Cell* 2019; 177(4): 1067-79.
- Liu JJ, Orlova N, Oakes BL, Ma E, Spinner HB, Baney KL, Chuck J, Tan D, Knott GJ, Harrington LB, Al-Shayeb B. CasX enzymes comprise a distinct family of RNA-guided genome editors. *Nature* 2019; 566(7743): 218.
- Technology Review, 2019, <http://www.technologyreview.com>. Last accessed June 3, 2019.
- Thakore PI, Black JB, Hilton IB, Gersbach CA. Editing the epigenome: technologies for programmable transcription and epigenetic modulation. *Nat Methods* 2016; 13: 127-37.
- Klann TS. CRISPR-Cas9 epigenome editing enables high-throughput screening for functional regulatory elements in the human genome. *Nat Biotechnol* 2017; 35: 561-68.

37. Simeonov DR. Discovery of stimulation-responsive immune enhancers with CRISPR activation. *Nature* 2017; 549:111-5.
38. Liu SJ, CRISPRi-based genome-scale identification of functional long noncoding RNA loci in human cells. *Sci* 2017; aah7111.
39. Fujita T, Fujii H. Efficient isolation of specific genomic regions and identification of associated proteins by engineered DNA-binding molecule-mediated chromatin immunoprecipitation (enChIP) using CRISPR. *Biochem Biophys Res Commun* 2013; 439: 132–36.
40. Fujita T, Fujii H. Identification of proteins associated with an IFN γ -responsive promoter by a retroviral expression system for enChIP using CRISPR. *PLOS ONE* 9 2014; e103084.
41. Sanjana NE. Genome-scale CRISPR pooled screens. *Anal Biochem* 2017; 532: 95-99.
42. Shalem O, Sanjana NE, Zhang F. High-throughput functional genomics using CRISPR-Cas9. *Nat Rev Genet* 2015;16: 299–311.
43. Shi J, Wang E, Milazzo JP, Wang Z, Kinney JB, Vakoc CR. Discovery of cancer drug targets by CRISPR-Cas9 screening of protein domains. *Nat Biotech* 2015;33: 661–67.
44. Chen Y, Zhang Y. Application of the CRISPR/Cas9 system to drug resistance in breast cancer. *Adv Sci* 2018; 5:1700964.
45. Parnas O, Jovanovic M, Eisenhaure Thomas M, Herbst Rebecca H, Dixit A, Ye Chun J, Przybylski D, Platt Randall J, Tirosch I, Sanjana Neville E, et al. A genome-wide crispr screen in primary immune cells to dissect regulatory networks. *Cell* 2015;162:675–86.
46. Zhou Y, Zhu S, Cai C, Yuan P, Li C, Huang Y, Wei W. High-throughput screening of a CRISPR-Cas9 library for functional genomics in human cells. *Nature* 2014;509:487–91.
47. Kiani S, Chavez A, Tuttle M, Hall RN, Chari R, Ter-Ovanesyan D, Qian J, Pruitt BW, Beal J, Vora S, et al. Cas9 gRNA engineering for genome editing, activation and repression. *Nat Methods* 2015;12:1051–54.
48. Sun Y, Jiao G, Liu Z, Zhang X, Li J, Guo X, Xia L. Generation of high-amylose rice through CRISPR/Cas9-mediated targeted mutagenesis of starch branching enzymes. *Front Plant Sci* 2017; 8: 298.
49. Rodríguez-Leal D, Lemmon ZH, Man J, Bartlett ME, Lippman ZB. Engineering quantitative trait variation for crop improvement by genome editing. *Cell* 2017; 171(2): 470-80.
50. Soyk S, Müller NA, Park SJ, Schmalenbach I, Jiang K, Hayama R, Lippman ZB. Variation in the flowering gene SELF PRUNING 5G promotes day-neutrality and early yield in tomato. *Nat Genet* 2017; 49(1): 162.
51. Hu B, Li D, Liu X, Qi J, Gao D, Zhao S, Yang L. Engineering non-transgenic gynoecious cucumber using an improved transformation protocol and optimized CRISPR/Cas9 system. *Mol Plant* 2017; 10(12): 1575-78.
52. Okuzaki A, Ogawa T, Koizuka C, Kaneko K, Inaba M, Imamura J, Koizuka N. CRISPR/Cas9-mediated genome editing of the fatty acid desaturase 2 gene in *Brassica napus*. *Plant Physiol Biochem* 2018; 131: 63-69.
53. Li J, Meng X, Zong Y, Chen K, Zhang H, Liu J, Gao C. Gene replacements and insertions in rice by intron targeting using CRISPR–Cas9. *Nat Plants* 2016; 2(10): 16139.
54. Shimatani Z, Ariizumi T, Fujikura U, Kondo A, Ezura H, Nishida K. Targeted base editing with crispr-deaminase in tomato. In *plant genome editing with crispr systems*. Humana Press, New York 2019; 297-307.
55. Peng A, Chen S, Lei T, Xu L, He Y, Wu L, Yao L, Zou X. Engineering canker-resistant plants through CRISPR/Cas9-targeted editing of the susceptibility gene Cs LOB 1 promoter in citrus. *Plant Biotechnol J* 2017; 15(12): 1509-19.
56. Zhang A, Liu Y, Wang F, Li T, Chen Z, Kong D, Bi J, Zhang F, Luo X, Wang J, Tang J, Yu X, Liu G, Luo L. Enhanced rice salinity tolerance via CRISPR/Cas9-targeted mutagenesis of the OsRR22 gene. *Mol Breeding* 2019; 39(3): 47.
57. Paixão JFR, Gillet FX, Ribeiro TP, Bournaud C, Lourenço-Tessutti IT, Noriega DD, Grossi-de-Sa MF. Improved drought stress tolerance in Arabidopsis by CRISPR/dCas9 fusion with a Histone Acetyltransferase. *Sci Rep* 2019; 9(1): 8080.
58. McGill M. Plant Genome Editing Using CRISPR/Cas9: Investigating the role of ten1 in the maintenance and protection of telomeres in Arabidopsis thaliana 2019; Celebrating Scholarship and Creativity Day. 60.
59. Zhao P, You Q, Lei MA. CRISPR/Cas9 deletion into the phosphate transporter SIPHO1; 1 reveals its role in phosphate nutrition of tomato seedlings. *Physiol Plant* 2018.
60. Veillet F, Perrot L, Chauvin L, Kermarrec MP, Guyon-Debast A, Chauvin JE, Mazier M. Transgene-free genome editing in tomato and potato plants using agrobacterium-mediated delivery of a CRISPR/Cas9 cytidine base editor. *Int J Mol Sci* 2019; 20(2): 402.
61. Zsögön A, Čermák T, Naves ER, Notini MM, Edel KH, Weinl S, Peres LEP. De novo domestication of wild tomato using genome editing. *Nature Biotechnol* 2018; 36: 1211–16.
62. Calyxt, First commercial sale of calyxt high oleic soybean oil on the U.S. market, Press Release, 2019.
63. Jiang Y, Chen B, Duan C, Sun B, Yang J, Yang S. Multigene editing in the *Escherichia coli* genome via the CRISPR-Cas9 system. *Appl Environ Microbiol* 2015; 81(7): 2506-14.
64. Wang Y, Zhang ZT, Seo SO, Lynn P, Lu T, Jin YS, Blaschek HP. Gene transcription repression in *Clostridium beijerinckii* using CRISPR-dCas9. *Biotechnol Bioeng* 2016 113(12): 2739-43.
65. Zhu DK, Yang XQ, He Y, Zhou WS, Song XH, Wang JB, Zhang Y, Liu MF, Wang MS, Jia RY, Chen S, Sun KF, Yang Q, Wu Y, Chen XY, Cheng AC. Comparative genomic analysis identifies structural features of CRISPR-Cas systems in *Riemerella anatipestifer*. *BMC genomics* 2016; 17(1): 689.
66. Song X, Huang H, Xiong Z, Ai L, Yang S. CRISPR-Cas9D10A nickase-assisted genome editing in *Lactobacillus casei*. *Appl Environ Microbiol* 2017 83(22): e01259-17.
67. Aparicio T, de Lorenzo V, Martínez-García E. CRISPR/Cas9-based counter selection boosts recombinering efficiency in *Pseudomonas putida*. *Biotechnol J* 2018; 13(5): 1700161.
68. Medina-Aparicio L, Dávila S, Rebollar-Flores JE, Calva E, Hernández-Lucas I. The CRISPR-Cas system in Enterobacteriaceae. *Pathogens and disease* 2018; 76(1): fty002.
69. Li K, Cai D, Wang Z, He Z, Chen S. Development of an efficient genome editing tool in *Bacillus licheniformis* using CRISPR-Cas9 nickase. *Appl Environ Microbiol* 2018; 84(6): e02608-17.
70. Xiao Y, Wang S, Rommelfanger S, Balassy A, Barba-Ostria C, Gu P, Galazka JM, Zhang F. Developing a Cas9-based tool to engineer native plasmids in *Synechocystis* sp. PCC 6803. *Biotechnol Bioeng* 2018; 115(9): 2305-14.
71. Li L, Wei K, Zheng G, Liu X, Chen S, Jiang W, Lu Y. CRISPR-Cpf1-assisted multiplex genome editing and transcriptional repression in *Streptomyces*. *Appl Environ Microbiol* 2018 84(18): e00827-18.
72. Wang Y, Liu Y, Liu J, Guo Y, Fan L, Ni X, Zhang X, Wang M, Zheng P, Sun J, Ma Y. MACBETH: multiplex automated Corynebacterium glutamicum base editing method. *Metab Eng* 2018; 47:200-10.
73. Shariat N. The combination of CRISPR–MVLST and PFGE provides increased discriminatory power for differentiating human clinical isolates of *Salmonella enterica* subsp. *enterica* serovar *Enteritidis*. *Food Microbiol* 2013; 34: 164–73.
74. Barrangou R. Genomic impact of CRISPR immunization against bacteriophages. *Biochem Soc Trans* 2013; 41: 1383–91.
75. Barrangou R, Horvath P. CRISPR: new horizons in phage resistance and strain identification. *Annu Rev Food Sci Technol* 2013; 3: 143–62.

76. Gomaa AA. Programmable removal of bacterial strains by use of genome-targeting CRISPR-Cas systems. *MBio* 2014; 5: e00928–e1013.
77. Bondy-Denomy J, and Davidson AR. To acquire or resist: the complex biological effects of CRISPR-Cas systems. *Trends Microbiol* 2014; 22: 218–25.
78. Martin-Laffon J, Kuntz M, Ricroch AE, inventors. Worldwide CRISPR patent landscape shows strong geographical biases. *Nat Biotechnol* 2019; 37(6):613-20.
79. Jinek M, Chylinski K, Fonfara I, Hauer M, Doudna JA, Charpentier E. A programmable dual-RNA-guided DNA endonuclease in adaptive bacterial immunity. *Sci* 2012; 337(6096): 816-21.
80. Swiech L, Heidenreich M, Banerjee A, Habib N, Li Y, Trombetta J, Zhang, F. In vivo interrogation of gene function in the mammalian brain using CRISPR-Cas9. *Nature Biotechnol* 2015; 33(1): 102.
81. Jacobi AM, Rettig GR, Turk R, Collingwood MA, Zeiner SA, Quadros RM, Gurumurthy CB. Simplified CRISPR tools for efficient genome editing and streamlined protocols for their delivery into mammalian cells and mouse zygotes. *Methods* 2017; 121: 16-28.
82. Amoasii L, Hildyard JC, Li H, Sanchez-Ortiz E, Mireault A, Caballero D, Bassel-Duby R. Gene editing restores dystrophin expression in a canine model of Duchenne muscular dystrophy. *Sci* 2018; 362(6410): 86-91.
83. Santiago-Fernández O, Osorio FG, Quesada V, Rodríguez F, Basso S, Maeso D, Freije JM. Development of a CRISPR/Cas9-based therapy for Hutchinson–Gilford progeria syndrome. *Nat Med* 2019; 1.
84. Ihry RJ, Worringer KA, Salick MR, Frias E, Ho D, Theriault K, Randhawa R. p53 inhibits CRISPR-Cas9 engineering in human pluripotent stem cells. *Nat Med* 2018; 24(7): 939.
85. Schaefer KA, Wu WH, Colgan DF, Tsang SH, Bassuk AG, Mahajan VB. Unexpected mutations after CRISPR-Cas9 editing in vivo. *Nat Met* 2017; 14(6): 547.
86. Beaumont KA, Shekar SN, Cook AL, Duffy DL, Sturm RA. Red hair is the null phenotype of MC1R. *Hum Mutat* 2008; 29(8): E88-E94.
87. Deng S, Kongpan LI, Wang F, Ning LI, Liu G, Zhao Y, Lian Z. One-step generation of myostatin gene knockout sheep via the CRISPR/Cas9 system 2014; 1: 2-5.
88. Lu Y, Xue J, Deng T, Zhou X, Yu K, Huang M, Gong Y. A phase I trial of PD-1 deficient engineered T cells with CRISPR/Cas9 in patients with advanced non-small cell lung cancer. 2018.
89. June CH, O'Connor RS, Kawalekar OU, Ghassemi S, Milone MC. CAR T cell immunotherapy for human cancer. *Sci* 2018; 359(6382): 1361-65.
90. Normile D. Shock greets claim of CRISPR-edited babies 2018.
91. Wei X, Nielsen R. CCR5-Δ 32 is deleterious in the homozygous state in humans. *Nat Med* 2019; 1.
92. OGTR, Office of the Gene Technology Regulator, Questions & answers on the technical review of the gene technology regulations 2001 (10 April 2019).
93. World Trade Organization (WTO) Committee on Sanitary and Phytosanitary Measures, International Statement on Agricultural Applications of Precision Biotechnology (Oct. 30, 2018).
94. Eriksson D, Kershen D, Nepomuceno A, Pogson BJ, Prieto H, Purnhagen K, Whelan A. A comparison of the EU regulatory approach to directed mutagenesis with that of other jurisdictions, consequences for international trade and potential steps forward. *New Phytol* 2019; 222(4): 1673-84.
95. Dobrovidova O. Russia joins in global gene-editing bonanza. *Nature* 2018; 569(7756): 319.
96. NHK World–Japan. 2018.Govt. Panel to not regulate some genome editing. [WWW document] URL https://www3.nhk.or.jp/nhkworld/en/news/20180821_14/ [accessed 21 August 2018].
97. Callaway E. CRISPR plants now subject to tough GM laws in European Union 2018; *Nature* 560(7716):16.
98. Kupferschmidt K. EU verdict on CRISPR crops dismays scientists 2018.
99. Euractive. The EU future of new plant breeding techniques, Special Report May 2019 <http://eurac.tv/9qiu>
100. Jeggo PA. Identification of genes involved in repair of DNA doublestrand breaks in mammalian cells. *Radiat Res* 1998; 150(5s): S80-S91.

The Effect of Body Shape Type on Differentiability of Traditional and Geometric Morphometric Methods: A Case Study of *Channa gachua* (Hamilton, 1822)

Atta Mouludi-Saleh¹ , Soheil Eagderi¹ , Hadi Poorbagher¹ ,
Shirin Kazemzadeh¹ 

¹University of Tehran, Faculty of Natural Resources, Department of Fisheries, Karaj, Iran

ORCID IDs of the authors: A.M.S. 0000-0002-0939-0901; S.E. 0000-0001-8649-9452; H.P. 0000-0003-0546-8713; S.K. 0000-0003-0253-4148

Please cite this article as: Mouludi Saleh A, Eagderi S, Poorbagher H, Kazemzadeh S. The Effect of Body Shape Type on Differentiability of Traditional and Geometric Morphometric Methods: A Case Study of *Channa gachua* (Hamilton, 1822). Eur J Biol 2019; 78(2): 161-164. DOI: 10.26650/EurJBiol.2019.0011

ABSTRACT

Objective: The morphological differences of two populations of the Dwarf snakehead, *Channa gachua* (Hamilton, 1822) from Sarbaz (Makran basin) and Halil (Hamun-e Jaz Murian basin) rivers were studied using geometric and traditional morphometrics (GM and TM) methods to test the hypothesis that the type of body shape can produce different results.

Materials and Methods: A total of 16 landmark-points and 12 distance measurements were defined to analyse the body shape differences and the extracted data were analyzed using GM and TM methods.

Results: Our findings reject the hypothesis, and the results revealed that GM is more effective in detecting meticulous morphological differences.

Conclusion: In addition, the results suggest selecting a proper method i.e. GM or TM, based on the degree of accuracy needed i.e. if we need to find small shape differences within its signification, GM is a superior technique, or to show the type of differences, then we can use TM.

Keywords: Freshwater Fish, Morphology, Phenotypic Plasticity, Generalized Procrustes Analysis

INTRODUCTION

Comparative studies on the body shape in fishes are commonly used to understand many aspects such as resource management, evolution, behaviour, ecology and phenotype plasticity (1-6). In many works, which have investigated the morphological variation of the biological structures using traditional (TM) (7-9) and geometric morphometric (GM) (10-17) techniques, it has been suggested that GM is more effective to detect morphological disparities (4, 8). Additionally, it has been shown that both methods can lead to similar (12) or different results (9).

It bring to us this hypothesis that such differences may be related to the body shape type of the studied organisms. For instance, if a fish's body shape is simple, then we can expect similar results of both TM and GM methods; and if the body shape is complex, then we can expect a different result. Therefore, this study was conducted to compare the body shape of the dwarf snakehead, *Channa gachua*, using TM and GM methods.

Channa gachua is a species with large head scales and elongate dorsal and anal fins, and with the ability to breathe from air inhabiting tropical and sub-tropical water bodies (18). It is a fish species with a bottom rover



Corresponding Author: Soheil Eagderi E-mail: soheil.eagderi@ut.ac.ir

Submitted: 29.05.2019 • **Revision Requested:** 24.07.2019 • **Last Revision Received:** 20.08.2019 • **Accepted:** 04.09.2019

© Copyright 2019 by The Istanbul University Faculty of Science • Available online at <http://ejb.istanbul.edu.tr> • DOI: 10.26650/EurJBiol.2019.0011

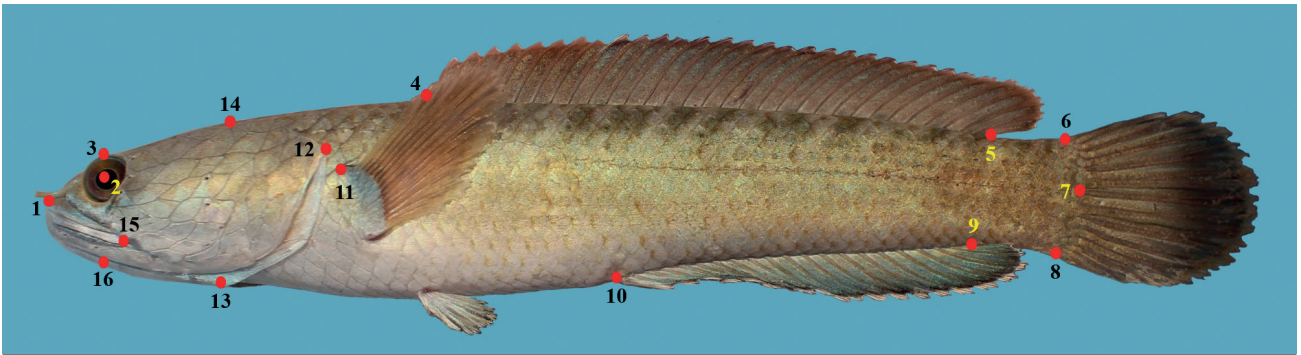


Figure 1. Defined landmark-points to extract the body shape data of *Channa gachua*. (1) anterior-most point of the snout tip on the upper jaw, (2) center of the eye, (3) dorsal edge of the head perpendicular to the center of eye, (4) origin and (5) insertion point of the dorsal-fin base, (6) postero-dorsal end of the caudal peduncle at its connection to the caudal fin, (7) posterior end of the medial region of the caudal peduncle, (8) postero-ventral end of the caudal peduncle at its connection to the caudal fin, (9) insertion and (10) origin point of the anal-fin base, (11) most anterior point of the pectoral fin, (12) posterior edge of the opercle, (13) ventral end of the gill slit, (14) the line extends perpendicularly to the most basic part of the gill slit above the head, (15) The terminus of the oral clefts in the upper jaw and (16) ventral edge of the head perpendicular to the center of eye.

body shape pattern i.e. a simple body shape that expects the same results of both TM and GM methods. The biggest population of this species in the western Asia, is found in the Makran, Mashkid and Hamun-e Jaz Murian basins of Iran (18).

MATERIALS AND METHODS

In total, 40 specimens of *C. gachua* representing two different populations were collected from the Halil (n= 17, 28°40'29.43"N, 57°42'22.96"E, Hamun-e Jaz Murian basin) and Sarbaz (n= 23, 26°37'47"N, 61°15'31"E, Makran basin) rivers using an electrofishing device (Samus MP750). After anesthesia, the left sides of the fresh collected specimens were photographed using a copy-stand equipped with a digital camera (Kodak EasyShare Z650 with a 6 MP resolution) with fins erected by insect pins. Then, the sampled specimens were fixed in the buffered formalin and transferred to a laboratory.

For the GM method, a total of 16 homologous landmark-points were digitized using tpsDig2 software (version 2.16) (Figure 1) on 2D pictures. A Generalized Procrustes analysis (GPA) was used to remove non-shape data, including size, position and direction. The resulting data were analyzed using discriminant function analysis (DFA) and Hotelling's T-test to investigate the morphological distinction between the populations. Morphological disparities between the populations were visualized using deformation grids in MorphoJ software.

For the TM method, 12 distance measurements, including SL (standard length), SnL (snout length), ED (eye horizontal diameter), HL (head length), HW (maximum head width), HDO (head depth at posterior edge of the opercle), HDE (head depth at middle of the eye), BD (body depth at dorsal-fin origin), DFL (dorsal-fin length), AFL (anal-fin length) and CPL (caudal peduncle length) were taken using dial calipers to the nearest 0.1 mm. To remove the size from data, they were standardized using the Beacham formula as following (19):

$$M_{(t)} = M_{(0)} \left(\frac{L}{L_{(0)}} \right)^b$$

Where $M_{(t)}$ is standardized values of characters, $M_{(0)}$ = characters of the observed length L = standard length mean of all samples, $L_{(0)}$ = a standard length of each sample and b = regression coefficient between $\log L_{(0)}$ and $\log M_{(0)}$.

Analyses for GM method were performed using PAST and MorphoJ (version 1.01) softwares. Levin's test and DFA/ Hotelling's T-test in TM method were performed in SPSS V.19 and PAST software, respectively.

RESULTS AND DISCUSSION

Geometric Method

DFA and Hotelling's T-test showed that the two populations can be significantly differentiated in terms of the body shape ($P > 0.0001$) (Figure 2). The wireframe of the body shape showed differences in position of the snout and caudal peduncle length. In the Halil River population, the body was deeper and the eyes

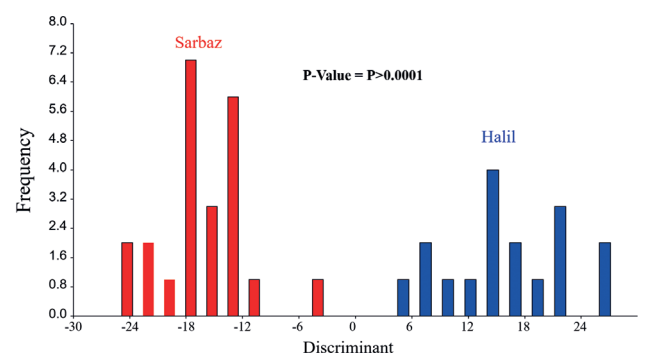


Figure 2. Discriminant function analysis of *Channa gachua* populations from the Halil and Sarbaz rivers in GM method.

Table 1. Levin’s test and mean (\pm standard deviation) of each morphological character measured in *Channa gachua* from Sarbaz and Halil rivers populations (All measurements are shown in mm. Variables for which significant differences were obtained are highlighted in bold).

Characters	Sarbaz River (mean \pm SD)	Halil River (mean \pm SD)	F	P-value
SL	98.48 \pm 0.00	98.48 \pm 0.00		-
SnL	4.28 \pm 0.94	4.48 \pm 1.19	7.37	0.01
ED	4.4 \pm 0.43	4.29 \pm 0.98	12.92	0.001
HL	29.98 \pm 2.03	30.1 \pm 2.47	2.86	0.98
HW	21.09 \pm 0.83	20.96 \pm 0.99	1.61	0.212
HDO	19.14 \pm 1.02	18.93 \pm 1.1	0.401	0.53
HDE	10.05 \pm 0.84	10.12 \pm 0.91	1.31	0.294
BH	19.81 \pm 1.27	19.49 \pm 1.20	0.085	0.772
DFL	53.12 \pm 1.38	53.04 \pm 1.3	0.074	0.788
AFL	33.81 \pm 1.79	33.24 \pm 1.19	1.93	0.177
CPL	8.5 \pm 0.90	8.3 \pm 0.87	0.029	0.885

AFL = anal-fin length, BD = body depth at dorsal-fin origin, CPL = caudal peduncle length, DFL = dorsal-fin length, ED = eye horizontal diameter, HDE = head depth at middle of the eye, HDO = head depth at posterior edge of the opercle, HL = head length, HW = maximum head width, SnL = snout length, and SL = standard length.

and snout had a more ventral position than those of the Sarbaz River one (Figure 3).

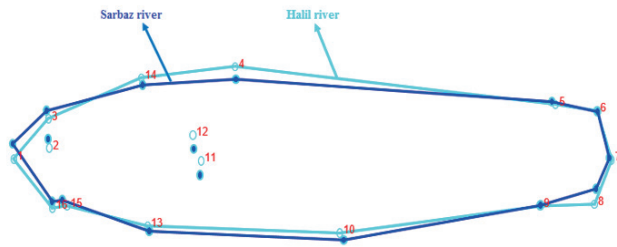


Figure 3. Wireframe diagram consensus body shape graph of *Channa gachua* populations from the Halil and Sarbaz rivers in GM method.

Traditional Method

The results showed normality of the data. Levene’s test showed significant differences in the snout length and eye diameter (Table 1) ($P < 0.05$). DFA/Hotelling’s T-test showed no significant difference between the two studied populations ($P = 0.975$, $F = 0.334$, Hotelling’s $t^2 = 5.64$) (Figure 4).

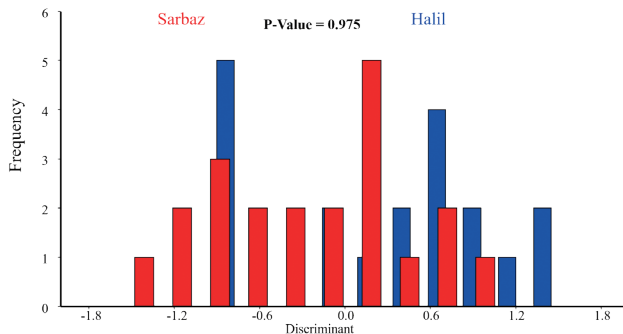


Figure 4. Discriminant function analysis of *Channa gachua* populations from the Halil and Sarbaz rivers in TM method.

Morphological variations in fishes are considered to be an important adaptive strategy for populations experiencing inconsistent environments such as rivers (20). In addition, fishes show a variety of body form associated with functions such as swimming and feeding to overcome different habitats and lifestyles (10, 21). The body shape can even display the lifestyles of a fish. Therefore, based on the diversity of the habitat features or lifestyles, the degree of a biological structure can show a higher plasticity (22), e.g. those fishes with a generalized body shape, are fusiform with a pointed head and forked tail. Therefore, fusiform body designs have a lot of variations in different parts of their body shape.

In the present study, the multivariate analysis did not show a significant difference in TM. However in TM, comparing each morphometric data revealed differences in SnL and ED similar to the results of the GM method. Our findings reject the hypothesis that differences may be related to the body shape type using GM or TM.

However, it is suggested to select a proper method viz GM or TM, prior to the analysis of the data based on the aim of the study and particularly degree of accuracy needed i.e. if we need to find small shape differences within its signification, then we can apply GM, or if our aim is to find traits which show differences, then we can use TM as well. Both methods reveal real differences but GM better signifies difference due to its higher detection ability.

Peer-review: Externally peer-reviewed.

Author Contributions: Conception/Design of study: S.E., A.M.S; Data Acquisition: S.E., A.M.S, S.K.; Data Analysis/Interpretation: S.E., A.M.S., S.K.; Drafting Manuscript: S.E., A.M.S. Critical Revision of Manuscript: S.E.; Final Approval and Accountability: S.E., H.P.; Technical or Material Support: S.E.; Supervision: S.E.

Conflict of Interest: The authors declare that they have no conflicts of interest.

Financial Disclosure: There are no funders to report for this submission

Acknowledgements: This research was financially supported by the University of Tehran. The authors are thankful for M. Nasri for his help during the sampling.

REFERENCES

- Ambrosio PP, Costa C, Sánchez P, Flos R. Stocking density and its influence on shape of Senegalese sole adults. *Aqua Inter* 2008; 16(4): 333.
- Jalili P, Eagderi S, Keivany Y. Body shape comparison of Kura bleak (*Alburnus filippii*) in Aras and Ahar-Chai rivers using geometric morphometric approach. *Res Zool* 2015; 5(1): 20-4.
- Karpouzi VS, Stergiou KI. The relationships between mouth size and shape and body length for 18 species of marine fishes and their trophic implications. *J fish biol* 2003; 62(6): 1353-65.
- Loy A, Cataudella S, Corti M. Shape changes during the growth of the sea bass, *Dicentrarchus labrax* (Teleostea: Perciformes), in relation to different rearing conditions. In *Advances in morphometrics* (1996; 399-405). Springer, Boston, MA.
- Smith TB, Skulason S. Evolutionary significance of resource polymorphisms in fishes, amphibians, and birds. *Annu Rev Ecol Syst* 1996, 111-33.
- Webb PW. Locomotor patterns in the evolution of actinopterygian fishes. *Am Zool* 1982; 22: 329-42.
- Mouludi Saleh A, Keivany Y, Jalali SAH. Biometry of Chub (*Squalius namak Khaefi* et al., 2016) in rivers of Namak Basin. *J Experiment Anim Biol* 2018; 7(1): 107-18.
- Radkhah A, Poorbagher H, Eagderi S. Investigation of morphological differences of *Capoeta capoeta* populations in the upstream and downstream of Zarinerood River in Urmia Lake Basin. *J Anim Env* 2016; 8(3): 167-74.
- Salehinia D, Eagderi S, Khorasani NA, Zamani-Faradonbeh M. Impact of Sangban Dam on the morphological characteristics of Siah mahi (*Capoeta gracilis*, keyserling, 1864) populations using traditional and geometric morphometrics techniques. *J Anim Env* 2016; 8(2): 97-104.
- Eagderi S, Esmailzadegan E, Madah A, Body shape variation in riffle minnows (*Alburnoides eichwaldii* De Filippii, 1863) populations of Caspian Sea basin. *J Biosystem Taxon* 2013; 5(14): 1-8.
- Eagderi S, Esmailzadegan E, Pirbeigi A. Morphological responses of *Capoeta gracilis* and *Alburnoides eichwaldii* populations (Cyprinidae) fragmented due to Tarik Dam (Sefidrud River, Caspian Sea basin, Iran). *Iranian J Ichthyol* 2014; 1(2): 114-20.
- Mouludi-Saleh A, Keivany Y. Morphological diversity in three species of Chubs (*Squalius* spp.) populations in Iranian Basins. *Nova Biol Reperta* 2018a; 5(2): 192-204.
- Mouludi-Saleh A, Keivany Y. Morphometric analysis of *Squalius namak Khaefi* et al. 2016 in Khaznagh and Ghare-Chai rivers. *Sri Lanka J Aqua Sci* 2018b; 23(2): 173-8.
- Nasri M, Eagderi S, Farahmand H, Segherloo IH, Body shape comparison of *Cyprinion macrostomum* (Heckel, 1843) and *Cyprinion watsoni* (Day, 1872) using geometric morphometric method. *Inter J Aqua Biol* 2013; 1(5): 240-4.
- Nasri M, Eagderi S, Keivany Y, Farahmand H, Dorafshan S, Nezhadheydari H. Morphological diversity of *Cyprinion* Heckel, 1843 species (Teleostei: Cyprinidae) in Iran. *Iranian J Ichthyol* 2018; 5(2): 96-108.
- Razavipour P, Eagderi S, Poorbagher H, Javanshir Khooi A, Keivany Y. Comparative study of morphological characteristics of Tuini fish (*Capoeta damascina*) in inland water of Iran using geometric morphometric method. *J Fish* 2015; 8(1): 79-90.
- Zamani Faradonbeh M, Eagderi S, Nasri M. Geometrics morphometric comparison of populations of waspi *Cabdio morar* (Hamilton, 1822) in Mashkil and Mokran basins. *Iranian Sci Fish J* 2014; 23(2): 57-67.
- Coad BW, Freshwater Fishes of Iran (Available at <http://www.briancoad.com>) (accessed on 4 March 2019).
- Elliott NG, K. Haskard JA. Koslow. Morphometric analysis of orange roughy (*Hoplostethus atlanticus*) off the continental slope of southern Australia. *J Fish Biol* 1995; 46:202-20.
- Zamani Faradonbe M, Eagderi S, Moradi M. Patterns of Body Shape Variation in *Capoeta gracilis* (Pisces: Cyprinidae) in Relation to Environmental Variables in Sefidrud River Basin, Iran. *J Appl Biol Sci* 2015; 9(1): 36-42.
- Langerhans RB, Layman CA, Langerhans AK, DeWitt TJ. Habitat-associated morphological divergence in two Neotropical fish species. *Biol J Linn Soc* 2003; 80: 689-98.
- Kassen B, Bell G. Experimental evolution in *Chlamydomonas*. IV. Selection in Environments that vary through time at different scales. *Heredity* 1998; 80:732-41.